

The copyright of this thesis vests in the author. No quotation from it or information derived from it is to be published without full acknowledgement of the source. The thesis is to be used for private study or non-commercial research purposes only.

Published by the University of Cape Town (UCT) in terms of the non-exclusive license granted to UCT by the author.

**Humpback whales, rock lobsters and mathematics:  
Exploration of assessment models incorporating stock-  
structure**

*Andrea Müller*

Dissertation presented for the degree of Master of Science  
in the Department of Mathematics and Applied Mathematics

University of Cape Town

April 2011

## **Declaration**

I know the meaning of plagiarism and declare that all of the work in the dissertation, save for that which is properly acknowledged, is my own.

---

University of Cape Town

---

**Contents**

<b>Abstract</b> .....	<b>6</b>
<b>1 Introduction</b> .....	<b>8</b>
1.1 Thesis overview.....	8
<b>SECTION A</b>	
<b>2 Statistical and mathematical background to population assessments</b> .....	<b>11</b>
2.1 Population assessments.....	11
2.2 Model dynamics.....	11
2.2.1 Age- and sex-aggregated models.....	11
2.2.2 Age- and sex-disaggregated models.....	12
2.3 Assessment procedure.....	12
2.3.1 Frequentist approach.....	13
2.3.2 Bayesian approach.....	13
2.3.3 Simulation of the posterior distribution.....	14
2.4 Sampling importance re-sampling (SIR).....	15
2.4.1 Theoretical background.....	15
2.4.2 The SIR process.....	17
2.4.3 Convergence diagnostics.....	18
2.5 Markov Chain Monte Carlo (MCMC) methods.....	19
2.5.1 Markov chains.....	19
2.5.2 Gibbs sampling.....	20
2.5.3 Metropolis-Hastings algorithm.....	20
2.5.4 Sampling and convergence.....	21
<b>SECTION B</b>	
<b>3 Background information for the Southern Hemisphere humpback whales</b> .....	<b>26</b>
3.1 Introduction.....	26
3.1.1 Stock structure and locations.....	26
3.1.2 Catch history and IWC management.....	26
3.2 Data.....	27
3.2.1 Abundance estimates.....	27
3.2.2 Capture-recapture data.....	27
3.2.3 $N_{\min}$ constraints.....	28
3.3 Assessment methodology.....	28
3.3.1 Bayesian framework.....	28
3.3.2 Likelihood function.....	29
3.4 SH humpback whale assessments presented in this thesis.....	31

<b>4</b>	<b>The incorporation of length data into an assessment of the Southern Hemisphere humpback whale Breeding Stock C</b>	<b>53</b>
4.1	Introduction	53
4.1.1	Background information	53
4.1.2	The question of interchange between sub-stocks and model selection	54
4.1.3	Expansion of the assessment to include catch-at-length data	55
4.2	Data	56
4.2.1	Historic catch data	56
4.2.2	Abundance and trend data	56
4.3	Methods	57
4.3.1	Model Dynamics	57
4.3.2	Growth curves and catch-at-length	61
4.3.3	Likelihood function	62
4.3.4	Estimation process	63
4.4	Results	64
4.5	Discussion	65
4.6	Future work	68
<b>5</b>	<b>Exploration of stock-structure models for the Southern Hemisphere humpback whale Breeding Stock B</b>	<b>87</b>
5.1	Introduction	87
5.2	Data	89
5.2.1	Historic Catch data	89
5.2.2	Absolute abundance data	90
5.2.3	Capture-recapture data	90
5.3	Methods	91
5.3.1	Model dynamics	91
5.3.2	Bayesian framework	99
5.3.3	Likelihood function	99
5.3.4	$N_{\min}$ constraints	100
5.4	Results	100
5.5	Discussion	102
5.6	Future work	104
<b>6</b>	<b>Initial results for a combined assessment of all seven Southern Hemisphere humpback whales breeding stocks</b>	<b>123</b>
6.1	Introduction	123
6.2	Data	124
6.2.1	Historic Catch data	124
6.2.2	Abundance and trend data	124
6.3	Methods	124
6.3.1	Breeding stock population dynamics	124

6.3.2	Catch Allocation.....	125
6.3.3	Estimation procedure.....	126
6.3.4	Contributions to the likelihood function and priors.....	127
6.3.5	$N_{\min}$ constraints.....	128
6.4	Results .....	128
6.5	Discussion.....	129
6.6	Future work.....	130

## SECTION C

<b>7</b>	<b>Initial results from an assessment of the South African <i>Palinurus delagoae</i> rock lobster resource to investigate the recovery of the resource between two periods of experimental trap-fishing.....</b>	<b>138</b>
7.1	Introduction.....	138
7.1.1	Biological background .....	138
7.1.2	Trawl fishery .....	138
7.1.3	Trap fishery .....	138
7.1.4	Purpose of the assessment .....	139
7.2	Data.....	139
7.2.1	Historic catch data .....	139
7.2.2	Trend information.....	139
7.2.3	Tag-recapture data .....	140
7.3	Methods .....	140
7.3.1	Model Dynamics: .....	140
7.3.2	The likelihood function .....	141
7.3.3	Estimation process.....	144
7.3.4	Assumptions made in this assessment .....	144
7.4	Results .....	144
7.5	Discussion.....	145
7.6	Future work.....	147

## SECTION D

<b>8</b>	<b>Overall discussion and closing remarks .....</b>	<b>169</b>
	<b>Acknowledgements.....</b>	<b>171</b>
	<b>References .....</b>	<b>172</b>

---

## Abstract

This thesis presents four marine resource assessments; three concern the Southern Hemisphere (SH) humpback whale (*Megaptera novaeangliae*) and one the South African east coast rock lobster *Palinurus delagoae*. It also sets out the statistical background to the methodology employed in the assessments, including an outline of the Bayesian approach, Bayes' theorem, and the sampling-importance re-sampling (SIR) as well as the Markov Chain Monte Carlo (MCMC) methods.

Assessments of the SH humpback whale population are currently being undertaken by the Scientific Committee (SC) of the International Whaling Commission (IWC). In 1998, this whale species in the SH was divided into seven breeding stocks (A–G) for assessment and management purposes (IWC, 1998), and since then assessments of Breeding Stocks A, G (IWC, 2007) and C (IWC, 2010) have been completed.

The SH humpback whale Breeding Stock C breeds off the east coast of southern Africa and is thought to consist of two sub-stocks (IWC, 2007). Catch-at-length data from the 1900s are available for this breeding stock, and a paper (Best and Brandão, 2009) presented at an intersessional meeting held by the IWC SC noted that the catches taken off the African coast showed different trends in age- and sex-structure to those taken off Madagascar. Four explanations for this observation were put forward at the meeting: (i) that two separate stocks which had undergone different levels of exploitation were involved, (ii) that animals of different ages migrate to different regions, so that this could account for the observed differences in the catch compositions, (iii) that the body sizes of the two breeding stocks are slightly different, and (iv) that whaling selectivity occurred differently between the two regions. The meeting suggested that these ideas be explored using a simple age-based model with knife-edge catch-at-age selectivity. This was undertaken as part of the work for this thesis.

The results showed a relatively poor fit of the model-predicted catch-at-length frequencies to those observed, suggesting that: (i) differential past exploitation alone is not sufficient to account for the differences observed in the catch-at-length distributions off the African mainland and around Madagascar, (ii) the reported catches are not representative of the entire population, as a smaller proportion of large animals was caught than would have been expected given the model estimates, (iii) if the body sizes of the two stocks are different, then this difference would need to be quite substantial to account for the observed dissimilarities observed in the catch-at-length distributions, and (iv) a geographical age-specific separation might be a more likely explanation, as an initial impression is that whaling selectivity is unlikely to be substantially different between the two regions (Africa and Madagascar) since the whaling techniques are considered to be identical.

The SH humpback whale Breeding Stock B is located off the west coast of Africa, from South Africa to Gabon. This breeding stock is currently under assessment by the IWC SC and several stock-structure hypotheses have been put forward. Genetic differences have been detected between the whales found off west South Africa (WSA) and those found in the waters off Gabon and it has been proposed that either: (i) Breeding Stock B actually consists of two sub-stocks; or (ii) there is only one breeding stock, but that maternally directed fidelity to the feeding grounds could account for the observed genetic differences. The proposed stock-structure hypotheses explore both these assumptions, as well as alternative possible migration routes, breeding grounds and further stock sub-structuring. Six models are analysed for the work presented in this thesis, and the results indicate that the various stock-structure hypotheses serve primarily to assist an understanding of the implications of different behaviours of the whales, rather than to obtain substantially different estimates of current population status. The

---

input data for these assessments are currently under review by the IWC SC for finalisation for the 2011 meeting of this committee. As such, the results presented in this thesis are of an initial nature, to be developed further once consensus is reached within the committee regarding assumptions about input data.

The SH humpback whales migrate to the Antarctic over summer, where they feed and the stocks mix to some extent. Historic catch records are given by position, and thus allocation of these catches to the respective breeding stocks requires assumptions to be made about where each stock is located on the feeding grounds. It has been proposed at an intersessional meeting of the IWC SC to develop a model that combines all seven breeding stocks into a single assessment, to allow for uncertainty in the high-latitude boundaries set between the stocks in a consistent manner, and perhaps even allow these boundaries to be estimated rather than fixed. This last study in this thesis relating to the SH humpback whale provides the first step within this larger assessment. It combines all seven breeding stocks into a single assessment and allocates catches from areas where neighbouring stocks are assumed to overlap (in the feeding grounds) in proportion to the relative sizes of those stocks. This assessment proved to be challenging, as the allocation of catches in this manner introduces interdependence in the estimation of the demographic parameters for the individual stocks. This resulted in a lack of stability and convergence in the results. As far as it has been taken here, this study serves to illustrate the processes involved and to provide some initial insights into this proposed combined stock assessment. Further developments in this regard will however be required before reliable results become available.

Under the common theme of exploring situations where stock-structure is important though poorly known, an assessment was undertaken of the South African east coast rock lobster (*Palinurus delagoae*) to investigate the recovery of the resource between two periods of experimental trap-fishing, as well as to assess the current stock levels and potential for future sustainable catches. An age-structured model of a single homogeneous stock was developed that incorporated a catch per unit effort (CPUE) series, as well as catch-at-length frequency data. This allowed for the population trajectory of the stock to be estimated, including the extent of the stock's recovery to its pristine level, as well as possible sustainable future catches for the stock. A complete data set was not available for this particular assessment. As such, several assumptions had to be made that render the results of the assessment as preliminary until the full data set can be located and the assessment updated. Even so, the results indicate problems in trying to reconcile observations with the past dynamics of this population unless a more complex spatial/stock structure is to be assumed.

Work presented in this thesis served to inform and facilitate ongoing research into stock assessments commissioned by the IWC and the South African Department of Agriculture, Forestry and Fisheries (DAFF), and has fulfilled the objective of providing some initial insights into questions posed by these management bodies.

## 1 Introduction

The topics addressed in this thesis, some briefly but others more comprehensively, perhaps span an unusually broad spectrum. An underlying theme of the tasks tackled has been the use of available data to investigate hypotheses put forward concerning stock and/or spatial structuring of the population under study. The degree to which this structuring applies differs for the various cases considered. At one end of the spectrum, a population might be hypothesised to consist of independent stocks that experience reproductive isolation (Chapter 5). At the other extreme, a population might be thought to consist of a single stock, but spatially separated with movement occurring between the population components (Chapter 7). Work has involved the adaption of population dynamics models commonly used in marine assessments to incorporate these extreme, as well as intermediate, population structurings. Each chapter presents a study that aims to answer particular questions that require exploration of the data through the development of population models. This thesis pulls together the primary assessments (though in some cases these are still of an initial nature) performed over a two-year period.

### 1.1 Thesis overview

The thesis consists of four sections.

#### *Section A*

Section A sets the platform for the thesis by giving the details of the mathematical and statistical methods employed in the assessments undertaken. It gives an introduction to marine population assessments and the basics of age- and sex-aggregated and disaggregated models. It contrasts the frequentist and Bayesian approaches to statistical analyses, and presents the theoretical background to the Bayesian methods implemented in some of the assessments reported on in this thesis.

#### *Section B*

This section pertains to the application of the methods given in Section A to the Southern Hemisphere (SH) humpback whale populations. Chapter 3 introduces this whale species, particularly in relation to its stock structure and the history of its assessment and management by the International Whaling Commission (IWC). It presents the data available (as of February 2011) for the SH humpback whale species, and details the Bayesian framework within which these assessments take place.

The SH humpback whale population has been divided into seven breeding stocks for assessment and management purposes by the IWC (IWC, 1998). Three different humpback assessments relating to these breeding stocks were undertaken and are presented in Chapters 4 to 6. Each of these chapters has its own introduction giving the details of the nature of the assessment to be undertaken as well as the biological and historical information needed as background knowledge.

Chapter 4 presents the results of the incorporation of length data into an assessment of the SH humpback whale Breeding Stock C (found off the east coast of Africa), while Chapter 5 reports on the exploration of several proposed stock-structure models for the SH humpback whale Breeding Stock B (found off the west coast of Africa). Chapter 6 reports on an assessment that attempts to combine all the seven breeding stocks (previously

only individually assessed) into a single assessment. Each chapter includes a discussion of the results and suggested future work.

#### *Section C*

Section C consists of a single chapter reporting on the results of an initial assessment of the *P. delagoae* rock lobster (found off the east coast of South Africa) that aims to investigate (a) the extent of recovery of the resource between two periods of experimental trap-fishing and (b) the potential for sustainable fishing of the resource. Background information on this lobster species as well as details of its catch history and the data available are presented in this chapter, along with results, discussion and suggested future work.

#### *Section D*

An overall discussion of the work completed for the thesis is given in this section. As the previous chapters provide detailed discussion of the work they present, as well as suggested future work, Section D serves primarily to tie the individual chapters together through general comments and observations.

University of Cape Town

University of Cape Town

**SECTION A:**

**Statistical and mathematical background**

## 2 Statistical and mathematical background to population assessments

### 2.1 Population assessments

Surveys, catch records and experiments all provide information about the status of a marine population. Surveys for example can give estimates of current abundance (in relative or absolute terms), or track a population's migratory habits. Historical catch records give an indication of past population sizes that could have yielded such catches, while catch per unit effort (CPUE) values give indications of a population increasing or declining. Very seldom, however, do data such as these provide direct estimates of quantities such as the population's intrinsic growth rate, or its pre-exploitation (pristine) level – two quantities that provide valuable information to help inform management decisions. An estimate of abundance  $N$ , for instance, provides only limited information in the absence of an estimate of the pristine population level, i.e. the important question is what the population status is relative to that pristine level. The intrinsic growth rate allows predictions to be made about the future status of a population under various assumptions and management schemes. In fisheries, another important use of these two quantities is the estimation of the maximum sustainable yield (MSY), i.e. the highest quantity that can be harvested from a population annually while maintaining the stock at a constant level. Techniques that utilise available data to estimate these quantities are of great importance, and fall into the realm of population assessments.

### 2.2 Model dynamics

In any population assessment, the first step after obtaining data is to decide on the population dynamics model to be utilised. These generally discrete models determine how the size of a population will change from year to year given an intrinsic growth rate, pristine population level and historic catch records. Depending on the complexity of the model, additional biological parameter values may need to be set on input or estimated.

#### 2.2.1 Age- and sex-aggregated models

At its simplest, a population model is age- and sex- aggregated, such as the Pella-Tomlinson model:

$$N_{y+1} = N_y + r N_y \left( 1 - \left( \frac{N_y}{K} \right)^\mu \right) - C_y \quad (2.1)$$

where

- $N_y$  is the size of the population at the start of year  $y$ ,
- $r$  is the intrinsic growth rate of the population,
- $\mu$  is the parameter that determines the population size where productivity is maximum, also known as a “degree of compensation” parameter,
- $K$  is the pristine (pre-exploitation) abundance or carrying capacity for the population, and
- $C_y$  is the catch taken in year  $y$ .

The model assumes that next year's population size is simply this year's population size, plus the natural growth, less the catches taken. It is a logistic-type model, and the natural growth term:

$$G(N_y) = r N_y \left( 1 - \left( \frac{N_y}{K} \right)^\mu \right) \quad (2.2)$$

follows the logic that as the population size reaches its carrying capacity, the growth rate must tend to zero.

The Pella-Tomlinson model is a generalisation of the logistic or Schaefer model (where  $\mu$  is set to 1) and allows for skewness of the stock production curve (Pella and Tomlinson, 1969). Appendix 2.1 illustrates this curve, as well as the effect of adjusting the  $\mu$  and  $r$  values. Additionally, Appendix 2.1 shows how the maximum sustainable yield (MSY), the maximum sustainable yield level (MSYL) and the maximum sustainable rate (MSYR) are calculated. Given estimated values for the population parameters  $r$ ,  $K$  and  $\mu$ , these quantities can be computed and management decisions made accordingly.

### 2.2.2 Age- and sex-disaggregated models

In certain instances, there is information available that is sex or age specific. Such information could include catches for which the sex and length (which is an indication of age) have been recorded. Since data are often scarce in the field of marine population assessments, this is valuable additional information that should be included in population models where possible. To incorporate sex or age specific data, however, a move away from a simpler model (like the Pella-Tomlinson) to a more complicated age- and/or sex-disaggregated model is needed.

Two such models have been utilised in this thesis; one both age- and sex-disaggregated (Chapter 4), and one only age-disaggregated (Chapter 7). The equations for the dynamics are given in the relevant chapters.

An age- and sex-disaggregated model is somewhat more detailed than an aggregated model and as such requires more assumptions to be made. Some assumptions are biological, such as those made about the initial age structure of the population at its pristine level (see Appendix 2.2), natural mortality, pregnancy rates and age at maturity. Others relate to catch information, a major assumption being that of the catch selectivity function. For many species, young animals are less likely to be caught than the older, larger animals (because of, for example, larger mesh-sizes in nets), while for some species older animals have techniques for evading nets and are thus harder to catch. Such facts are taken into account in an assessment through a catch selectivity-at-age function that effectively specifies the extent to which various portions of a population are available for catching. Sometimes this function is estimated, but if there are insufficient data it is fixed and alternative functions are tested as sensitivities.

When an age- and/or sex-disaggregated model is developed, the question needs to be asked if the available age- and sex-specific data are sufficient to estimate the additional parameters (to validate the additional assumptions) that arise in an age- and/or sex-disaggregated assessment. If the answer is yes, then such an assessment could produce a considerable amount of information about the population in question that would not be possible to obtain from an age- and sex- aggregated model.

## 2.3 Assessment procedure

Robert (1994) suggests that the main purpose of a statistical analysis (within a population assessment) is to take observations of a population into consideration and to make inferences about the probability distributions

underlying various aspects of interest concerning that population. This information is used either to investigate the possible cause of an observed effect, or to make predictions about the probabilities of possible future occurrences and population trends. A statistical analysis aims to give an interpretation of the phenomenon concerned, rather than an explanation (Robert, 1994).

‘Interpretation’, however, implies a certain degree of subjectivity, which is evident in the many and varied approaches that are taken to statistics. The most widely used is the frequentist approach, which interprets the probability of an event occurring as the proportion of times the event would occur in a long series of repeated experiments.

### 2.3.1 Frequentist approach

Assume  $\theta$  is a parameter of interest for some population under observation. In the frequentist approach,  $\theta$  is treated as an unknown but fixed parameter, which does not allow a probability distribution to be associated with  $\theta$  directly. The only probability distribution considered is what is known as the sampling distribution<sup>1</sup>, for which the probabilities and statistics of interest concerning  $\theta$  are calculated.

In the context of population assessments, there are usually some biological parameters that are unknown and need to be estimated. These parameters could include, for example, the intrinsic growth rate, natural mortality, the pristine population level or recruitment parameters. These parameters usually cannot be computed directly from samples taken from the population. Rather, they are estimated through the fitting of a population dynamics model to biological data, such as an abundance estimate or trend information. While the actual values of the parameters are unknown, there may very often be some sort of prior information available about the parameters, such as natural bounds<sup>2</sup>. Prior information cannot easily be incorporated into a frequentist analysis, as the parameters are considered fixed constants. They should therefore not be more likely to take on values between certain bounds than others *before* the data have been incorporated into the assessment.

### 2.3.2 Bayesian approach

Bayesian methodology, on the other hand, does allow for the incorporation of such prior information. Here, parameters are treated as random variables, i.e. they are assumed to have some underlying distribution associated with this inherent uncertainty. This distribution reflects the strength of one’s belief about the possible values that the parameter in question can assume and is known as a *prior distribution* (Freund, 2004). The Bayesian approach aims to update the prior distribution using the available data to construct a *posterior distribution*. The posterior distribution thus incorporates both the prior information about the parameter in question, and the available data for the population. It is from this distribution that statistics of interest, such as a posterior median value and

---

<sup>1</sup> Let  $Y_i = \{Y_{i_1}, Y_{i_2}, \dots, Y_{i_n}\}$  be a random sample of  $n$  values from a distribution that depends on  $\theta$ . Suppose statistic  $X$  is a quantity of interest that can be calculated from the random sample of these data (for example the mean, median, standard deviation). Suppose this statistic  $X$  is calculated for each possible random sample of size  $n$ . Then the distribution of these values is called the *sampling distribution* of the statistic.  $X$  can thus be interpreted as a random variable, and the sampling distribution gives an indication of how  $X$  varies over all possible random samples of size  $n$  (Bolstad, 2007).

<sup>2</sup> Intrinsic growth rates, for example, cannot be negative and very often have an upper bound beyond which growth rates become biologically infeasible.

probability intervals are calculated. The updating of a prior to a posterior distribution is accomplished through the following theorem.

#### *Bayes' theorem*

Suppose that for a particular population, the following  $N$  parameters are to be estimated:  $\theta_1, \theta_2, \dots, \theta_N$ . Let  $\underline{\theta}^k = \{\theta_1^k, \theta_2^k, \dots, \theta_N^k\}$  be a particular set of possible values that these parameters can have. A function is defined that assesses how likely it is to have observed the data available for the population, given this parameter value combination  $\underline{\theta}^k$  (McAllister *et al.*, 1994). This function is known as the *likelihood function*,  $L$ . Each  $\underline{\theta}^k$  is then assigned a likelihood,  $L(\text{data} | \underline{\theta}^k)$ .

Suppose each  $\theta_i$ ,  $i \in [1, N]$  has a prior probability distribution  $p_i(\theta_i)$ , from which values can be drawn. Assuming that the prior distributions  $p(\theta_i)$  are independent<sup>3</sup>, the joint prior distribution is given by:

$$p(\underline{\theta}^k) = p(\theta_1^k, \theta_2^k, \dots, \theta_N^k) = p_1(\theta_1^k) \times p_2(\theta_2^k) \times \dots \times p_N(\theta_N^k) \quad (2.3)$$

Bayes' theorem states that the posterior distribution, or the distribution of  $\underline{\theta}^k$  given the available data, is given by (McAllister *et al.*, 1994):

$$P(\underline{\theta}^k | \text{data}) = \frac{L(\text{data} | \underline{\theta}^k) p(\underline{\theta}^k)}{\int L(\text{data} | \underline{\theta}) p(\underline{\theta}) d\underline{\theta}} \quad (2.4)$$

#### **2.3.3 Simulation of the posterior distribution**

This posterior distribution (particularly the integration over the likelihood function and prior distribution) is very often neither analytically computable, nor easily approximated. When this is the case, the posterior distribution needs to be simulated on the basis of a large number of draws (Rubin, 1988). Monte Carlo methods are the most commonly used to accomplish this simulation (McAllister and Ianelli, 1997). Two such methods, the Sampling-Importance Resampling (SIR) algorithm and the Markov Chain Monte Carlo (MCMC) method, will be described here for the following problem:

Suppose a particular population under assessment has  $N$  estimable parameters,  $\theta_1, \theta_2, \dots, \theta_N$ , each with their own prior distribution. There are certain data available for the population (such as abundance estimates or trend information, as well as a catch history), and a population dynamics model has been selected that accounts for the annual natural growth and mortality rates of the population. Thus, given a set of values for  $\{\theta_1, \theta_2, \dots, \theta_N\}$ , the population trajectory can be computed.

The aim is to estimate the posterior median values of  $\theta_1, \theta_2, \dots, \theta_N$ .

<sup>3</sup> Following the likelihood principle, two fully dependent parameters bring the same information to the likelihood function (Robert, 1994). Therefore, only independent parameters should be used jointly in the likelihood evaluation. McAllister *et al.* (1994) states that two parameters,  $\theta_1$  and  $\theta_2$ , are considered to be independent if no combinations of values for  $\theta_1$  and  $\theta_2$  are assumed to be more likely than others when these two parameters are considered jointly.

## 2.4 Sampling importance re-sampling (SIR)

“The SIR algorithm has been proposed as one of the simplest, most versatile Bayesian Monte Carlo methods for drawing a sample from the posterior.” (McAllister *et al.*, 1994)

### 2.4.1 Theoretical background

Suppose  $h(\underline{\theta})$  is a rough approximation of the posterior distribution. The better this approximation is, the more efficient the generation of the posterior distribution becomes (Rubin, 1988).  $h(\underline{\theta})$  is called the *importance function*. McAllister *et al.* (1994) explains the SIR process:

Let  $M$  parameter combinations  $\underline{\theta}^k = \{\theta_1^k, \theta_2^k, \dots, \theta_N^k\}$ ,  $k \in [1, M]$  be drawn from a common probability density,  $h(\underline{\theta})$ , the importance function. Suppose  $g(\underline{\theta} = \{\theta_1, \theta_2, \dots, \theta_N\})$  is some function of interest<sup>4</sup>. Assuming that  $\underline{\theta}$  is a vector of continuous random variables, with  $P(\underline{\theta} | \text{data})$  as its probability distribution, the expected value of  $g(\underline{\theta})$  is given by:

$$\begin{aligned} E^{P(\underline{\theta}|\text{data})}[g(\underline{\theta})] &= \int g(\underline{\theta})P(\underline{\theta} | \text{data})d\underline{\theta} \\ &= \frac{\int g(\underline{\theta})L(\text{data} | \underline{\theta})p(\underline{\theta})d\underline{\theta}}{\int L(\text{data} | \underline{\theta})p(\underline{\theta})d\underline{\theta}} \end{aligned} \quad (2.5)$$

The next step is to multiply the integrand in the numerator by  $h(\underline{\theta})/h(\underline{\theta})$ :

$$\begin{aligned} \int g(\underline{\theta})L(\text{data} | \underline{\theta})p(\underline{\theta})d\underline{\theta} &= \int \frac{g(\underline{\theta})L(\text{data} | \underline{\theta})p(\underline{\theta})h(\underline{\theta})}{h(\underline{\theta})} d\underline{\theta} \\ &= E^{h(\underline{\theta})} \left[ \frac{g(\underline{\theta})L(\text{data} | \underline{\theta})p(\underline{\theta})}{h(\underline{\theta})} \right] \end{aligned} \quad (2.6)$$

Using the strong law of large numbers, it follows that (McAllister *et al.*, 1994):

$$\lim_{M \rightarrow \infty} \frac{1}{M} \sum_{k=1}^M \left[ \frac{g(\underline{\theta}^k)L(\text{data} | \underline{\theta}^k)p(\underline{\theta}^k)}{h(\underline{\theta}^k)} \right] = \int g(\underline{\theta})L(\text{data} | \underline{\theta})p(\underline{\theta})d\underline{\theta} \quad (2.7)$$

Equation (2.5) then becomes:

$$E^{P(\underline{\theta}|\text{data})}[g(\underline{\theta})] \cong \frac{\sum_{k=1}^M g(\underline{\theta}^k)w(\underline{\theta}^k)}{\sum_{k=1}^M w(\underline{\theta}^k)} = \sum_{k=1}^M \left[ g(\underline{\theta}^k) \frac{w(\underline{\theta}^k)}{\sum_{k=1}^M w(\underline{\theta}^k)} \right] \quad (2.8)$$

<sup>4</sup> For example,  $g(\underline{\theta})$  could be a population's current size as a function of pristine population level and another  $N-1$  parameters to make up  $\underline{\theta} = \{\theta_1, \theta_2, \dots, \theta_N\}$ .  $E(g(\underline{\theta}))$  is then the posterior mean of the current population size distribution.

where  $w(\underline{\theta}^k)$  is known as the *importance ratio* of  $\underline{\theta}^k$ , and is given by:

$$w(\underline{\theta}^k) = \frac{L(\text{data} | \underline{\theta}^k) p(\underline{\theta}^k)}{h(\underline{\theta}^k)} \quad (2.9)$$

Note that if  $X$  is a discrete random variable with  $f(x)$  the value of its probability distribution at  $X=x$ , the expected value of  $g(X)$  is given by:

$$E[g(X)] = \sum_x g(x).f(x) \quad (2.10)$$

(Freund, 2004).

Comparison of Equation (2.10) to Equation (2.8) shows that  $\underline{\theta}^k$  can be seen as a discrete random variable with an underlying distribution:

$$f(\underline{\theta}^k) = \frac{w(\underline{\theta}^k)}{\sum_{k=1}^M w(\underline{\theta}^k)} \quad (2.11)$$

The distribution  $f(\underline{\theta})$  is taken as an estimate of the actual posterior distribution, i.e.:

$$P(\theta^k | \text{data}) \cong \frac{w(\theta^k)}{\sum_{k=1}^M w(\theta^k)} \quad (2.12)$$

### 2.4.2 The SIR process

Sampling from this estimated posterior distribution takes place in four steps (Rubin, 1988; McAllister *et al.*, 1994):

- Step 1:* The importance function  $h(\underline{\theta})$  is chosen. Since sampling takes place from  $h(\underline{\theta})$ , the closer  $h(\underline{\theta})$  is to the posterior distribution, the more computationally efficient the process will be<sup>5</sup>.
- Step 2:*  $M$  parameter combinations,  $\{\underline{\theta}^1, \underline{\theta}^2, \dots, \underline{\theta}^M\}$  are drawn from  $h(\underline{\theta})$ . If the final aim is to produce  $m$  samples from the posterior distribution from which to compute the posterior medians, probability intervals and whatever other statistics that are of interest, then  $M$  should be substantially larger than  $m$ . Rubin (1988) notes that if  $h(\underline{\theta})$  is a good approximation of  $P(\underline{\theta}|data)$ , then the ratio  $M/m$  can be small, but as  $h(\underline{\theta})$  gets poorer,  $M/m$  needs to increase.
- Step 3* For each  $k \in [1, M]$ , the population dynamics model is projected forward from pristine population levels, under the assumption that the parameter values in  $\underline{\theta}^k = \{\theta_1^k, \theta_2^k, \dots, \theta_N^k\}$  are true. The likelihood function, prior distribution, and importance functions are evaluated at  $\underline{\theta}^k$ , i.e.  $L(\underline{\theta}^k | data)$ ,  $p(\underline{\theta}^k)$  and  $h(\underline{\theta}^k)$  are computed. From these the importance ratio  $w(\underline{\theta}^k)$  is calculated using Equation (2.9).  $w(\underline{\theta}^k)$  is the weight of  $\underline{\theta}^k$  in the simulated posterior distribution in Equation (2.12). Note that if a serious case of lack of biological reality occurs (such as the catch exceeding the size of the population available),  $w(\underline{\theta}^k)$  is set to zero.
- Step 4* Finally,  $m$  samples  $\underline{\theta}^*$  are drawn randomly from  $\{\underline{\theta}^1, \underline{\theta}^2, \dots, \underline{\theta}^M\}$ , with probabilities proportional to  $w(\underline{\theta}^1)$ ,  $w(\underline{\theta}^2)$ , ...,  $w(\underline{\theta}^M)$ . The resulting sample,  $\{\underline{\theta}^{*1}, \underline{\theta}^{*2}, \dots, \underline{\theta}^{*m}\}$ , is an approximation of a sample drawn from the joint posterior distribution of  $\underline{\theta}$ . It is from this sample that the statistics of interest, such as posterior medians or probability envelopes, are calculated.

#### A note on prior distributions

Prior distributions can be either informative or uninformative. Informative priors convey some prior knowledge about a parameter, whereas uninformative priors convey ignorance or objectivity with respect to the parameters of interest (McAllister *et al.*, 1994).

<sup>5</sup> For example, in the case of a single parameter  $\theta$ , if the posterior distribution is Gaussian, but  $h(\theta)$  is taken to be a uniform distribution, many of the samples will be drawn from the (less likely) values in the tails of the Gaussian distribution. If  $h(\theta)$  however is also Gaussian, then more samples will be drawn from around the mean of the distribution than from the tails. Note that in such a case, a t-distribution with thick tails and a large variance is usually chosen for  $h(\theta)$ , to allow for error in what the posterior distribution is suspected to be and to ensure numerical stability (if the tails of  $h(\theta)$  are narrower than the true posterior, SIR will be unstable). McAllister *et al.* (1994) note that for simplicity the prior distribution is sometimes used as the importance function. In this case the importance ratio is simply the value of the likelihood function, i.e. Equation (2.9) reduces to  $w(\underline{\theta}^k) = L(data | \underline{\theta}^k)$ .

It is important to note that the prior distributions should be updated by the data and not the model dynamics themselves. In other words, once  $M$   $\underline{\theta}^k$  parameter combinations have been taken through the population dynamics, the distribution of the parameters (known as the post-model pre-data distributions) should match their prior distributions.

When data contain little information, the posterior distribution tends to reflect the prior distribution. As data become more informative,  $L(\text{data}|\underline{\theta})$  becomes the driving factor in the resultant posterior distribution (Equation (2.4)), and the influence of the priors is reduced (McAllister *et al.*, 1994). Considering that many population assessments have only scant data available, it becomes important that the prior distributions chosen are not unjustifiably informative.

### 2.4.3 Convergence diagnostics

Three convergence diagnostics are outlined here for an assessment utilising the SIR approach:

- 1 *Maximum importance ratio as a proportion of the sum of all importance ratios* (McAllister and Ianelli, 1997):

$$M(\underline{\theta}) = \frac{\max(w(\underline{\theta}^k))}{\sum_{k=1}^M w(\underline{\theta}^k)} \quad (2.13)$$

If this ratio is too big, then  $\max(w(\underline{\theta}^k))$  will dominate in the re-sampling process and this could bias the results. This ratio should ideally be less than 0.01.

- 2 *CV in the average importance ratio* (McAllister and Kirchner, 2002).

$$CV(\bar{w}(\underline{\theta})) = \frac{\sqrt{\frac{1}{N} \sum_{k=1}^N w(\underline{\theta}^k)^2 - \frac{1}{N^2} \left( \sum_{k=1}^N w(\underline{\theta}^k) \right)^2}}{\sqrt{N} \sum_{k=1}^N w(\underline{\theta}^k)} \quad (2.14)$$

This provides an approximation of the expected coefficient of variation in the estimate of the marginal posterior probability distribution. As a rule of thumb, this ratio should be less than 0.04.

- 3 *CV in the importance ratio* (McAllister and Ianelli, 1997).

$$CV(w(\underline{\theta}^k)) = \frac{SD(w(\underline{\theta}^k))}{\frac{1}{M} \sum_{k=1}^M w(\underline{\theta}^k)} \quad (2.15)$$

This is an indicator of the sampling efficiency, and should ideally be less than 50 for relatively simple models.

Convergence diagnostics such as these should be tested for any assessment implementing the SIR methodology.

## 2.5 Markov Chain Monte Carlo (MCMC) methods

For many problems, especially high dimensional ones, it may be quite difficult or even impossible to find an importance function that is a good approximation of the posterior distribution, but still easy to sample (Carlin and Louis, 2009). In such cases MCMC, the second method mentioned for simulating the posterior distribution, offers an alternative approach.

While the statistical theory behind the SIR process is by no means simple, the process is however fairly intuitive. MCMC is far less transparent, and the full justification of why it works is beyond the scope of many books outlining the process<sup>6</sup>. This section aims to provide a basic explanation of the theory and an outline of the processes involved.

### 2.5.1 Markov chains

A Markov chain is a special type of stochastic process that deals with the characterization of random variables, where successive quantities are described probabilistically according to the value of their immediate predecessors (Gamerman, 1997). Let  $S$  denote the sample space (for example parameter values for the posterior), i.e. the (often high-dimensional) space containing the possible values  $\underline{\theta}^k = \{\theta_1^k, \theta_2^k, \dots, \theta_N^k\}$  can take. A Markov chain simulates a random walk of the vector of parameters (Cunningham, 2002) through the parameter space. Any such chain would have some starting position  $\underline{\theta}^0 \in S$  and each successive step or iteration is determined by a random draw from a proposal or jumping distribution.

In most cases, if a chain is run for long enough it will settle on some limiting distribution<sup>7</sup>. MCMC techniques enable sampling from a distribution of interest by embedding it as a limiting distribution of a Markov chain (Gamerman, 1997).

The question now is how to construct a Markov chain whose limiting distribution is exactly the joint posterior distribution of interest. Gamerman (1997) notes that there are large classess of schemes that provide these answers, but that two commonly used algorithms are *Gibbs sampling* and *Metropolis-Hastings* algorithms. A brief outline is given of these two methods based on the descriptions given in Gamerman (1997).

Two definitions are provided before continuing:

- i. In a homogeneous<sup>8</sup> Markov chain, the *transition kernel* is a set  $P(\underline{\theta}, A)$  such that for all  $\underline{\theta} \in S$ ,  $P(\underline{\theta}, \cdot)$  is a probability distribution, and for all  $A \subset S$ , the function  $\underline{\theta} \mapsto P(\underline{\theta}, A)$  can be evaluated. The transition kernel in essence captures the probabilities associated with moving from one point in the sample space  $S$  to another in a single iteration, and if the chain has converged, in any number of iterations.
- ii. The posterior distribution  $P(\underline{\theta} | \text{data})$  will be denoted by  $\pi(\underline{\theta})$  from now on.

<sup>6</sup> Carlin and Louis (2009) for example give an in depth discussion of MCMC, but avoid full justification because of the complexity of the Markov theory upon which the MCMC approach is based.

<sup>7</sup> A Markov chain has a “distribution” associated with it in the sense that random samples can be drawn from the chain, just as they can from a probability density distribution.

<sup>8</sup> A Markov chain is said to be homogeneous if the probabilities associated with moving from one point to another in the sample space  $S$  do not depend on the iteration number  $k$  in the chain (thus allowing the transition kernel to be defined).

### 2.5.2 Gibbs sampling

Gibbs sampling is a MCMC scheme where the transition kernel is formed by the full conditional distributions,  $\pi_i(\theta_i) = \pi(\theta_i | \theta_{\ell \neq i})$  for  $i \in [1, 2, \dots, N]$ . This method therefore requires that these conditional distributions are completely known and can be sampled, and is achieved through the following three steps:

*Step 1:* Set the iteration counter of the chain to be  $k=1$  and set the initial starting position  $\underline{\theta}^0 = \{\theta_1^0, \theta_2^0, \dots, \theta_N^0\}$ <sup>9</sup>.

*Step 2:* Obtain a new value  $\underline{\theta}^k = \{\theta_1^k, \theta_2^k, \dots, \theta_N^k\}$  from  $\underline{\theta}^{k-1}$  by drawing each  $\theta_i^k$  ( $k \in [1, N]$ ) from its conditional distribution, i.e.

$$\begin{aligned}\theta_1^k &\sim \pi(\theta_1 | \theta_2^{k-1}, \theta_3^{k-1}, \dots, \theta_N^{k-1}) \\ \theta_2^k &\sim \pi(\theta_2 | \theta_1^{k-1}, \theta_3^{k-1}, \dots, \theta_N^{k-1}) \\ &\vdots \\ \theta_N^k &\sim \pi(\theta_N | \theta_1^{k-1}, \theta_2^{k-1}, \dots, \theta_{N-1}^{k-1})\end{aligned}$$

*Step 3* Change the iteration counter  $k$  to  $k+1$  and return to *Step 2* until convergence is reached.

Gamerman (1997) shows that the equilibrium distribution of a chain constructed in this manner is in fact  $\pi$ . Thus when convergence is reached, the resulting vector  $\underline{\theta}^k$  is a draw from  $\pi$ .

### 2.5.3 Metropolis-Hastings algorithm

The Metropolis-Hastings algorithm originally dealt with the calculation of properties of chemical substances, but has much broader applications in statistics and simulation (Gamerman, 1997). As for Gibbs sampling, the Metropolis-Hastings algorithm is a technique for constructing a Markov chain whose limiting distribution is the posterior distribution of interest,  $\pi$ , however unlike Gibbs sampling, it can be implemented when the conditional distributions are not known. The method is implemented through the following four steps (Gamerman, 1997):

*Step 1:* Set the iteration counter of the chain to be  $k=1$  and set the initial starting position  $\underline{\theta}^0 = \{\theta_1^0, \theta_2^0, \dots, \theta_N^0\}$ .

*Step 2:* The move from position with iterate  $k-1$  to position  $k$  is made according to a uniform distribution<sup>10</sup> centred at  $\underline{\theta}^k$ .

<sup>9</sup> Generally any value that could occur in the sample is acceptable as a starting position, as long it is not too far out in the tails of the posterior distribution. A starting position near the joint posterior mode is usually a safe option (Cunningham, 2002).

<sup>10</sup> This is the jumping distribution (or an element of the transition kernel) and may also have a different shape, such as a multivariate normal or t-distribution. Gamerman (1997) explains why the transition kernel can be kept arbitrary.

- Step 3* The ratio of the likelihood multiplied by the prior at  $\underline{\theta}^k$  to the likelihood multiplied by the prior at  $\underline{\theta}^{k-1}$  is computed and denoted by  $r$ . If  $r > 1$  (i.e.  $\underline{\theta}^k$  is an improvement in terms of the likelihood) then the step is accepted automatically. If  $r < 1$ , then  $\underline{\theta}^k$  has a probability of being accepted that is proportional the magnitude of  $r$ .<sup>11</sup>
- Step 4* Change the iteration counter  $k$  to  $k+1$  and return to *Step 2* until convergence is reached.

Again, details as to why  $\pi$  is the limiting distribution of a chain constructed in this manner are given in Gamerman (1997). Note that in contrast to Gibbs sampling, the move from one point in the sample space to the next now depends on the proposed transition as well as an evaluation of this proposal.

#### 2.5.4 Sampling and convergence

With these two techniques available for constructing Markov chains with  $\pi$  as their limiting distributions, Gamerman (1997) suggests two approaches to sampling from them. Suppose a chain is assumed to reach convergence after  $q$  iterations, and that  $m$  samples are required from  $\pi$ . The first method constructs  $m$  chains in parallel, each initialised from an independent and unique starting position. The  $q^{\text{th}}$  element in each is taken as a sample from  $\pi$ . This method produces  $m$  independent samples, but requires  $m$  chains to be generated and is therefore computationally inefficient. The second method considers a single chain, where the elements of the chain before convergence are discarded (known as a *burn-in* phase) before sampling takes place. This method is computationally much more efficient, but the samples are also no longer independent. This issue is addressed by sampling from only every  $T^{\text{th}}$  element after burning, a process called *thinning*. Since any element in a Markov chain in theory only depends on its immediate predecessor, this leaves  $m$  independent samples. Larger thinning gaps require longer chains and so the advantage of more independent samples must be weighed against the computational cost (Cunningham, 2002). Gamerman (1997) notes that it is generally agreed that running  $n$  parallel chains is in practice computationally inefficient and unnecessary. It is, however, recommended to run at least a few parallel chains in order to check if they converge to common values. If convergence has occurred, then a single chain can be used for sampling. If not, then there may be secondary modes in the posterior distribution and the parallel chains should be run for longer.

The discussion above is based on the assumption that the chains have converged. An important issue is clearly that of testing convergence. There are many possible tests for this, some theoretical and some statistical. The statistical methods are generally preferred, as the theoretical tests are often not very easy to implement in practice. Even amongst the statistical methods, various options have been proposed (such as those described in Gamerman, 1997). For this thesis, the only application of MCMC (Chapter 6) showed a lack of convergence, which could be judged by a graphical display of the chains in question. Further details of convergence diagnostics are thus not given here.

<sup>11</sup> In practice, such an acceptance probability can be constructed by drawing a random number  $u \in U [0, 1]$ . If  $u < r$ , then the move to  $\underline{\theta}^k$  is accepted, whereas if  $u > r$ , then the move to  $\underline{\theta}^k$  is rejected and the chain remains at  $\underline{\theta}^{k-1}$ , i.e.  $\underline{\theta}^k = \underline{\theta}^{k-1}$ . In other words, the closer the ratio is to one (and the closer  $\underline{\theta}^k$  is to  $\underline{\theta}^{k-1}$  in terms of the likelihood), the more likely the move to  $\underline{\theta}^k$  is to be accepted.

## Appendix 2.1

### Illustration of the Pella-Tomlinson stock production curve, and an explanation and derivation of MSYL, MSY and MSYR

Consider the Pella-Tomlinson equation:

$$N_{y+1} = N_y + r N_y \left( 1 - \left( \frac{N_y}{K} \right)^\mu \right) - C_y \quad (\text{A2.1.1})$$

The maximum sustainable yield level (MSYL) is the population level at which a maximum sustainable yield (MSY) can be taken. A sustainable yield is defined the taking of an annual catch that corresponds to a population's natural growth during that year:

$$SY = r N_y \left( 1 - \left( \frac{N_y}{K} \right)^\mu \right) \quad (\text{A2.1.2})$$

Since a sustainable catch in any year harvests the same amount by which the population grows in that year, the population is kept at a constant level. A plot of the sustainable yield as a function of the population size is shown below.

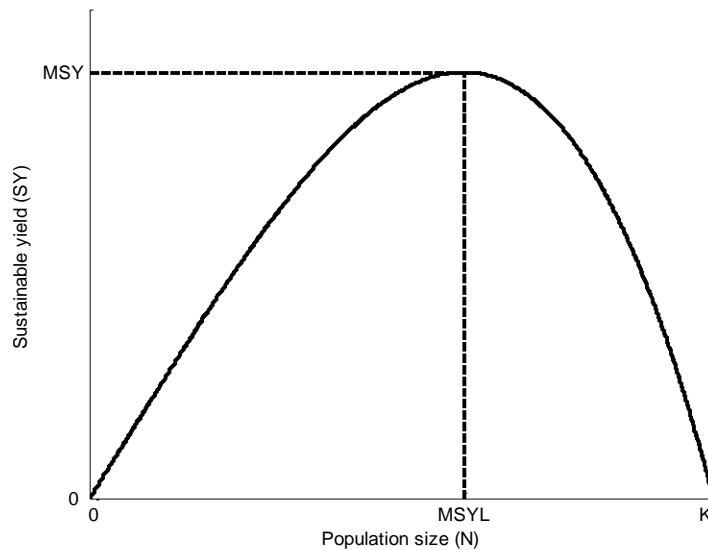


**Figure A2.1.1:** Plot showing sustainable yield,  $SY$ , against population size,  $N$ .

The curve above is also known as the stock production curve (Pella and Tomlinson, 1969). The major driving factors behind the shape of the curve are the intrinsic growth rate  $r$  and the parameter  $\mu$ , which determines the population size where productivity is at a maximum. This is illustrated in Figure A2.1.2 (a) and (b), where it can be seen that the value of  $\mu$  affects the skewness of the curve, while the value of  $r$  determines the magnitude of MSY.

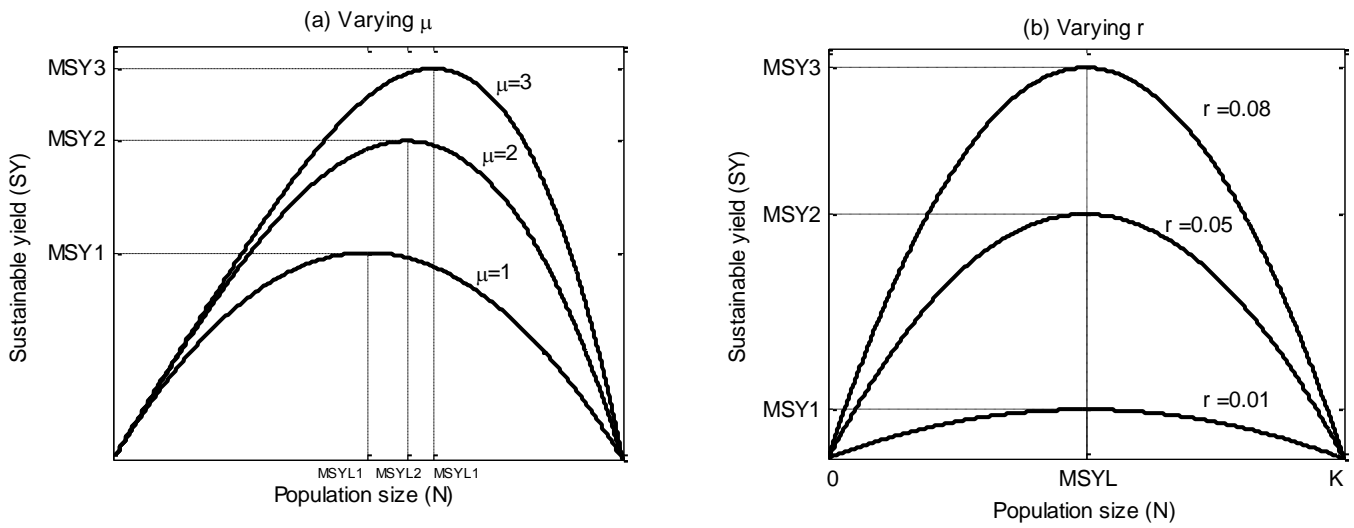


**Figure A2.1.2 (a) and (b):** The Pella-Tomlinson stock production curves for a range of  $\mu$  and  $r$  values. The MSY and MSYL values are indicated for each case.

The MSYL, MSY and MSYR are found analytically by simple differentiation of Equation (A2.1.2)

$$MSYL = K \left[ \frac{1}{1 + \mu} \right]^{1/\mu} \quad (A2.1.3)$$

$$MSY = rK \left[ \frac{1}{1 + \mu} \right]^{1/\mu} \left[ \frac{\mu}{1 + \mu} \right] \quad (A2.1.4)$$

$$MSYR = \frac{MSY}{MSYL} = r \left[ \frac{\mu}{1 + \mu} \right] \quad (A2.1.5)$$

## Appendix 2.2

### Derivation of the initial (pristine) population age structure for an age-disaggregated model

For any age-disaggregated model used in an assessment, population estimates and parameters for the year  $y+1$  are based on the numbers from year  $y$ . Thus, given a pristine total abundance,  $K$ , the initial population structure (in terms of age) needs to be computed.

Assume that at the pristine level, there are  $R_0$  new recruits (i.e. animals of age 0) into the population each year. Given an instantaneous natural mortality rate,  $M$ , the following year will see  $R_0(1-e^{-M})$  deaths, leaving  $R_0e^{-M}$  animals of age 1. Continuing in this fashion the pristine population composition is given by Equation (A2.2.1) below.

$$K = R_0 + R_0e^{-M} + R_0e^{-2M} + \dots + R_0e^{-(m-1)M} + \frac{R_0e^{-mM}}{1-e^{-M}} \quad (\text{A2.2.1})$$

where  $m$  is the plus-group age.

The last term of Equation (A2.2.1) is derived making use of the fact that the equation represents a geometric series, and as such

$$\sum_{a=0}^{\infty} R_0e^{-aM} = \frac{R_0}{1-e^{-M}} \quad (\text{A2.2.2})$$

and

$$\sum_{a=0}^{m-1} R_0e^{-aM} = \frac{R_0(1-e^{-mM})}{1-e^{-M}} \quad (\text{A2.2.3})$$

Equation (A2.2.2) shows that  $K = \frac{R_0}{1-e^{-M}}$ , and therefore, given the pristine population abundance  $K$  and the natural mortality  $M$ , the pristine recruitment level  $R_0$  can be computed. Figure A2.2.1 below illustrates a typical age-structure for a population at its pristine level.

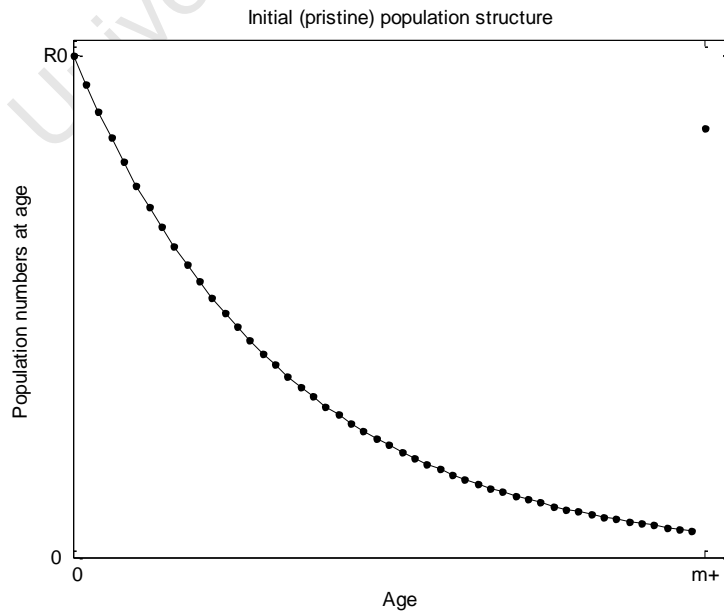


**Figure A2.2.1:** Illustration of the initial, pristine population structure.

**SECTION B:**

**Applications to the Southern Hemisphere humpback whale**

***(Megaptera novaeangliae)***

University of Cape Town

### 3 Background information for the Southern Hemisphere humpback whales

#### 3.1 INTRODUCTION

The Southern Hemisphere (SH) humpback whale is a medium-sized species of baleen whale, reaching a length of about 15m, with a weight of up to 34 tonnes (Johnson and Wolman, 1984). It has a distinctive rounded body shape, with unusually long pectoral fins (up to one-third of the total body length) and a knobbly head (Johnson and Wolman, 1984). Humpback whales in the Southern Hemisphere reside in high-latitude feeding grounds over the summer and migrate north in winter to breed (IWC, 2006b).

##### 3.1.1 Stock structure and locations

In 1998, at the 48<sup>th</sup> annual meeting of the Scientific Committee (SC) of the International Whaling Commission (IWC), the SH humpback whale species was divided into seven breeding stocks<sup>12</sup> for assessment purposes. These divisions relate the high latitude feeding grounds to low-latitude breeding grounds and are given in Table 3.1 below. The boundaries were based on catch positions of previous Soviet Antarctic catches, capture-recapture information and distributions of sightings on IDCR<sup>13</sup> cruises (IWC, 1998).

**Table 3.1:** Geographical summer feeding regions allocated to each of the seven humpback breeding stocks (IWC, 1998).

Breeding stock	Antarctic Longitudinal band	Geographical location of breeding area
Breeding Stock A	70°W – 20°W	Brazil
Breeding Stock B	20°W – 10°E	Angola and Gabon
Breeding Stock C	10°E – 60°E	Mozambique, Comores and Madagascar
Breeding Stock D	60°E – 120°E	Western Australia
Breeding Stock E	120°E – 170°W	Eastern Australia, Tonga and New Zealand
Breeding Stock F	170°W – 120°W	Oceania
Breeding Stock G	120°W – 70°W	Columbia

Although breeding regions are demarcated reasonably well, the stocks mix on their high latitude feeding grounds (IWC, 2009b). The allocation of similar boundaries in the high-latitudes is therefore more complicated, and various hypotheses have been proposed over the years. Figure A3.1.1 of Appendix 3.1 shows a map illustrating the high-latitude boundaries set by the latest hypothesis currently in use, as well as the original high-latitude boundaries given in Table 3.1. These stock boundaries are particularly important in relation to the allocation of high-latitude catches to the respective breeding stocks.

##### 3.1.2 Catch history and IWC management

Like other large whales, humpbacks have been a target for the whaling industry and were subject to heavy whaling in the 20<sup>th</sup> century, leading to a large population decline (Baker *et al.*, 1993). Following a ban on

<sup>12</sup> Some of these stocks were later divided into further sub-stocks based on genetic differentiation in samples taken from the stock (IWC, 2006a).

<sup>13</sup> International Decade of Cetacean Research.

humpback whaling in 1966 (Johnson and Wolman, 1984), stocks have partially recovered. In 1998, the IWC SC appointed a sub-committee for the individual assessment of the seven SH humpback stocks to estimate the extent of recovery and other biological parameters of interest (IWC, 1998). Considerable time and effort has been invested in the collection of information relating to stock-boundary locations, in the collation of historic catches, and in the collection and analysis of genetic and photographic capture-recapture data as well as sighting survey data.

## 3.2 DATA

There are several forms of data available for the SH humpback whale stocks. These include:

- Catch data
- Absolute abundance estimates
- Relative abundance estimates
- Capture-recapture data
- $N_{min}$  constraints (genetics-based limits on minimum possible historic population size)

Appendix 3.1 gives the details of the catch series on record, and the catch-allocation methods and assumptions used. Appendix 3.2 lists data available (as of February 2011) for the seven humpback whale breeding stocks. The methods used to incorporate various forms of data into the assessments presented in this thesis are described in the relevant sections.

### 3.2.1 Abundance estimates

Abundance estimates (both absolute and relative) generally arise from line transect sightings surveys using ships and/or aircraft, or from shore-based surveys along coastal migration paths. Line transect surveys involve systematic observational sampling along predetermined paths through a sampling area. Sightings are recorded in terms of numbers and locations, and this information can be used to calculate abundance estimates (e.g. Andriolo *et al.*, 2006). Shore-based surveys usually take place during peak migration and count the numbers of whales passing the survey site in a given period of time. Often two or more survey sites are used in order to give an estimate of whales that might have been missed at any one of the sites to attempt to convert a relative index of abundance into an absolute estimate (e.g. Noad *et al.*, 2006).

### 3.2.2 Capture-recapture data

Capture-recapture information arises from databases of photographs and biopsies. The photographs collected and genetic signals from biopsy samples are compared across years and matches found are recorded. Data arising in this manner are used to obtain abundance estimates (using the MARK program<sup>14</sup>) and also provide information about migratory habits.

---

<sup>14</sup> The program MARK is a software application used for the ‘analysis of data from marked individuals’ (Cooch and White, 2011). In the case of the humpback whales, the animals are not physically marked (or tagged), but ‘captured’ either through photographs or biopsy samples. If these photographs and samples are of good quality, then they can be used to ‘recapture’ (i.e. re-identify) an individual when photographs and/or biopsies are taken in successive years. The MARK program can be used to analyse this data in order to obtain abundance estimates or estimate survival rates.

### 3.2.3 $N_{min}$ constraints

Rosenbaum *et al.* (2006b) undertook an analysis of mitochondrial DNA sequences for the seven humpback whale breeding stocks and provided estimates of the current number of mitochondrial haplotypes present in the respective populations. Jackson *et al.* (2006) point out that the minimum effective female population size must have been greater than this number of haplotypes and explain why the effective female population is generally considered to be one quarter of the total population, as a conservative estimate. As such, the trajectory for the total population should not drop below four times this haplotype number, a value that is referred to in this thesis as the  $N_{min}$  constraint. These values are incorporated into the model fitting processes as biological constraints.

## 3.3 ASSESSMENT METHODOLOGY

### 3.3.1 Bayesian framework

It is common procedure to implement the Bayesian SIR methodology (see Section 2.4.2) in humpback assessments<sup>15</sup>. The parameters of interest are usually the population's intrinsic growth rate  $r$  and the pre-exploitation population level  $K$ . These two quantities are, however, not independent.

Suppose a target current abundance estimate is given for a population, and an intrinsic growth rate  $r$  and pristine population level  $K$  are to be estimated so that the resulting population trajectory hits the abundance estimate. Section A3.3.1 of Appendix 3.3 shows that if the estimated value for  $r$  is low, then a high value for  $K$  is required to match the abundance estimate. Similarly, a high  $r$  requires a low  $K$ . Therefore the combination (low  $r$ , high  $K$ ) for example is much more likely than the combination (low  $r$ , low  $K$ ). The intrinsic growth rate  $r$  thus contains inherent information about the pristine population level  $K$  and *vice versa*. This complicates the SIR process, as the parameters themselves (in addition to their prior distributions and the data) now bring information to the relative probabilities of different scenarios.

Should  $r$  and  $K$  values nonetheless be drawn directly from their respective prior distributions, this approach is known as the 'Forwards' method. Section A3.3.2 of Appendix 3.3 explains a further problem with this method and reinforces why an alternative method known as the 'Backwards' method is often preferred. In this approach, a prior distribution is assumed on the target abundance estimate,  $N_{target}^{obs}$ , rather than on  $K$ . Combinations of ( $r$ ,  $N_{target}^{obs}$ ) are drawn, and for each combination, a value of  $K$  is found (using a simple simplex minimisation routine) such that the estimated population trajectory matches the drawn target abundance. The prior distributions for  $r$  and  $N_{target}^{obs}$  are assumed to be independent and the SIR process can be implemented as described in Section 2.4.

Where the Bayesian approach has been used for individual assessments presented in this thesis, the prior distributions assumed are detailed in the relevant sections. Generally, the prior distribution from which the target abundance estimate  $\tilde{N}_{target}^{obs}$  is drawn at random is assumed to be uniform on a natural logarithmic scale with lower and upper bounds set in relation to the value of its CV. This provides a prior that is uninformative but bounded for reasonable computational efficiency.

<sup>15</sup> The SIR methodology was employed in the IWC SC assessment breeding stocks A, G (IWC, 2006) and C (IWC, 2009).

### 3.3.2 Likelihood function

The methods for incorporating available abundance and trend data into the likelihood function are common across humpback assessments and are explained below.

#### 3.3.2.1 Absolute abundance data

Given an absolute abundance estimate,  $N_{target}^{obs}$ , this is assumed to be log-normally distributed with the log of the estimate as the mean and the CV as the standard deviation<sup>16</sup>. Thus the likelihood contribution is:

$$\frac{1}{2CV^2} (\ln N_{target}^{obs} - \ln N_{target})^2 \quad (3.1)$$

where

$N_{target}^{obs}$  is the absolute abundance estimate obtained from observations,

$N_{target}$  is the model-estimated population size for the year of the abundance estimate, and

CV is the coefficient of variation of the  $N_{target}^{obs}$  estimate.

#### 3.3.2.2 Relative abundance data

These estimates are given in a series spanning several years. Each year has a relative abundance index  $I_y$ , obtained from observations. It is assumed that this index is log-normally distributed about its expected value:

$$I_y = qN_y e^{\varepsilon_y} \quad (3.2)$$

where

$I_y$  is the relative abundance estimate for year  $y$ ,

$q$  is a constant of proportionality,

$N_y$  is the model estimate of observed population size at the start of year  $y$ , and

$\varepsilon_y$  is from  $N(0, \sigma^2)$  (see Equation (3.3) below).

The  $\sigma$  parameter is the residual standard deviation, which is estimated in the fitting procedure by its maximum likelihood value:

$$\hat{\sigma} = \sqrt{1/\bar{n} \sum_y (\ln I_y - \ln q - \ln N_y)^2} \quad (3.3)$$

where

$\bar{n}$  is the number of data points in the series, and

$q$  is a constant of proportionality, estimated by its maximum likelihood value:

<sup>16</sup> If  $N$  is assumed to be log-normally distributed, then  $\ln N$  is normally distributed with some mean  $\mu$  and standard deviation  $\sigma$ . The median value of  $N$  is then  $e^\mu$  while the CV of  $N$  is given by  $\sqrt{e^{\sigma^2} - 1}$ . Solving backwards for  $\mu$  and  $\sigma$  (with the use of the Taylor expansion for  $e^{\sigma^2}$ ),  $\mu$  is found to be the log of the median value for  $N$  and  $\sigma$  is simply the CV of  $N$ .

$$\ln \hat{q} = 1/\bar{n} \sum_y (\ln I_y - \ln N_y) \quad (3.4)$$

The negative log-likelihood component for the relative abundance data is given by:

$$\bar{n} \ln \sigma + \frac{1}{2\sigma^2} \sum_y (\ln I_y - \ln q - \ln N_y)^2 \quad (3.5)$$

In the Bayesian context,  $q$  and  $\sigma$  are “nuisance parameters, i.e. parameters that need to be estimated but are not of interest themselves (McAllister *et al.*, 1994). Walters and Ludwig (1994) show that the above approach is essentially a shortcut to avoid integrating over the prior distributions parameters and corresponds to the assumption that these priors are uniformly distributed in log-space.

### 3.3.2.3 Capture-recapture data

These data are usually given in the form a matrix showing counts of animals that were seen in a specific year and re-seen in a subsequent year. The method for incorporating this information into the likelihood is given below, for the case where a breeding stock can consist of several sub-stocks associated with particular regions.

The capture-recapture data give:

- $n_y^i$ , the number of animals captured in region  $i$ <sup>17</sup> in year  $y$ , and
- $m_{y,y'}^{i,j}$ , the number of animals captured in year  $y$  in region  $i$  that were recaptured in year  $y'$  in region  $j$ .

If  $p_y^i$  is the probability that an animal is seen in region  $i$  in year  $y$ , then the number of animals captured in region  $i$  in year  $y$  is given by:

$$n_y^i = p_y^i N_y^i \quad (3.6)$$

where  $N_y^i$  is the total (1+) population in region  $i$ .

Suppose further that there are two regions  $i$  and  $j$ , and that  $\alpha^i$  is the probability that an animal from region  $i$  moves to region  $j$  in any given year<sup>18</sup>, then the number of animals captured in region  $i$  in year  $y$  is given by:

$$n_y^i = p_y^i [(1 - \alpha^i) N_y^i + \alpha^j N_y^j] \quad (3.7)$$

Bearing in mind that the capture-recapture data give  $m_{y,y'}^{i,j}$  (the number of animals captured in year  $y$  in region  $i$  that were recaptured in year  $y'$  in region  $j$ ) the model-predicted equivalent,  $\hat{m}_{y,y'}^{i,j}$ , needs to be computed.

Given a natural mortality rate  $M$  (set here to equal  $0.03 \text{ yr}^{-1}$  as recommended by the IWC SC), a proportion  $e^{-M(y'-y)}$  of the animals survive through to year  $y'$ . The model predicted number of animals captured in region  $i$  in year  $y$  that were recaptured in region  $j$  in year  $y'$  is then given by:

<sup>17</sup> For breeding stocks B and C (the only stocks for which capture-recapture data are available) the index ‘ $i$ ’ (and ‘ $j$ ’) refers to the region associated with a particular sub-stock (i.e. B1/ B2 or C1/C3, see Chapters 4 and 5).

<sup>18</sup> There are several assumptions that can be made as to how long such an animal will remain in a neighbouring sub-stock (some examples are given in Chapter 4), but for the purpose of this illustration, the assumption is made that an animal only ‘visits’ a neighbouring sub-stock and will return to its own sub-stock in the following year.

$$\hat{m}_{y,y'}^{i,j} = p_y^i [(1 - \alpha^i) N_y^i e^{-M(y'-y)} \alpha^i + \alpha^j N_y^j e^{-M(y'-y)} (1 - \alpha^j)] p_{y'}^j \quad (3.8)$$

where  $(1 - \alpha^i) N_y^i e^{-M(y'-y)} \alpha^i$  is the number of animals originally from region  $i$  that moved to region  $j$  in year  $y'$ , and  $\alpha^j N_y^j e^{-M(y'-y)} (1 - \alpha^j)$  is the number of animals from region  $j$  that were in region  $i$  in year  $y$ , but have subsequently remained in region  $j$ .

The model predicted number of animals captured in region  $i$  in year  $y$  that were recaptured in the same region  $i$  in year  $y'$  is given by:

$$\hat{m}_{y,y'}^{i,i} = p_y^i [(1 - \alpha^i) N_y^i e^{-M(y'-y)} (1 - \alpha^i) + \alpha^j N_y^j e^{-M(y'-y)} \alpha^j] p_{y'}^i \quad (3.9)$$

Note that if  $\alpha^i = 0$  (i.e. no interchange is assumed), Equation (3.8) reduces to zero and Equation (3.9) becomes

$$\hat{m}_{y,y'}^{i,i} = p_y^i N_y^i e^{-M(y'-y)} p_{y'}^i \quad (3.10)$$

The probability of an observed  $m_{y,y'}^{i,j}$ , given the model-predicted  $\hat{m}_{y,y'}^{i,j}$ , is determined assuming a Poisson distribution<sup>19</sup>, with the associated likelihood contribution given by:

$$\frac{(\hat{m}_{y,y'}^{i,j})^{m_{y,y'}^{i,j}}}{m_{y,y'}^{i,j}!} e^{-\hat{m}_{y,y'}^{i,j}} \quad (3.11)$$

The final component for the negative of the log-likelihood for capture-recapture data is then given by:

$$\sum_i \sum_j \sum_{y=y_0}^{y_f-1} \sum_{y'=y+1}^{y_f} [-m_{y,y'}^{i,j} \ln \hat{m}_{y,y'}^{i,j} + \hat{m}_{y,y'}^{i,j}] \quad (3.12)$$

where  $y_0$  is the first year of captures and  $y_f$  is the last year of recaptures.

Note that if an animal is re-seen a second time, this is treated as a new sighting when compiling the capture-recapture matrices.

### 3.4 SH HUMPBACK WHALE ASSESSMENTS PRESENTED IN THIS THESIS

The following three chapters each present an assessment of the SH humpback whale species that makes use of the methodology described above. These studies were carried out under the recommendation of the IWC SC, and their results have been presented to the IWC SC for discussion. Each chapter gives the aims of the study, as well as necessary background information, and provides discussion of the results obtained.

<sup>19</sup> Equations (3.6) to (3.11) imply a multinomial distribution. However, because the annual capture probabilities are so small, the Poisson distribution is an adequate and convenient approximation.

## Appendix 3.1

### Historic catches of Southern Hemisphere humpback whales

This Appendix lists the historic catches available for Southern Hemisphere humpback whales. Catches taken north of 40°S are straightforward to allocate to the seven breeding stocks, as these catches (listed in Table A3.1.1) were taken in the vicinities of the reasonably well defined breeding regions. The allocation of catches taken in the high latitude feeding areas (south of 40°S) is more complicated, as neighbouring stocks are assumed to mix there.

#### *A3.1.1 Allocation of catches taken south of 40 °S*

Initial catch allocation models were proposed in 1997 at IWC SC 49 (IWC, 1998) based on various assumptions about the locations of the seven breeding stocks in the feeding regions, as well as the degree of overlap between neighbouring stocks. As new information became available in the years that followed, a number of modifications were made to these models. A working group was appointed at an intersessional meeting in Seattle, February 2009 to review and clarify the various catch allocation hypotheses (Findlay *et al.*, 2009). The report of this working group is given in Appendix 2 of IWC (2010). Two catch allocation hypotheses (Hypothesis 1 and Hypothesis 2) were proposed.

In Hypothesis 1, each breeding stock is associated with a ‘Nuclear’ area in the feeding ground, where 100% of catches taken there are allocated to that breeding stock. Areas between Nuclear regions are denoted as ‘Margin’ areas, and here catches are allocated to the associated adjacent east and west stocks in a 50:50 ratio.

Hypothesis 2 takes into account that data connecting breeding and feeding grounds suggest that, on average, there is a roughly symmetric distribution of animals on the feeding grounds up to 30° east and west of the median longitude associated with a breeding stock. Thus given a median feeding ground longitude for a particular breeding stock, catches taken up to 30° east and west of that longitude are allocated to that stock. Areas where there is an overlap between neighbouring stocks are designated Margin areas and catches split in a 50:50 ratio, as for Hypothesis 1.

The report of the working group noted that these hypotheses are subject to change as new data to inform on the boundaries become available, and are by no means the only option for catch allocation. The hypotheses were presented rather as a useful way of dealing with catch allocation, especially for the breeding stocks for which there are few data available to suggest alternative catch allocation assumptions. Groups involved with individual breeding stock assessments were however encouraged to explore alternative catch allocation models independently (IWC, 2010).

The IWC SC agreed to use Hypothesis 1 as a reference case, and accordingly the catch allocations for the assessments in this thesis adhere to Hypothesis 1. Figure A3.1.1 shows the Hypothesis 1 boundary assumptions, and Table A3.1.2 lists the catch series.

### A3.1.2 Sex-disaggregation of catches taken from breeding sub- stocks C1 and C3

This section details the sex-disaggregation of the C1 and C3 catches for the age- and sex-disaggregated model in Chapter 4. The methodology detailed below and the tables with the corresponding catch series were compiled by S.J. Johnston and C. Allison and taken from Müller *et. al* (2009).

#### Catches North of 40°S

Catches from the C1 and C3 breeding stocks are reported as combined (male+female) catches. For C1 catches reported for Southern Cape, Natal and Mozambique have been combined, and the C3 catches are from Western Indian Ocean. Russian catches taken between 10° – 60°E are split equally between the two stocks.

#### *C1 Catches*

For certain periods the catches have been either totally or partially sexed. In order to produce a sex-disaggregated catch series for the full time period, the following rules were applied:

- The observed sex ratio was used in years for which this was available.
- For years for which there was no sex-ratio information:
  1. 1900-1930 period – the average of available sex ratio data from 1918-1930 was used for the missing years (=55.71% male). Note that when calculating the average, the ratio total males/total whales over the 1900-1930 period was used.
  2. 1939-1945 period – the average sex ratio reported for the five years before and five years after this period was used (=53.14% male).
  3. 1968+ period: for years with no sex ratio data, the average of the 1955-1967 period was used (=58.67%).

The final sex-disaggregated catch series for C1 is reported in Table A3.1.3.

#### *C3 Catches*

As with C1, for certain periods the catches have been either totally or partially sexed. In order to produce a sex-disaggregated catch series for the full time period, the following rules were applied:

- The observed sex ratio was used in years for which this was available.
- For years for which there was no sex-ratio information:
  1. For pre-1940 - the 1937 sex ratio was used (61.65% male).
  2. For 1951+, the average (over the 1951+ period) was used for the years for which sex ratio information was not available (62.5% male).

The final sex-disaggregated catch series for C3 is reported in Table A3.1.4.

#### Catches South of 40°S

These catches are from 10° – 60°E, with no differentiation between C1 and C3. All but three years (1957-1959) have sex ratio information. For these three years, the average of the 1948-1967 period (42.5%) was used. Table A3.1.5 reports the final sex-disaggregated catch series for catches south of 40°S.

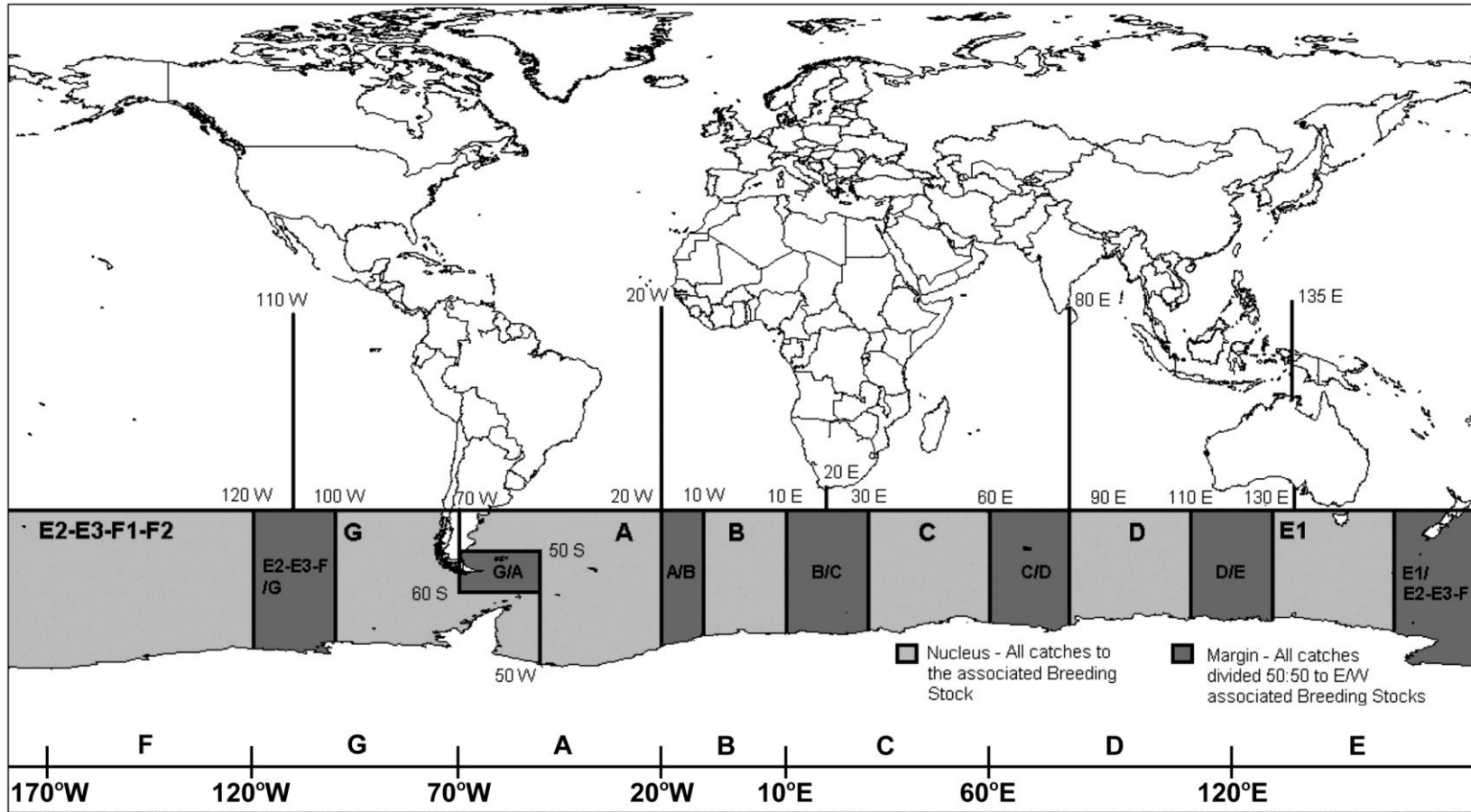


**Figure A3.1.1:** Nucleus and Margin regions associated with each of the seven breeding stocks according to Hypothesis 1 (map adapted from IWC, 2010). The Antarctic longitudinal bands given in Table 3.1 are indicated.

**Table A3.1.1:** Historic catch series for all stocks for the breeding areas north of 40°S (C. Allison, *pers. comm.*).

Year	A	B	C1	C3	D	E	F	G
1900	0	0	0	0	0	8	0	0
1901	0	0	0	0	0	8	0	0
1902	0	0	0	0	0	8	0	0
1903	0	0	0	0	0	8	0	0
1904	0	0	0	0	0	8	0	0
1905	0	0	0	0	0	8	0	0
1906	0	0	0	0	0	8	0	0
1907	0	0	0	0	0	8	0	0
1908	0	0	104	0	0	8	0	16
1909	0	576	149	0	0	16	0	44
1910	0	962	632	0	0	77	0	62
1911	102	2603	1580	0	0	77	0	92
1912	342	4692	2313	25	234	224	0	86
1913	352	5962	1805	0	993	440	0	45
1914	317	2873	830	0	1968	93	0	195
1915	82	169	334	0	1297	106	0	30
1916	68	70	94	0	388	82	0	15
1917	62	10	7	0	0	94	0	15
1918	62	10	9	0	0	90	0	23
1919	29	17	91	0	0	119	0	24
1920	0	40	148	0	0	107	0	21
1921	0	0	251	0	0	89	0	21
1922	0	626	285	0	155	57	0	19
1923	0	899	183	0	166	79	0	16
1924	0	662	187	0	0	107	0	34
1925	0	842	372	0	669	96	0	248
1926	0	442	124	0	735	78	0	277
1927	0	47	86	0	996	127	0	40
1928	0	68	62	0	1035	105	0	36
1929	0	50	99	0	0	102	0	26
1930	0	614	134	0	0	78	0	33
1931	0	0	72	0	0	109	0	53
1932	0	0	307	0	0	18	0	21
1933	0	0	162	0	0	44	0	11
1934	0	723	514	0	0	52	0	13
1935	0	1238	418	0	0	57	0	31
1936	0	869	300	0	3076	69	0	18
1937	0	327	242	1223	3250	55	0	28
1938	0	0	177	1752	917	75	0	6
1939	0	0	200	1240	0	80	0	7
1940	0	0	176	0	0	107	0	0
1941	0	0	79	0	0	86	0	0
1942	0	0	156	0	0	71	0	0
1943	0	0	80	0	0	90	0	0
1944	0	0	115	0	0	88	0	0
1945	0	0	116	0	0	107	0	0
1946	0	0	93	0	0	110	0	15
1947	11	5	89	0	2	101	0	19
1948	23	14	182	0	4	92	0	5
1949	17	1371	190	1333	190	144	0	6
1950	26	1411	151	714	388	79	0	5
1951	28	1114	103	0	1224	111	0	26
1952	9	280	111	0	1187	721	0	27
1953	8	9	89	0	1300	809	0	29

1954	18	0	28	0	1320	898	0	106
1955	9	0	49	0	1126	832	0	7
1956	17	0	36	0	1119	1013	0	10
1957	3	3	34	0	1120	1025	16	5
1958	5	2	39	0	967	1023	16	0
1959	8	168	38	0	700	1278	16	3
1960	13	4	36	0	545	1341	16	2
1961	13	23	36	0	580	981	16	3
1962	11	15	38	1	548.2	209	0	4
1963	12	9	39.6	1.6	87	9	0	1
1964	0	1	4	4	2	0	0	35
1965	0	1	4.5	4.5	75.8	2.5	0	143
1966	0	9	119	119	30	0	0	58
1967	189	3	33.5	33.5	12	0	0	0
1968	0	0	0	0	0	0	0	3
1969	0	0	0	0	0	0	0	1
1970	0	0	0	0	0	0	0	0
1971	0	0	0	0	0	0	0	0
1972	0	0	0	0	0	0	0	0
1973	0	0	1	0	0	0	3	0
1974	0	0	0	0	0	0	4	0
1975	0	0	0	0	0	0	8	0
1976	0	0	0	0	0	0	4	0
1977	0	0	0	0	0	0	4	0
1978	0	0	0	0	0	0	11	0
1979- 2009	0	0	0	0	0	0	0	0

**Table A3.1.2:** Historic catch series for all stocks for the feeding areas, south of 40°S (C. Allison, *pers. comm.*). The columns with grey shading are those corresponding to catches taken in the nucleus regions; the columns in white show the catches taken in marginal regions. Note that the assumptions underlying the distribution of catches between stocks can result in non-integer values.

Year	A	A/B	B	B/C	C	C/D	D	D/E	E	E/F	F	F/G	G	G/A
1900	0	0	0	0	0	0	0	0	0	0	0	0	0	0
1901	0	0	0	0	0	0	0	0	0	0	0	0	0	0
1902	0	0	0	0	0	0	0	0	0	0	0	0	0	0
1903	0	0	0	0	0	0	0	0	0	0	0	0	1	0
1904	180	0	0	0	0	0	0	0	0	0	0	0	0	0
1905	288	0	0	0	0	0	0	0	0	0	0	0	23	0
1906	240	0	0	0	0	0	0	0	0	0	0	0	498	0
1907	1261	0	0	0	0	0	0	0	0	0	0	0	366	0
1908	1849	0	0	0	0	217	0	0	0	0	0	0	1246	9
1909	3391	0	0	0	0	118	0	0	0	0	0	0	1481	94
1910	6468	0	0	0	0	83	0	0	0	0	0	0	2527	70
1911	5730	0	0	0	0	0	0	0	0	0	0	0	2039	17
1912	2539	0	0	0	0	0	0	0	0	0	0	0	976	8
1913	647	0	0	0	0	0	0	0	0	0	0	0	1038	7
1914	838	0	0	0	0	0	0	0	0	0	0	0	656	12
1915	1615	0	0	0	0	0	0	0	0	0	0	0	219	0
1916	379	0	0	0	0	0	0	0	0	0	0	0	21	0
1917	59	0	0	0	0	0	0	0	0	0	0	0	69	0
1918	67	0	0	0	0	0	0	0	0	0	0	0	81	0
1919	82	0	0	0	0	0	0	0	0	0	0	0	181	0
1920	102	0	0	0	0	0	0	0	0	0	0	0	149	0
1921	9	0	0	0	0	0	0	0	0	0	0	0	0	0

Chapter 3 – Background information for the Southern Hemisphere humpback whales

1922	364	0	0	0	0	0	0	0	0	0	0	0	189	0
1923	133	0	0	0	0	0	0	0	0	0	0	0	96	0
1924	266	0	0	0	0	0	0	0	0	0	0	0	102	0
1925	254	0	0	0	0	0	0	0	0	0	0	0	163	0
1926	7	0	0	0	0	0	0	0	0	82	0	0	0	0
1927	0	0	0	0	0	0	0	0	0	16	0	0	0	2
1928	18	0	0	0	0	11	0	0	0	17	0	0	0	0
1929	50	9	8	4	0	11	0	0	0	775	0	0	0	0
1930	107	26	37	111	38	4	23	1	81	58	96	0	0	0
1931	18	1	2	0	2	109	52	0	0	0	0	0	0	0
1932	23	2	16	9	28	3	79	0	0	0	0	0	0	0
1933	132	38	47	9	45	101	500	0	0	0	0	0	0	0
1934	57	14	24	265	277	92	1252	0	0	0	0	0	0	0
1935	48	201	99	1518	351	1	940	0	4	0	0	0	0	0
1936	105	88	162	2390	293	15	1420	0	0	0	0	0	1	0
1937	242	65	123	498	281	57	650	161	0	0	0	0	0	0
1938	0	0	0	0	0	0	655	204	24	0	0	0	0	0
1939	2	0	0	4	0	0	0	0	0	0	0	0	0	0
1940	36	111	131	0	0	0	0	342	1026	684	342	0	1	0
1941	13	0	0	0	0	0	0	0	0	0	0	0	0	0
1942	0	0	0	0	0	0	0	0	0	0	0	0	0	0
1943	4	0	0	0	0	0	0	0	0	0	0	0	0	0
1944	60	0	0	0	0	0	0	0	0	0	0	0	0	0
1945	238	0	0	0	0	0	0	0	0	0	0	0	0	0
1946	30	1	0	0	0	0	0	0	0	0	0	0	0	0
1947	24	1	0	0	0	1	0	0	0	0	0	0	0	0
1948	25.3	38.1	45.4	33.2	1	0	0	0	0	0	0	0	0	0
1949	66	257.5	207.8	350.7	44	0	665	119	908	0	0	0	0	0
1950	672.6	27.9	201	69.9	3	5	1110	0	0	85	403	0	271.8	0
1951	17.6	114.9	313	209.6	1	104	626	402	1	169	227	0	0	0
1952	24.6	33.4	168.1	193.9	14	3	190	0	0	382	148	0	0	0
1953	132.2	31.2	69.8	51.7	14	0	259	0	0	0	150	0	0	0
1954	25.1	52.1	265.4	42.3	7	0	26	0	751	22	507	0	0	0
1955	87.3	83.2	60.2	22.4	6	111	546	919	1962	0	334	0	14	0
1956	150.2	65.2	30.5	0	3	0	0	0	0	0	10	66	626.2	2.8
1957	57.5	32.4	28	55.3	11	70.3	1828	12	87	133	167	31	59	0
1958	10.9	6.5	80.6	55.3	63.6	297.3	2106	2158	447.5	735.2	0	0	0	52.4
1959	7.7	7.7	53	130	21.8	11.6	205.7	85.8	8774	3227	757	81.1	19	0
1960	14.2	4	113.2	27	44.2	51.6	427.3	242.3	2090	6334	3498	0	81	5.8
1961	0	0	18	25	3	2	241	134	511	923	2401	98	1166	1
1962	12.6	4	10	19	55	120	1474	176.4	93.3	311.4	294.9	42.5	255.1	49.4
1963	0	0	2	0	38.8	79.2	256.2	23.7	45.7	238	0	0	0	0
1964	0	0	0	0	48	16	55.8	17.9	40.3	45	0	0	0	0
1965	52	34	880	64	11	6.5	76.4	17.6	82.8	177.1	562.2	0	0	0
1966	0	0	147	137	59	6	90	33	8	25	253	0	0	0
1967	0	6	359	35	31	11	66	12	12	14	111	0	0	0
1968	0	0	0	0	0	0	0	0	0	0	0	0	0	0
1969	0	0	0	0	0	0	0	0	0	0	0	0	0	0
1970	0	0	0	0	0	0	0	0	0	0	0	0	0	0
1971	0	0	0	0	0	0	0	0	0	0	0	3	0	0
1972	2	0	1	0	0	0	0	0	0	2	0	0	0	0
1973-2009	0	0	0	0	0	0	0	0	0	0	0	0	0	0

**Table A3.1.3:** Sex disaggregated catches for breeding sub-stock C1 for catches taken north of 40°S.

Year	Total C1 annual catches	Total C1 whales sexed	C1 male values	% male catches	C1 female catches	Year	Total C1 annual catches	Total C1 animals sexed	C1 male values	% male catches	C1 female catches	Year	Total C1 annual catches	Total C1 animals sexed	C1 male values	% male catches	C1 male catches	C1 female catches
1900	0	0	55.71	0	0	1927	86	86	52.33	45	41	1954	28	27	48.15	13	15	
1901	0	0	55.71	0	0	1928	62	62	41.94	26	36	1955	49	49	63.27	31	18	
1902	0	0	55.71	0	0	1929	99	50	56.00	55	44	1956	36	36	50.00	18	18	
1903	0	0	55.71	0	0	1930	134	131	56.49	76	58	1957	34	34	67.65	23	11	
1904	0	0	55.71	0	0	1931	72	72	47.22	34	38	1958	39	39	64.10	25	14	
1905	0	0	55.71	0	0	1932	307	307	55.70	171	136	1959	38	38	55.26	21	17	
1906	0	0	55.71	0	0	1933	162	162	51.23	83	79	1960	36	36	50.00	18	18	
1907	0	0	55.71	0	0	1934	514	514	53.31	274	240	1961	48	44	55.68	27	21	
1908	104	0	55.71	58	46	1935	418	417	50.60	212	206	1962	39	37	50.00	20	20	
1909	149	0	55.71	83	66	1936	300	300	50.33	151	149	1963	38.5	37.5	62.67	24	14	
1910	632	0	55.71	352	280	1937	242	242	52.07	126	116	1964	6.5	3.5	28.57	2	5	
1911	1580	0	55.71	880	700	1938	177	177	50.28	89	88	1965	4.5	2.5	60.00	3	2	
1912	2313	0	55.71	1289	1024	1939	200	0	53.14	106	94	1966	31	31	54.84	17	14	
1913	1805	0	55.71	1006	799	1940	176	0	53.14	94	82	1967	41	33	75.76	31	10	
1914	830	0	55.71	462	368	1941	79	0	53.14	42	37	1968	0	0	58.67	0	0	
1915	334	0	55.71	186	148	1942	156	0	53.14	83	73	1969	0	0	58.67	0	0	
1916	94	0	55.71	52	42	1943	80	0	53.14	43	37	1970	0	0	58.67	0	0	
1917	7	0	55.71	4	3	1944	115	0	53.14	61	54	1971	0	0	58.67	0	0	
1918	9	2	100.00	9	0	1945	116	0	53.14	62	54	1972	0	0	58.67	0	0	
1919	91	0	55.71	51	40	1946	93	93	61.29	57	36	1973	1	1	100.00	1	0	
1920	148	50	50.00	74	74	1947	89	89	57.30	51	38	1974	0	0	58.67	0	0	
1921	251	0	55.71	140	111	1948	182	182	57.69	105	77	1975	0	0	58.67	0	0	
1922	285	285	62.46	178	107	1949	190	190	62.11	118	72	1976	0	0	58.67	0	0	
1923	183	109	48.62	89	94	1950	151	151	46.36	70	81	1977	0	0	58.67	0	0	
1924	187	187	57.22	107	80	1951	103	103	53.40	55	48	1978	0	0	58.67	0	0	
1925	372	167	59.28	221	151	1952	111	111	51.35	57	54	1979	0	0	58.67	0	0	
1926	124	124	49.19	61	63	1953	89	89	49.44	44	45							

**Table A3.1.4:** Sex disaggregated catches for breeding sub-stock C3 for catches taken north of 40°S.

Year	Total C3 annual catches	Total animals sexed	C3 % male	C3 male catches	C3 female catches	Year	Total C3 annual catches	Total animals sexed	C3 % male	C3 male catches	C3 female catches	Year	Total C3 annual catches	Total animals sexed	C3 % male	C3 male catches	C3 female catches
1900	0	0	61.65	0	0	1927	0	0	61.65	0	0	1954	0	0	62.50	0	0
1901	0	0	61.65	0	0	1928	0	0	61.65	0	0	1955	0	0	62.50	0	0
1902	0	0	61.65	0	0	1929	0	0	61.65	0	0	1956	0	0	62.50	0	0
1903	0	0	61.65	0	0	1930	0	0	61.65	0	0	1957	0	0	62.50	0	0
1904	0	0	61.65	0	0	1931	0	0	61.65	0	0	1958	0	0	62.50	0	0
1905	0	0	61.65	0	0	1932	0	0	61.65	0	0	1959	0	0	62.50	0	0
1906	0	0	61.65	0	0	1933	0	0	61.65	0	0	1960	0	0	62.50	0	0
1907	0	0	61.65	0	0	1934	0	0	61.65	0	0	1961	12	8	56.25	7	5
1908	0	0	61.65	0	0	1935	0	0	61.65	0	0	1962	2	1	50.00	1	1
1909	0	0	61.65	0	0	1936	0	0	61.65	0	0	1963	1	1	100.00	1	0
1910	0	0	61.65	0	0	1937	1223	1223	61.65	754	469	1964	7	4	28.57	2	5
1911	0	0	61.65	0	0	1938	1752	0	61.65	1080	672	1965	4	3	60.00	2	1
1912	25	0	61.65	15	10	1939	1240	0	61.65	764	476	1966	31	31	54.84	17	14
1913	0	0	61.65	0	0	1940	0	0	61.65	0	0	1967	41	33	75.76	31	10
1914	0	0	61.65	0	0	1941	0	0	61.65	0	0	1968	0	0	62.50	0	0
1915	0	0	61.65	0	0	1942	0	0	61.65	0	0	1969	0	0	62.50	0	0
1916	0	0	61.65	0	0	1943	0	0	61.65	0	0	1970	0	0	62.50	0	0
1917	0	0	61.65	0	0	1944	0	0	61.65	0	0	1971	0	0	62.50	0	0
1918	0	0	61.65	0	0	1945	0	0	61.65	0	0	1972	0	0	62.50	0	0
1919	0	0	61.65	0	0	1946	0	0	61.65	0	0	1973	0	0	62.50	0	0
1920	0	0	61.65	0	0	1947	0	0	61.65	0	0	1974	0	0	62.50	0	0
1921	0	0	61.65	0	0	1948	0	0	61.65	0	0	1975	0	0	62.50	0	0
1922	0	0	61.65	0	0	1949	1333	1333	61.37	818	515	1976	0	0	62.50	0	0
1923	0	0	61.65	0	0	1950	714	707	34.37	245	469	1977	0	0	62.50	0	0
1924	0	0	61.65	0	0	1951	0	0	62.50	0	0	1978	0	0	62.50	0	0
1925	0	0	61.65	0	0	1952	0	0	62.50	0	0	1979	0	0	62.50	0	0
1926	0	0	61.65	0	0	1953	0	0	62.50	0	0						

**Table A3.1.5:** Breeding Stock C sex disaggregated catches for south of 40°S.

Year	South annual catches	Total animals sexed	% male	South male catches	South female catches	Year	South annual catches	Total animals sexed	% male	South male catches	South female catches	Year	South annual catches	Total animals sexed	% male	South male catches	South female catches
1900	0	0		0	0	1927	0	0	0.00	0	0	1954	50	29	31.03	16	34
1901	0	0		0	0	1928	0	0	0.00	0	0	1955	28	14	35.71	10	18
1902	0	0		0	0	1929	4	3	66.67	3	1	1956	4	3	33.33	1	3
1903	0	0		0	0	1930	150	113	45.13	68	82	1957	66	0	42.50	28	38
1904	0	0		0	0	1931	2	2	100.00	2	0	1958	120	0	42.50	51	69
1905	0	0		0	0	1932	38	37	45.95	17	21	1959	152	0	42.50	65	87
1906	0	0		0	0	1933	54	54	62.96	34	20	1960	72	46	39.13	28	44
1907	0	0		0	0	1934	554	541	47.69	264	290	1961	28	28	53.57	15	13
1908	0	0		0	0	1935	1870	1868	45.77	856	1014	1962	74	74	41.89	31	43
1909	0	0		0	0	1936	2684	2683	51.99	1396	1288	1963	40	28	42.86	17	23
1910	0	0		0	0	1937	780	774	43.93	343	437	1964	48	48	29.17	14	34
1911	0	0		0	0	1938	0	0	0.00	0	0	1965	76	74	60.81	46	30
1912	0	0		0	0	1939	4	4	25.00	1	3	1966	196	195	48.72	95	101
1913	0	0		0	0	1940	0	0	0.00	0	0	1967	66	66	39.39	26	40
1914	0	0		0	0	1941	0	0	0.00	0	0	1968	0	0	0.00	0	0
1915	0	0		0	0	1942	0	0	0.00	0	0	1969	0	0	0.00	0	0
1916	0	0		0	0	1943	0	0	0.00	0	0	1970	0	0	0.00	0	0
1917	0	0		0	0	1944	0	0	0.00	0	0	1971	0	0	0.00	0	0
1918	0	0		0	0	1945	0	0	0.00	0	0	1972	0	0	0.00	0	0
1919	0	0		0	0	1946	0	0	0.00	0	0	1973	0	0	0.00	0	0
1920	0	0		0	0	1947	0	0	0.00	0	0	1974	0	0	0.00	0	0
1921	0	0		0	0	1948	34	7	14.29	5	29	1975	0	0	0.00	0	0
1922	0	0		0	0	1949	396	195	38.97	154	242	1976	0	0	0.00	0	0
1923	0	0		0	0	1950	74	20	45.00	33	41	1977	0	0	0.00	0	0
1924	0	0		0	0	1951	212	14	28.57	61	151	1978	0	0	0.00	0	0
1925	0	0		0	0	1952	208	14	35.71	74	134	1979	0	0	0.00	0	0
1926	0	0		0	0	1953	66	18	27.78	18	48	1980	0	0	0.00	0	0

## Appendix 3.2

### Abundance and trend data for Southern Hemisphere humpback whales

The data currently available for the various breeding populations of Southern Hemisphere (SH) humpback whales are reported here.

There are three basic forms of data on abundance and possibly also trend.

1. Absolute abundance estimates
2. Relative abundance estimates
3. Capture-recapture data

The minimum number of haplotypes for each population is also given. These numbers are used as an indication of what the minimum size of the populations may have been. Their values multiplied by four give the actual estimates of the minimum population size (see Section 3.2.3) and can be incorporated into the population models as lower bounds.

#### A3.2.1 Breeding Stock A

##### Absolute abundance estimates

**Table A3.2.1:** Abundance estimate from a fixed-wing aircraft survey off Brazil (Andriolo *et al.*, 2006).

Year	N	CV
2005	6251	0.17

##### Relative abundance estimates

**Table A3.2.2:** Breeding ground index of abundance from aerial line transect surveys conducted off the north-eastern coast of Brazil (5-12°S) from 2002-2004 (Andriolo *et al.*, 2006). These estimates of abundance were obtained using comparable methodology, but covered only a portion of the range of the stock (12-21°S) and are therefore used as an index of relative abundance (Zerbini *et al.*, in press).

Year	N	CV
2002	2305	0.20
2003	2539	0.19
200	3615	0.19

**Table A3.2.3:** Feeding ground abundance index: IDCR/SOWER<sup>20</sup> estimates from Branch (in press).

Year	N	CV
1981	45	0.88
1986	259	0.62
1997	200	0.64

<sup>20</sup> Southern Ocean Whale and Ecosystem Research.

Minimum number of haplotypes62 (Rosenbaum *et al.*, 2006b)**A3.2.2 Breeding Stock B**Absolute abundance estimates

**Table A3.2.4:** The estimates given below are for the year 2003 and result from the MARK program when fitted to the photo-ID capture-recapture data from Iguela only (lower estimate of 6342 in 2003) and the genetic data from Iguela only (upper estimate of 7196 in 2003) (Collins *et al.*, 2008).

lower	6432	CV	0.18
upper	7196	CV	0.15

Relative abundance estimates

**Table A3.2.5:** IDCR/SOWER estimates for the feeding grounds south of 60°S over 20°W-10°E (Branch, in press).

Year	N	CV
1980	692	0.84
1986	70	0.63
1995	595	0.51

Capture-recapture

Photographs and biopsies were collected from the coastal waters of Gabon during the austral winter (July-October) in each year between 2001 and 2006. Data analysed were from two field sites: Iguela (1°51'S, 9°20'E) and Mayumba (3°22'S, 10°38'E) (Collins *et al.*, 2008).

**Table A3.2.6:** Photo-ID (total sample from all sites) [ $n$  = number of different individuals sighted each year,  $m$  = total recaptures between pairs of years].

$n$	2000	2001	2002	2003	2004	2005	2006
	24	111	233	161	138	216	199

$m$	2000	2001	2002	2003	2004	2005	2006
2000	X	0	1	0	0	0	0
2001		X	5	6	5	2	1
2002			X	12	2	2	4
2003				X	7	2	1
2004					X	2	2
2005						X	6
2006							X

**Table A3.2.7:** Photo-ID (Iguela only) [ $n$  = number of different individuals sighted each year,  $m$  = total recaptures between pairs of years].

$n$	2001	2002	2003	2004	2005
	111	143	161	138	123

$m$	2001	2002	2003	2004	2005
2001	X	4	6	5	1
2002		X	6	6	1
2003			X	7	1
2004				X	0
2005					X

**Table A3.2.8:** Genotypes (total samples from all sites) (secondary data) [ $n$  = number of different individuals sighted each year,  $m$  = total recaptures between pairs of years].

$n$	2000	2001	2002	2003	2004	2005	2006
	82	155	257	270	188	296	207

$m$	2000	2001	2002	2003	2004	2005	2006
2000	X	1	1	4	2	3	0
2001		X	6	8	6	3	2
2002			X	6	6	6	4
2003				X	8	7	1
2004					X	3	3
2005						X	11
2006							X

**Table A3.2.9:** Genotypes (Iguela only) (secondary data) [ $n$  = number of different individuals sighted each year,  $m$  = total recaptures between pairs of years].

$n$	2001	2002	2003	2004	2005
	155	170	270	188	137

$m$	2001	2002	2003	2004	2005
2001	X	6	8	6	0
2002		X	4	2	6
2003			X	8	4
2004				X	6
2005					X

**Table A3.2.10:** West South African photo-ID capture-recapture data based on right-dorsal fin features (Barendse *et al.*, 2010).

<i>n</i>	2001	2002	2003	2004	2005	2006
	39	58	14	20	25	27

<i>m</i>	2001	2002	2003	2004	2005	2006
2001	X	7	1	2	0	1
2002		X	0	4	2	2
2003			X	0	0	0
2004				X	1	0
2005					X	0
2006						X

**Table A3.2.11:** WSA photo-ID capture-recapture data based on fluke fin features (J. Barendse, *pers. comm.*).

<i>n</i>	2001	2002	2003	2004	2005	2006
	15	16	10	7	9	16

<i>m</i>	2001	2002	2003	2004	2005	2006
2001	X	3	1	0	0	0
2002		X	0	1	0	1
2003			X	1	0	0
2004				X	0	0
2005					X	1
2006						X

**Table A3.2.12:** WSA genetic capture-recapture data based on microsatellite matches (Barendse *et al.*, 2010).

<i>n</i>	2001	2002	2003	2004	2005	2006
	34	41	20	27	22	22

<i>m</i>	2001	2002	2003	2004	2005	2006
2001	X	9	1	1	1	1
2002		X	1	5	0	1
2003			X	1	1	1
2004				X	1	2
2005					X	1

Minimum number of haplotypes

Total: 147

Gabon (B1): 92

Angola and West South Africa: 55 (Rosenbaum *et al.*, 2006b).

### A3.2.3 Breeding Stock C

#### Absolute abundance estimates

The C1 estimate is from a shipboard line transect survey detailed in Findlay *et al.* (in press). C3 estimates were obtained from the application of MARK to photo-ID and genotypic capture-recapture data collected in Antongil Bay from 2000-2006 (lower estimate 6737, CV=0.31, upper estimate 7715, CV=0.24) (Cerchio *et al.*, 2008a).

**Table A3.2.13:** Absolute abundance data for Breeding Stock C.

	Year	Estimate	CV
C1	2003	5965	0.17
C3	2005	7715	0.24

#### Relative abundance estimates

**Table A3.2.14:** Cape Vidal sightings per unit effort data for the 1988-2002 period (Findlay and Best, 2006). These data are obtained from shore-based surveys of northwards-migrating humpback whales at Cape Vidal, north Kwa-Zulu Natal.

Year	Estimate
1988	358
1989	249
1990	359
1991	587
2002	1673

**Table A3.2.15:** IDCR/SOWER estimates for the breeding grounds (10°E-60°E) (Branch, in press).

Year	N	CV
1979	104	0.62
1987	926	0.50
1993	2391	0.41

#### Capture-recapture

These data are reported in Cerchio *et al.* (2008a and b) except for the addition of C1 data for 2007 provided by K. Findlay (*pers. comm.*). They consist of photo-ID capture-recapture data from Antongil Bay (C3) (Cerchio *et al.*, 2008a), as well as photo-ID capture-recapture data for C1 (Cerchio *et al.*, 2008b). The years 2000 and 2004 for C1 and the year 2002 for C3 are excluded in the assessment due to poor temporal coverage of capture effort.

**Table A3.2.16:** Capture recapture data: Seen in C1 and re-seen in C1 [ $n$  = number of different individuals sighted each year,  $m$  = total recaptures between pairs of years].

$n$	2000	2001	2002	2003	2004	2005	2006	2007
	3	24	49	115	21	134	112	167

$m$	2000	2001	2002	2003	2004	2005	2006	2007
2000	X	0	0	0	0	0	0	0
2001		X	1	0	0	0	0	0
2002			X	1	1	0	0	1
2003				X	0	0	0	1
2004					X	1	0	0
2005						X	2	3
2006							X	1

**Table A3.2.17:** Capture recapture data: Seen in C3 and re-seen in C3. [ $n$  = number of different individuals sighted each year,  $m$  = total recaptures between pairs of years].

$n$	2000	2001	2002	2003	2004	2005	2006
	89	159	16	126	151	144	158

$m$	2000	2001	2002	2003	2004	2005	2006
2000	X	2	1	3	1	0	1
2001		X	1	3	3	3	2
2002			X	3	0	0	0
2003				X	2	1	3
2004					X	4	3
2005						X	4

**Table A3.2.18:** Photographic capture-recapture data between C1 and C3 [ $n$  is number of different individuals sighted each year,  $m$  is total recaptures between pairs of years]. The entries above the diagonal in the matrix reflect animals first seen in C3 and later re-sighted in C1, whereas entries below the diagonal reflect the reverse, animals first seen in C1 and later re-sighted in C3.

$n$	2000	2001	2002	2003	2004	2005	2006
C1	89	159	16	126	151	144	158
C3	3	24	49	115	21	134	112

$m$	2000	2001	2002	2003	2004	2005	2006
2000	X	0	0	0	0	0	0
2001	0	X	0	0	0	0	0
2002	0	0	X	0	0	0	0
2003	0	0	0	X	0	0	0
2004	0	0	0	0	X	0	0
2005	0	0	0	0	0	X	0
2006	0	0	0	1	0	0	X

Minimum number of haplotypes

Total: 188

C1: 62

C2: 38

C3: 88 (Rosenbaum *et al.*, 2006b)C2 and C3: 93 (H. Rosenbaum, *pers. comm.*)**A3.2.4 Breeding Stock D**Absolute abundance estimate

Single platform aerial line transect and land-based surveys yielded an estimated abundance of northward-migrating whales from 2 June to 7 Sep 2008 of 21750 (95% CI: 17550-43000). This value is based on an estimate of abundance of surfaced whales of 11850 (9550-23450) and an estimated  $g(0)$  (the proportion of whales seen on the survey trackline) of 0.54 ( $\pm 0.21$ ). Note the numbers in parenthesis are 95% percentile intervals and do not include variance in the estimate of  $g(0)$  (Hedley *et al.*, 2008).

Relative abundance estimates**Table A3.2.19:** Aerial survey relative abundance estimates (Bannister and Hedley, 2001).

Year	Estimate
1982	10.2
1986	16.2
1988	12.7
1991	23.6
1994	36.0

**Table A3.2.20:** JARPA<sup>21</sup> surveys conducted during 1989/90-2004/05 austral summer seasons (January and February) alternating survey areas between Area IV (70°E-130°E) and Area V (130°E-170°W), all south of 60°S. Areas IV and V were divided into 2 sectors, western and eastern. Each sector was divided into northern (60°S to 45 nm from ice-edge) and southern (from ice-edge to 45 nm away). Breeding Stock D corresponds to Area IV (Matsuoka *et al.*, in press).

Year	Estimate	CV	Year	Estimate	CV
1989	5325	0.302	1997	10657	0.166
1991	5408	0.188	1999	16751	0.143
1993	2747	0.153	2001	31134	0.123
1995	8066	0.142	2003	27783	0.115

**Table A3.2.21:** IDCR/SOWER estimates from Branch (in press) (60°E-120°E).

Year	Estimate	CV
1978	1219	0.46
1988	422	0.52
1997	17959	0.17

**Table A3.2.22:** Catch per unit effort data from four catchers operating on the west coast of Australia from June 25 to August 26 each year (Chittleborough, 1965) (Area IV: 70°E-130°E).

Year	Estimate
1950	0.475
1951	0.424
1952	0.347
1953	0.353
1954	0.351
1955	0.244
1956	0.178
1957	0.146
1958	0.123
1959	0.090
1960	0.062
1961	0.055
1962	0.051

Minimum number of haplotypes

51 (Rosenbaum *et al.*, 2006b)

<sup>21</sup> Japanese Whale Research Program in the Antarctic.

### A3.2.5 Breeding Stock E

#### Absolute abundance estimate

In 2004 a land-based survey was conducted at Point Lookout on the east coast of Australia over 14 weeks from 25 May to 27 August. The Hermite polynomial method was used to arrive at an absolute abundance estimate of 7090  $\pm$  660 (95% CI) for 2004 (Noad *et al.*, 2006). Observations from two locations were used to estimate proportions missed from a single location.

#### Relative abundance estimates

**Table A3.2.23:** Estimates from land-based surveys conducted at Point Lookout and two other locations. The values give the number of whales passing per 10h during four weeks of the peak migration. (Values provided by M. Noad (*pers. comm.*) and are as used for the assessment in Noad *et al.*, 2008).

Year	Estimate	Year	Estimate
1984	6.12	1994	17.75
1985	5.92	1996	20.91
1986	8.25	1998	28.45
1987	8.53	1999	27.45
1988	9.15	2001	34.67
1989	10.22	2002	37.34
1990	11.58	2004	47.11
1991	12.93	2007	70.73
1992	14.36		

**Table A3.2.24:** Catch per unit effort data from two catchers operating on the east coast of Australia from June 10 to August 5 each year (Chittleborough, 1965) (Area V: 130°E-170°W).

Year	Estimate
1953	0.97
1954	0.76
1955	0.78
1956	0.70
1957	0.71
1958	0.75
1959	0.74
1960	0.52
1961	0.23
1962	0.69

**Table A3.2.25:** JARPA surveys conducted during 1989/90-2004/05 austral summer seasons (January and February) alternating survey areas between Area IV (70°E-130°E) and Area V (130°E-170°W), all south of 60°S. Areas IV and V were divided into two sectors, western and eastern. Each sector was divided into northern (60°S to 45 n. miles from ice-edge) and southern (from ice-edge to 45 n. miles away). Breeding Stock E corresponds to Area V (Matsuoka *et al.*, in press).

Year	Estimate	CV
1990	602	0.343
1992	4388	0.623
1994	3678	0.307
1996	1474	0.274
1998	3831	0.430
2000	5128	0.215
2002	2873	0.157
2004	9342	0.337

**Table A3.2.26:** IDCR/SOWER estimates for the breeding grounds (Branch, in press). Breeding Stock E estimates here correspond to south of 60°S and between 120°E-170°W.

Year	N	CV
1980	995	0.58
1985	622	0.50
1992	3484	0.33
2001	13300	0.22

#### Minimum number of haplotypes

Total: 108

E2: 60

E3: 48 (Rosenbaum *et al.*, 2006b)

E1: 42 (Olavarría *et al.*, 2006)

### **A3.2.6 Breeding Stock F**

#### Absolute abundance estimate

**Table A3.2.27:** The estimate arises from a sighting-resighting analysis of individual identification photos collected from 1999 to 2004. Survey areas were New Caledonia and Tonga (E2 and E3), the Cook Islands and French Polynesia (F) (Baker *et al.*, 2006).

Year	N	CV
2002	3827	0.12

#### Relative abundance estimates

**Table A3.2.28:** IDCR/SOWER estimates are given for the breeding grounds (Branch, in press), in which F corresponds to the area south of 60°S and between 170°W-110°W, according to the assumptions of the naïve catch allocation model (IWC, 1998).

Year	N	CV
1983	3240	0.47
1990	2976	0.51
1997	3852	0.22

Minimum number of haplotypes

Total: 230

F1: 131

F2: 99 (Rosenbaum *et al.*, 2006b)

---

**A3.2.7 Breeding Stock G**

Absolute abundance estimate

**Table A3.2.29:** Breeding ground estimate is from a photographic capture-recapture study in Ecuador, and is based on Chapman modified-Peterson estimator (Felix *et al.*, in press).

Year	N	CV
2006	6504	0.21

Relative abundance estimates

**Table A3.2.30:** IDCR/SOWER estimates for the breeding grounds (Branch, in press). The area for G is 110°W-50°W, south of 60°S.

Year	N	CV
1982	1452	0.65
1989	2817	0.38
1996	3310	0.21

Minimum number of haplotypes

148 (Rosenbaum *et al.*, 2006b)

### Appendix 3.3

#### Bayesian framework for estimating values for the intrinsic growth rate $r$ and pristine population level $K$ in Southern Hemisphere humpback whale assessments

##### A3.3.1 The $r$ - $K$ dependence

Suppose a target current abundance estimate is given for a population, and an intrinsic growth rate  $r$  and pristine population level  $K$  are to be estimated so that the resulting population trajectory hits the abundance estimate.

Figure A3.3.1 (a) shows two population trajectories, one with a low  $r$  value of 0.02 and one with a high  $r$  value of 0.08. Both trajectories hit the 2010 target abundance estimate of 6000, but have very different estimated  $K$  values. A population with a low intrinsic growth rate (such as  $r=0.02$ ) has a much slower recovery rate, implying that its pristine population level must have been high to be able to yield the catches taken and still recover to a size of 6000 by 2010. A population with a faster recovery rate (such as a population with  $r=0.08$ ) can start initially at a lower pre-exploitation (pristine) size and still yield the reported catches and recover sufficiently by 2010. Figure A3.3.1 (a) illustrates this inverse relationship between the two parameters

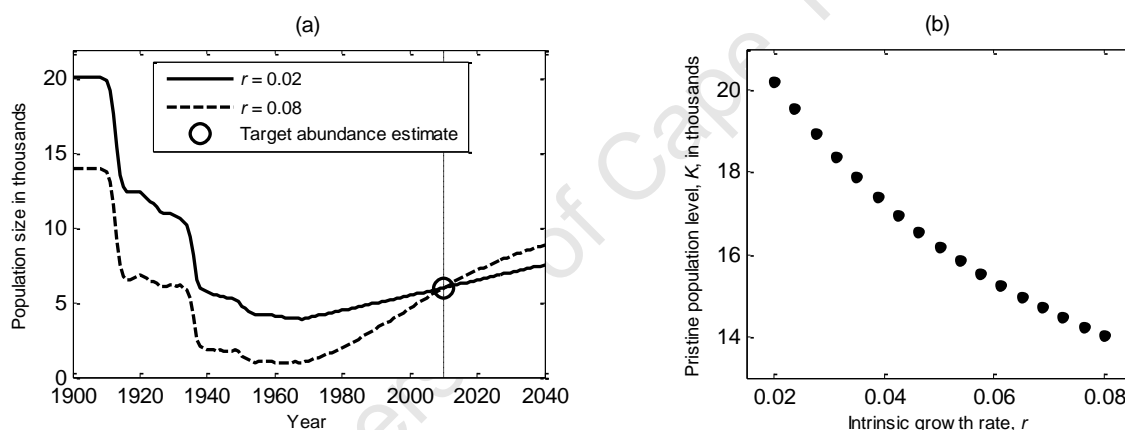


**Figure A3.3.1 (a) and (b):** An illustration of the  $r$ - $K$  dependence: (a) shows two population trajectories where  $r$  has been set on input and  $K$  estimated so that the resulting population trajectory hits the abundance estimate of 6000, whereas (b) shows a series of  $r$  values and the corresponding estimated  $K$  values, illustrating the inverse relationship between the two parameters.

##### A3.3.2 Problems associated with the ‘Forwards’ method

The figures above show that the intrinsic growth rate  $r$  contains inherent information about the pristine population level  $K$  and *vice versa*. If the  $r$  and  $K$  values are drawn directly from their respective prior distributions (i.e. the ‘Forwards’ method), the parameters themselves (in addition to their prior distributions and the data) now bring information to the posterior distribution. This additional information complicates the SIR process, and consequently the ‘Backwards’ method is generally preferred in humpback assessments.

Further, Butterworth and Punt (1997) argue that the ‘Forwards’ and ‘Backwards’ methods will yield different results when applied to the same prior for initial population size,  $K$ . They show that given a uniform prior on a current abundance estimate, the value of the intrinsic growth rate  $r$  determines how large the range of estimated  $K$

values is that are obtained through the ‘Backwards’ method. The following illustration is adapted from the one given in Butterworth and Punt (1997).

Suppose a population is assumed to follow the Pella Tomlinson model as described in Appendix 2.1, with  $\mu$  set to 2.39 as per standard practice in humpback assessments. Suppose also that the only information, apart from historical catches, is a year 2000 abundance estimate,  $N_{2000}^{obs} = 6000$ . Consider two values of MSYR: 1.5% and 6% (corresponding to intrinsic growth rates of roughly 0.02 and 0.08 respectively<sup>22</sup>).

*Backwards method:*

- i)  $N$  values of  $N_{2000}^{obs}$  are drawn from a uniform prior distribution  $U[4000, 8000]$  and for each, a value for  $K$  is found such that the population trajectory matches the drawn value of  $N_{2000}^{obs}$ . This procedure is followed for both an MSYR of 1.5% and 6%.
- ii) The estimated  $K$  values for MSYR=1.5% fall within the range  $A$  (see Figure A3.3.2), and  $B$  indicates the range of  $K$  values for MSYR=6%. The uniform interval on  $N_{2000}^{obs}$  is marked by  $I$ .
- iii) Since these trajectories are generated from the uniform interval  $I$ , they are all equally likely and receive equal weight from a uniform prior on  $K$ ,  $U[10\ 000, 30\ 000]$ . The MSYR values of 1.5% and 6% are then also equally likely in the posterior distribution for MSYR.

*Forwards method:*

- i)  $N'$  equally likely trajectories are generated with  $K$  from  $U[10\ 000, 30\ 000]$ , for both values of MSYR.
- ii) The proportion of MSYR=1.5% trajectories with an  $N_{2000}$  that falls within the acceptable range  $[4000, 8000]$  will be proportional to  $A$ , whereas the proportion of acceptable trajectories for MSYR=6% will be proportional to  $B$ .
- iii) Since  $A > B$ , more of the 1.5% trajectories will be accepted. Thus the post-model pre-data distribution for MSYR gives a greater weight to MSYR=1.5% than to MSYR=6%.

Therefore, given an uniform prior on  $K$ , the Backwards and Forwards methods must yield different results.

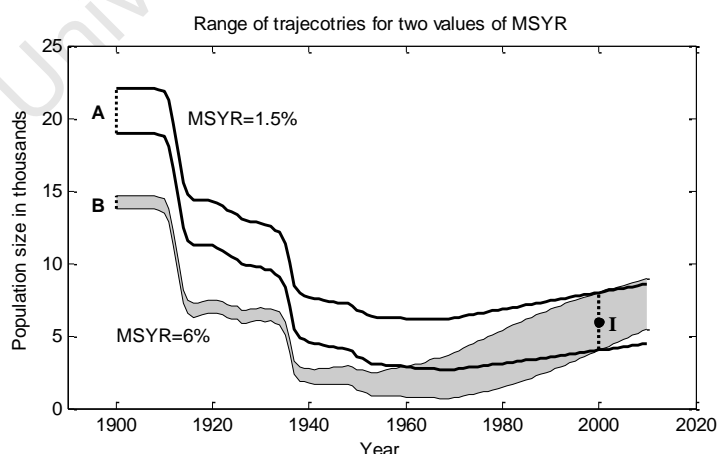


**Figure A3.3.2:** The upper and lower limits of the range of estimated trajectories for each value of MSYR are shown here.  $A$  and  $B$  (for MSYR=1.5% and MSYR=6% respectively) indicate the range of estimated  $K$  values generated from the uniform interval  $I$  on  $N_{2000}^{obs}$ . The 2000 abundance estimate of 6000 is shown by the black dot.

<sup>22</sup> The value of  $\mu=2.39$  sets  $MSYR=0.71r$  (see Appendix 2.1).

## 4 The incorporation of length data into an assessment of the Southern Hemisphere humpback whale Breeding Stock C

### 4.1 INTRODUCTION

#### 4.1.1 Background information

The Southern Hemisphere humpback whale Breeding Stock C is found to the east of southern Africa. Originally, it was hypothesised to consist of four sub-stocks, C1-C4 (IWC, 2007):

- C1-S (South) – includes East South Africa and Mozambique as far north as Mozambique Island.
- C1-N (North) – extends northwards from Mozambique Island to the northern limit of the range (southern Tanzania possibly into Kenya).
- C2 – includes Mayotte Island, the Comoros Islands and the Mozambique Channel.
- C3 – around Madagascar.
- C4 – extends across the Mascarene group of islands, including Mauritius and Reunion.

Figure 4.1 provides a map detailing the four sub-stocks and their respective regions. C1-S and C1-N have been combined into a single breeding sub-stock, C1, for assessment purposes (IWC, 2007). Furthermore, genetic analyses show no significant differentiation between C2 and C3 (Rosenbaum *et al.*, 2006b). This, along with the fact that there are no catch records or abundance estimates for C2 (IWC, 2009b), has led to the decision to combine C2 and C3 into one sub-stock, under the name of C3 (IWC, 2007). The hypothesis of a discrete breeding sub-stock C4 was based on relatively scant data, and it has thus also been absorbed into C3 for assessment purposes (IWC, 2007). As such, assessments of Breeding Stock C involve two sub-stocks, namely C1 and C3.

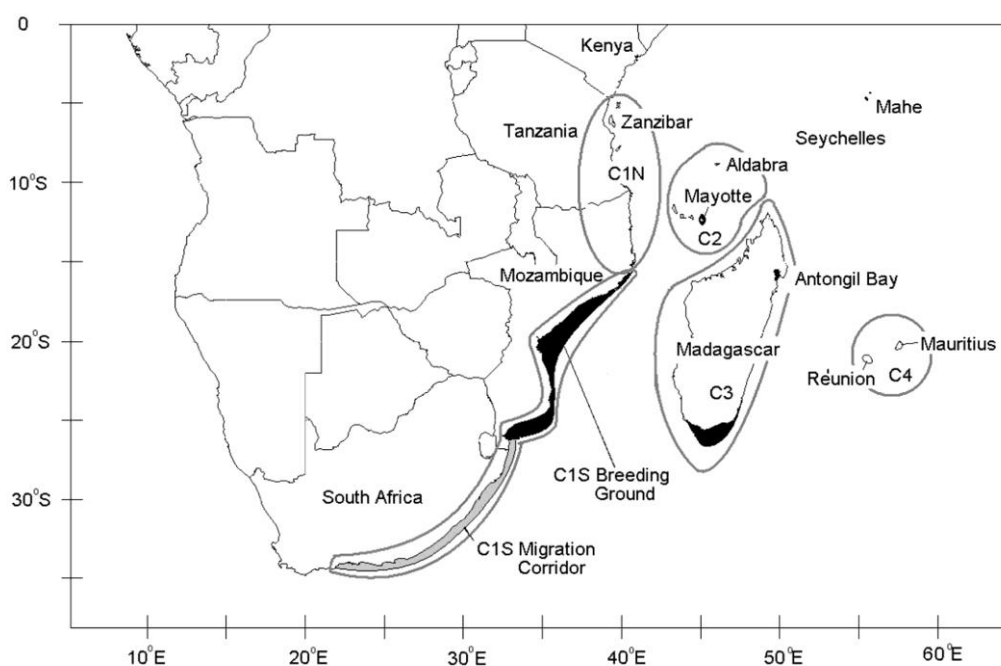


**Figure 4.1:** Sub-stock division of breeding stock C Figure taken from IWC (2008).

#### 4.1.2 The question of interchange between sub-stocks and model selection

While C1 and C3 are treated as independent in terms of breeding, photo-ID matches have shown a link between them: a whale that was seen in C1 in 2003 was seen in C3 three years later (Cerchio *et al.*, 2008a). This observation raised the question as to what extent the animals move between C1 and C3, and hence the need also to allow for movement between the sub-stocks in the assessment models.

As a result, ten interchange hypotheses were proposed and discussed at the MARAM International Stock Assessment Workshop, Cape Town, 2008 (Johnston and Butterworth, 2008b). From these hypotheses, the following four were selected as most realistic (MARAM, 2008; and IWC, 2010).

- (1) The *Resident model*, which assumes no interchange between sub-stocks C1 and C3.
- (2) The *Sabbatical model*, which assumes that in any year there is a particular probability that a whale from sub-stock C1 will travel to the C3 region and *vice versa*. This movement does not affect the whale in the following year, when it is more likely to stay in its home breeding ground. The model thus assumes that an animal will visit only one of these two regions in any one year.
- (3) The *Migrant model* is similar to the Sabbatical model, except that if a whale from C1 moves to C3 (or *vice versa*) then it will join the C3 stock and behave as a C3 animal from then on. It will have the same probability as any C3 whale of migrating back to C1.
- (4) The *Tourist model* is an adaptation of the Resident model where whales from one breeding sub-stock, in addition to returning to their own breeding area each year, have a probability of also visiting the breeding area for the other sub-stock that same year (without joining this other sub-stock).

Appendix 4.1 gives a diagrammatic representation and the details of the Sabbatical model. The availability of photo-ID capture-recapture data<sup>23</sup> allows for the estimation of the interchange rates (IWC, 2010) and assessments, checked by simulation testing, were carried out for the four models (Johnston and Butterworth, 2009). Results relevant to this thesis are given in Appendix 4.1.

These models and their assessment results were presented at two consequent international workshops<sup>24</sup>, and while it was noted that these conceptual models represent extreme examples of movement, with true behaviour likely to fall somewhere in between (IWC, 2009b), the Sabbatical model was chosen as a base case for further assessments<sup>25</sup>.

---

<sup>23</sup> Genotypic capture-recapture data are also available, but the IWC SC recommended that these should not be included until genotyping errors can be taken into account in the modelling process (IWC, 2008).

<sup>24</sup> The Intersessional Meeting on Southern Hemisphere Humpback Whale Assessment Methodology, Seattle, February 2009, and the 61<sup>st</sup> Meeting of the Scientific Committee (SC) of the International Whaling Commission (IWC), Madeira, June 2009.

<sup>25</sup> Since movement between the stocks has been documented, the Resident model cannot serve as a base case as it does not allow for any interchange to take place. However, as there has been only one interchange observed, there is insufficient information to strongly support any one of the remaining hypotheses. The Sabbatical model was chosen as a base case since the other models are essentially adaptations of this model, and because more sensitivity tests had been carried out based on this model than on any of the others (MARAM, 2008).

### 4.1.3 Expansion of the assessment to include catch-at-length data

At an intersessional meeting on Southern Hemisphere humpback whale assessment methodology, held in Seattle in February 2009, a paper (Best and Brandão, 2009) was presented giving an account of historic humpback whaling in Madagascar for the years 1910-1950. This paper illustrated that while catches off Durban and the north C1 region show similar age- and sex-structure, catches off Madagascar show a different pattern. Considering that these catches were taken in the same season on the same expedition, Best and Brandão (2009) suggested that these differences in age and sex between regions indicated that two different populations were being exploited over this period, and also that possibly a heavier exploitation on the C1 stock than the C3 stock had taken place. Figure 4.2 (a) and (b) illustrate these differences.

The meeting proposed four alternative explanations for the data (IWC, 2009b):

- *Explanation 1:* Stocks are at different levels of depletion (implying no/low interchange).
- *Explanation 2:* Animals migrate to different regions based on age (does not imply low interchange) so that stocks tend to be geographically segregated and relative proportions may be different purely as a result of biology rather than exploitation. It was observed that vessel catches that occurred along the African coast were consistent in terms of their length distributions (Figure 4.2 (c) shows the cumulative distributions over the years), and it was suggested that the African mainland catches are thus representative of the C1 population.
- *Explanation 3:* Body sizes of the whales from the two stocks are slightly different, due to either strong differences in natural selection between habitats (which does not imply low interchange) or from selection and/or genetic drift (which does imply low interchange). Under this hypothesis, the difference in body size would not necessarily imply different depletion levels in the two populations.
- *Explanation 4:* Whaling selectivity (with regard to age) occurred differently between regions, although catches in both regions were made by the same vessel.

The meeting suggested that these ideas be explored using a simple age-based model with knife-edge selectivity to test the implications of catch selectivity on the length distributions of whales caught<sup>26</sup>, and to investigate if length distribution differences between the two regions are a reflection of different levels of past exploitation. This exploration was undertaken as part of the work done for this thesis, and the methods and results follow from this point. The assessment is based on the Resident model, which is much simpler than the base-case Sabbatical model. Future work will aim to apply an age-disaggregated model to the Sabbatical scenario.

---

<sup>26</sup> Given the estimated catch-at-age proportions from an age-disaggregated model, these can be converted to catch-at-length estimates (see Section 4.3.2), which can then be compared to the observed catch-at-length frequencies.

## 4.2 DATA

### 4.2.1 Historic catch data

There are two sets of historic catch data that relate to breeding sub-stocks C1 and C3:

- i) Catches north of 40°S
- ii) Catches south of 40°S.

Note that not all the historic catches have been sexed as required for this analysis. Appendix 3.1 outlines the method used to obtain a sex-disaggregated catch series, and Table A3.1.3 through to Table A3.1.5 of this Appendix list these catches.

#### *Catch-at-length data*

Catch-at-length frequency data held by the IWC Secretariat are available for the periods 1936-1937 and 1949-1950 from the following sources:

- i) Whale station at Durban (1936 and 1937)
- ii) Union Whaling Company (*Uniwaleco*) expeditions in 1937 (Africa and Madagascar)
- iii) *Anglo Norse* expeditions in 1949 and 1950.

Catches landed at Durban are assumed to be from breeding sub-stock C1. The 1937 *Uniwaleco* expedition to Madagascar took catches off the African coast, as well as off Madagascar, and the catches have accordingly been allocated to C1 and C3 respectively (Best and Brandão, 2009). The catches taken from the *Anglo Norse* expedition to Madagascar have been allocated to C3.

Plots of these data accumulated over years for Africa (C1) and Madagascar (C3) are shown split by sex in Figure 4.3 (a)-(d). The “stretching<sup>27</sup>” of whales to above the 35 ft minimum size limit which applied during the period for the C3 catches is very evident (see Figure 4.3 (c) and (d)). Figure 4.2 (a) and (b) show a comparison of the observed catch-at-length proportions between the Africa (C1) and Madagascar (C3) catches for both males and females, and immediately indicates the differences between C1 and C3.

### 4.2.2 Abundance and trend data

#### *Absolute abundance data*

The absolute abundance data considered in this analysis are presented in Table A3.2.13 of Appendix 3.2. For sub-stock C1, a line transect survey estimate of 5965 (CV = 0.17) for the 2003 season is available from Findlay *et al.* (in press). C3 estimates for 2005 are provided by MARK when applied to capture-recapture data from Antongil Bay for both photo-ID and genotypic data (lower estimate of 6737, CV=0.31, upper estimate of 7715, CV=0.24) (Cerchio *et al.* 2008a).

---

<sup>27</sup> A minimum length of 35 feet for humpback catches was introduced in June 1937 (effective from the 1938 season) and as such if whales under the legal size limit were caught, they were often recorded as larger animals, i.e. “stretched” (P. Best, *pers. comm.*). Note that the C1 catches are from the Durban (1936-1937) and *Uniwaleco* (1937) records. As the size restriction took effect only in the 1938 season, the C1 catches are not affected by this restriction, unlike the C3 catches, the majority of which were taken by the *Anglo Norse* expedition (1949-1950).

### Trend information

Cape Vidal sightings per unit effort data are for the 1988-2002 period (Findlay and Best, 2006). They are obtained from shore-based surveys of northwards-migrating humpback whales at Cape Vidal, South Africa, each year between 1988 and 1991, and in 2002, and are given in Table A3.2.14 of Appendix 3.2.

### Capture-recapture data

The capture-recapture data used here are as reported in Cerchio *et al.* (2008a and b) except for the addition of C1 data for 2007 provided by K. Findlay (*pers. comm.*). They consist of photo-ID capture-recapture data from Antongil Bay (C3) (Cerchio *et al.*, 2008a), as well as photo-ID capture-recapture data for C1 (Cerchio *et al.*, 2008b). The data span the period 2000-2007 for C1 and 2000-2006 for C3. The years 2000 and 2004 for C1 and the year 2002 for C3 are however excluded in the assessment due to poor temporal coverage of capture effort and low number of samples collected (IWC, 2009a). These data are listed in Table A3.2.16 to Table A3.2.18 of Appendix 3.2.

## 4.3 METHODS

In this assessment the generalized BALEEN II population dynamics model is used as in the HITTER-FITTER package (Punt, 1996).

### 4.3.1 Model Dynamics

BALEEN II is an age- and sex-structured model, and considers animals as being either recruited or unrecruited<sup>28</sup>. It assumes that all whaling takes place at the start of the year, and that all animals are recruited (and have reached the age at first parturition) by the age  $m-1$ . The dynamics of the population are assumed to be governed by the equations:

$$\begin{aligned}
 N_{y+1,a}^{C1,s} &= \begin{cases} 0 & \text{if } a = 0 \\ (N_{y,a-1}^{C1,s} - C_{y,a-1}^{C1,s})S_{y,a-1}^s + U_{y,a-1}^{C1,s}S_{y,a-1}^s\delta_a^s & \text{if } 1 \leq a \leq m-1 \\ (N_{y,m}^{C1,s} - C_{y,m}^{C1,s})S_{y,m}^s + (N_{y,m-1}^{C1,s} - C_{y,m-1}^{C1,s})S_{y,m-1}^s & \text{if } a = m \end{cases} \\
 U_{y+1,a}^{C1,s} &= \begin{cases} 0.5P_{y+1}^{C1,M}f_{y+1}^{C1} & \text{if } a = 0 \\ U_{y,a-1}^{C1,s}S_{y,a-1}^s(1 - \delta_a^s) & \text{if } 1 \leq a \leq m-1 \end{cases} \quad (4.1) \\
 N_{y+1,a}^{C3,s} &= \begin{cases} 0 & \text{if } a = 0 \\ (N_{y,a-1}^{C3,s} - C_{y,a-1}^{C3,s})S_{y,a-1}^s + U_{y,a-1}^{C3,s}S_{y,a-1}^s\delta_a^s & \text{if } 1 \leq a \leq m-1 \\ (N_{y,m}^{C3,s} - C_{y,m}^{C3,s})S_{y,m}^s + (N_{y,m-1}^{C3,s} - C_{y,m-1}^{C3,s})S_{y,m-1}^s & \text{if } a = m \end{cases} \\
 U_{y+1,a}^{C3,s} &= \begin{cases} 0.5P_{y+1}^{C3,M}f_{y+1}^{C3} & \text{if } a = 0 \\ U_{y,a-1}^{C3,s}S_{y,a-1}^s(1 - \delta_a^s) & \text{if } 1 \leq a \leq m-1 \end{cases}
 \end{aligned}$$

<sup>28</sup> A recruited animal is considered available for catching.

where

- $N_{y,a}^{C1,s}$  is the number of recruited animals of age  $a$  and sex  $s$  ( $m/f$ ) at the start of year  $y$  for the C1 sub-stock,
- $N_{y,a}^{C3,s}$  is the number of recruited animals of age  $a$  and sex  $s$  ( $m/f$ ) at the start of year  $y$  for the C3 sub-stock,
- $U_{y,a}^{C1,s}$  is the number of unrecruited animals of age  $a$  and sex  $s$  at the start of year  $y$  for the C1 sub-stock,
- $U_{y,a}^{C3,s}$  is the number of unrecruited animals of age  $a$  and sex  $s$  at the start of year  $y$  for the C3 sub-stock,
- $\delta_a^s$  is the proportion of unrecruited animals of sex  $s$  which recruit at age  $a$ ,
- $S_{y,a}^s$  is the annual survival rate of animals of sex  $s$  and age  $a$  during year  $y$ ,
- $C_{y,a}^{C1,s}$  is the total catch (in terms of animals) in year  $y$  for sex  $s$  and age  $a$  from breeding population C1,
- $C_{y,a}^{C3,s}$  is the total catch (in terms of animals) in year  $y$  for sex  $s$  and age  $a$  from breeding population C3,
- $P_y^{C1,M}$  is the number of C1 females which have reached the age at first parturition by the start of year  $y$ ,
- $f_y^{C1}$  is pregnancy rate during year  $y$  for sub-stock C1,
- $P_y^{C3,M}$  is the number of C3 females which have reached the age at first parturition by the start of year  $y$ ,
- $f_y^{C3}$  is pregnancy rate during year  $y$  for sub-stock C3, and
- $m$  is the maximum (lumped or plus-group) age-class (all animals of ages  $m$  and  $m-1$  are assumed to be recruited and to have reached the age at first parturition).

Note that these equations assume a 50:50 sex ratio at birth.

The annual survival rate is given by:

$$S_{y,a}^s = \exp(-M) \quad (4.2)$$

where  $M$  (set to  $0.03 \text{ yr}^{-1}$ ) is the instantaneous rate of natural mortality for animals of sex  $s$  and age  $a$  in year  $y$ , and is assumed to be independent of both  $a$  and  $y$  for these analyses.

#### Density dependence

Density dependence in fecundity for whale populations is conventionally modelled by writing the pregnancy rate,  $f_y$ , as follows:

$$f_y^{Ci} = f_{-\infty} \left[ 1 + A_f \left\{ 1 - \left( P_y^{Ci,D} / K^{Ci,D} \right)^{Z_f} \right\} \right] \quad (4.3)$$

where

- $C_i$  is either C1 or C3,
- $f_{-\infty}$  is the pregnancy rate at the pre-exploitation equilibrium<sup>29</sup>,
- $A_f$  is the resilience parameter,
- $Z_f$  is the degree of compensation,
- $K^{C_i,D}$  is the pre-exploitation equilibrium size of the component of the  $C_i$  population to which density dependence is functionally related, and
- $P_y^{C_i,D}$  is the size, at the start of year  $y$ , of the component of the population to which density dependence is functionally related, taken to be the number of females which have reached the age at first parturition  $P_y^{C_i,M}$ , where

$$P_y^{C_i,M} = \sum_{a=a_{\min}}^m \beta_a (N_{y,a}^{C_i,f} + U_{y,a}^{C_i,f}) \quad (4.4)$$

where

- $a_{\min}$  is the minimum age at which a female can reach first parturition, and
- $\beta_a$  is the fraction of females of age  $a$  which have reached the age at first parturition.

#### Recruitment and maturity

The fraction of unrecruited animals of sex  $s$  and age  $a$  which recruit at age  $a+1$ ,  $\delta_{a+1}^s$ , is given by:

$$\delta_{a+1}^s = \begin{cases} (\alpha_{a+1}^s - \alpha_a^s) / (1 - \alpha_a^s) & \text{if } \alpha_a^s < 1 \\ 1 & \text{if } \alpha_a^s = 1 \end{cases} \quad (4.5)$$

where

- $\alpha_a^s$  is the proportion of animals of sex  $s$  and age  $a$  which would be recruited if the population were at pre-exploitation equilibrium:

$$\alpha_a^s = \begin{cases} 0 & \text{if } a = 0 \\ \left[ 1 + \exp\left\{-\left(a - r_{50}^s\right) / \sigma_r^s\right\}\right]^{-1} & \text{if } 1 \leq a \leq m - 2 \\ 1 & \text{if } a \geq m - 1 \end{cases} \quad (4.6)$$

where

- $r_{50}^s$  is the age at 50% recruitment for animals of sex  $s$ , and
- $\sigma_r^s$  is a parameter which determines the width of the recruitment ogive for animals of sex  $s$ .

<sup>29</sup> At pre-exploitation levels,  $P_y^{C_i,D} = K^{C_i,D}$ , and  $f_0^{C_i} = f_{-\infty}$  (from Equation (4.3)). Applying this equality to the unrecruited population component in Equation (4.1), it can be shown that  $f_{-\infty} = R_0 / P_0^{C_i,M}$ , where  $R_0$  is the number of animals of age 0 at pre-exploitation equilibrium.

The proportion of females of age  $a$  that have reached the age at first parturition is given by:

$$\beta_a = \begin{cases} 0 & \text{if } a < a_{\min} \\ \left[1 + \exp\left\{-\left(a - p_{50}\right) / \sigma_p\right\}\right]^{-1} & \text{if } a_{\min} \leq a \leq m - 2 \\ 1 & \text{if } a \geq m - 1 \end{cases} \quad (4.7)$$

where

$p_{50}$  is the age at 50% maturity plus one year (to allow for the gestation period), and

$\sigma_p$  is a parameter which determines the width of the maturation ogive.

The parameter values used for these analyses are given in Table 4.1 (note that the parameter values were chosen so that the recruitment and maturity-at-age vectors are knife-edge).

The applications in this assessment assume that the maximum sustainable yield level (MSYL) and the maximum sustainable yield rate (MSYR)<sup>30</sup> refer to the total (1+) component of the population, and that density dependence acts on the mature female component. While values of the  $A_f$  and  $z_f$  parameters can be computed in the model, in the interest of time they were instead obtained from the HITTER-FITTER package (C. de Moor, *pers. comm.*) for different MSYR values and the biological parameters applicable. These values are listed in Table 4.2. Where a required MSYR value was not in the table, the  $A_f$  and  $z_f$  values were obtained by linear interpolation between the values given.

#### Catches

The total yearly catch by sex  $s$  is given by:

$$C_y^{C1,s} = C_y^{C1,s,B} + C_y^{C1,s,F} \quad (4.8)$$

$$C_y^{C3,s} = C_y^{C3,s,B} + C_y^{C3,s,F} \quad (4.9)$$

where

$C_y^{C1,s}$  is the total catch (in terms of animals) in year  $y$  from breeding population C1,

$C_y^{C3,s}$  is the total catch (in terms of animals) in year  $y$  from breeding population C3,

$C_y^{C1,s,B}$  are the catches of animals in year  $y$  for sex  $s$  from the C1 sub-stock in either breeding area<sup>31</sup>,

$C_y^{C1,s,F}$  are the catches of animals in year  $y$  for sex  $s$  from the C1 sub-stock in the feeding area,

<sup>30</sup> See Appendix 2.1 for more details on MSY, MSYL and MSYR.

<sup>31</sup> For models allowing interchange (such as the Sabbatical model), breeding ground catches for each region would need to be split according to the animals present there (which will not necessarily correspond to the total sub-stock associated with that region). However, since the Resident model has been implemented here, no interchange is assumed to take place, and catches are allocated entirely to the sub-stock associated with each breeding region.

$C_y^{C3,s,B}$  are the catches of animals in year  $y$  for sex  $s$  from the C3 sub-stock in either breeding area<sup>31</sup>, and  
 $C_y^{C3,s,F}$  are the catches of animals in year  $y$  for sex  $s$  from the C3 sub-stock in the feeding area.

To split the feeding ground catches between the two sub-stocks, it is assumed that the catches from each sub-stock each year are proportional to their relative abundances in the feeding area (given that complete mixing is assumed). Thus the breakdown of feeding ground catches is calculated as follows:

$$C_y^{C1,s,F} = C_y^{s,F} \frac{N_y^{C1,s}}{(N_y^{C1,s} + N_y^{C3,s})} \quad (4.10)$$

$$C_y^{C3,s,F} = C_y^{s,F} \frac{N_y^{C3,s}}{(N_y^{C1,s} + N_y^{C3,s})} \quad (4.11)$$

where

$N_y^{C1,s}$  is the total number of recruited C1 animals of sex  $s$  at the start of the year  $y$ , and

$N_y^{C3,s}$  is the total number of recruited C3 animals of sex  $s$  at the start of the year  $y$

given by:

$$N_y^{C1,s} = \sum_{a=1}^m N_{y,a}^{C1,s} \quad (4.12)$$

$$N_y^{C3,s} = \sum_{a=1}^m N_{y,a}^{C3,s} \quad (4.13)$$

The catch in year  $y$  at age  $a$  is assumed to be taken non-selectively across all recruited animals and is calculated as follows:

$$C_{y,a}^{C1,s} = C_y^{C1,s} N_{y,a}^{C1,s} / N_y^{C1,s} \quad (4.14)$$

$$C_{y,a}^{C3,s} = C_y^{C3,s} N_{y,a}^{C3,s} / N_y^{C3,s} \quad (4.15)$$

#### 4.3.2 Growth curves and catch-at-length

Chittleborough (1965) provides sex-specific length-at-age data from the 1950's, which were used to obtain separate growth "curves" for males and females. Because of a relatively poor fit to the von Bertalanffy growth curve, an alternative approach has been taken in which four straight lines are fit to the data, with parameters estimated to give best possible fit to the data. These fits, as well as the process used to obtain them, are given in Appendix 4.2.

These growth "curves" can be used to obtain catch-at-length estimates from the catch-at-age estimates provided by the BALEEN II model. Given the model estimates of catches-at-age,  $C_{y,a}^{C_i,s}$ , where  $i = \{1,3\}$ , these estimates can be converted into proportions of the catch of age  $a$ :

$$p_{y,a}^{Ci,s} = C_{y,a}^{Ci,s} / \sum_a C_{y,a}^{Ci,s} \quad (4.16)$$

Using the above-mentioned growth “curves”, these proportions at age can be converted to model estimates of proportions at length, under the assumption that the length-at-age distributions remain constant over time:

$$p_{y,\ell}^{Ci,s} = \sum_a p_{y,a}^{Ci,s} A_{a,\ell}^{Ci,s} \quad (4.17)$$

where  $A_{a,\ell}^{Ci,s}$  is the proportion of animals of age  $a$  and sex  $s$  that fall into length group  $\ell$  for sub-stock  $C_i$ , where  $i = \{1,3\}$ . The  $A$  matrix has been calculated under the assumption that for each age  $a$ , the length-at-age is normally distributed about a mean length given by the above-mentioned growth curves. The standard deviation used for this normal distribution is a function of age and proportional to the mean length:

$$\sigma_a^{Ci,s} = 0.05 \bar{\ell}_a^{Ci,s} \quad (4.18)$$

where  $\bar{\ell}_a^{Ci,s}$  is the mean length for age  $a$ , sex  $s$  and sub-stock  $C_i$  ( $i = \{1,3\}$ ) obtained from the growth “curve”. The value of 0.05 implies that with mean lengths of typically 30-40 ft, 95% of the length-at-age distribution varies over  $\pm 3$  to  $\pm 4$  ft. Several alternatives to 0.05 were explored before settling on this value as providing a reasonable fit to the data.

### 4.3.3 Likelihood function

#### Absolute abundance data

The absolute abundance estimate for C1 is assumed to be log-normally distributed with the log of the estimate as a mean and the CV as a standard deviation (see Section 3.3.2.1 for more detail). Thus its negative log likelihood contribution is:

$$\frac{1}{2CV^2} (\ln N_{target}^{obs} - \ln N_{target})^2 \quad (4.19)$$

where

$N_{target}^{obs}$  is the observed absolute abundance estimate obtained from the survey,

$N_{target}$  is the model-estimated population size for the year of the survey abundance estimate, and

CV is the coefficient of variation of  $N_{target}^{obs}$ .

#### Relative abundance data

The Cape Vidal relative abundance estimates are assumed to be log-normally distributed about their expected value, and their negative log-likelihood contribution is given by:

$$\bar{n} \ln \sigma + \frac{1}{2\sigma^2} \sum_y (\ln I_y - \ln q - \ln N_y)^2 \quad (4.20)$$

where

- $\bar{n}$  is the number of data points in the series,
- $\sigma$  is the residual standard deviation,
- $l_y$  is the relative abundance estimate for year  $y$ ,
- $q$  is a constant of proportionality, and
- $N_y$  is the model estimate of observed population size at the start of year  $y$ .

(See Section 3.3.2.2 for more details.)

#### Capture-recapture data

The capture-recapture data described in the data section have been incorporated into the likelihood using a Poisson distribution (see Section 3.3.2.3 for more details) and make the following contribution to the negative log likelihood:

$$\sum_i \sum_j \sum_{y=y_0}^{y_f-1} \sum_{y'=y+1}^{y_f} [-m_{y,y'}^{i,j} \ln \hat{m}_{y,y'}^{i,j} + \hat{m}_{y,y'}^{i,j}] \quad (4.21)$$

where

- $m_{y,y'}^{i,j}$  is the number of animals captured in year  $y$  in region  $i$  that were recaptured in year  $y'$  in region  $j$ ,
- $\hat{m}_{y,y'}^{i,j}$  is the model-predicted number of animals captured in year  $y$  in region  $i$  that were recaptured in year  $y'$  in region  $j$ , and
- $y_0$  is the first year of captures and  $y_f$  is the last year of recaptures.

Note that:

- The C3 absolute abundance estimates have not been used in the fitting process, as they have obtained directly from the capture-recapture data (which are included in the likelihood).
- The catch at length data have not been used in the fitting process, but instead serve as a reality check.
- The record of the interchange between C1 and C3 has been ignored for this assessment as the Resident model (i.e. no interchange) has been implemented here, so that terms for  $i \neq j$  in equation (4.21) are ignored.

#### 4.3.4 Estimation process

In order to obtain the  $A_f$  and  $z_f$  values required for Equation (4.3), the MSYR(1+) value is required as described in the recruitment and maturity section above. Initially, MSYR was treated as an estimable parameter, but this approach led to convergence difficulties (largely due to number of catches exceeding number of whales in particular age and sex cells during the minimisation search). Thus the following estimation approach was adopted:

MSYR<sup>32</sup> is set at a range of values, and for each of these values,  $K^{C1}$  and  $K^{C3}$  (referring to the 1+ population), are estimated using a simplex minimisation routine to maximise the likelihood described above.

As such, this assessment (because of its exploratory nature) makes use of only maximum likelihood estimation, rather than the standard Bayesian approach used in other Southern Hemisphere humpback assessments.

This estimation approach has been described in more detail in Appendix 4.3. Note that for each MSYR value, a ( $K^{C1}$ ,  $K^{C3}$ ) combination that resulted in the number of catches exceeding the number of animals estimated for either males or females (for any year and any age) was discarded on account of biological implausibility.

#### 4.4 RESULTS

##### *Convergence*

Figure 4.4 (a) and (b) verify that the results reflect convergence. Figure 4.4 (a) shows how for various different starting selections for the minimisation procedure, the results converge on the same point. This commonality indicates that a global minimum has been found, rather than a local minimum. Figure 4.4 (b) shows negative log-likelihood values associated with each of the steps shown in Figure 4.4 (a). These values similarly converge to the same minimum negative log-likelihood value of 22.77.

##### *General assessment results*

The results for the main analysis are reported in Table 4.3. The maximum likelihood estimates are given for the pristine population sizes, in terms of the total, age 1+ and the mature population components. The estimate of the minimum population size (corresponding to the total population) is also given, as well as this minimum as a fraction of total pristine population. “Current” abundances are given in numbers and as fractions of the pristine population sizes. Finally predicted population sizes for the year 2040 (where trajectories were projected forward under the assumption of zero catch) are given as a proportion of pristine population sizes. These proportions give an estimated extent of recovery to pristine level for the year 2040 under the assumption that the catch remains zero.

Note that the table reports the maximum likelihood estimates only. No probability envelopes can be provided at this stage, as this would require an extension of the current approach to Bayesian methods. Such an extension will be undertaken in future work.

Figure 4.5 (a) and (b) illustrate the population trajectories and data fits for the C1 and C3 populations respectively. Both the total population and the age 1+ population are shown. The C1 relative abundance data and absolute abundance estimate used in the fitting process have been plotted in Figure 4.5 (a). Figure 4.5 (b) shows the upper and lower C3 capture-recapture abundance estimates as a reality check. These estimates have not been used in the fitting process as the capture-recapture data underlying them have been used instead (Johnston and Butterworth, in prep.).

<sup>32</sup> Note that the same MSYR value was used for C1 and C3 here, since there are too few data available to reliably obtain two different values from the assessment.

Figure 4.6 (a) and (b) provide a comparison between the median trajectories of the C1 and C3 (1+) population from the sex-disaggregated model and the corresponding trajectories from Johnston and Butterworth (in prep.). Note that only the absolute abundance estimates have been shown here. The Cape Vidal data are relative indices of abundance and therefore scale in accordance to the population size in such a plot. Since the median trajectories from the two models are different, the Cape Vidal series also differs and becomes awkward to plot on the same figure.

#### *Fit to length distribution data*

Figure 4.7 (a)-(d) compare the model predicted catch-at-length frequencies to those reported. Since the catches were taken on various expeditions over several years, the data have been accumulated (over the years and expeditions) to give total C1 and C3 male and female catch-at length distributions. Therefore, the C1 catches shown were taken in the years 1936 and 1937, and the C3 catches shown were taken in the 1937, 1949 and 1950.

Because of the “stretching” observed in Figure 4.3 (c) and (d), model implementations for C3 group all lengths below 35 ft into a single “35-“ group. As already noted, since the C1 catches (1936-1937) were taken before the size-limits were enforced (1938), they were presumably not subject to “stretching”, as there was no reason to record the catches incorrectly.

## 4.5 DISCUSSION

### *General assessment results (in comparison to the results of Johnston and Butterworth (in prep.))*

Johnston and Butterworth (in prep.) present the results of a Bayesian stock assessment of breeding sub-stocks C1 and C3 for the Sabbatical, Tourist, Migrant and Resident models. The results of the resident model are of particular interest as a comparison to the results presented in this thesis, as both assessments, though employing different estimation techniques, are based on the same population structure hypothesis and use the same input data. The results from Johnston and Butterworth (in prep.) are given in Table A4.1.1 of Appendix 4.1. Before entering into the following discussion, it needs to be emphasised that the Johnston and Butterworth (in prep.) model is *not* sex- or age-disaggregated.

Qualitatively, the results of Johnston and Butterworth (in prep.) show a slightly better fit<sup>33</sup> (see Figure A4.1.2 in Appendix 4.1), compared to 1+ population trajectory (dashed line) in Figure 4.5 (a)), as they manifest a somewhat greater rate of increase. This improved fit may arise from the fact that for the age- and sex-specific model, biological plausibility requires that for any year the male/female catches may not exceed the male/female population size. This constraint proved problematic in the age- and sex-disaggregated assessment presented in this thesis, as the model-estimated male population size in the 1960s regularly went below that which was required to achieve the observed male catches in the model fitting process. This problem led to the alternative approach of specifying MSYR on input rather than estimating it, finding the best results that still respected this biological constraint (see Appendix 4.3) and then choosing the MSYR value with the best associated log likelihood. In an

---

<sup>33</sup> A note for comparing the results of the two assessments: The sighting surveys that give rise to the abundance and trend data treat calves separately. Thus the data (and the consequent estimated population sizes) correspond to the 1+ population and the values obtained in Johnston and Butterworth (in prep.) are comparable with the 1+ population in the results of this section.

age- and sex-aggregated model (as the one Johnston and Butterworth (in prep.) used to obtain the results in Appendix 4.1) catches are lumped into a single group, as are the male and female population components. Thus there is a reduced sensitivity to detailed aspects of the catch and a greater range of parameter values can consequently be available in the estimation process. This in turn may allow for a better fit to the trend data.

Appendix 2.1 shows that given an intrinsic growth rate parameter  $r$  and  $\mu=2.39$ , an MSYR value of roughly  $0.7r$  would be expected. Thus given the Johnston and Butterworth (in prep.)  $r^{C1}$  and  $r^{C3}$  values in Table A4.1.1 of Appendix 4.1, MSYR(1+) values of 0.059 and 0.036 would be expected for C1 and C3 respectively. These values are both higher than the MSYR(1+) value of 0.34 that yielded the best likelihood for this sex-disaggregated assessment (see Appendix 4.3). This feature of the results has not as of yet been further explored.

In general, considering that the results from this assessment fall within the Johnston and Butterworth (in prep.) 90% probability intervals (see Figure 4.6 (a) and (b)), the differences between the two have not been considered to be of great consequence. Future work involving catch-at-length data, however, will need to refer back to the results of Johnston and Butterworth (in prep.), or updates thereof, for comparative purposes and as a consistency check.

Based on the results shown in Table 4.3, sub-stock C1 is currently<sup>34</sup> at 74% of its pristine level, and sub-stock C3 is at 86% (compared to the 83% and 87% reported for C1 and C3 respectively in Table A4.1.1 of Appendix 4.1 for the comparative age- and sex-aggregated model). For both assessments, the C1 and C3 stocks are expected to recover completely or almost completely to their pre-exploitation levels by 2040 under the assumption of zero future catch.

#### *Fits to length distribution data*

The fits of the model-predicted catch-at-length distributions to those observed are given in Figure 4.7 (a)-(d). These comparisons are shown averaged over years because of low sample sizes in individual years. Only the year-averaged observed C3 female length distribution is well fitted by the model. For C3 males, the model predicts a greater proportion of smaller whales caught than was observed. The reverse is true for the C1 population, where the proportion of smaller males and even more so of smaller females caught is appreciably greater than the model predicts.

The aim of exploring an age- and sex- disaggregated model was to address the questions raised at the February 2009 IWC Intersessional Meeting in Seattle regarding the length distribution differences between the C1 and C3 regions (see Section 4.1.2). The four explanations put forward there for the differing size and sex structure of the catches are addressed below:

- *Explanation 1: Stocks are at different levels of depletion:*

The results of the assessment demonstrate that differential past exploitation alone is not sufficient to account for the (quite appreciable) differences in catch-at-length distributions off the African mainland and around Madagascar (see Figure 4.2 (a)-(b)).

---

<sup>34</sup> The ‘current’ abundance estimate is given for 2006 as this value is comparable to the assessment results reported in Johnston and Butterworth (in prep.).

- *Explanation 2: Animals migrate to different regions based on age:*

The analyses do suggest that the catches off the African mainland are not representative of the complete C1 population, since, based on the assessment results, a larger proportion of large animals would have been expected to be caught than was in fact observed. In light of the age- and sex-disaggregated assessment carried out here, the combined facts that catches at different locations along the African coast are similar in terms of length distributions (see Figure 4.3 (c)) and that the operations from which the length data were obtained were conducted in a manner identical to those off Madagascar, could indicate that older C1 animals are preferentially located further offshore on migrations or do not all migrate very far north every year. This would contradict the suggestion made at the February 2009 meeting that the African mainland catches are representative of the C1 population (see Section 4.1.3).

- *Explanation 3: Body sizes of the two stocks are slightly different:*

An initial impression from the modelling conducted is that the effect of different body sizes would have to be extremely strong to account for what are relatively substantial observed differences. Further, this suggested mechanism seems unlikely given that feeding is primarily in the Antarctic where the two groups of whales would be highly mixed.

- *Explanation 4: Whaling selectivity is occurring differently between regions:*

If, as mentioned above, the older C1 animals are located further offshore on migrations, or do not migrate as far north every year, then this would result in non-uniform selectivity-at-age in the catches. This non-uniformity would then be owing to the whales' behaviour rather than the whaling techniques, which are considered to have been identical in both regions (P. Best, *pers. comm.*).

#### *Uncertainty about catch splits*

When considering the points discussed above, the uncertainty about the catch data used in the assessment also needs to be taken into account. One area of uncertainty, for example, is the allocation of the *Uniwaleco* catches between C1 and C3. Best and Brandão (2009) report that the cruise track was partly reconstructed from newspaper records and locations of all the whales caught. These catches are most likely to have been recorded for the noon position of the factory (as only one position was given per day) and as such the allocation of catches between C1 and C3 is not straightforward. The main uncertainties arise when the expedition crossed the Mozambique Channel, where the catches could have been taken in either African or Mozambique coastal waters. The final decisions made for the allocations are given in Best and Brandão (2009).

A further uncertainty arises from the fact that a large proportion of catches are of unknown sex. More precisely only 56.4% of C catches are of known sex (IWC, 2009b). Therefore assumptions had to be made about sex ratios for both breeding and feeding stocks and applied to catches of unknown sex. The details of these allocations are given in Appendix 3.1.

Variations or errors in the catch series have important implications to the estimation of pre-exploitation size (IWC, 2008), and as such the results and discussion given here, while of interest, are subject to change if the catch series should be modified later in the light of further investigation.

*Points arising from the 61<sup>st</sup> annual meeting of the IWC*

A paper on this work (Müller *et al.*, 2009) was presented at the 61<sup>st</sup> annual meeting of the IWC SC, Madeira, June 2009. The following comments were made by the sub-committee on Other Southern Hemisphere Humpback Whale Stocks, and are taken from IWC (2010):

“It was observed that while differences in male and female body lengths may imply unequal visitation of the breeding grounds by different age-sex classes, it is also possible that sex-specific differences may be explained by any one of the following:

- females not migrating
- shorter sex-specific residencies on breeding grounds
- differences in sex-specific behaviour (i.e. adult male aggregation).

It was suggested that migratory pulses of animals of different ages may also explain length-at-catch differences between years. The sub-committee agreed that it would be useful to explore the length-at-catch data further at a generic level for Southern Hemisphere stocks, but felt it was a lesser priority for the SC62 [the 62<sup>nd</sup> meeting of the Scientific Committee]”.

#### **4.6 FUTURE WORK**

*Estimation process*

The first and primary criticism of the methodology used here is the use of the maximum likelihood approach, as it assumes that the parameters are fixed and does not allow for prior information about the parameters to be incorporated as can be done using Bayesian (SIR/MCMC) methods. Therefore the next step in this assessment will be to extend the current model to make use of Bayesian methodology. Careful consideration will have to be given to the treatment of the catches in the context of addressing the issue of age-specific catches exceeding the estimated numbers-at-age. One possible approach is to implement a non knife-edge selectivity-at-age function. The estimation process should ideally also be expanded to include the catch-at-length data in the likelihood, but this first requires a refinement of the model to be compatible with those data<sup>35</sup>.

*Model assumptions*

Sensitivity to the values reported in Table 4.1 could be investigated. Some of these would play an important role in implementing alternative catch selectivity-at-age functions.

Once the assessment based on the Resident model has been sufficiently advanced, the underlying model would need to be extended to the Sabbatical model form, which is considered as the reference model by the IWC.

---

<sup>35</sup> The current combination of model dynamics, trend data and selectivity-at-catch is not compatible with the catch-at-length data. So before the catch-at-length data can be incorporated into the likelihood, some changes will need to be made to the current model structure. Most likely this will involve adjustment of the selectivity-at-catch function.

*Future of age- and sex-disaggregated models*

Currently, assessments of the Southern Hemisphere humpback whales primarily make use of age- and sex-aggregated models. Development of age- and sex-disaggregated models allows sex and length specific data to be incorporated into assessments that would otherwise not be taken into account. Such data could provide a valuable contribution to the assessments, considering the scarcity of data available for many of the stocks. This assessment has shown that while the catches with sex and length information have introduced new challenges, they have also provided useful insight into the appropriateness of the model and model parameters chosen, by providing a reality check.

Lack of sex- and length-specific data may prevent age- and sex-disaggregated models from becoming standard implementation in current humpback assessments, but where these data are available, it would definitely be informative to include them.

University of Cape Town

**Table 4.1:** Model parameters used in this assessment<sup>36</sup>. Note that an unselective harvest from age 1 and above is assumed.

<b>General population parameters</b>		
$m$	<i>Plus-group age</i>	50 yrs
$M$	<i>Natural mortality rate</i>	0.03 yr <sup>-1</sup>
$a_r$	<i>Age at recruitment</i>	1 yr
$a_{min}$	<i>Minimum age at first parturition</i>	5 yrs
<b>Parameter values for Equations (4.6) and (4.7)</b>		
$r_{50}^m$		1
$r_{50}^f$		1
$\sigma_r^m$		0
$\sigma_r^f$		0
$p_{50}$		5
$\sigma_p$		0

**Table 4.2:**  $A_f$  and  $z_f$  values for fixed MSYR(1+).

MSYR (1+)	$A_f$	$Z_f$
0.000	0.00	2.389
0.005	0.27	2.181
0.010	0.58	1.989
0.015	0.91	1.813
0.020	1.28	1.651
0.025	1.69	1.501
0.030	2.15	1.363
0.035	2.67	1.235
0.040	3.26	1.116
0.045	3.93	1.006
0.050	4.71	0.903
0.055	5.62	0.806
0.060	6.69	0.716
0.065	7.97	0.632
0.070	9.52	0.553
0.075	11.44	0.479
0.080	13.89	0.410
0.085	17.09	0.344
0.090	21.47	0.283
0.095	27.81	0.225
0.100	37.78	0.170

<sup>36</sup> The value for age at first parturition was taken from Chittleborough (1965). The values for the parameters in Equations (4.6) and (4.7) were chosen in such a way as to make the effective selectivity-at-catch function knife-edge about the value  $p_{50}$ . An age of five corresponds to the ~35ft enforced minimum catch length (see Figure A4.2.2), and thus five was chosen for  $p_{50}$ .

**Table 4.3:** Assessment results for the age- and sex-disaggregated Resident model.

	Sub-stock C1	Sub-stock C3
<b>Historic catch</b>	<b>Feeding grounds split</b>	<b>Feeding grounds split</b>
<b>Recent abundance</b>	<b>proportional to abundance</b>	<b>proportional to abundance</b>
<b>Trend information</b>	<b>5965 (2003)</b>	<b>None</b>
<b>Capture-recapture data</b>	<b>Cape Vidal</b>	<b>None</b>
	<b>"All" photo-ID data*</b>	<b>"All" photo-ID data*</b>
<i>MSYR(I+)</i>	0.034	0.034
<i>K (total population)</i>	10212	9189
<i>K (age I+)</i>	9910	8916
<i>K (mature population)</i>	8790	7908
<i>N<sub>min</sub> (total)</i>	1168	1031
<i>N<sub>min</sub>/K (total)</i>	0.1179	0.1156
<i>N<sub>2006</sub> (total)</i>	7569	8014
<i>N<sub>2006</sub> (I+)</i>	7162	7662
<i>N<sub>2006</sub> (mat)</i>	5670	6329
<i>N<sub>2006</sub>/K (total)</i>	0.7412	0.8722
<i>N<sub>2006</sub>/K (I+)</i>	0.7227	0.8594
<i>N<sub>2006</sub>/K (mat)</i>	0.6452	0.8003
<i>N<sub>2040</sub>/K (total)</i>	0.9943	0.9955
<i>N<sub>2040</sub>/K (I+)</i>	0.9936	0.9952
<i>N<sub>2040</sub>/K (mat)</i>	0.9883	0.9935

\* As per the decision of IWC (2009a), these photo-ID data exclude the years 2000 and 2004 for C1, and 2002 for C3, because of poor temporal coverage of capture effort.

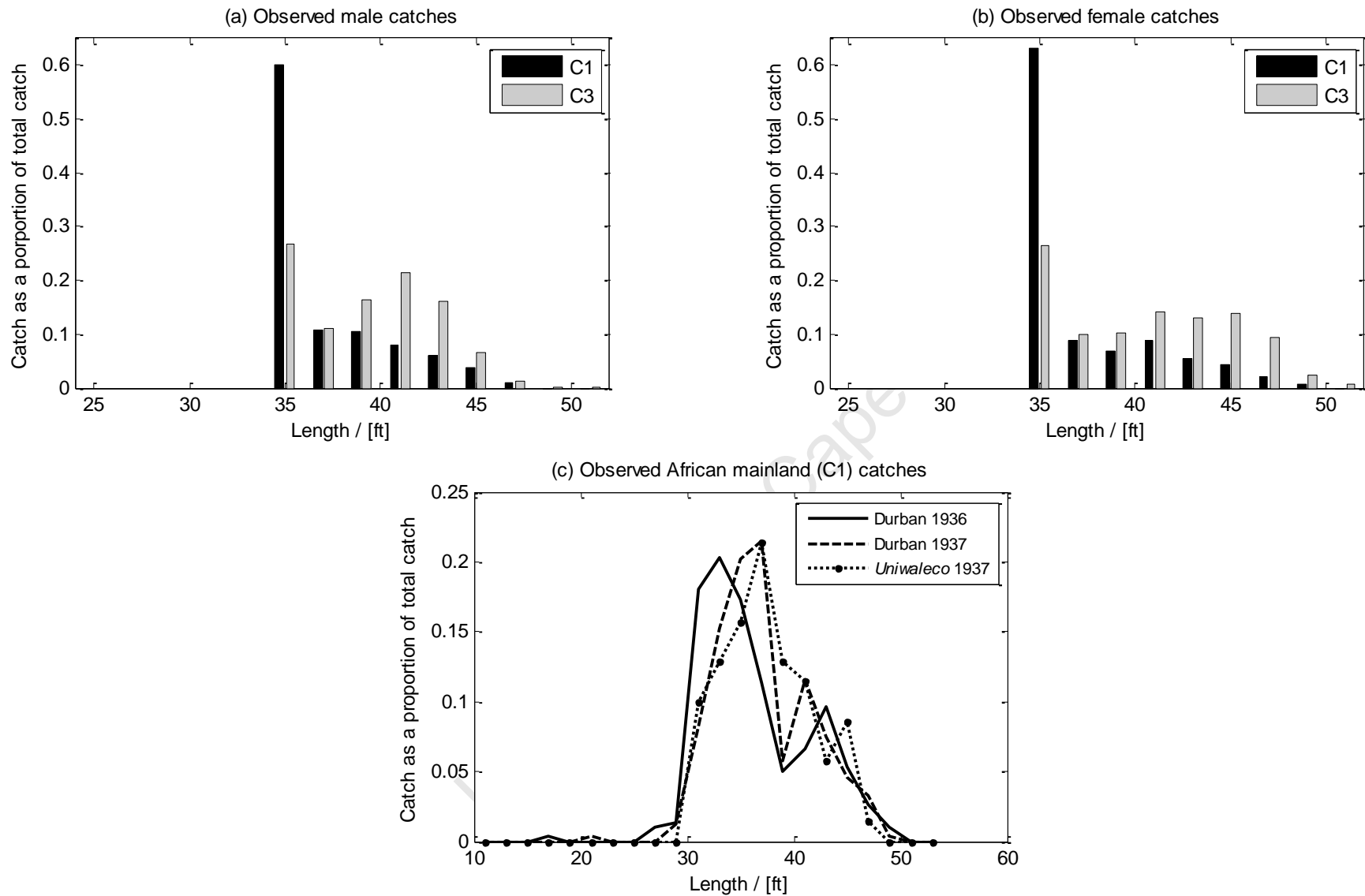


**Figure 4.2 (a)-(c):** Comparisons of observed catches by region: (a) and (b) show the catch length-frequency proportions cumulated over years, comparing the Africa (C1) and the Madagascar (C3) catches; (c) shows the African mainland catches (males and females combined) for the Durban 1936 and 1937 and *Uniwaleco* 1937 catches. Note that in (a) and (b) catches of 35ft or less have been grouped into a 35- group for comparability given the evident ‘stretching’ of C3 catches.

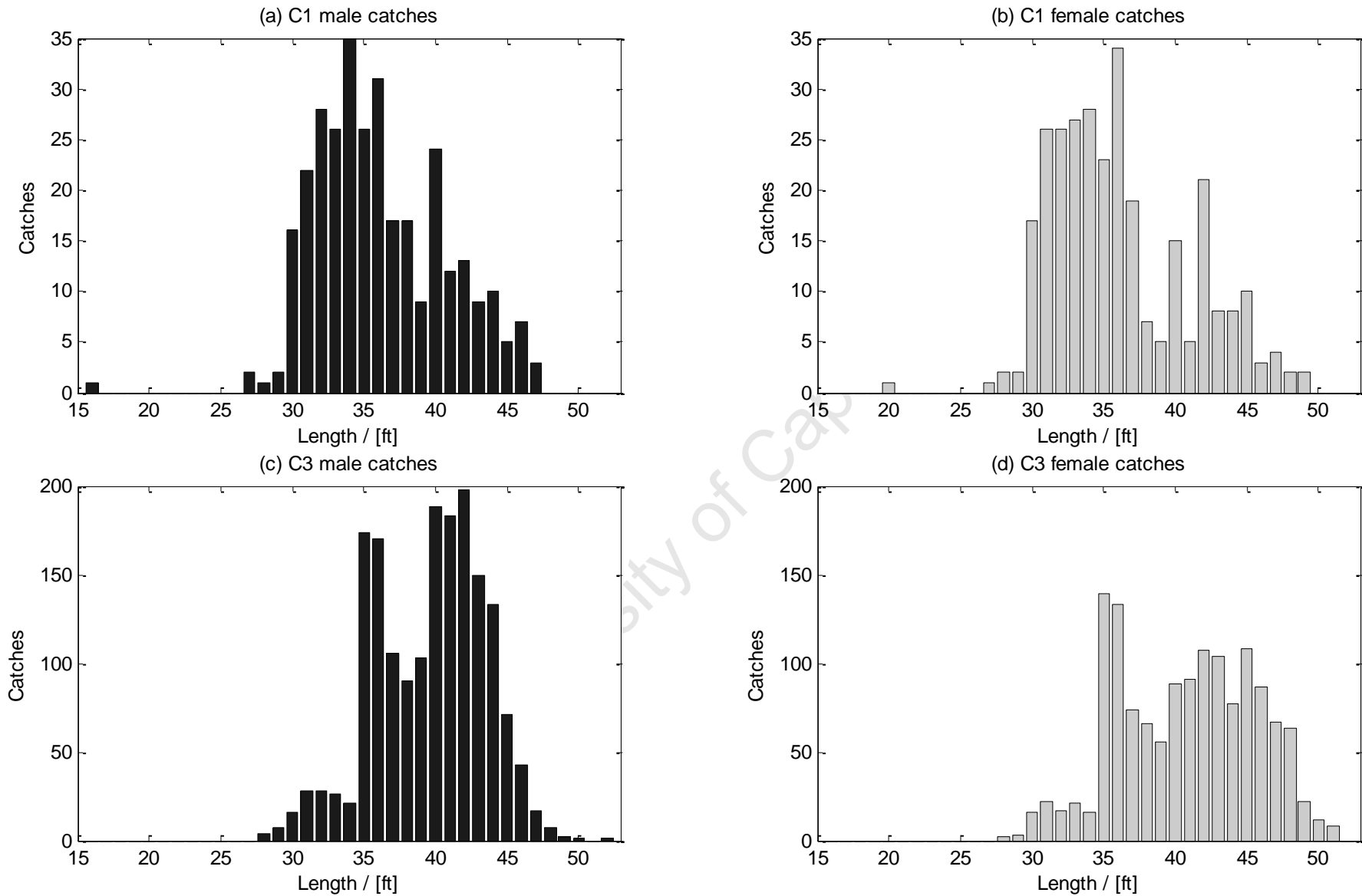


**Figure 4.3 (a)-(d):** Reported catch-at-length data. Note that the C1 catches are from Durban (1936 and 1937) as well as from the *Uniwaleco* catches allocated to C1, and the C3 catches are from *Uniwaleco* catches allocated to C3, as well as from the *Anglo Norse* expedition (1949 and 1950).

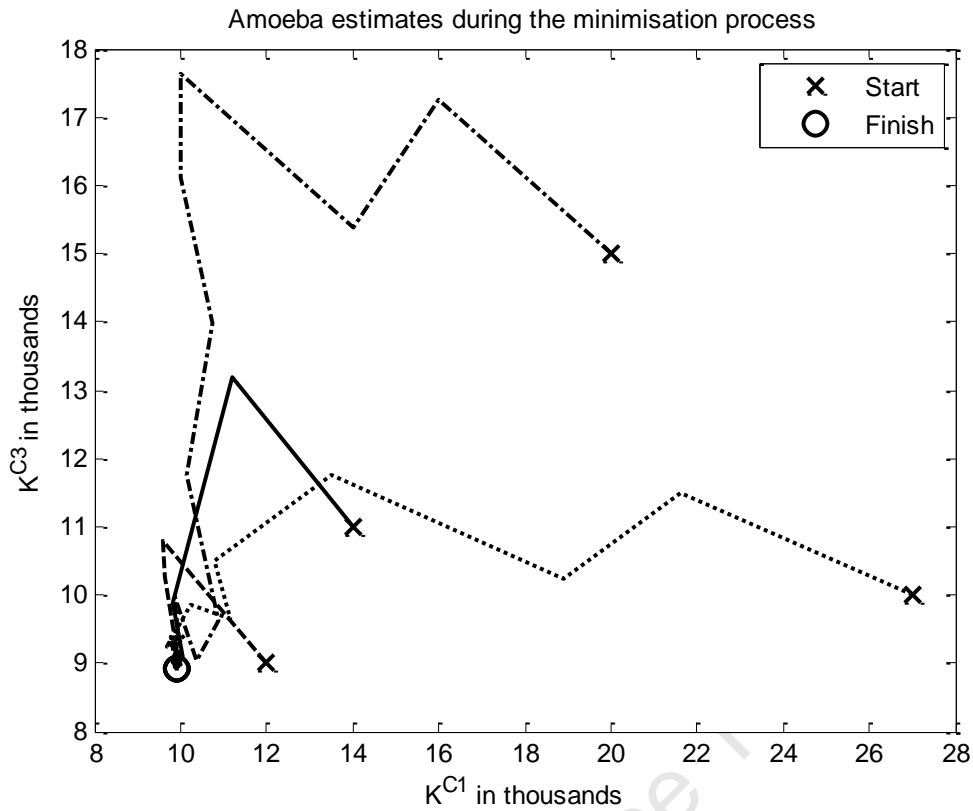


**Figure 4.4 (a):** Ameoba (Press *et al.*, 1992) minimisation routine for four different starting positions. Since two values,  $K^{C1}$  and  $K^{C3}$ , are being estimated, each iteration or ‘step’ in the procedure has an associated a three dimensional simplex. The proceeding step is a move in the ‘best’ direction. What are shown here are the points in each simplex with the highest likelihood, i.e. the best estimates in each simplex.

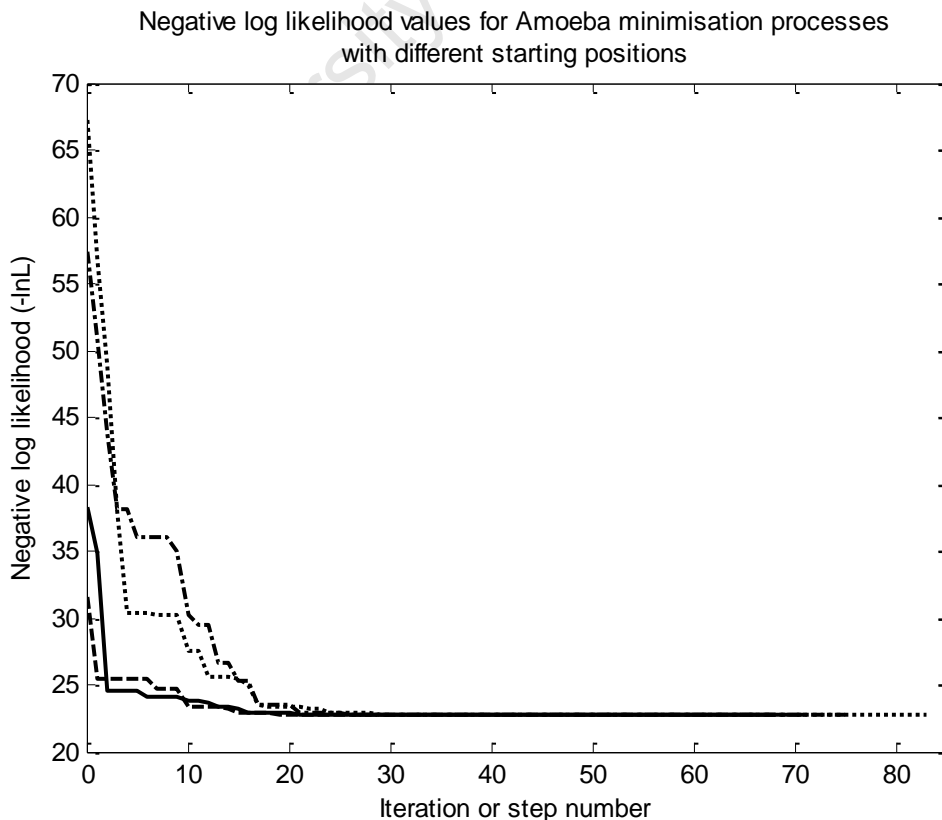


**Figure 4.4 (b):** Negative log-likelihood values associated with the trajectories shown in Figure 4.4 (a).

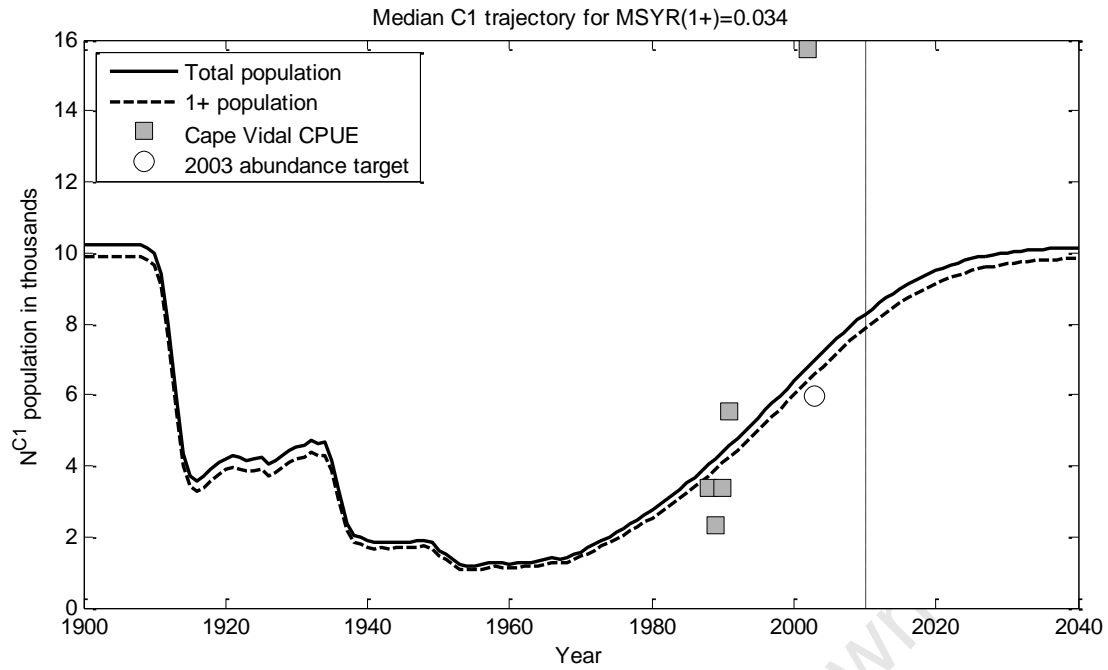


**Figure 4.5 (a):** Fit of the age- and sex-disaggregated Resident model to C1 trend data (Cape Vidal), capture-recapture data and the 2003 abundance estimate for C1. The trajectory to the right of the vertical dashed line is a projection into the future under the assumption of zero catch.

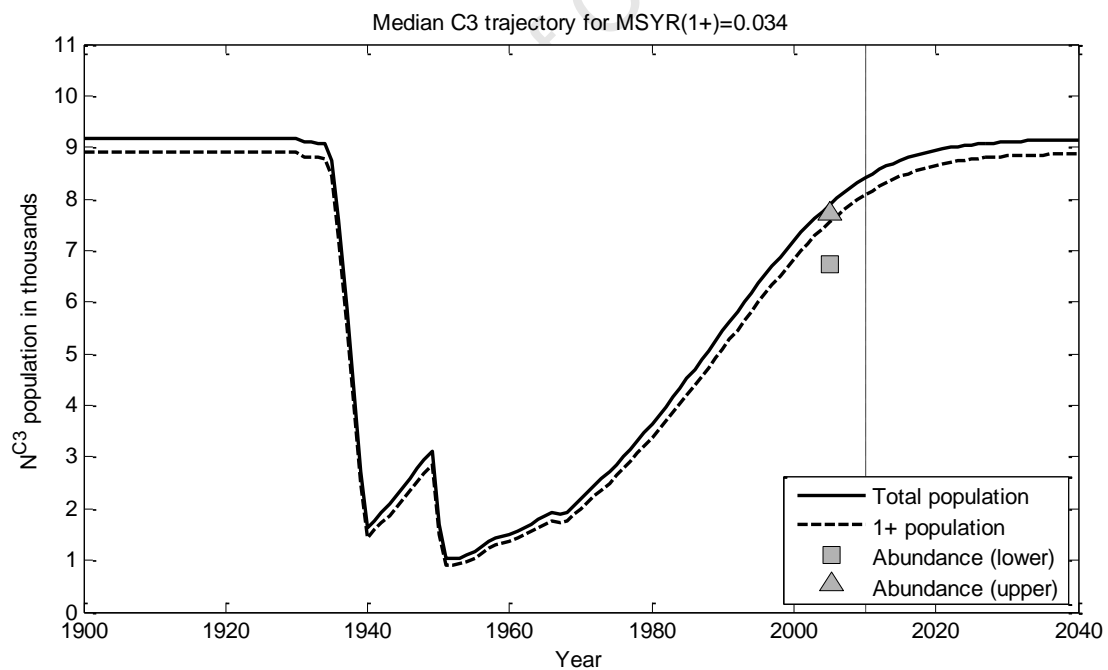


**Figure 4.5 (b):** Fit of the age- and sex-disaggregated Resident model to C3, capture-recapture data. The trajectory to the right of the vertical dashed line is a projection into the future under the assumption of zero catch. Note that the upper and lower abundance estimates have not been used in the fitting process, as the capture-recapture data underlying them have been used instead (Johnston and Butterworth, in prep.). They have been included in the plot as a reality check.

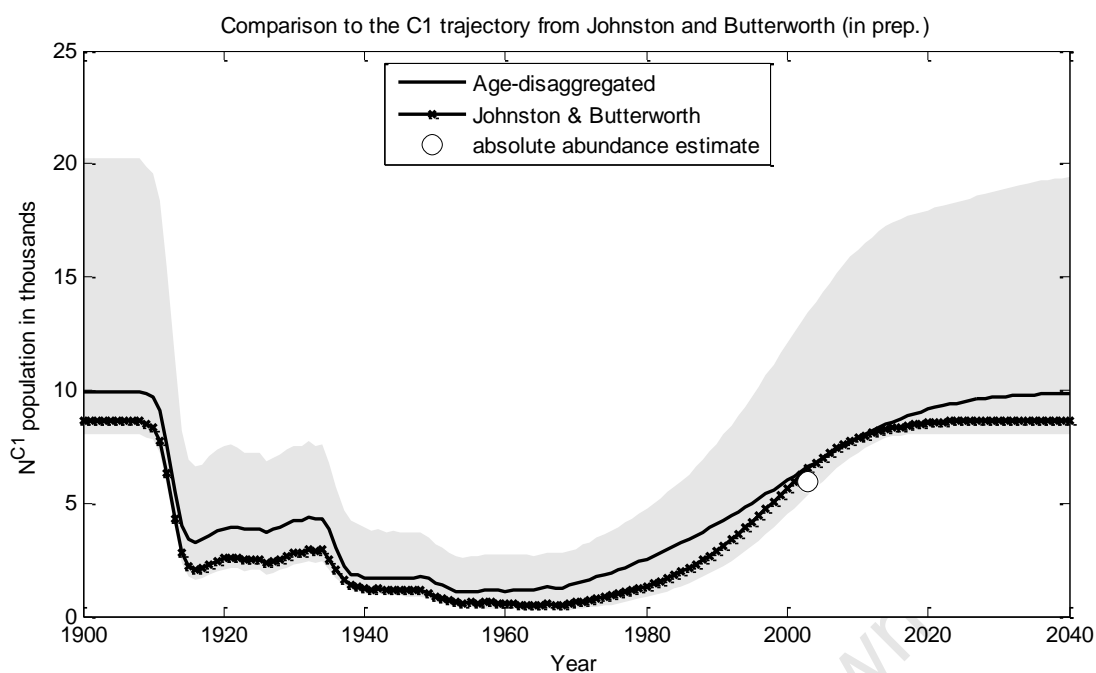


**Figure 4.6 (a):** The median C1 trajectory of the age 1+ population from the age- and sex-disaggregated model plotted together with the results from the corresponding Resident model in Johnston and Butterworth (in prep.). The shaded region is the 90% probability envelope from Johnston and Butterworth (in prep.).

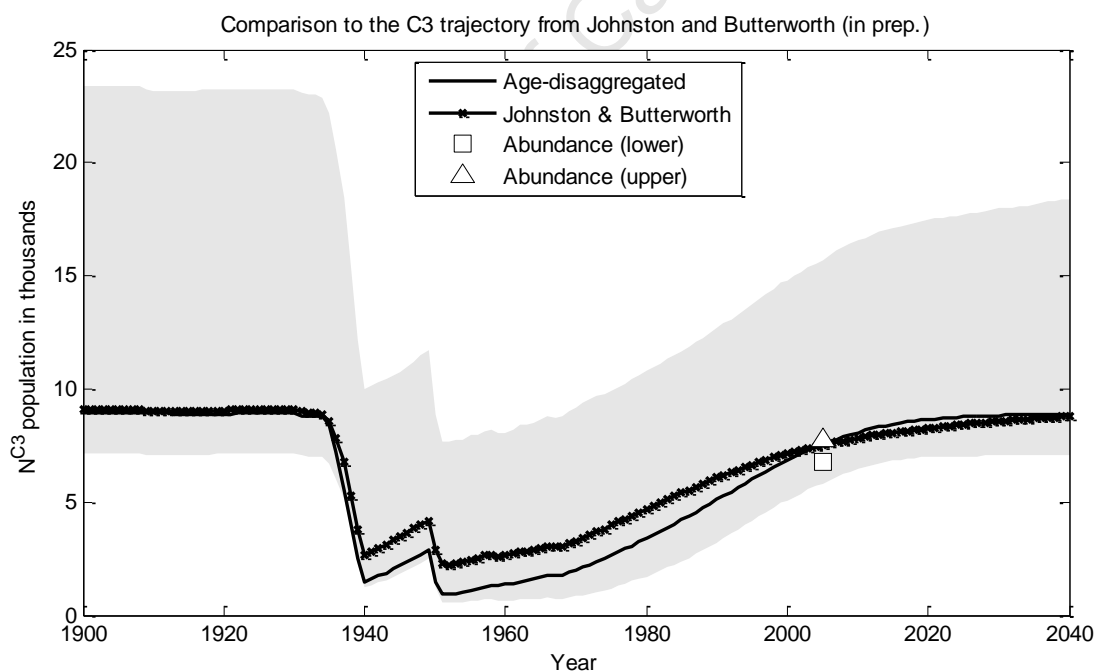


**Figure 4.6 (b):** The median C3 trajectory of the age 1+ population from the age- and sex-disaggregated model plotted together with the results from the corresponding Resident model in Johnston and Butterworth (in prep.). The shaded region is the 90% probability envelope from Johnston and Butterworth (in prep.).

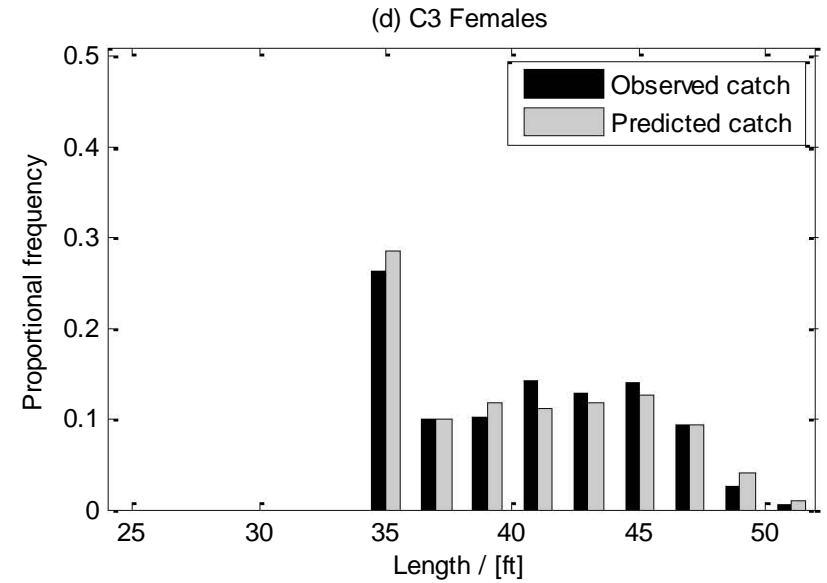
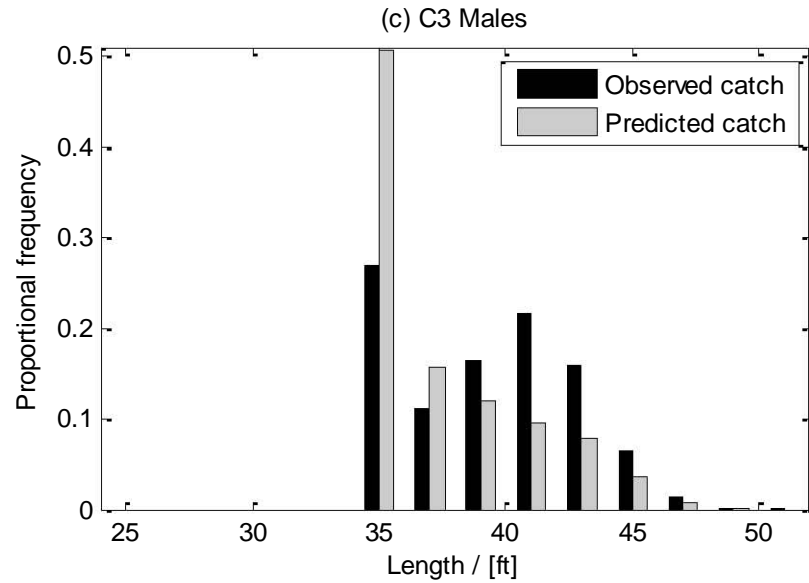
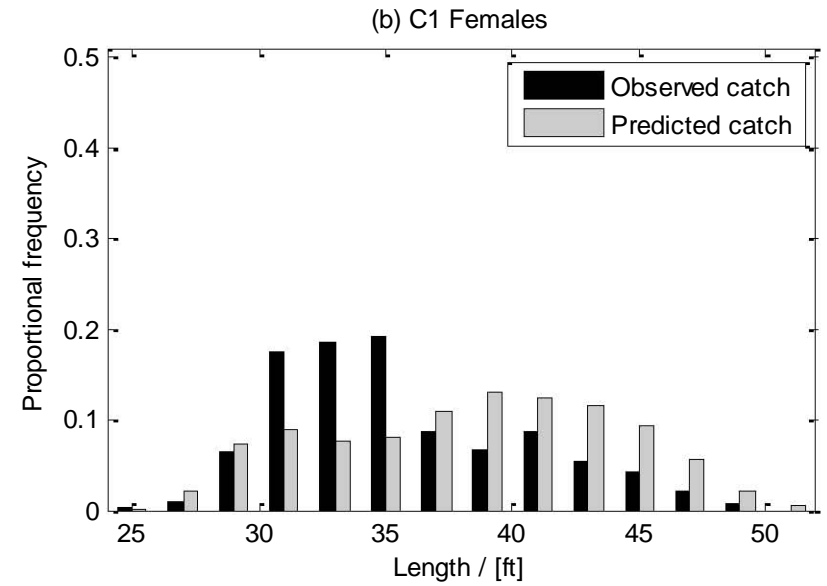
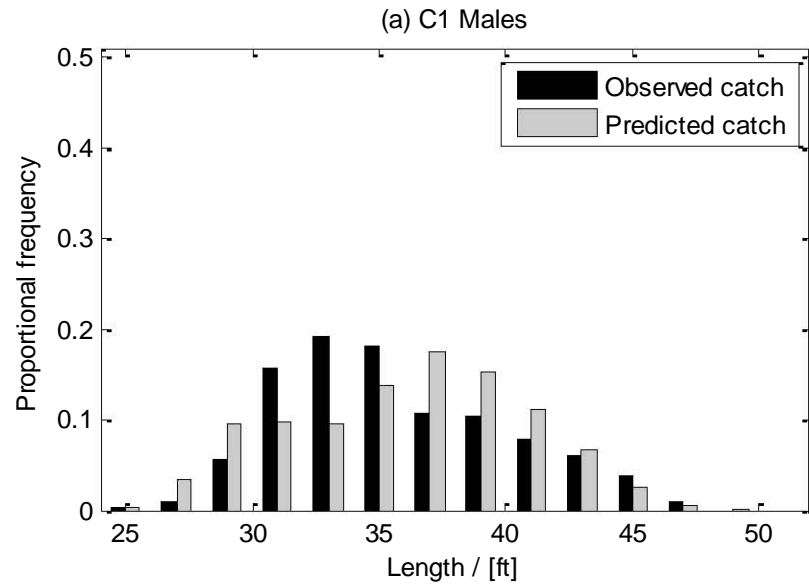


**Figure 4.7 (a)-(d):** Comparison of the model-predicted catches-at-length to observed catches. The C1 catches are accumulated for the years 1936 and 1937, and the C3 catches are accumulated for the years 1937, 1949 and 1950.

### Appendix 4.1

#### Population dynamics for the Sabbatical model and assessment results for the Resident model for breeding sub-stocks C1 and C3, both taken from Johnston and Butterworth (in prep.).

##### Sabbatical interchange modelling approach

The sabbatical interchange model, which is not age- and sex-disaggregated, is shown schematically below. There are two breeding sub-stocks C1 and C3 of sizes  $N^{C1}$  and  $N^{C3}$  respectively. However each year there is a probability  $\alpha^{C1}$  that an animal from sub-stock C1 travels to the C3 region instead of C1, and similarly a probability  $\alpha^{C3}$  that one from sub-stock C3 travels to the C1 region instead of C3. Note that the model thus assumes that an animal “visits” only one of these two regions in any one year. The observed numbers in regions C1 and C3 each year are then given by  $\eta^{C1}$  and  $\eta^{C3}$  respectively, and these are the variables to which observations apply (both capture-recapture and survey data).

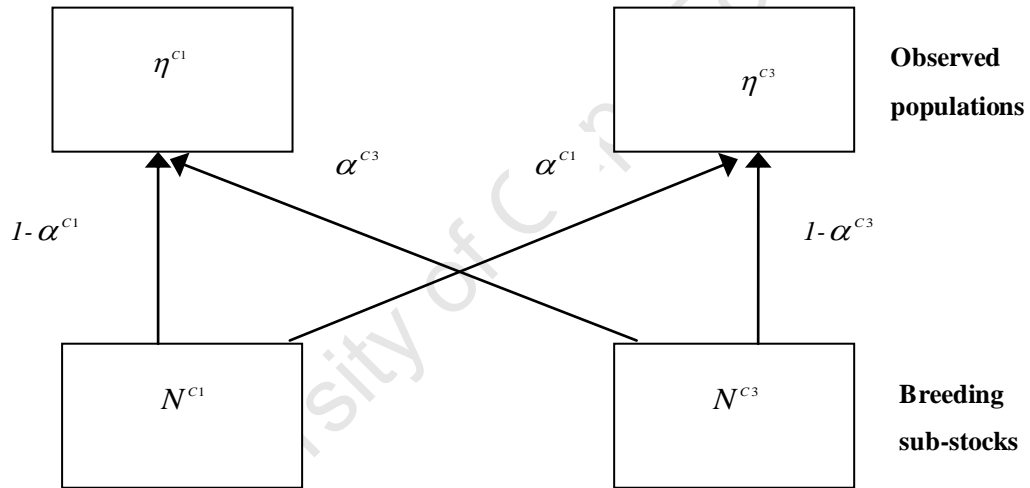


**Figure A 4.1.1:** Schematic representation of the Sabbatical model.

The following equations then apply:

##### *Breeding sub-stock population dynamics*

$$N_{y+1}^{B,C1} = N_y^{B,C1} + r^{C1} N_y^{B,C1} \left( 1 - \left( \frac{N_y^{B,C1}}{K^{C1}} \right)^\mu \right) - C_y^{C1} \quad (\text{A4.1.1})$$

$$N_{y+1}^{B,C3} = N_y^{B,C3} + r^{C3} N_y^{B,C3} \left( 1 - \left( \frac{N_y^{B,C3}}{K^{C3}} \right)^\mu \right) - C_y^{C3} \quad (\text{A4.1.2})$$

where

- $N_y^{B,C1}$  is the number of whales in the breeding population C1 at the start of year  $y$ ,
- $N_y^{B,C3}$  is the number of whales in the breeding population C3 at the start of year  $y$ ,
- $r^{C1}$  is the intrinsic growth rate for breeding population C1,
- $r^{C3}$  is the intrinsic growth rate for breeding population C3,
- $K^{C1}$  is the carrying capacity of breeding population C1,
- $K^{C3}$  is the carrying capacity of breeding population C3,
- $\mu$  is the “degree of compensation” parameter, which is set at 2.39, and hence fixes the MSY level to  $MSYL=0.6K$ , as conventionally assumed by the IWC SC,
- $C_y^{C1}$  is the total catch (in terms of animals) in year  $y$  from breeding population C1, and
- $C_y^{C3}$  is the total catch (in terms of animals) in year  $y$  from breeding population C3.

#### Feeding stocks

Mixing of the breeding populations in the feeding area (defined by 10°E – 60°E (see Appendix 3.1)) yields:

$$N_y^F = N_y^{B,C1} + N_y^{B,C3} \quad (A4.1.3)$$

which is assumed to reflect complete mixing of sub-stocks C1 and C3 in the feeding area.

#### Observed populations

$$\eta_y^i = (1 - \alpha^i)N_y^i + \alpha^j N_y^j \quad \left\{ \begin{matrix} i \\ j \end{matrix} \right\} = \left\{ \begin{matrix} C1 \\ C3 \end{matrix} \right\} \text{ or } \left\{ \begin{matrix} C3 \\ C1 \end{matrix} \right\} \quad (A4.1.4)$$

where

- $\eta_y^i$  is the observed population size in year  $y$  in breeding region  $i$ ,
- $\alpha^i$  is the probability that animal from breeding population  $i$  moves (for one year) to the observation area for breeding population  $j$  instead of that for breeding population  $i$ .

#### Catches

$$C_y^{C1} = C_y^{C1,B} + C_y^{C1,F} \quad (A4.1.5)$$

$$C_y^{C3} = C_y^{C3,B} + C_y^{C3,F} \quad (A4.1.6)$$

where

- $C_y^{C1,B}$  are the catches of animals in year  $y$  from the C1 sub-stock in either breeding area,
- $C_y^{C1,F}$  are the catches of animals in year  $y$  from the C1 sub-stock in the feeding area,

$C_y^{C3,B}$  are the catches of animals in year  $y$  from the C3 sub-stock in either breeding area, and

$C_y^{C3,F}$  are the catches of animals in year  $y$  from the C3 sub-stock in the feeding area.

The reported breeding area catches ( $C_y^{C1,B,reported}$  and  $C_y^{C3,B,reported}$ ) are provided in Table A3.1.1 of Appendix 3.1, but

only the combined catch ( $C_y^F = C_y^{C1,F} + C_y^{C3,F}$ ) for the feeding area is provided in Table A3.1.2 of Appendix 3.1.

To split this feeding ground catch, it is assumed that the catches each year are proportional to their relative abundances in the feeding area (given that complete mixing is assumed). Thus the breakdown of feeding ground catches is calculated as follows:

$$C_y^{C1,F} = C_y^F \frac{N_y^{C1,B}}{(N_y^{C1,B} + N_y^{C3,B})} \quad \text{and} \quad (\text{A4.1.7})$$

$$C_y^{C3,F} = C_y^F \frac{N_y^{C3,B}}{(N_y^{C1,B} + N_y^{C3,B})} \quad (\text{A4.1.8})$$

The reported breeding ground catches are also split proportional to the relative abundance of each breeding sub-stock in each area as follows:

$$C_y^{C1,B} = C_y^{C1,B,reported} \frac{(1-\alpha^1)N_y^{C1,B}}{((1-\alpha^1)N_y^{C1,B} + \alpha^3 N_y^{C3,B})} + C_y^{C3,reported} \frac{\alpha^1 N_y^{C1,B}}{(\alpha^1 N_y^{C1,B} + (1-\alpha^3)N_y^{C3,B})} \quad (\text{A4.1.9})$$

$$C_y^{C3,B} = C_y^{C1,B,reported} \frac{\alpha^3 N_y^{C3,B}}{((1-\alpha^1)N_y^{C1,B} + \alpha^3 N_y^{C3,B})} + C_y^{C2+3,reported} \frac{(1-\alpha^3)N_y^{C3,B}}{(\alpha^1 N_y^{C1,B} + (1-\alpha^3)N_y^{C3,B})} \quad (\text{A4.1.10})$$

### Migrant model

The Migrant model is similar to the Sabbatical model, except that if a whale from C1 moves to C3 (or *vice versa*) then it will join the C3 stock and behave as a C3 animal from then on. It will have the same probability as any C3 whale of migrating back to C1.

The  $\alpha$  parameter is replaced by  $\beta$ . Further, Equations (A4.1.1) and (A4.1.2) change to:

$$N_{y+1}^{B,C1} = N_y^{B,C1} + r^{C1} N_y^{B,C1} \left( 1 - \left( \frac{N_y^{B,C1}}{K^{C1}} \right)^\mu \right) - C_y^{C1} - \beta^{C1} N_y^{B,C1} + \beta^{C3} N_y^{B,C3} \quad (\text{A4.1.11})$$

$$N_{y+1}^{B,C3} = N_y^{B,C3} + r^{C3} N_y^{B,C3} \left( 1 - \left( \frac{N_y^{B,C3}}{K^{C3}} \right)^\mu \right) - C_y^{C3} - \beta^{C3} N_y^{B,C3} + \beta^{C1} N_y^{B,C1} \quad (\text{A4.1.12})$$

### Tourist Model

The Tourist model is an adaptation of the Resident model where whales from one breeding sub-stock, in addition to returning to their own breeding area each year, have a probability of also visiting the breeding area for the other sub-stock that same year (without joining this other sub-stock).

The  $\alpha$  parameter is replaced by  $\gamma$ . Further the model-predicted number of animals captured in year  $y$  and recaptured in year  $y'$  (Equations (3.8) and **Error! Reference source not found.** in Section 3.3.2.3) are adjusted by replacing  $(1-\alpha)$  by  $\gamma$ .

### **Resident Model**

The Resident model is identical to the Sabbatical model, except that  $\alpha^{C1}$  and  $\alpha^{C3}$  are both zero.

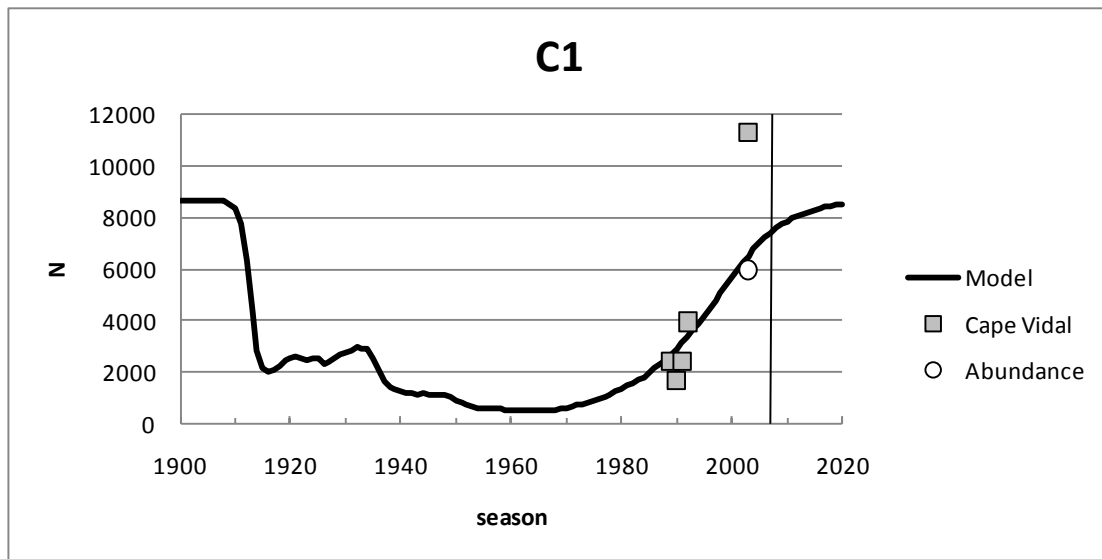
### **Results**

Table A4.1.1 below gives the assessment results from Johnston and Butterworth (in prep.) for the Resident model. These results are given to provide a comparison for the age- and sex-disaggregated Breeding Stock C assessment presented in this thesis.

**Table A4.1.1:** Resident model assessment results (posterior medians with 5<sup>th</sup> and 95<sup>th</sup> percentiles in parenthesis).

	<b>Sub-stock C1</b>	<b>Sub-stock C3</b>
<b><i>r</i> prior</b>	<b>U[0, 0.106]</b>	<b>U[0, 0.106]</b>
<b>Historic catch</b>	<b>Feeding grounds split proportional to abundance</b>	<b>Feeding grounds split proportional to abundance</b>
<b>Recent abundance</b>	<b>5,965 (2003)</b>	<b>None</b>
<b>Trend information</b>	<b>Cape Vidal trend data only</b>	<b>None</b>
<b>Capture-recapture data</b>	<b>'All' photo-identification data*</b>	<b>'All' photo-identification data*</b>
<i>r</i>	0.084 [0.037; 0.103]	0.051 [0.006; 0.100]
<i>K</i>	8,676 [8,082; 12,141]	9,093 [7,128; 16,239]
<i>α</i>	-	-
<i>N<sub>min</sub></i>	473 [264; 2220]	2,145 [553; 6,384]
<i>N<sub>2006</sub></i>	7,233 [6,249; 8,479]	7,593 [5,958; 9,957]
<i>η<sub>2006</sub></i>	7,233 [6,249; 8,479]	7,593 [5,958; 9,957]
<i>N<sub>min</sub>/K</i>	0.055 [0.033; 0.190]	0.233 [0.074; 0.417]
<i>N<sub>2006</sub>/K</i>	0.828 [0.595; 0.951]	0.865 [0.448; 1.000]
<i>N<sub>2020</sub>/K</i>	0.989 [0.823; 0.998]	0.975 [0.486; 1.000]
<i>N<sub>2040</sub>/K</i>	1.000 [0.965; 1.000]	1.000 [0.582; 1.000]

\* As per the decision of IWC (2009a), the photo-ID data used exclude the years 2000 and 2004 for C1, and 2002 for C3, because of poor temporal coverage of capture effort. Further, for the resident model, the one recapture that reflects movement between C1 and C3 is excluded.



**Figure A4.1.2:** Resident model fit to C1 trend data (Cape Vidal), as well as the recent abundance estimate (2003). The model trajectory follows the Bayesian posterior median values of  $\eta_y^{c1}$ , the whales in the C1 breeding grounds. The vertical line shows 2006; projections thereafter assume zero catch.

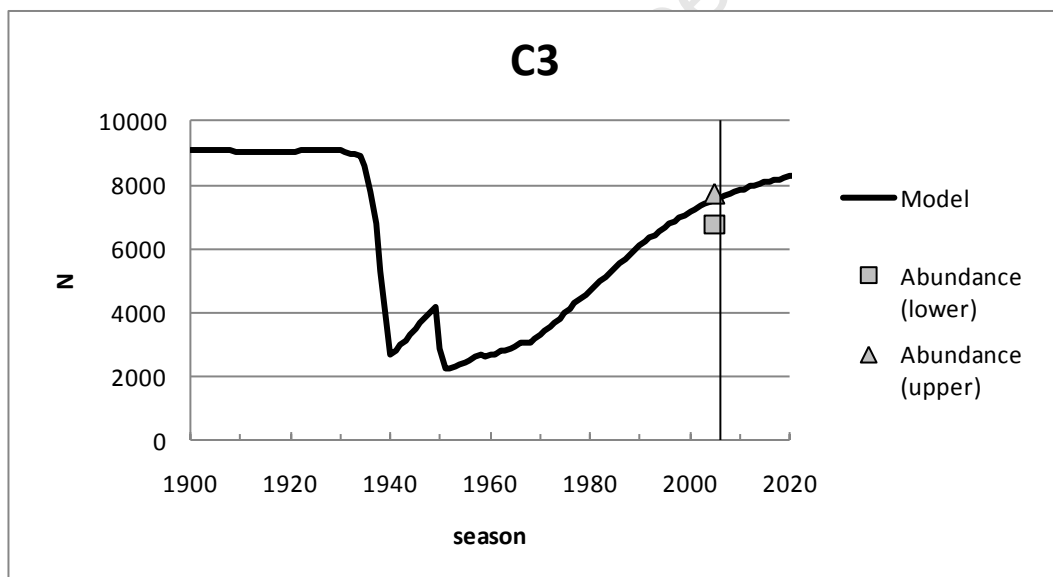


**Figure A4.1.3:** Resident model trajectories follows the Bayesian posterior median values of  $\eta_y^{c3}$ , the whales in C3 breeding grounds. The vertical line shows 2006. The triangle and square symbols show the upper and lower abundance estimates from Cerchio (2008a) respectively for comparative purposes – these estimates are not used in fitting the model because the capture-recapture data underlying them are used instead.

## Appendix 4.2

### Fit of a growth curve to Southern Hemisphere humpback whale Breeding Stock C growth data

Chittleborough (1965) provides sex-specific length-at-age data from the 1950's. In addition to these data, length at birth has been assumed to be 14ft (P. Best, *pers. comm.*). The von Bertalanffy growth curve, given by Equation (A4.2.1) below, is commonly used to model growth:

$$L(a) = L_{\infty} \left( 1 - e^{-\kappa(a-a_0)} \right) \quad (\text{A4.2.1})$$

where

- $L(a)$  is the length at age  $a$ ,
- $L_{\infty}$  is the maximum length the animals are assumed to attain,
- $\kappa$  is a growth rate parameter, and
- $a_0$  is the (non-biological) age at which length is zero, effectively provided by projecting backwards from length at birth.

As females are on average larger than males, the Chittleborough (1965) data were fitted to the von Bertalanffy curve for males and females separately.  $L_{\infty}$ ,  $\kappa$  and  $a_0$  values were found using Excel solver which requires that the sum of squared errors between the data points and the fitted curve is minimised (results in Table A4.2.1).

This fit, however, is poor (see Figure A4.2.1 (a) and (b)). The von Bertalanffy curve battles to fit both the high growth in the early years and the reduced growth rate in the later years. Adjustment of the estimated parameter values showed that a better fit to one half of these data inherently implies a worse fit to the other.

An alternative approach was therefore taken in which several straight lines were fitted to the data. The method used was to choose ages at which a changeover from one line to the next was to occur and the corresponding lengths for those ages were estimated<sup>37</sup>. Several options were explored in terms of the number of lines used, and the ages at which the changeover occurs from one line to the next. The final choice was four lines: one between the ages zero and one; the next between the ages one and four; the third between the ages four and 20; and the final line for ages greater than 20. The results are shown in Table A4.2.2, and the fits to the data are illustrated in Figure A4.2.2(a) and (b).

**Table A4.2.1:** Table of the parameter values estimated for the von Bertalanffy growth curve.

Parameter value	Males	Females
$L_{\infty}$ (ft)	41.51	44.15
$\kappa$ ( $\text{yr}^{-1}$ )	0.29	0.20
$a_0$ (yr)	-1.92	-2.83

**Table A4.2.2:** Table of estimated length-at-age values used to obtain the growth “curves” used in the analysis.

Line	Males	Females
	Estimated length (ft) at starting point of line	Estimated length (ft) at starting point of line
1 (ages 0-1 yrs)	29.00	29.00
2 (ages 2-4 yrs)	35.45	35.49
3 (ages 4-20 yrs)	41.83	43.60
4 (ages 20+ yrs)	42.41	45.40

<sup>37</sup> Linear interpolation between the chosen ages and the corresponding lengths yielded the intermediate length-at-age values. The estimation process took place through minimisation of the sum of the square of the errors between data and estimated points.

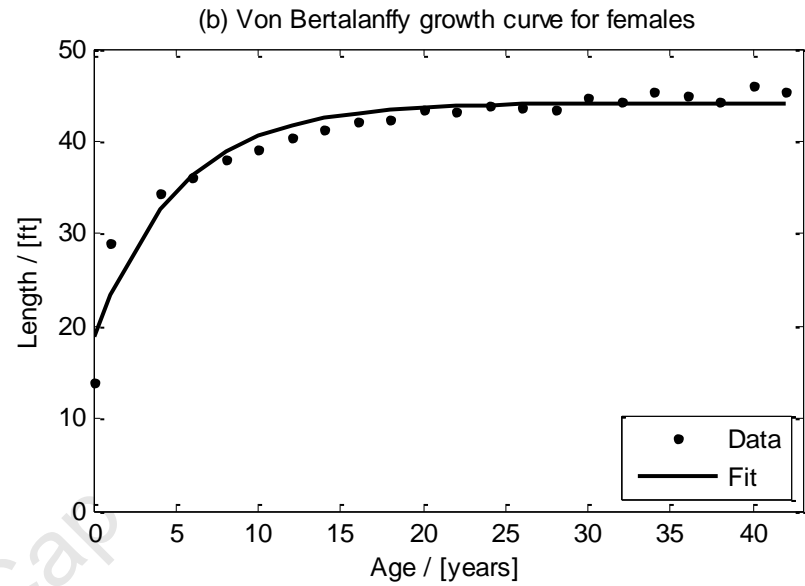
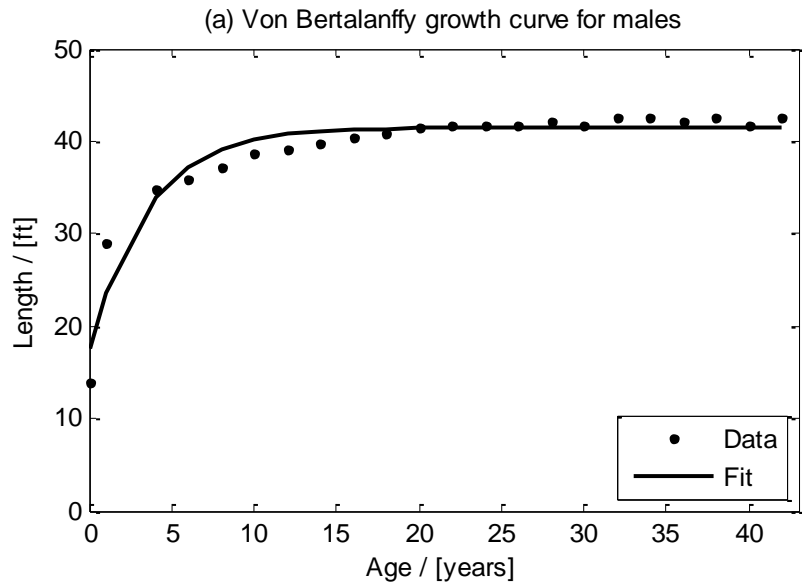


Figure A4.2.1 (a) and (b): Fit to the data using the von Bertalanffy growth curve.

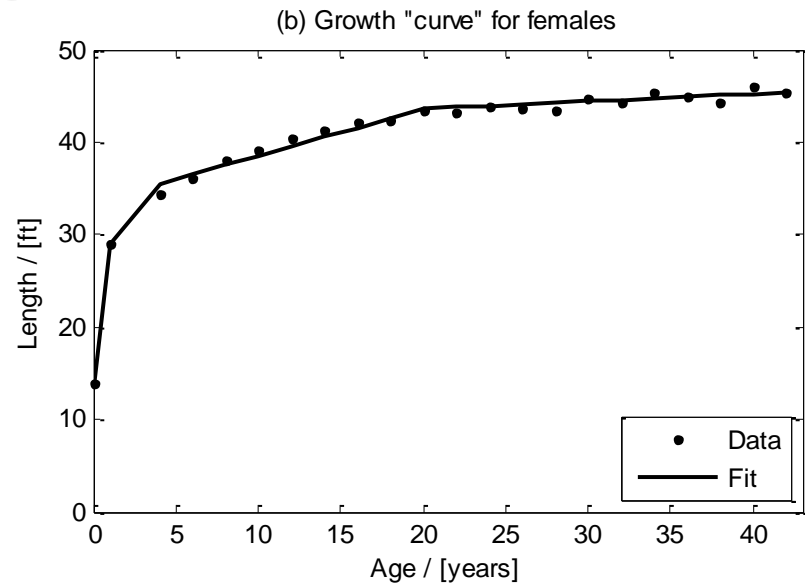
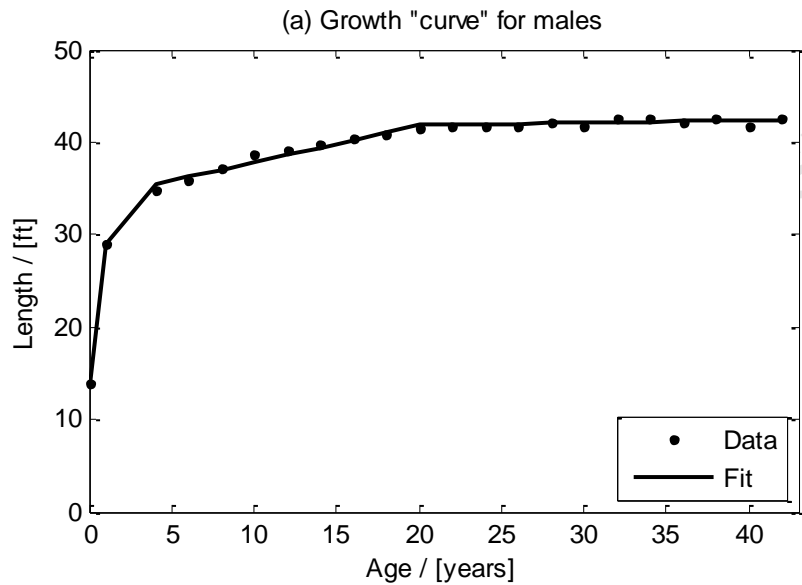


Figure A4.2.2 (a) and (b): Fit to the data using four lines, with changeover points at the ages 1, 4 and 20.

### Appendix 4.3

#### Estimation process for the assessment of the Southern Hemisphere humpback whale Breeding Stock C.

MSYR is set at a range of values and for each the values of  $K^{C1}$  and  $K^{C3}$  (referring to the 1+ population) are estimated using the simplex minimisation routine to maximise the likelihood described in Section 4.3.3.

The results of a manual exploration of the likelihood profile are shown in Figure A4.3.1. This figure shows a clear minimum in the negative log likelihood (and therefore a maximum in the likelihood) at an MSYR(1+) of roughly 0.034, the value used for the assessment.

Figure A4.3.2 (a) and (b) show the population trajectories for a range of MSYR values. In general, the lower MSYR is, the higher the estimated  $K^{C1}$  and  $K^{C3}$  values are. At this point, it is important to remember that given the typical humpback Pella Tomlinson growth model, with  $\mu = 2.39$ , one would expect an MSYR(1+) of  $0.71r$  (see Appendix 2.1). Therefore MSYR and  $r$  are linearly related and the low MSYR to high  $K$  relationship observed in Figure A4.3.2 (a) and (b) conforms to expectation (see Appendix 3.3). It is interesting to note is that the value of MSYR has a much greater effect on the shape of the trajectory for C3 (Figure A4.3.2 (b)).

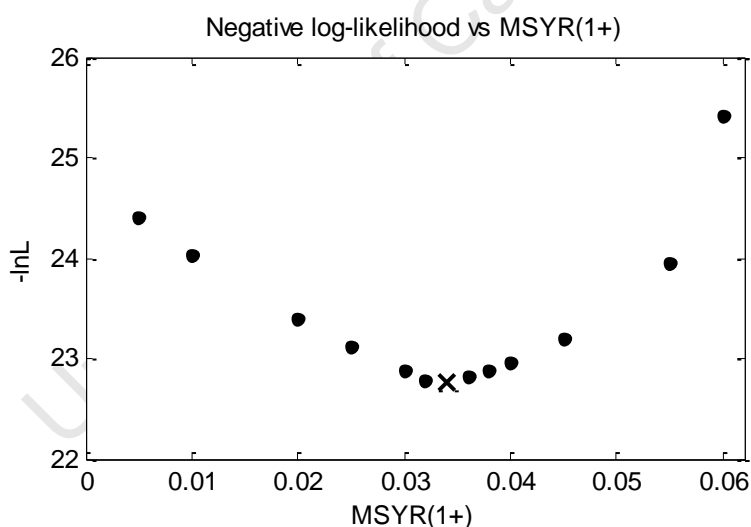


**Figure A4.3.1:** Negative log-likelihood values plotted against MSYR. The X marks the best-estimate MSYR of 0.034 (used in this assessment)

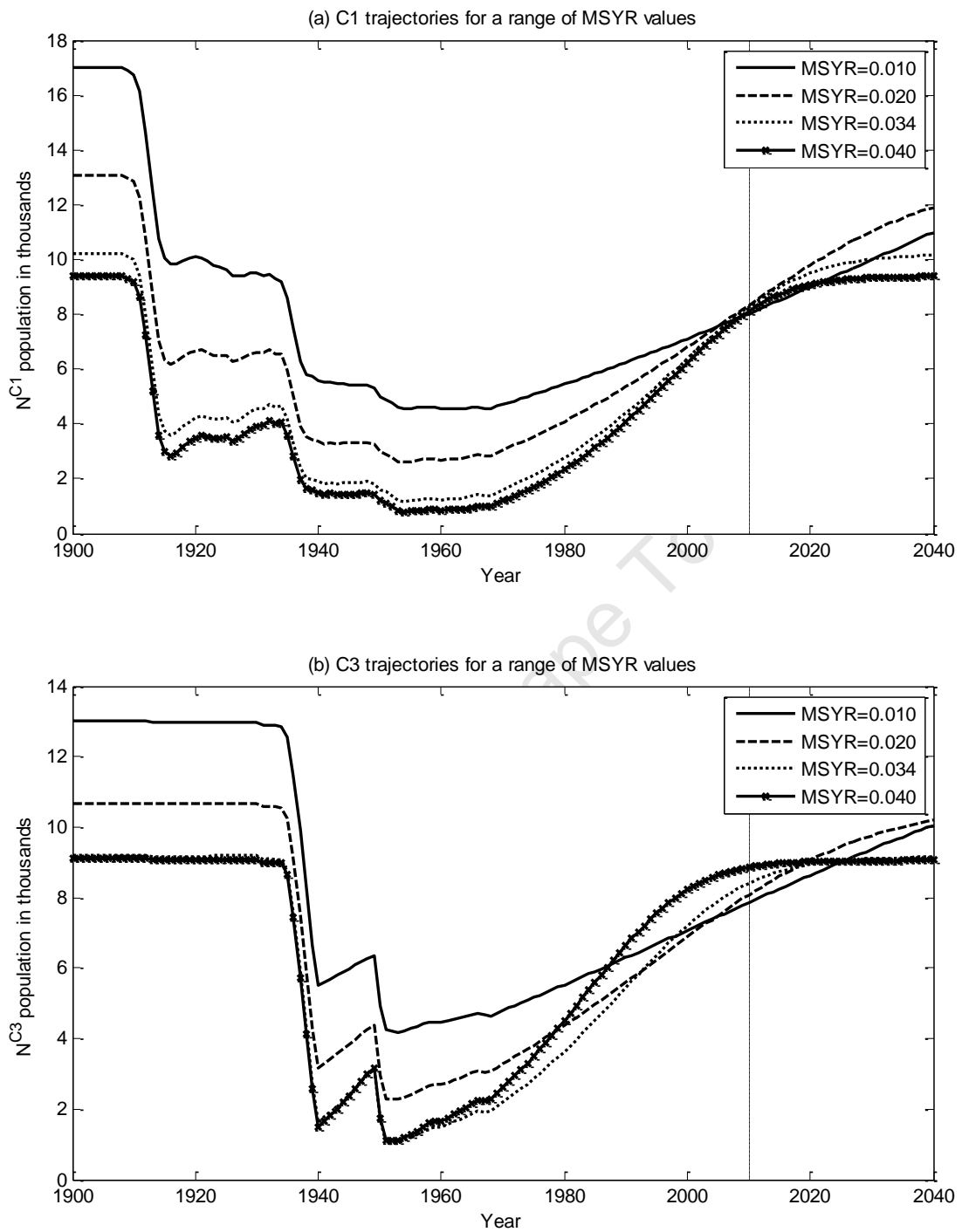


**Figure A4.3.2 (a) and (b):** C1 and C3 median trajectories for a range of MSYR(1+) values. Values to the right of the vertical dashed line represent projections into the future under the assumption of zero catch.

## 5 Exploration of stock-structure models for the Southern Hemisphere humpback whale Breeding Stock B

### 5.1 INTRODUCTION

The humpback whale population that is found off the west coast of Africa is known within the International Whaling Commission's Scientific Committee (IWC SC) as Breeding Stock B (BSB). Humpback whales are migratory animals, usually utilising low latitude regions for winter breeding and high latitude regions for summer feeding (IWC, 2006b). Available data relating to the behaviour of the humpback whales off the African west coast appear consistent with different assumptions as to what activities (migrating, breeding or feeding) take place in various locations off that coast. The coastal waters of Gabon, for example, have been identified by the IWC SC as a breeding ground (IWC, 2011). Geographically, western South Africa (WSA) would be expected to function as a migratory corridor; however, evidence of feeding, defecation, as well as a regular and lengthy presence of whales during summer suggests that the region may also serve as a summer feeding ground (IWC, 2006b; Barendse *et al.*, 2006). Historical catches taken in this region over the summer period support this postulate (IWC, 2006b; Barendse *et al.*, 2006). This summer feeding behaviour is unusual for the Southern Hemisphere humpback whales (which feed primarily in the high latitudes in the Antarctic); however the existence of this low-latitude feeding ground may be a result of the productivity associated with the Benguela upwelling system (IWC, 2006b; Barendse *et al.*, 2006; IWC, 2009b).

The issue of possible stock sub-structure arose when genetic evidence (Barendse *et al.*, 2006; Carvalho *et al.* 2010) showed statistically significant (at the 5% level) differences between the whales found in Gabon waters and those off the west coast of South Africa. Two hypotheses were put forward (IWC, 2011):

1. Breeding Stock B actually consists of two sub-stocks, B1 and B2. B1 is thought to winter (and breed) along the central African west coast and around the northern islands of the Gulf of Guinea (IWC, 2006b). B2 is thought to migrate northwards close to the west coast of Africa, possibly through the breeding ground of B1, but its own breeding ground is unknown (IWC, 2011).
2. There is only one breeding stock, but maternally directed fidelity<sup>38</sup> to feeding grounds accounts for the genetic differences (IWC, 2011).

Much debate in the IWC SC has centred on these two hypotheses and the general discussion of stock-structure. At an intersessional workshop in Hobart, April 2006, it was agreed to set the border between B1 and B2 at 18°S.

Figure 5.1 shows the known Breeding Stock B territory off the African coast as well as the hypothesised breeding stock sub-structuring.

---

<sup>38</sup> Maternally directed fidelity occurs when a now fully-grown calf continues to follow the same migratory route as it followed with its mother.

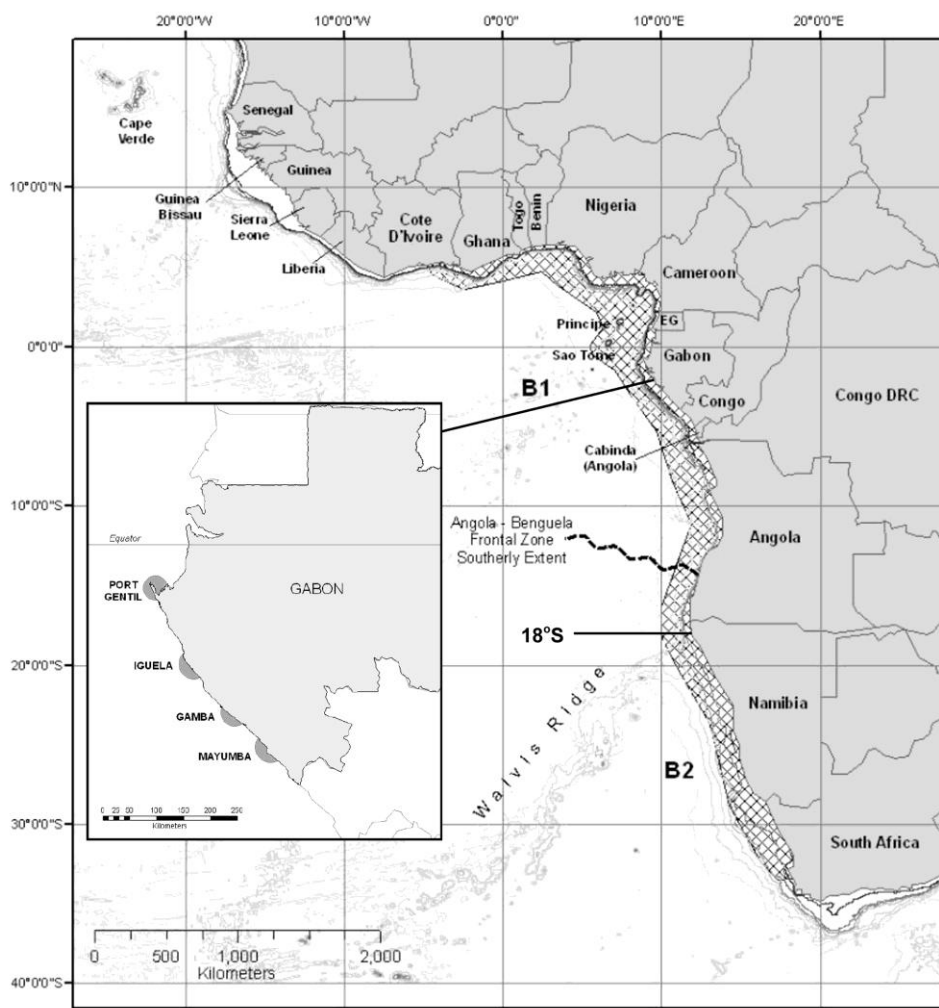


**Figure 5.1:** Distribution of humpback whale Breeding Stock B in western Africa, adapted from Collins *et al.* (2008). The four field sites on the coast of Gabon are indicated (see Section 5.2.2).

In 2009, the completion of the assessment of Breeding Stock B was made a priority by the IWC SC and the sub-committee for Southern Hemisphere humpback whales recommended the development of population dynamic models to test the implications of different stock-structure hypotheses (IWC, 2010). Müller *et al.* (2010) proposed three models for a preliminary exploration of these implications, and the corresponding assessments form a contribution to this thesis. The detailed descriptions, diagrammatic representations, as well as the equations setting out the population dynamics of these models are given in Section 5.3.1.

The models and their results were presented at the 63<sup>rd</sup> Meeting of IWC SC, Morocco, June 2010 (Müller *et al.*, 2010). Following discussion within the sub-committee responsible for issues pertaining to the SH humpback whales, two of the three models were no longer considered plausible<sup>39</sup> in light of new genetic and photographic data that had been presented at the meeting (IWC, 2011). The results will, however, still be reported on in this thesis as they provide a convenient comparative background. Six additional models were developed and the corresponding assessments carried out during the meeting. The results suggested that the various stock-structure hypotheses had little impact on the estimated status of sub-stock B1, breeding off Gabon, but they did have a

<sup>39</sup> The reasons are given in Section 5.3.

substantial impact on the other (smaller) sub-stock (B2), found off WSA (IWC, 2011). While time constraints at the meeting prevented further model developments, the sub-committee did however agree on nine final stock-structure hypotheses (three with high priority and the remaining six to be considered for sensitivity purposes) that would likely be the most informative for assessments (IWC, 2011). Assessments in terms of these models are to be carried out before the 2011 IWC SC meeting, during which the final assessment of Breeding Stock B is planned to be completed. The assessments of the three priority models have been undertaken as part of this thesis, and these models as well as their results are presented here.

## 5.2 DATA

### 5.2.1 Historic Catch data

There are two sources of historic catch data that relate to populations B1 and B2. Appendix 3.1 gives the details of the catch hypothesis currently in use for humpback assessments and presents the catch series on record.

#### i) Catches north of 40°S

B1: The catches taken north of 18°S: those from “Congo”, “Congo/Ang”, and “Angola” from Allison’s database (C. Allison, *pers. comm.*).

B2: The catches taken south of 18°S: those from “Namib” and “SWCap” from Allison’s database (C. Allison, *pers. comm.*).

Records of a series of Russian catches are also available for 10 degree longitude and latitude bands (C. Allison, *pers. comm.*). Catches for 20°W-10°E have been allocated to Breeding Stock B with catches taken above 18°S allocated to B1 and those below 18°S to B2. Figure A3.1.1 of Appendix 3.1 shows the geographical location of the regions associated with Breeding Stock B.

#### ii) Catches south of 40°S

These catches include both B1 and B2 whales. Table A3.1.2 of Appendix 3.1 reports this historic catch series.

### 5.2.2 Absolute abundance data

Photographs and biopsies were collected from four field sites on the coast of Gabon, and data from two sites (Iguela and Mayumba, see Figure 5.1) were analysed (Collins *et al.*, 2008). An absolute abundance estimate for B1 is available from the application of MARK to the photo-ID (fluke) capture-recapture data from Iguela only<sup>40</sup> (lower estimate of 6432 in 2003, CV=0.18) and the genetic data from Iguela only (upper estimate of 7196 in 2003, CV=0.15). Recent capture-recapture data for B2 have been used to obtain a ball-park estimate of 500 for 2004 for B2.<sup>41</sup>

### 5.2.3 Capture-recapture data

#### Data for B1

The capture-recapture data used here are as reported in Collins *et al.* (2008). Photographs and biopsies were collected from the coastal waters of Gabon during the austral winter (July-October) in each year between 2001 and 2006. The data used in these assessments are based on fluke feature identifications<sup>42</sup> from several sites and are reported in Table A3.2.6 of Appendix 3.2.

#### Data for B2

Recent capture-recapture data (Barendse *et al.*, 2010) have led to the results presented in Table A3.2.10 and Table A3.2.11 of Appendix 3.2. These data came from an electronic image database compiled for humpback whales photographed off the west coast of South Africa. Information is recorded when positive identification matches are made using fluke features and right or left dorsal fin features and microsatellite data. Varying combinations of these features have been used in the assessments conducted for the IWC SC.

---

<sup>40</sup> Estimates using data from all four sites were considered unreliable for several reasons (Collins *et al.* 2008).

<sup>41</sup> The number of humpback whales found off WSA is estimated to be between 200 (using genetic microsatellite data) to 300 (using left-dorsal fin photographic data), but not exceeding 500 (J. Barendse, *pers. comm.*). The ball-park estimate used here thus represents an upper limit for the numbers of humpbacks off WSA. This value, however, should not have a substantial effect on the assessment results, as its role is merely to reduce an otherwise very large uniform prior distribution in the interest of computational efficiency.

<sup>42</sup> There has been much debate within the IWC SC as to which data are the best to use: photo-ID (using flukes, right- or left-dorsal), or genetic (microsatellite) data. It has been argued that only a proportion of a whale population show their tail flukes, and that fluke estimates thus give an under-estimate (Barendse *et al.*, 2010). Barendse *et al.*, (2010) also note that estimates arising from right-dorsal fin data may be positively biased owing to possible higher numbers of false negatives. The IWC SC sub-committee for SH humpback whales considered that microsatellite based estimates would likely be the least biased, provided that a correction is made for genotype matching errors (IWC, 2010). It was agreed that if no such correction could be made, fluke data would be used, as has been done here for these assessments.

## 5.3 METHODS

### 5.3.1 Model dynamics

Diagrammatic representations, as well as the model descriptions and details of the dynamics for the six models presented in this thesis are given below. Table 5.1 below provides the explanations of the symbols used in this section.

**Table 5.1:** List of symbol explanations for the model descriptions in Section 5.3.1.

$N_y^B$	is the number of whales in the single breeding population B at the start of year $y$ ,
$N_y^{B1}$	is the number of whales in the breeding population B1 at the start of year $y$ ,
$N_y^{B2}$	is the number of whales in the breeding population B2 at the start of year $y$ ,
$N_y^{B1,W}$	is the number of whales in the western sub-stock of B1 at the start of year $y$ ,
$N_y^{B1,E}$	is the number of whales in the eastern sub-stock of B1 at the start of year $y$ ,
$r^{B1}$	is the intrinsic growth rate <sup>43</sup> for B1,
$r^{B2}$	is the intrinsic growth rate for B2,
$K^B$	is the carrying capacity for the single population B,
$K^{B1}$	is the carrying capacity for population B1,
$K^{B2}$	is the carrying capacity for population B2,
$\mu$	is the “degree of compensation” parameter, which is set at 2.39, and hence fixes the MSY level to $MSYL=0.6K$ , as conventionally assumed by the IWC SC,
$C_y^B$	is the total catch from population B (in terms of animals) in year $y$ ,
$C_y^{B1}$	is the total catch from population B1 (in terms of animals) in year $y$ ,
$C_y^{B2}$	is the total catch from population B2 (in terms of animals) in year $y$ ,
$C_y^{B1,W}$	is the total number of western B1 animals caught in year $y$ ,
$C_y^{B1,E}$	is the total number of eastern B1 animals caught in year $y$ ,
$C_y^G$	is the catch taken in the Gabon breeding area in year $y$ ,
$C_y^{WSA}$	is the catch taken off west South Africa in year $y$ , and
$C_y^A$	is the high latitude southern feeding grounds catch taken in year $y$ .

<sup>43</sup> The intrinsic growth rate is the maximum per capita growth rate the population can achieve when its size is very low.

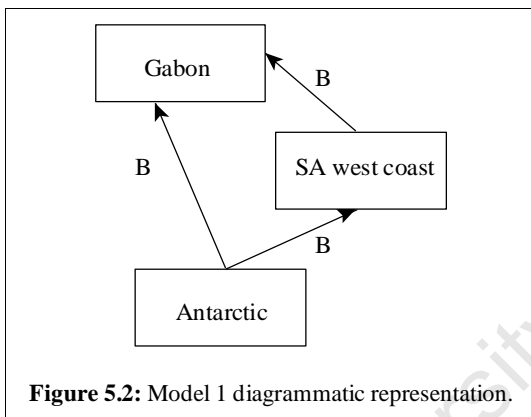
**Models 1-3 proposed for IWC SC 62, Morocco 2010***Trend data utilised for Models 1-3*

The capture-recapture data used for B1 are the data for all sites combined, and includes both photo-ID and genetic information (Table A3.2.6 of Appendix 3.2). The capture-recapture data used for B2 are the data from matches using the right dorsal fin features for identification as well as the microsattelites matches (Table A3.2.10 of Appendix 3.2).

Note that the input data used here were discussed and updated at IWC 62 for incorporation into consequent models (discussed later).

*N<sub>min</sub> constraints*

For these initial illustrative assessments, an arbitrary N<sub>min</sub> constraint of 400 was applied to B1 and a constraint of 10 to B2.

*5.3.1.1 Model 1*

**Figure 5.2:** Model 1 diagrammatic representation.

*Model description:*

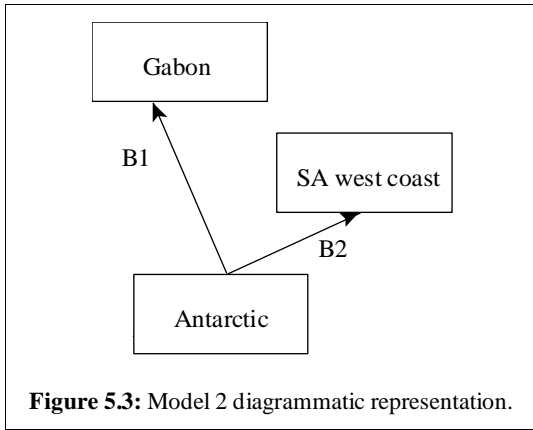
Model 1 assumes only one breeding stock (i.e. B1 and B2 are combined as one homogeneous population). The population splits as it departs from high latitude feeding grounds, and follows two migratory routes to the breeding area off Gabon.

**Table 5.2:** Breeding stock dynamics, catch equations and trend data information for Model 1.

<i>Breeding stock population dynamics:</i>	$N_{y+1}^B = N_y^B + r^B N_y^B \left( 1 - \left( \frac{N_y^B}{K^B} \right)^\mu \right) - C_y^B \quad (5.1)$
<i>Catches:</i>	$C_y^B = C_y^G + C_y^{WSA} + C_y^A \quad (5.2)$
<i>Trend data:</i>	The model is fit to the Gabon capture-recapture data (photo-ID and genetic) and an $N_{min}$ constraint of 400 has been applied.

*Note: Model 1 was considered implausible by the working group at IWC SC 62 since it assumes that the whales found in WSA waters and off Gabon are from the same breeding stock (when genetic differences indicating separate breeding stocks have in fact been found (Rosenbaum et al., 2006a; Carvalho et al., 2010)).*

5.3.1.2 Model 2



*Model description:*

Model 2 assumes two independent breeding populations which mix for feeding in the Antarctic. Breeding population B1 then migrates northwards to its breeding area in Gabon, whereas breeding population B2 migrates along the coast of WSA to its breeding grounds.

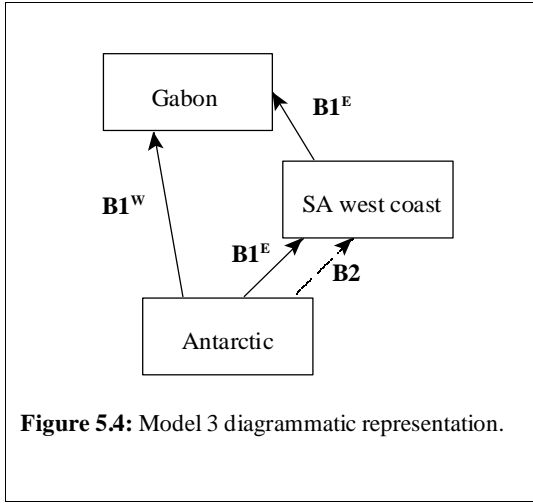
**Figure 5.3:** Model 2 diagrammatic representation.

**Table 5.3:** Breeding stock dynamics, catch equations and trend data information for Model 2.

<i>Breeding stock population dynamics:</i>	$N_{y+1}^{B2} = N_y^{B2} + r^{B2} N_y^{B2} \left( 1 - \left( \frac{N_y^{B2}}{K^{B2}} \right)^\mu \right) - C_y^{B2} \quad (5.3)$
	$N_{y+1}^{B1} = N_y^{B1} + r^{B1} N_y^{B1} \left( 1 - \left( \frac{N_y^{B1}}{K^{B1}} \right)^\mu \right) - C_y^{B1} \quad (5.4)$
<i>Catches:</i>	$C_y^{B1} = C_y^G + p_y C_y^A \quad (5.5)$ $C_y^{B2} = C_y^{WSA} + (1 - p_y) C_y^A \quad (5.6)$ <p>where <math>p_y = \frac{N_y^{B1}}{N_y^{B1} + N_y^{B2}}</math>, i.e. the catches from each stock are proportional to their relative abundances (full mixing).</p>
<i>Trend data:</i>	<p>Gabon capture-recapture data (photo-ID and genetic) are fit and an <math>N_{min}</math> constraint of 400 applied to <math>N_y^{B1}</math>, and the WSA data (right dorsal fin and microsatellite) are fit and an <math>N_{min}</math> constraint of 10 applied to <math>N_y^{B2}</math>.</p>

*Note: Model 2 was considered implausible by the working group at IWC SC 62 as it does not allow for any movement between WSA and Gabon, when gene flow has in fact been observed from WSA to Gabon (IWC, 2011).*

## 5.3.1.3 Model 3



## Model description:

Model 3 assumes two breeding populations, B1 and B2, as for Model 2. B1 is however assumed to be comprised of two sub-stocks, one of which ( $B1^E$ ) passes through the WSA coastal waters before going to Gabon, while the other ( $B1^W$ ) migrates directly to the Gabon breeding region. Given the carrying capacity for B1,  $K^{B1}$ , the carrying capacities for its sub-stocks are given by:

$$K^{B1,W} = XK^{B1} \quad \text{and} \quad K^{B1,E} = (1-X)K^{B1}$$

where  $X$  is a fixed parameter.

**Table 5.4:** Breeding stock dynamics, catch equations and trend data information for Model 3.

Breeding stock population dynamics:	$N_{y+1}^{B1,W} = N_y^{B1,W} + r^{B1} N_y^{B1,W} \left( 1 - \left( \frac{N_y^{B1,W} + N_y^{B1,E}}{K^{B1}} \right)^\mu \right) - C_y^{B1,W} \quad (5.7)$
	$N_{y+1}^{B1,E} = N_y^{B1,E} + r^{B1} N_y^{B1,E} \left( 1 - \left( \frac{N_y^{B1,W} + N_y^{B1,E}}{K^{B1}} \right)^\mu \right) - C_y^{B1,E} \quad (5.8)$
	$N_{y+1}^{B2} = N_y^{B2} + r^{B2} N_y^{B2} \left( 1 - \left( \frac{N_y^{B2}}{K^{B2}} \right)^\mu \right) - C_y^{B2} \quad (5.9)$
Catches:	$C_y^{B1,W} = \frac{N_y^{B1,W}}{N_y^{B1,W} + N_y^{B1,E}} C_y^G + \frac{N_y^{B1,W}}{N_y^{B1,W} + N_y^{B1,E} + N_y^{B2}} C_y^A \quad (5.10)$
	$C_y^{B1,E} = \frac{N_y^{B1,E}}{N_y^{B1,W} + N_y^{B1,E}} C_y^G + \frac{N_y^{B1,E}}{N_y^{B1,E} + N_y^{B2}} C_y^{WSA} + \frac{N_y^{B1,E}}{N_y^{B1,W} + N_y^{B1,E} + N_y^{B2}} C_y^A \quad (5.11)$
	$C_y^{B2} = \frac{N_y^{B2}}{N_y^{B1,E} + N_y^{B2}} C_y^{WSA} + \frac{N_y^{B2}}{N_y^{B1,W} + N_y^{B1,E} + N_y^{B2}} C_y^A \quad (5.12)$
Trend data:	<p>Gabon data (photo-ID and genetic) are fit and an <math>N_{min}</math> constraint of 400 applied to <math>N_y^{B1,W} + N_y^{B1,E}</math>, and WSA data (right dorsal fin and microsatellite) are fit and an <math>N_{min}</math> constraint of 10 applied to <math>N_y^{B1,E} + N_y^{B2}</math>.</p>

**Priority Models Ia-IIIa identified by the Scientific Committee at IWC SC 62 in June 2010**

*Trend data utilised for Models Ia-IIIa*

IWC (2011) recommended that microsatellite data should be used for the reference case, but only if genotyping errors can be incorporated into the assessment models. As the data to quantify such errors are not available at this point, the photo-ID data using flukes for identification have been used (as recommended in IWC, 2011). Thus the Gabon population is fitted to the photo-ID data from all sites combined (as before) and the WSA population is fitted to new photo-ID data using fluke features from the coast of WSA (Barendse *et al.*, 2010, see Table A3.2.11 of Appendix 3.2).

*N<sub>min</sub> constraints*

An  $N_{min}$  constraint of 272 has been applied to the whale population found in Gabon and a constraint of 96 to the whale population passing through the coastal waters of WSA, as recommended in IWC (2011).

University of Cape Town

## 5.3.1.4 Model Ia

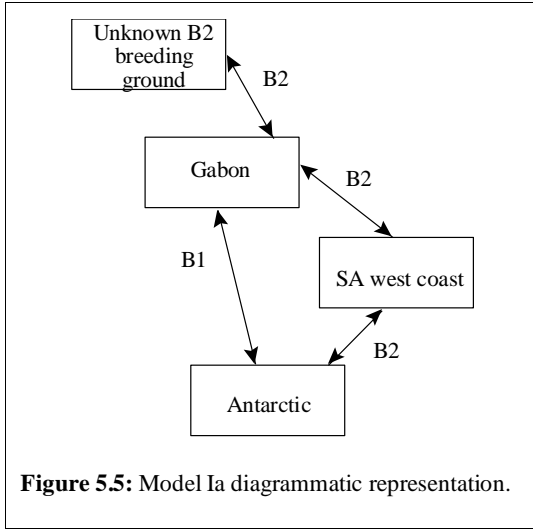


Figure 5.5: Model Ia diagrammatic representation.

## Model description:

Model Ia assumes two independent breeding sub-stocks which can mix on Antarctic feeding grounds. Whales from breeding sub-stock B1 feed in the Antarctic and migrate to Gabon for breeding. Whales from breeding sub-stock B2 feed off WSA and migrate along the West African coast through Gabon to a separate unidentified breeding ground. Additionally, some portion of B2 animals migrate to the Antarctic feeding grounds.

Table 5.5: Breeding stock dynamics, catch equations and trend data information for Model Ia.

Breeding stock population dynamics:	$N_{y+1}^{B1} = N_y^{B1} + r^{B1}N_y^{B1} \left[ 1 - \left[ \frac{N_y^{B1}}{K^{B1}} \right]^\mu \right] - C_y^{B1} \quad (5.13)$
	$N_{y+1}^{B2} = N_y^{B2} + r^{B2}N_y^{B2} \left[ 1 - \left[ \frac{N_y^{B2}}{K^{B2}} \right]^\mu \right] - C_y^{B2} \quad (5.14)$
Catches:	$C_y^{B1} = p_y^{A,B1}C_y^A + p_y^{G,B1}C_y^G \quad (5.15)$
	$C_y^{B2} = p_y^{A,B2}C_y^A + C_y^{WSA} + p_y^{G,B2}C_y^G \quad (5.16)$ <p>where the proportions <math>p_y^{A/G, B1/B2}</math> are proportional splits of catches by sub-stock, given by:</p> $p_y^{A,B1} = \frac{N_y^{B1}}{N_y^{B1} + p_1 N_y^{B2}} \quad \text{and} \quad p_y^{A,B2} = \frac{p_1 N_y^{B2}}{N_y^{B1} + p_1 N_y^{B2}}$ $p_y^{G,B1} = \frac{N_y^{B1}}{N_y^{B1} + p_2 N_y^{B2}} \quad \text{and} \quad p_y^{G,B2} = \frac{p_2 N_y^{B2}}{N_y^{B1} + p_2 N_y^{B2}}$ <p>and <math>p_1</math> is the proportion of B2 animals that migrate to the Antarctic (set at 0.5). <math>p_2</math> is the probability of sighting (or catching) a B2 animal as it transits through the Gabon breeding area relative to the probability for a B1 animal in that area (<math>p_2</math> has been set at 0.5).</p>
Trend data:	<p>Gabon data (photo-ID and genetic) are fit and an <math>N_{min}</math> constraint of 272 applied to <math>N_y^{B1} + p_2 N_y^{B2}</math>, and the WSA data (flukes) are fit and an <math>N_{min}</math> constraint of 96 applied to <math>N_y^{B2}</math>.</p>

## 5.3.1.5 Model IIa

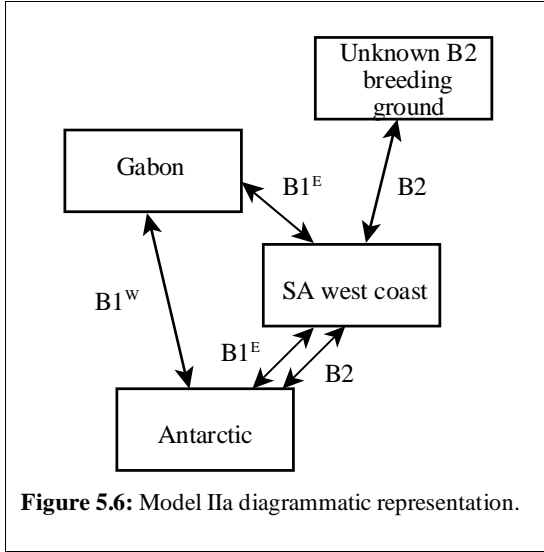


Figure 5.6: Model IIa diagrammatic representation.

Model IIa assumes two breeding sub-stocks B1 and B2. B1 has two migratory components B1<sup>W</sup> and B1<sup>E</sup>. Whales from B1<sup>W</sup> migrate from the Antarctic feeding grounds directly to Gabon while whales from B1<sup>E</sup> migrate through the waters off WSA before continuing onto the Gabon breeding grounds. Whales from sub-stock B2 feed primarily off WSA and do not migrate past Gabon but instead to a separate unidentified breeding area. In addition, some portion of animals from sub-stock B2 migrates to Antarctic feeding grounds. Given the carrying capacity for B1, the carrying capacities for its sub-stocks are given by:

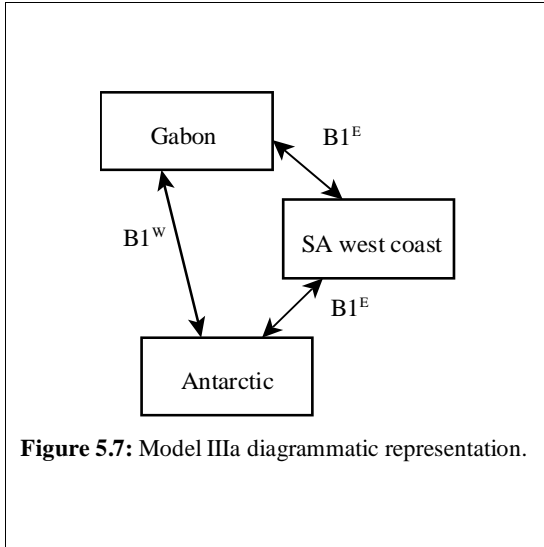
$$K^{B1,W} = XK^{B1} \quad \text{and} \quad K^{B1,E} = (1 - X)K^{B1}$$

where  $X$  is a fixed parameter.

Table 5.6: Breeding stock dynamics and catch equations for Model IIa.

Breeding stock population dynamics:	$N_{y+1}^{B1,W} = N_y^{B1,W} + r^{B1} N_y^{B1,W} \left[ 1 - \left[ \frac{N_y^{B1,W} + N_y^{B1,E}}{K^{B1}} \right]^\mu \right] - C_y^{B1,W} \quad (5.17)$
	$N_{y+1}^{B1,E} = N_y^{B1,E} + r^{B1} N_y^{B1,E} \left[ 1 - \left[ \frac{N_y^{B1,W} + N_y^{B1,E}}{K^{B1}} \right]^\mu \right] - C_y^{B1,E} \quad (5.18)$
	$N_{y+1}^{B2} = N_y^{B2} + r^{B2} N_y^{B2} \left[ 1 - \left[ \frac{N_y^{B2}}{K^{B2}} \right]^\mu \right] - C_y^{B2} \quad (5.19)$
Catches:	$C_y^{B1,W} = p_y^{A,B1,W} C_y^A + p_y^{G,B1,W} C_y^G \quad (5.20)$
	$C_y^{B1,E} = p_y^{A,B1,E} C_y^A + p_y^{WSA,B1,E} C_y^{WSA} + p_y^{G,B1,E} C_y^G \quad (5.21)$
	$C_y^{B2} = p_y^{A,B2} C_y^A + p_y^{WSA,B2} C_y^{WSA} \quad (5.22)$
	<p>where <math>p_y^{A/G/WSA, B1,W/B1,E/B2}</math> are proportional splits of catches by sub-stock:</p> $p_y^{A,B1,W} = \frac{N_y^{B1,W}}{N_y^{B1,W} + N_y^{B1,E} + p_1 N_y^{B2}}$ $p_y^{A,B1,E} = \frac{N_y^{B1,E}}{N_y^{B1,W} + N_y^{B1,E} + p_1 N_y^{B2}}$ $p_y^{A,B2} = \frac{p_1 N_y^{B2}}{N_y^{B1,W} + N_y^{B1,E} + p_1 N_y^{B2}}$ $p_y^{G,B1,W} = \frac{N_y^{B1,W}}{N_y^{B1,W} + N_y^{B1,E}} \quad \text{and} \quad p_y^{G,B1,E} = \frac{N_y^{B1,E}}{N_y^{B1,W} + N_y^{B1,E}}$ $p_y^{WSA,B1,E} = \frac{N_y^{B1,E}}{N_y^{B1,E} + N_y^{B2}} \quad \text{and} \quad p_y^{WSA,B2} = \frac{N_y^{B2}}{N_y^{B1,E} + N_y^{B2}}$ <p>and <math>p_1</math> is the proportion of B2 animals that migrate to the Antarctic, set at 0.5.</p>
Trend data:	<p>Gabon data (photo-ID and genetic) are fit and <math>N_{min}</math> constraint of 272 applied to <math>N_y^{B1,W} + N_y^{B1,E}</math>, and the WSA data (flukes) are fit and <math>N_{min}</math> constraint of 96 applied to <math>N_y^{B2} + N_y^{B1,E}</math>.</p>

## 5.3.1.6 Model IIIa



Model IIIa assumes a single breeding stock, B1, with two migratory components B1<sup>W</sup> and B1<sup>E</sup>. B1<sup>W</sup> migrates directly to Gabon from Antarctic feeding grounds, while B1<sup>E</sup> migrates through waters off WSA before continuing on to the Gabon breeding grounds. In this assessment the proportion of animals using each migratory route does not change with time (other than as a result of the differential impact of catches). Given the carrying capacity for B1, the carrying capacities for its sub-stocks are given by:

$$K^{B1,W} = XK^{B1} \quad \text{and} \quad K^{B1,E} = (1-X)K^{B1}$$

where  $X$  is a fixed parameter.

**Table 5.7:** Breeding stock dynamics and catch equations for Model IIIa

<i>Breeding stock population dynamics:</i>	$N_{y+1}^{B1,W} = N_y^{B1,W} + r^{B1} N_y^{B1,W} \left[ 1 - \left[ \frac{N_y^{B1,W} + N_y^{B1,E}}{K^{B1}} \right]^\mu \right] - C_y^{B1,W} \quad (5.23)$
	$N_{y+1}^{B1,E} = N_y^{B1,E} + r^{B1} N_y^{B1,E} \left[ 1 - \left[ \frac{N_y^{B1,W} + N_y^{B1,E}}{K^{B1}} \right]^\mu \right] - C_y^{B1,E} \quad (5.24)$
<i>Catches:</i>	$C_y^{B1,W} = p_y^{A,B1,W} C_y^A + p_y^{G,B1,W} C_y^G \quad (5.25)$ $C_y^{B1,E} = p_y^{A,B1,E} C_y^A + C_y^{WSA} + p_y^{G,B1,E} C_y^G \quad (5.26)$ <p>where the proportions <math>p_y^{A/G, B1,W/B1,E}</math> are proportional splits of catches by sub-stock, given by:</p> $p_y^{A,B1,W} = \frac{N_y^{B1,W}}{N_y^{B1,W} + N_y^{B1,E}} \quad \text{and} \quad p_y^{A,B1,E} = \frac{N_y^{B1,E}}{N_y^{B1,W} + N_y^{B1,E}}$ $p_y^{G,B1,W} = \frac{N_y^{B1,W}}{N_y^{B1,W} + N_y^{B1,E}} \quad \text{and} \quad p_y^{G,B1,E} = \frac{N_y^{B1,E}}{N_y^{B1,W} + N_y^{B1,E}}$
<i>Trend data:</i>	<p>Gabon data (photo-ID and genetic) are fit and an <math>N_{min}</math> constraint of 272 applied to <math>N_y^{B1,W} + N_y^{B1,E}</math>, and the WSA data (flukes) are fit and an <math>N_{min}</math> constraint of 96 applied to <math>N_y^{B1,E}</math>.</p>

### 5.3.2 Bayesian framework

The standard Bayesian SIR<sup>44</sup> approach commonly used in humpback assessments has been implemented for all the Breeding Stock B models. Information specific to the prior distributions assumed for these assessments is given below.

Prior distributions are defined as follows for the intrinsic growth rate  $r$  and the target abundance estimate  $N_{target}^{i,obs}$ :

- i)  $r^i \sim U[0, 0.106]$
- ii)  $\ln \tilde{N}_{target}^{i,obs} \sim U[\ln N_{target}^{i,obs} - 4CV, \ln N_{target}^{i,obs} + 4CV]$ .

(For models where the breeding stock is split into B1 and B2,  $i$  can reflect either B1 or B2. For Models assuming only one breeding population,  $i = B1$ .)

The uninformative  $r$  prior is bounded by zero (negative rates of growth are biologically implausible) and 0.106 (corresponding to the maximum growth rate for the species agreed by the IWC Scientific Committee (IWC, 2008)). The prior distribution from which target abundance estimate  $\tilde{N}_{target}^{i,obs}$  is drawn at random is assumed to be uniform on a natural logarithmic scale. The lower and upper bounds are set by the CV multiplied by four. The target abundance estimate used for B1 is the 2003 estimate of 7196 (CV=0.18) (Collins *et al.*, 2008), and the B2 capture-recapture data have been used to provide a B2 ball-park estimate for 2004 of 500 (CV=0.3) (see footnote 41).

### 5.3.3 Likelihood function

The capture-recapture data have been incorporated into the likelihood using a Poisson distribution (see Section 3.3.2.3 for more details) and make the following contribution to the negative log likelihood:

$$\sum_i \sum_j \sum_{y=y_0}^{y_f-1} \sum_{y'=y+1}^{y_f} [-m_{y,y'}^{i,j} \ln \hat{m}_{y,y'}^{i,j} + \hat{m}_{y,y'}^{i,j}] \quad (5.27)$$

where

$m_{y,y'}^{i,j}$  is the number of animals captured in year  $y$  in region  $i$  that were recaptured in year  $y'$  in region  $j$ ,

$\hat{m}_{y,y'}^{i,j}$  is the model-predicted number of animals captured in year  $y$  in region  $i$  that were recaptured in year  $y'$  in region  $j$ , and

$y_0$  is the first year of captures and  $y_f$  is the last year of recaptures.

Note that the absolute abundance estimates have not been incorporated into the final likelihood function<sup>45</sup>. Since there are no relative abundance data available for Breeding Stock B, the capture-recapture data are therefore the only data used in the final likelihood evaluation.

<sup>44</sup> For more details on this approach, see Chapter 2.

### 5.3.4 $N_{min}$ constraints

Estimates of the current number of mitochondrial haplotypes present in the Gabon and WSA populations were made available at IWC SC 62 (see Table A5.1.1 of Appendix 5.1). If the model-estimated population size drops below the  $N_{min}$  constraints arising from these numbers, a large penalty is added to the negative log-likelihood function so that parameter values that result in population trajectories that do not adhere to the constraint are excluded.

## 5.4 RESULTS

### Convergence

Table 5.9 reports the results of three convergence diagnostics tested. These results suggest that the SIR Bayesian integration process has converged for all six models.

### General assessment results

The tables and figures presenting the assessment results and population trajectories for each of the six models are summarised in Table 5.8 below:

**Table 5.8:** Summary of the location of the assessment results and population trajectories for the six BSB models.

Model	Assessment results	Population trajectory
Model 1	Table 5.10	Figure 5.8
Model 2	Table 5.11	Figure 5.9 (a)-(b)
Model 3	Table 5.12 (a)-(b)	Figure 5.10 (a)-(d)
Model Ia	Table 5.13 (a)-(b)	Figure 5.11 (a)-(d)
Model IIa	Table 5.14 (a)-(d)	Figure 5.12 (a)-(d)
Model IIIa	Table 5.15 (a)-(d)	Figure 5.13 (a)-(c)

Table 5.10 to Table 5.15 give the Bayesian assessment results for the six models in the form of posterior medians and 90% probability intervals<sup>46</sup> for the  $r$  and  $K$  parameters, as well as for various population sizes expressed both in absolute terms and as a fraction of the pristine population size,  $K$ . The estimated extent of recovery to pristine level for 2040,  $N_{2040}/K$ , is presented, where  $N_{2040}$  is the projected population size in 2040 under the assumption of zero future catch. Where the  $X$  parameter was a component of the assessment, the results for a range of  $X$  values have been given.

<sup>45</sup> As the capture-recapture data underlying the absolute abundance estimates have been used in the likelihood, the estimates themselves cannot be included as well. They are however used as a reality check, as well as in the initial step of model fitting procedure (backwards method) where, given a random draw from the prior for  $r^{B1}$  and a target recent abundance estimate, a corresponding value of  $K^{B1}$  is found by fitting exactly to the drawn abundance estimate (see Appendix 3.3).

<sup>46</sup> Given the  $n$  samples drawn in the SIR re-sampling process, the probability envelopes are computed by taking, for each year, the 5<sup>th</sup> and 95<sup>th</sup> percentiles of the ordered  $n$  population sizes for that year. These yearly values form the envelopes shown in the figures. The envelopes can be interpreted as follows: if the model assumptions are correct, the input data reliable and the priors appropriately specified, then there is a 90% probability each year that the true population will be within the envelope.

Plots of the corresponding median population trajectories for the six models are shown in Figure 5.8 to Figure 5.13. For models incorporating the  $X$  value, the trajectories for a range of  $X$  values are shown on a single plot for comparison purposes. In these cases, only the median trajectories have been shown in the interest of clarity; the 90% probability interval has only been included in plots containing a single population trajectory. In general, these probability intervals are wide except over the period for which the capture-recapture data are available (see for example Figure 5.8). Also noticeable is that the upper limit to the envelope is much further from the median trajectory than the lower (again evident in Figure 5.8). This asymmetry is in part a consequence of the implementation of the  $N_{min}$  constraints, which prevent population trajectories reaching much lower levels than those indicated by the lower side of the probability envelope.

The general form of the population trajectories is similar for all the models, as it is largely determined by the historic catches. Taking Figure 5.8 as an example, it is clear that when substantial whaling commenced around 1910, the population was reduced rapidly in the first few years of that whaling episode. Successive drops in the trajectories (such as the ones occurring in the late 1930's and early 1950's) are a result of more substantial catches again occurring. The rate of recovery depends on the estimated growth rate,  $r$ , which can be seen for example in Table 5.13a, where B2 has a much lower estimated  $r$  value than B1. Comparison of the  $N_{2040}/K$  values shows that B2 consequently has a much slower rate of recovery. Plots showing the trajectory for the B1 (Gabon) breeding population also show the lower and upper abundance estimates based on the application of MARK to the capture-recapture data described in section 5.2.2. These estimates have not been included in the likelihood function; they are shown here merely as a reality check.

#### *Model comparison*

Table 5.16 gives, for each model, the estimated population numbers (at pristine levels) found in each of the regions of Gabon and WSA, as well as the total number of Breeding Stock B animals. The 2010 estimates, as well as estimates of current and future extent of recovery towards pristine abundance are also given. For those models where results are available for several values of  $X$ , plots include results for only one such value, selected to be reasonably representative.<sup>47</sup> The corresponding median trajectories are shown in Figure 5.14 (a)-(c).

#### *Fit to capture-recapture data*

Unlike abundance estimates, capture-recapture data cannot be displayed on the population trajectory plots. Instead, estimated cumulative recapture numbers can be plotted against those observed. For each year, these estimates record the total number of accumulated recaptures that have taken place up to (and including) that year. Figure 5.15 (a)-(j) show the capture-recapture fits for Models 1-3 and Figure 5.16 (a)-(f) show those for Models Ia-IIIa. As for the population trajectory plots, the model-estimated median values are indicated with a solid line. For models without the  $X$  parameter, the 90% probability interval is shown; otherwise the median trajectories for a range of  $X$  values are shown on a single plot for comparison purposes.

<sup>47</sup> Recall that  $(1-X)$  is the proportion of B1 animals that migrate through the waters off WSA.  $X=0.8$  (i.e.  $1-X=0.2$ ) was chosen for Model 3 and Model IIa, as there is a B2 component present in these two models, and thus a smaller proportion of B1 animals is required to migrate through WSA to make up the numbers indicated by the data. A lower value of  $X=0.6$  (i.e.  $1-X=0.4$ ) was chosen for Model IIIa, as there is no B2 component there, and numbers observed off WSA need to be made up of the B1 animals migrating through WSA waters.

In general, the cumulative recapture numbers for the Gabon genetic data are fit well by the model estimates (see Figure 5.15 (b), (d) and (h), and Figure 5.16 (a), (c) and (e)). The cumulative recapture numbers from the photo-ID data are generally less consistent with the model predictions. The value of  $X$  makes little difference to the fit to the Gabon genetic data (for Model 3, see Figure 5.15 (h)), and to the Gabon photo-ID data (Models 3, IIa and IIIa, see Figure 5.15 (g) and Figure 5.16 (a), (c) and (e)). Alternative choices for  $X$  do however have a substantial effect on the fit to the WSA data, both photo-ID and genetic (see Figure 5.15 (i) and (j), and Figure 5.16 (b), (d) and (f)).

#### *$N_{min}$ constraints and prior incoherence*

Figure 5.17 (a)-(b) show the post-model, pre-data distributions for Model Ia without and with the re-sampling approach (see Appendix 5.2). This figure serves to illustrate how the re-sampling approach has helped reduce (though not eliminate) the problem of prior incoherence encountered in Models Ia-IIIa. The topic of prior incoherence is discussed in more detail below.

## 5.5 DISCUSSION

### *General assessment results*

Based on these assessments, current population status ( $N_{2010}/K$ ) ranges from 0.19 to 0.49 for the total Breeding Stock B population in posterior median terms (see Table 5.16). The extent of recovery towards pristine abundance by 2040 ranges from 0.26 to 1.00. This range is rather wide, as is the case for the estimated  $r$  values (see Table 5.10-Table 5.15). Also noteworthy is the fact that the growth rates estimated for B1 and B2 are in some cases substantially different (see for example Table 5.13 (a)-(b)), which is unexpected. At this point, it is important to note that the impact of prior incoherence has not fully been eliminated, and as such these results have to be seen as preliminary. Previous initial assessments of Breeding Stock B gave current status ( $N_{2006}/K$ ) estimates ranging from 0.65-0.91 and estimated intrinsic growth rates ( $r$ ) ranging from 0.042-0.065 (Johnston and Butterworth, 2008a). While those assessments use what is now considered to be outdated input data, such a large discrepancy would not have been expected. This suggests that the problem of prior incoherence arising from the introduction of the new  $N_{min}$  constraints is indeed having a considerable effect on the results reported here (see later discussion on prior incoherence).

### *Model comparison*

Some general points to note are:

- Models 1-3 use different input data to Models Ia-IIIa, and as such results for the two sets of models are not directly comparable.
- Model 1 and Model IIIa have the same basic structure, but in Model 1 there is no maternally-linked migration route fidelity, i.e. any whale is as likely to take the west as the east migration route.
- Model 3 and Model IIa are in essence the same – except that in Model IIa the B2 animals do not breed in the WSA waters. The differences observed in Figure 5.14 (a)-(c) will have resulted from different input capture-recapture data, as well as the different  $N_{min}$  constraints.

- The  $N_{2040}/K$  values given for Models 3, IIa and IIIa (Table 5.12, Table 5.14 and Table 5.15 respectively) can be misleading, as there is one overall pristine population level that is estimated,  $K^{B1}$ , which is split into  $B1^W$  and  $B1^E$  components using the value for  $X$ . The growth of the individual sub-populations is limited by the total  $K^{B1}$  and as such it is possible for either one of the two sub-populations to exceed its initial population level (i.e.  $N_{2040}/K$  to exceed one), provided the other population is at a low level.

Table 5.16 shows that Model 3 (at  $X=0.6$ ) yielded the lowest pristine total Breeding Stock B population estimate (median value of 19 800) and Model IIIa (at  $X=0.8$ ) yielded the highest (median value of 34 799). For the representative  $X$  values chosen (see footnote 47), this range is reduced, now from 21059 (Model 3 at  $X=0.8$ ) to 25732 (Model IIa at  $X=0.8$ ). Figure 5.14 (a) illustrates that the models (and therefore stock-structure hypotheses) have little influence on the total estimated Breeding Stock B numbers. There is similarly an unsubstantial effect on the number of animals estimated to be in Gabon (the  $B1^W$  component is likely too large in each case for the stock-structure hypothesis to affect it substantially). The major difference arises in the number of whales estimated to be in the WSA waters, where there is a fair spread over the various models. This contrast is to be expected as the major difference in the six stock-structure hypotheses is which breeding populations and sub-populations migrate through the WSA waters. Given the above, it seems appropriate to conclude that these stock structure hypotheses serve primarily to assist an understanding of the implications of different behaviours of the whales, rather than to obtain substantially different estimates of current population status.

#### *Fit to capture-recapture data*

The worst fits to the capture-recapture data are those relating to WSA (see Figure 5.16). As there are several factors influencing the estimated population in this region (such as model dynamics, value of  $X$ , as well as capture-recapture data), it is difficult to determine what might be causing the poor fit. The value of  $X$  substantially influences the numbers whales estimated to be in the WSA waters, so it is not unexpected that it has an appreciable effect on the fit to the WSA data. While the fits in general to the WSA data are not good, a high value of  $X=0.8$  gives the best fit for Models 3, IIa and IIIa. It should be noted here that the probability envelopes shown reflect uncertainties in expected numbers as a result of estimation imprecision, and do not include the further variability associated with sampling variance.

#### *$N_{min}$ constraints and prior incoherence*

A problem was encountered with the implementation of the new  $N_{min}$  constraints set at IWC 62. For Models Ia and IIa the estimated minimum B2 population size frequently went below the prescribed minimum, normally for a low  $K^{B2}$  value<sup>48</sup> when generating trajectories from the  $r$  and  $K$  priors. Since  $(r^{B2}, K^{B2})$  combinations that violate the  $N_{min}$  constraint are excluded, the assessment results generally show a somewhat higher  $K^{B2}$  and a lower  $r^{B2}$  than would otherwise be the case (see Table 5.13a (case A) and Table 5.14b). The realised prior distributions are then not as uniform and uninformative as they were first assumed to be, an effect known as prior incoherence. This is described in more detail in Appendix 5.2.

<sup>48</sup> Note that the B1 population is large enough not to violate its  $N_{min}$  constraint and as such is not affected directly by this problem of prior incoherence.

In Appendix 5.2, a re-sampling approach (Approach 1) that was taken in an attempt to correct for the prior incoherence has also been outlined. The results of this approach (shown in Table 5.13b) are only moderately better, as the estimated  $r^{B2}$  value is still much lower than would be expected, given humpback growth rates estimated for other breeding stocks (Zerbini *et al.*, 2008 for example estimate growth rates for humpback whales ranging from 0.043 to 0.112). Figure 5.17 (a)-(b) however show that while the post-model, pre-data distributions of the alternative re-sampling approach (Figure 5.17 (b)) are by no means ideal, they are considerably better than the results without re-sampling (Figure 5.17 (a)). The issue has been raised with an intersessional working group of the IWC Scientific Committee and the  $N_{min}$  constraints are currently under review. Once this review has been finalised, further work will be carried out on the models, and the alternative approaches described in the Appendix will be explored more comprehensively. The final results will be presented at the 63<sup>rd</sup> meeting of the IWC Scientific Committee, Norway, June 2011. Unfortunately the slow-moving pace of an international collaboration has prevented these results from being ready for inclusion in this thesis, and as such the purpose of the results and discussion given here is to present the results to date and illustrate the problems encountered.

#### *Effect of the choice of a value X*

In general, increasing  $X$  decreases the estimated  $r^{B1}$  value and increases the estimated  $K^{B1}$  (see Table 5.12a, Table 5.14a and Table 5.15a). It is difficult to provide a simple explanation for this pattern, as there are numerous factors influencing the results, and furthermore the  $r$  and  $K$  parameters are inversely related.

For Model IIIa, which is simpler because there is no B2 component, the only animals found in WSA waters are the B1<sup>E</sup> animals. Thus if only a small proportion of B1 animals go east (i.e. if  $X$  is big) the total B1 population would need to be large to provide the numbers that have been observed in WSA. This relationship seems likely to be the primary cause of the observed effect of the  $X$  parameter. For Models 3 and IIa the situation is less clear, as the presence of an independent B2 stock in WSA implies less dependence on the B1<sup>E</sup> component for numbers. Nonetheless, the same effect is observed, though it is difficult to tell if the effect can be explained through similar reasoning as for Model IIIa.

## 5.6 FUTURE WORK

#### *$N_{min}$ constraints and prior incoherence*

Once consensus has been reached within the IWC SC intersessional group as to which  $N_{min}$  constraints are to be used for the assessments, these limits will replace the values currently used. Thereafter, the issue of prior incoherence will need to be re-evaluated. If a substantial issue remains, then the approach to a solution would involve further exploration and refinement of the re-sampling approach to attempt to achieve less informative post-model distributions for  $r$ , as well as the exploration of Approaches 2 and 3 of Appendix 5.2. Alternative treatments of the  $N_{min}$  constraints may also be explored, such as applying the Gabon and WSA  $N_{min}$  constraints to B1+B2 combined.

It is important to note the possibility that the available data do not support some of the current hypothesised stock-structure models, and that the problem of prior incoherence is in fact a result of the more fundamental model

assumptions rather than an artefact of the estimation and sampling techniques. Further models may need to be explored<sup>49</sup>.

Prior incoherence is not an uncommon problem in whale assessments (see, for example, Brandon *et al.*, 2007), and the development of techniques for testing and correcting for this problem will form a valuable contribution to the field.

#### *Input data*

A table of input data (see Table A5.1.1 of Appendix 5.1) was produced at IWC SC 62 that details the capture-recapture data,  $N_{min}$  values, catch allocation assumptions and migration assumptions (such as proportion of WSA animals that migrate to the Antarctic for feeding) that are to be used in further assessments. The table presents input data considered suitable as a reference case and also lists some variants<sup>50</sup>. This table is currently under review, and the revised input data will need to be incorporated once the table has been finalised. Assessments will be carried out for the data and assumptions defined for the new reference case, as well as for various variants and sensitivities to the reference case that require testing. An important addition will be the inclusion of a struck-and-lost rate<sup>51</sup> of 0.15, which effectively increases the early reported catches by 15%.

#### *Model dynamics*

Assessments of the lower priority models (see Figure A5.1.1 of Appendix 5.1) put forward at IWC 62 will be carried out once the input data have been finalised. Based on current discussions within the intersessional group, at least one further alternative model will be put forward and assessed (see footnote 49).

Refinements of the current models may also be attempted, such as allowing the proportion of B1 animals using each migratory route (i.e.  $X$ ) to vary with time, or allowing for interchange to occur between B1 and B2 as was done for Breeding Stock C (see Section 4.1.2).

---

<sup>49</sup> One such model has been proposed by P. Best (*pers. comm.*), which addresses a concern that the WSA data are not representative of the whole B2 population. This new model allows the B2 population to split along two migratory routes, and the WSA data apply to whales taking the eastern migratory route only.

<sup>50</sup> Variants include capture-recapture data based on different identification techniques for matches, alternative catch assumptions and varying the proportion of B2 animals that migrate to the Antarctic. Note that the Model Ia-IIIa assessments presented in this thesis utilise the reference case input data specified at IWC62.

<sup>51</sup> ‘Struck-and-lost’ refers to whales that were killed or presumed mortally wounded but lost in the water before recovery (Best, 2010).

**Table 5.9:** Summary of the convergence diagnostics results.

		Maximum importance ratio as a proportion of the sum of all importance ratios (Should be less than 0.01)	CV in the average importance ratio (Should be less than 0.04)	CV in the importance ratio (Should be less than 50)
Model 1		0.0002	8.51E-08	2.69
Model 2		0.0018	1.75E-07	5.54
Model 3	X=0.6	0.0016	2.44E-07	7.70
	X=0.8	0.0016	1.89E-07	5.99
Model Ia	$N_{min}$ is 10	0.0004	2.78E-07	3.11
	$N_{min}$ is 96	0.0002	5.55E-08	4.97
	Resampling	0.0005	1.14E-07	3.62
Model IIa	X=0.5	0.0017	1.22E-06	13.69
	X=0.6	0.0042	1.01E-06	11.24
	X=0.7	0.0020	5.75E-07	6.43
	X=0.8	0.0015	5.27E-07	5.89
Model IIIa	X=0.5	0.0004	1.09E-07	6.34
	X=0.6	0.0006	8.74E-08	5.08
	X=0.7	0.0007	8.53E-08	4.95
	X=0.8	0.0004	8.63E-08	5.01

**Table 5.10:** Assessment results for **Model 1**. Posterior medians and 90% probability intervals are shown. This model is fit to Gabon data (photo-ID and genetics data from all sites).

Model 1	BSB
$r$	0.0633 [0.0192, 0.0860]
$K$	21424 [19301, 34151]
$N_{min}$	911 [435, 4913]
$N_{2006}$	10576 [8377, 12393]
$N_{min}/K$	0.042 [0.022, 0.136]
$N_{2010}/K$	0.501 [0.274, 0.642]
$N_{2040}/K$	0.985 [0.474, 0.999]

**Table 5.11:** Assessment results for **Model 2**. Posterior medians and 90% probability intervals are shown. The model fits  $N_y^{B1}$  to the Gabon data (photo-ID and genetics data from all sites), and  $N_y^{B2}$  to the WSA data (right dorsal fin and microsatellite data).

	BSB1	BSB2
$r$	0.0609 [0.0144, 0.0855]	0.0789 [0.0177, 0.1045]
$K$	18857 [16702, 30696]	2637 [2476, 4296]
$N_{min}$	974 [436, 4809]	31 [13, 255]
$N_{2010}$	10434 [8339, 11992]	734 [517, 987]
$N_{min}/K$	0.052 [0.026, 0.159]	0.012 [0.005, 0.058]
$N_{2010}/K$	0.553 [0.277, 0.698]	0.273 [0.124, 0.393]
$N_{2040}/K$	0.988 [0.413, 0.999]	0.978 [0.205, 0.999]

**Table 5.12 (a)-(d):** Assessment results for **Model 3**. The model fits  $N_y^{B1W} + N_y^{B1E}$  to the Gabon data (photo-ID and genetics data from all sites), and  $N_y^{B1E} + N_y^{B2}$  to the WSA data (right dorsal fin and microsatellite data). Posterior medians and 90% probability intervals are shown.  $X$  is the proportion of B1 animals that belong to B1<sup>W</sup>.

	<b>(a) B1</b>		<b>(b) B2</b>	
	X=0.6	X=0.8	X=0.6	X=0.8
$r$	0.080 [0.071, 0.088]	0.072 [0.025, 0.087]	0.063 [0.030, 0.099]	0.059 [0.005, 0.102]
$K$	19592 [18835, 20440]	19365 [17752, 28607]	177 [67, 532]	1044 [325, 3275]
$N_{min}$	509 [409, 674]	683 [420, 3337]	10 [10, 16]	59 [14, 128]
$N_{2010}$	11393 [10020, 12904]	10928 [8759, 12499]	83 [35, 167]	516 [63, 725]
$N_{min}/K$	0.026 [0.021, 0.033]	0.035 [0.023, 0.118]	0.063 [0.019, 0.152]	0.0409 [0.016, 0.377]
$N_{2010}/K$	0.582 [0.499, 0.672]	0.561 [0.308, 0.693]	0.700 [0.068, 0.999]	0.571 [0.025, 0.998]
$N_{2040}/K$	0.998 [0.992, 0.999]	0.995 [0.582, 0.999]	0.994 [0.170, 1.000]	0.985 [0.031, 1.000]
	<b>(c) B1<sup>W</sup></b>		<b>(d) B1<sup>E</sup></b>	
	X=0.6	X=0.8	X=0.6	X=0.8
$r$	$r^{B1}$	$r^{B1}$	$r^{B1}$	$r^{B1}$
$K$	11755 [11301, 12264]	15492 [14202, 22885]	7837 [7534, 8176]	3873 [3550, 5721]
$N_{min}$	480 [387, 627]	675 [412, 3274]	28 [17, 50]	6 [0, 129]
$N_{2010}$	10749 [9340, 12221]	10744 [8468, 12408]	644 [447, 863]	97 [1, 571]
$N_{min}/K$	0.041 [0.034, 0.052]	0.0437 [0.029, 0.142]	0.004 [0.002, 0.006]	0.002 [0.000, 0.021]
$N_{2010}/K$	0.914 [0.774, 1.066]	0.689 [0.373, 0.846]	0.081 [0.058, 0.110]	0.022 [0.000, 0.151]
$N_{2040}/K$	1.568 [1.525, 1.601]	1.219 [0.703, 1.248]	0.141 [0.095, 0.197]	0.042 [0.001, 0.254]

**Table 5.13 (a):** Assessment results for **Model Ia**. The parameter estimates are given for case A, where both the  $N_{min}$  constraints are in place ( $N_{min}^{B1} = 272$  and  $N_{min}^{B2} = 96$ ), as well as for case B where an arbitrary  $N_{min}$  constraint of 10 is placed on B2 to illustrate the extent of the effect of the 96 limit on results. The posterior medians and the 90% probability envelopes are shown.

	A: $N_{min}^{B2} = 96$		B: $N_{min}^{B2} = 10$	
	<b>B1</b>	<b>B2</b>	<b>B1</b>	<b>B2</b>
$r$	0.0623 [0.0107, 0.0998]	0.0189 [0.0021, 0.0403]	0.0633 [0.0130, 0.0946]	0.0579 [0.0081, 0.1007]
$K$	16169 [88949, 31219]	6256 [3952, 15425]	17329 [12172, 30045]	4009 [3114, 10568]
$N_{min}$	702 [223, 4276]	151 [96, 340]	688 [261, 4062]	37 [10, 232]
$N_{2010}$	7865 [5915, 9743]	335 [215, 672]	8103 [6078, 10223]	395 [242, 762]
$N_{min}/K$	0.046 [0.019, 0.138]	0.022 [0.014, 0.048]	0.040 [0.019, 0.131]	0.009 [0.003, 0.033]
$N_{2010}/K$	0.504 [0.205, 0.876]	0.052 [0.020, 0.138]	0.474 [0.209, 0.754]	0.096 [0.030, 0.217]
$N_{2040}/K$	0.985 [0.286, 1.000]	0.090 [0.024, 0.388]	0.983 [0.301, 1.000]	0.476 [0.042, 0.988]

**Table 5.13 (b):** Assessment results for **Model Ia** for the re-sampling approach. Posterior medians and 90% probability intervals are shown.

	<b>B1</b>	<b>B2</b>
$r$	0.0703 [0.0122, 0.1033]	0.0192 [0.0019, 0.0412]
$K$	15088 [8601, 30527]	6705 [4000, 15561]
$N_{min}$	546 [183, 3868]	148 [100, 317]
$N_{2010}$	7921 [5965, 9802]	351 [199, 705]
$N_{min}/K$	0.039 [0.016, 0.132]	0.021 [0.012, 0.045]
$N_{2010}/K$	0.550 [0.208, 0.889]	0.052 [0.017, 0.146]
$N_{2040}/K$	0.994 [0.303, 1.000]	0.091 [0.019, 0.416]

**Table 5.14 (a)-(d):** Assessment results for **Model IIa** for  $X=0.5$ ,  $X=0.6$ ,  $X=0.7$  and  $X=0.8$ , where  $X$  is the proportion of B1 whales that belong to  $B1^W$  before exploitation starts. Posterior medians and 90% probability intervals are shown.

$X$	<b>(a) B1</b>			
	0.5	0.6	0.7	0.8
$r$	0.0684 [0.0445,0.0848]	0.0605 [0.0410,0.0879]	0.0535 [0.0277, 0.0847]	0.0374 [0.0076, 0.0868]
$K$	20772 [19228, 24018]	21571 [18892, 24636]	22314 [18721, 27996]	24767 [17910, 37194]
$N_{min}$	539 [311, 1197]	732 [300, 1388]	929 [328, 2197]	1693 [308, 4784]
$N_{2010}$	8277 [6450, 10203]	8228 [6430, 10641]	8086 [6132, 10427]	7811 [5754, 10543]
$N_{min}/K$	0.026 [0.016, 0.051]	0.033 [0.016, 0.056]	0.041 [0.018, 0.080]	0.067 [0.017, 0.129]
$N_{2010}/K$	0.396 [0.274, 0.514]	0.387 [0.268, 0.555]	0.358 [0.223, 0.542]	0.314 [0.163, 0.565]
$N_{2040}/K$	0.978 [0.787, 0.997]	0.960 [0.714, 0.998]	0.919 [0.484, 0.998]	0.745 [0.206, 0.999]

$X$	<b>(b) B2</b>			
	0.5	0.6	0.7	0.8
$r$	0.0573 [0.0048,0.1006]	0.0638 [0.0044,0.1026]	0.0605 [0.0046, 0.1039]	0.0257 [0.0025, 0.0983]
$K$	10* [10*, 292]	116 [10*, 691]	241 [10, 1447]	862 [10*, 2423]
$N_{min}$	4 [1, 67]	37 [2, 135]	83 [3, 192]	97 [6, 195]
$N_{2010}$	10* [1, 177]	67 [3, 349]	176 [5, 489]	188 [10, 516]
$N_{min}/K$	0.390 [0.096, 0.610]	0.397 [0.091, 0.613]	0.390 [0.065, 0.664]	0.124 [0.049, 0.655]
$N_{2010}/K$	0.992 [0.121, 1.000]	0.997 [0.117, 1.000]	0.995 [0.089, 1.000]	0.322 [0.062, 1.000]
$N_{2040}/K$	1.000 [0.138, 1.000]	1.000 [0.133, 1.000]	1.000 [0.104, 1.000]	0.588 [0.071, 1.000]

$X$	<b>(c) B1<sup>W</sup></b>			
	0.5	0.6	0.7	0.8
$r$	$r^{B1}$	$r^{B1}$	$r^{B1}$	$r^{B1}$
$K$	10386 [9614, 12009]	12942 [11335,14782]	15620 [13105, 19597]	19813 [14328, 29755]
$N_{min}$	424 [253, 841]	640 [275,1140]	886 [317, 2000]	1652 [302, 4518]
$N_{2010}$	6405 [4596, 8178]	7295 [5390, 9885]	7677 [5542, 10197]	7641 [5503, 10329]
$N_{min}/K$	0.041 [0.026, 0.071]	0.049 [0.024, 0.078]	0.056 [0.024, 0.103]	0.082 [0.021, 0.152]
$N_{2010}/K$	0.613 [0.390, 0.828]	0.569 [0.370, 0.863]	0.488 [0.286, 0.753]	0.383 [0.191, 0.693]
$N_{2040}/K$	1.527 [1.086, 1.622]	1.409 [0.982, 1.559]	1.247 [0.624, 1.408]	0.918 [0.241, 1.231]

$X$	<b>(d) B1<sup>E</sup></b>			
	0.5	0.6	0.7	0.8
$r$	$r^{B1}$	$r^{B1}$	$r^{B1}$	$r^{B1}$
$K$	10386 [9614, 12009]	8628 [7557, 9855]	6694 [5616, 8399]	4953 [3582, 7439]
$N_{min}$	118 [60, 357]	91 [20, 247]	41 [4, 225]	29 [4, 301]
$N_{2010}$	1844 [1537, 2341]	938 [564, 1368]	411 [82, 741]	185 [52, 448]
$N_{min}/K$	0.011 [0.006, 0.030]	0.010 [0.003, 0.025]	0.006 [0.001, 0.027]	0.006 [0.001, 0.041]
$N_{2010}/K$	0.177 [0.146, 0.212]	0.109 [0.073, 0.145]	0.058 [0.014, 0.099]	0.038 [0.012, 0.078]
$N_{2040}/K$	0.427 [0.355, 0.501]	0.278 [0.156, 0.345]	0.140 [0.029, 0.213]	0.067 [0.024, 0.159]

\* There is a constraint built into the assessment that  $K^{B1}$  may not go below 10. This is a residue from earlier models where there were only B1 and B2 stocks (and as such the B2 population could not go extinct). The introduction of  $B1^E$  into the WSA region removes the need for this constraint and in future assessments it will be removed. Here, the 10\* indicates that the constraint has been hit (and the model most likely supports a zero B2 component).

**Table 5.15 (a)-(c):** Assessment results for **Model IIIa** for  $X=0.5$ ,  $X=0.6$ ,  $X=0.7$  and  $X=0.8$ , where  $X$  is the proportion of B1 whales that belong to  $B1^W$  before exploitation starts. Posterior medians and 90% probability intervals are shown.

$X$	<b>(a) B1</b>			
	0.5	0.6	0.7	0.8
$r$	0.0656 [0.0406, 0.0739]	0.0520 [0.0357, 0.0575]	0.0344 [0.0222, 0.0390]	0.0115 [0.0024, 0.0167]
$K$	21072 [20253, 24782]	22794 [22043, 25810]	26164 [25179, 29744]	34799 [32387, 40872]
$N_{min}$	578 [471, 1335]	948 [809, 1614]	1810 [1522, 2648]	4144 [3441, 5522]
$N_{2010}$	7891 [6201, 10030]	7723 [6028, 9437]	7238 [5740, 9236]	6594 [5179, 8350]
$N_{min}/K$	0.028 [0.023, 0.053]	0.042 [0.036, 0.063]	0.070 [0.058, 0.090]	0.118 [0.101, 0.142]
$N_{2010}/K$	0.372 [0.267, 0.491]	0.334 [0.241, 0.421]	0.275 [0.202, 0.365]	0.188 [0.135, 0.253]
$N_{2040}/K$	0.968 [0.738, 0.993]	0.894 [0.629, 0.960]	0.642 [0.387, 0.809]	0.261 [0.149, 0.393]

$X$	<b>(b) <math>B1^W</math></b>			
	0.5	0.6	0.7	0.8
$r$	$r^{B1}$	$r^{B1}$	$r^{B1}$	$r^{B1}$
$K$	10536 [10127, 12391]	13676 [13226, 15486]	18315 [17626, 20821]	27839 [25909, 32697]
$N_{min}$	448 [369, 907]	822 [706, 1290]	1681 [1418, 2344]	3952 [3326, 5100]
$N_{2010}$	6055 [4460, 7975]	6597 [5004, 8230]	6682 [5186, 8647]	6261 [4839, 8015]
$N_{min}/K$	0.043 [0.035, 0.074]	0.060 [0.052, 0.084]	0.092 [0.077, 0.116]	0.141 [0.120, 0.167]
$N_{2010}/K$	0.570 [0.378, 0.788]	0.480 [0.325, 0.621]	0.363 [0.258, 0.489]	0.224 [0.157, 0.305]
$N_{2040}/K$	1.496 [1.024, 1.592]	1.291 [0.843, 1.415]	0.850 [0.477, 1.087]	0.312 [0.171, 0.474]

$X$	<b>(c) <math>B1^E</math></b>			
	0.5	0.6	0.7	0.8
$r$	$r^{B1}$	$r^{B1}$	$r^{B1}$	$r^{B1}$
$K$	10536 [10127, 12391]	9118 [8817, 10324]	7849 [7554, 8923]	6960 [6477, 8174]
$N_{min}$	131 [98, 417]	127 [98, 321]	130 [99, 322]	199 [108, 432]
$N_{2010}$	1852 [1533, 2356]	1041 [889, 1443]	539 [436, 835]	316 [207, 507]
$N_{min}/K$	0.012 [0.010, 0.034]	0.014 [0.011, 0.031]	0.017 [0.013, 0.036]	0.028 [0.017, 0.053]
$N_{2010}/K$	0.174 [0.143, 0.212]	0.114 [0.096, 0.145]	0.069 [0.056, 0.095]	0.045 [0.031, 0.064]
$N_{2040}/K$	0.436 [0.385, 0.501]	0.296 [0.270, 0.352]	0.157 [0.136, 0.192]	0.061 [0.047, 0.081]

**Table 5.16:** Table showing the estimated population numbers (at pristine levels) found in each region, as well as the estimated current and future abundance for each region. The fields in grey indicate which population components are found in each region for the model under consideration.

	Gabon (pristine levels)	WSA (pristine levels)	Total BSB (pristine levels)	$N_{2010}$ (total)	$N_{2010}/K$ (total)	$N_{2040}/K$ (total)
Model 1	No split	No split	B			
	-	-	21424 [ 19301, 34151]	10576 [8377, 12393]	0.49 [0.25, 0.63]	0.98 [0.38, 1.00]
Model 2	B1	B2	B1+B2			
	18857 [16702, 30696]	2637 [2476, 4296]	21810 [ 19459, 33333]	11148 [ 9088, 12772]	0.51 [0.28, 0.64]	0.97 [0.45, 1.00]
Model 3	$B1^W+B1^E$	$B2+B1^E$	B1+B2			
	X=0.6 19592 [18835, 20440]	8057 [7844, 8321]	19801 [19244, 20551]	11481 [10111,12964]	0.58 [ 0.50, 0.67]	1.00 [ 0.98, 1.00]
	X=0.8 19365 [17552, 28607]	5213 [4620, 7172]	21059 [19331,29160]	11374 [ 8999,13088]	0.54 [ 0.31, 0.66]	0.97 [ 0.58, 1.00]
Model Ia	B1+B2	B2	B1+B2			
	23883 [ 20406, 35628]	6256 [ 3952, 15425]	23883 [ 20406, 35628]	8248 [ 6280, 10117]	0.35 [ 0.19, 0.49]	0.64 [ 0.27, 0.81]
Model IIa	$B1^W+B1^E$	$B2+B1^E$	B1+B2			
	X=0.5 20772 [ 19228, 24018]	10403 [ 9850, 12019]	20786 [ 19456, 24028]	8302 [ 6457, 10214]	0.40 [0.28, 0.52]	0.98 [0.79, 1.00]
	X=0.6 21571 [ 18892, 24636]	8798 [ 7863, 9882]	21699 [ 19210, 24646]	8332 [ 6461, 10818]	0.39 [0.27, 0.56]	0.95 [0.71, 1.00]
	X=0.7 22314 [ 18721, 27996]	7171 [ 6202, 8424]	22658 [ 19554, 28006]	8239 [ 6153, 10803]	0.36 [0.22, 0.54]	0.91 [0.49, 1.00]
	X=0.8 24767 [ 17910, 37194]	5955 [ 5247, 7453]	25732 [ 19950, 37204]	8023 [ 5872, 10841]	0.31 [0.16, 0.53]	0.73 [0.21, 0.96]
Model IIIa	$B1^W+B1^E$	$B1^E$	$B1^W+B1^E$			
	X=0.5 21072 [ 20253, 24782]	10536 [ 10127, 12391]	21072 [ 20253, 24782]	7891 [ 6201, 10030]	0.37 [0.27, 0.50]	0.97 [0.74, 0.99]
	X=0.6 22794 [ 22043, 25810]	9118 [ 8817, 10324]	22794 [ 22043, 25810]	7723 [ 6028, 9437]	0.33 [0.24, 0.42]	0.89 [0.63, 0.96]
	X=0.7 26164 [ 25179, 29744]	7849 [ 7554, 8923]	26164 [ 25179, 29744]	7238 [ 5740, 9236]	0.28 [0.20, 0.37]	0.64 [0.39, 0.81]
	X=0.8 34799 [ 32387, 40872]	6960 [ 6477, 8174]	34799 [ 32387, 40872]	6594 [ 5179, 8350]	0.19 [0.14, 0.25]	0.26 [0.15, 0.39]

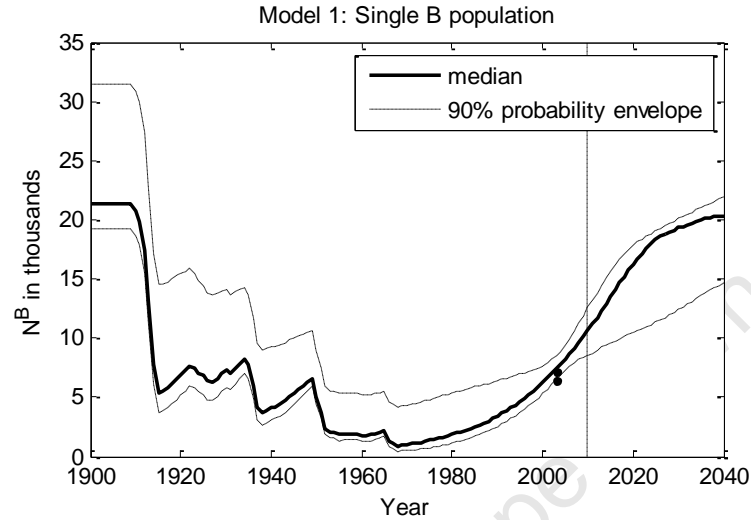


**Figure 5.8:** Model 1 median population trajectories for the single Breeding Stock B. The posterior medians and 90% probability interval envelopes are shown. Results shown for years to the right of the vertical dashed line are projections into the future under zero catch. The two dots indicate the lower and upper Gabon abundance estimates from MARK, shown here as a reality check.

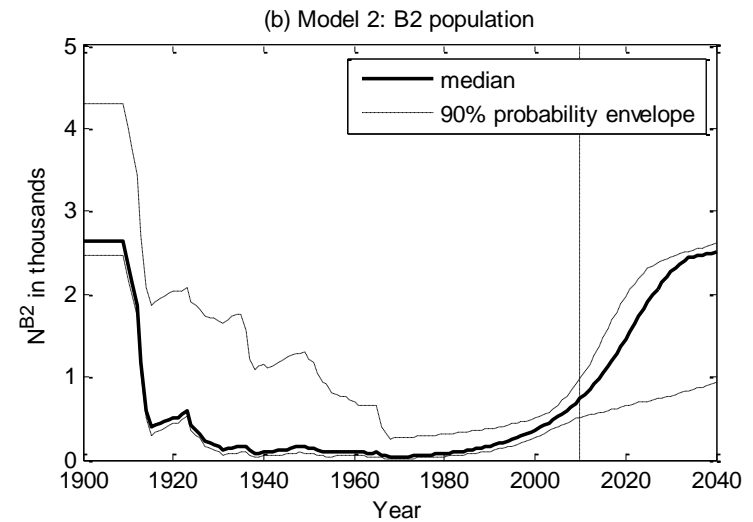
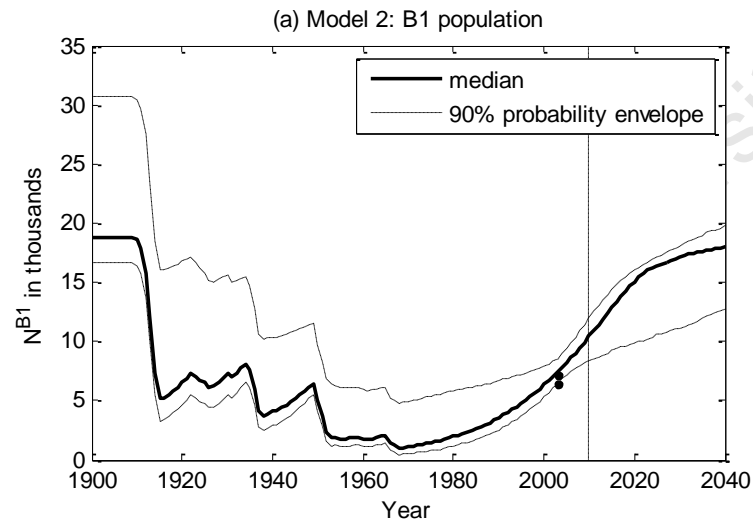


**Figure 5.9 (a)-(b):** Model 2 population trajectory for B1 and B2. The posterior medians and 90% probability interval envelopes are shown. Trajectories to the right of the vertical dashed line are projections under zero future catch. The two dots in (a) indicate the lower and upper Gabon abundance estimates from MARK, shown here as a reality check.

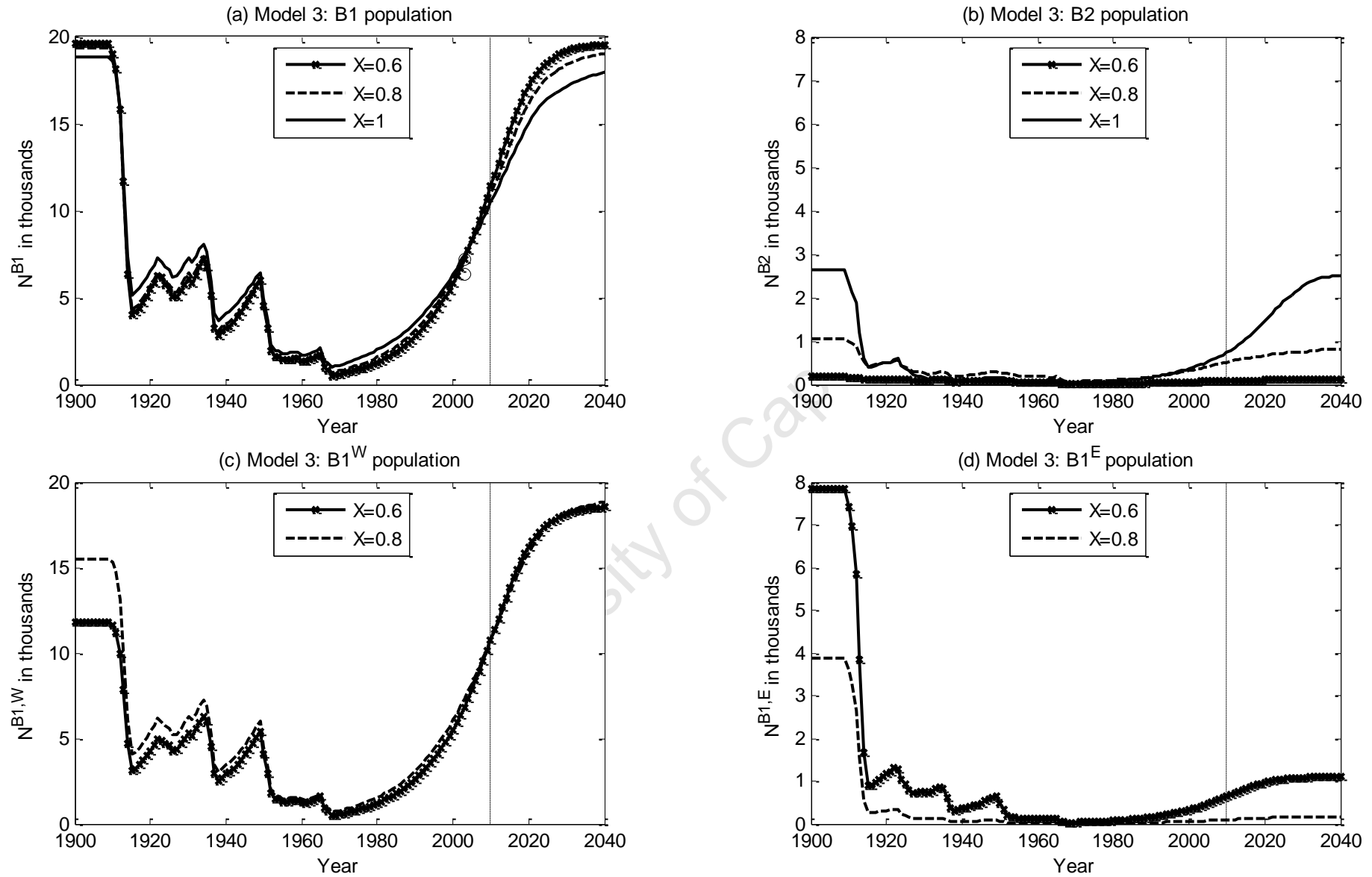


**Figure 5.10 (a)-(d):** A comparison of the posterior median trajectories for **Model 3** for  $X=1$ ,  $X=0.8$  and  $X=0.6$ . Note that Model 3 with  $X=1$  is identical to Model 2. The two circles in (a) indicate the lower and upper Gabon abundance estimates from MARK, shown here as a reality check.

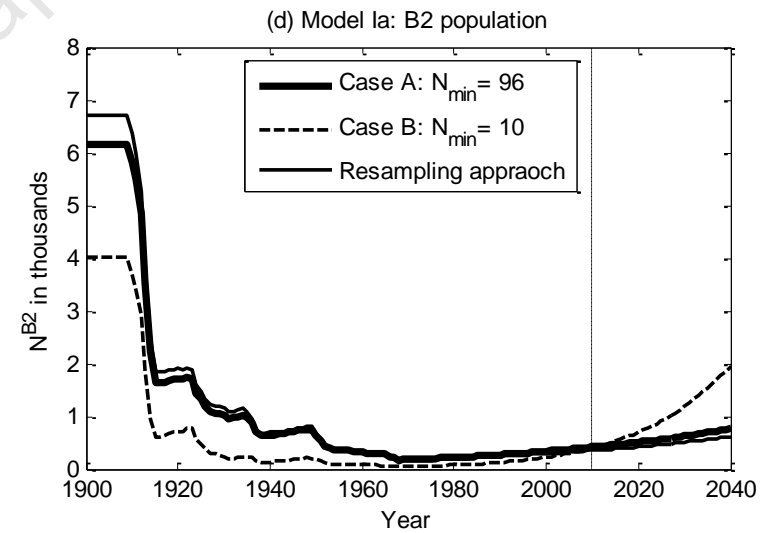
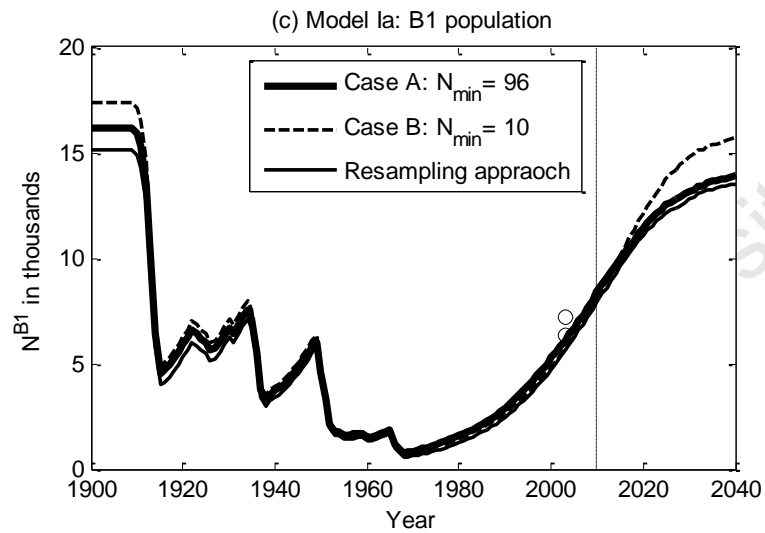
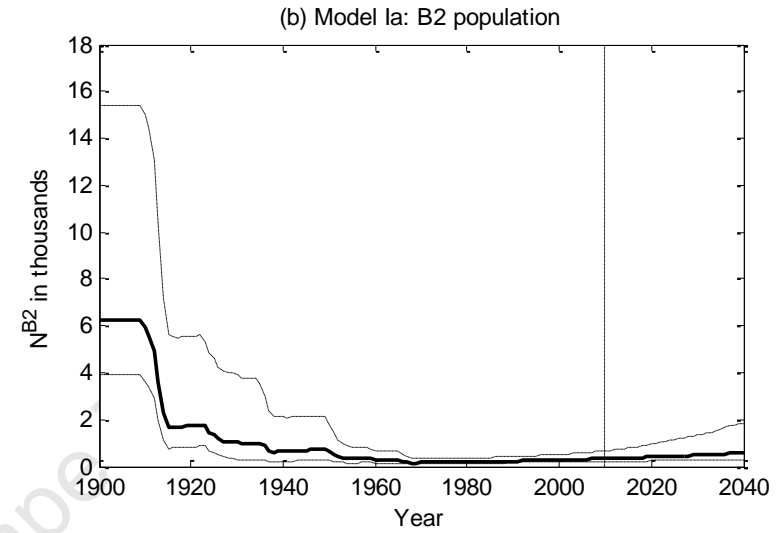
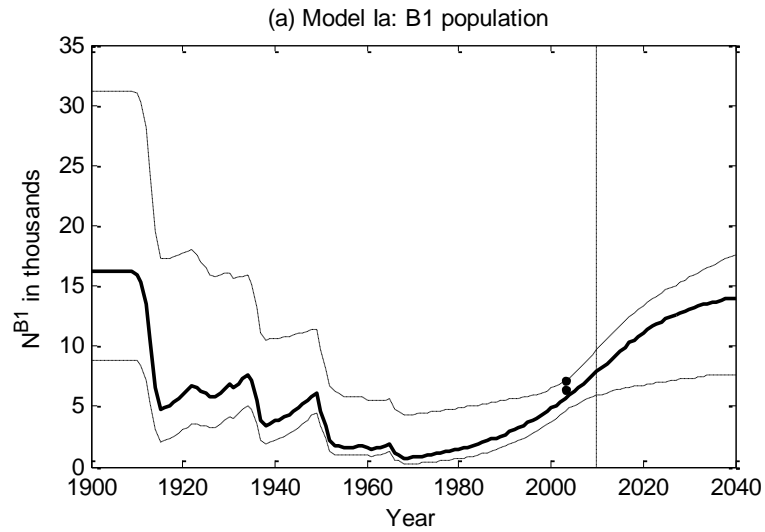


**Figure 5.11 (a)-(d):** The median **Model Ia** population trajectory and the 90% probability envelopes for B1 and B2 are shown in (a) and (b) for case A, where the  $N_{min}$  constraint on B2 is 96; (c) and (d) show a comparison of the **Model Ia** B1 and B2 median trajectories for (i) case A, where the  $N_{min}$  constraint on B2 is 96, (ii) case B, where the  $N_{min}$  constraint on B2 is 10 and (iii) the re-sampling approach. The two dots in (a) and the two circles in (c) indicate the lower and upper Gabon abundance estimates from MARK, shown here as a reality check.

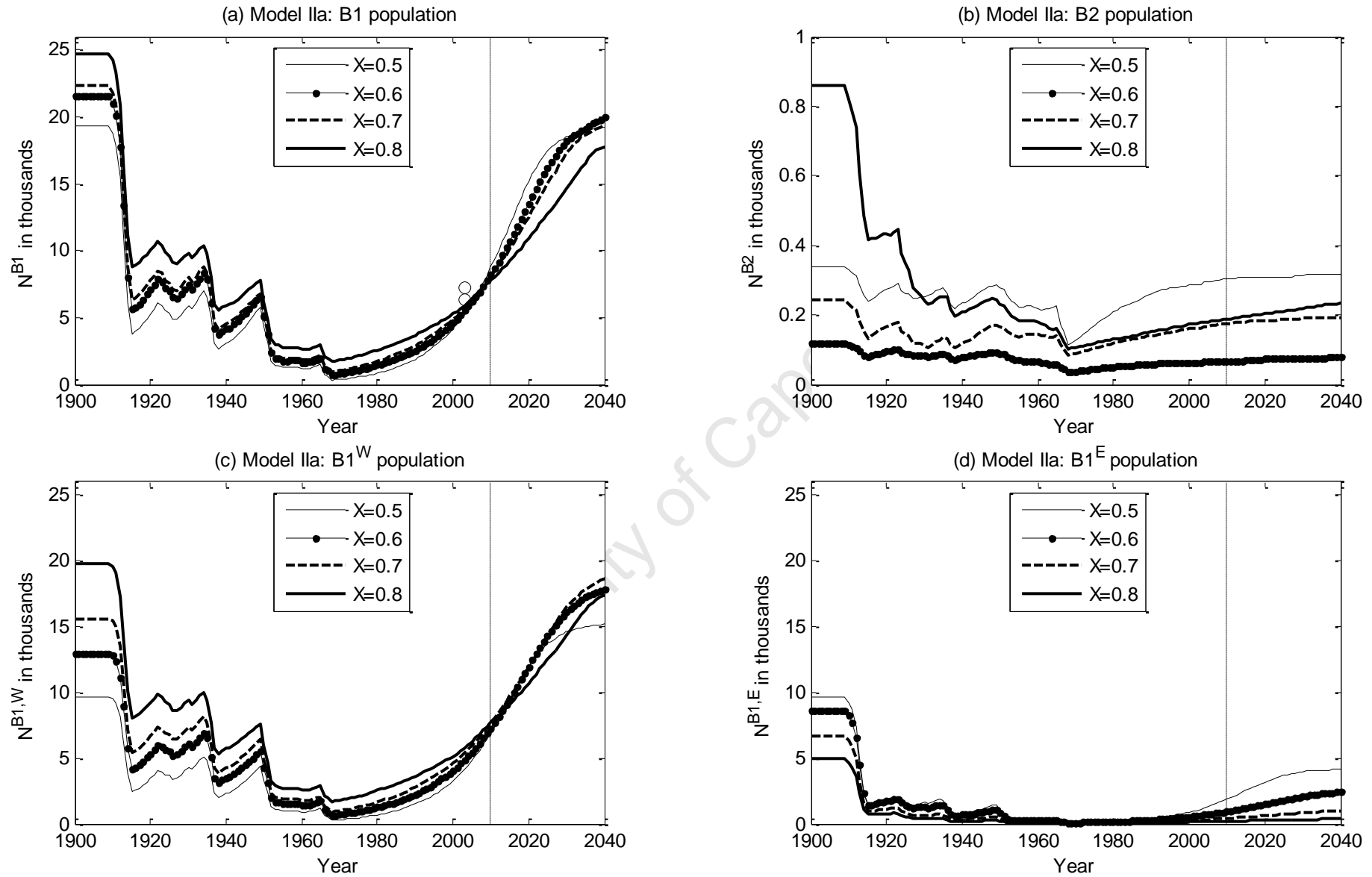


**Figure 5.12 (a)-(d):** Median trajectories for **Model IIa**, for  $X=0.5$ ,  $X=0.6$ ,  $X=0.7$ ,  $X=0.8$ . The two circles in (a) indicate the lower and upper Gabon abundance estimates from MARK, shown here as a reality check. Note the different vertical-axis scale in (b).

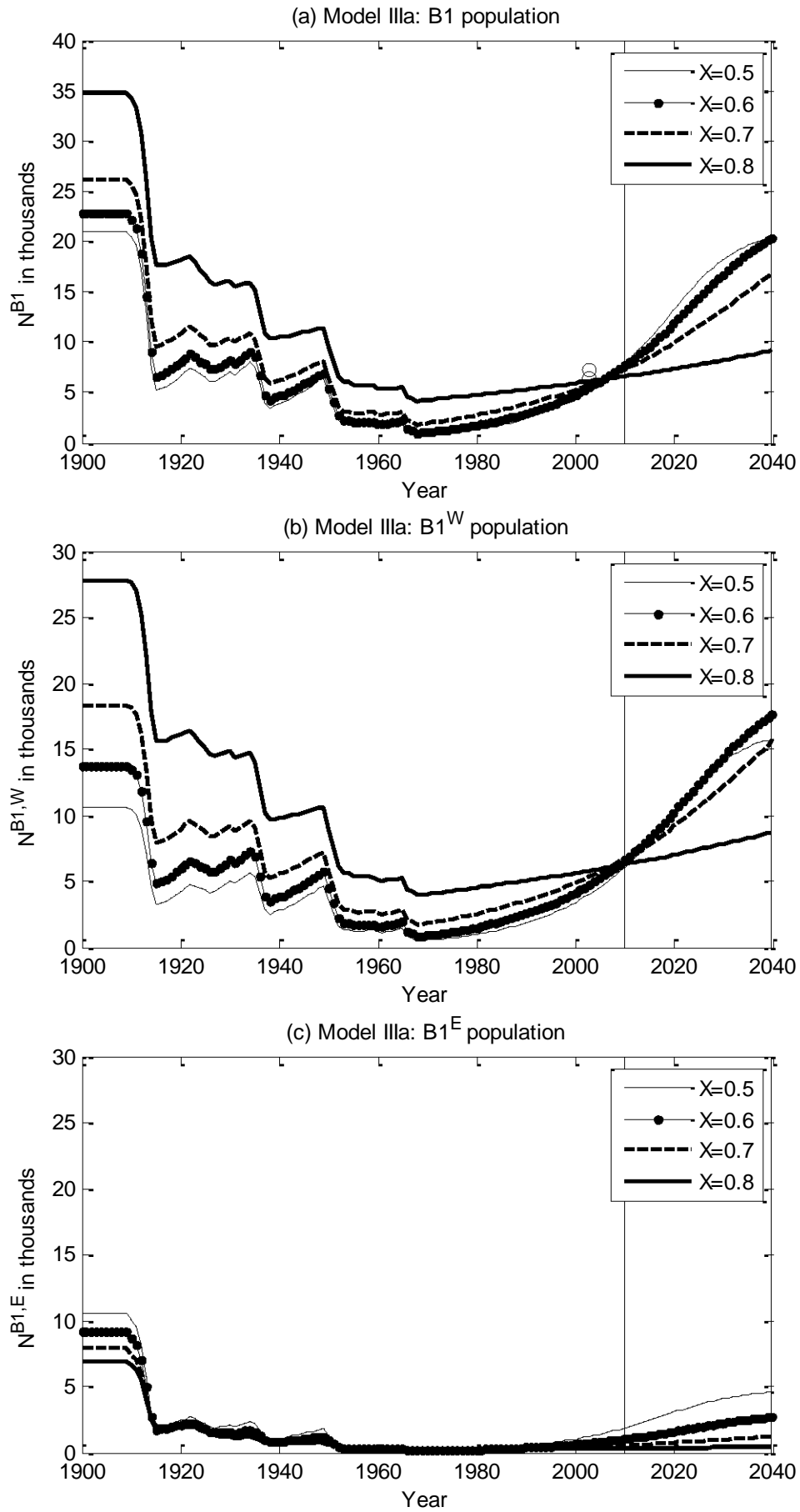


**Figure 5.13 (a)-(c):** Median trajectories for **Model IIIa**, for  $X=0.5$ ,  $X=0.6$ ,  $X=0.7$ ,  $X=0.8$ . The trajectories to the right of the vertical dashed lines represent projections into the future under the assumption of zero catch.

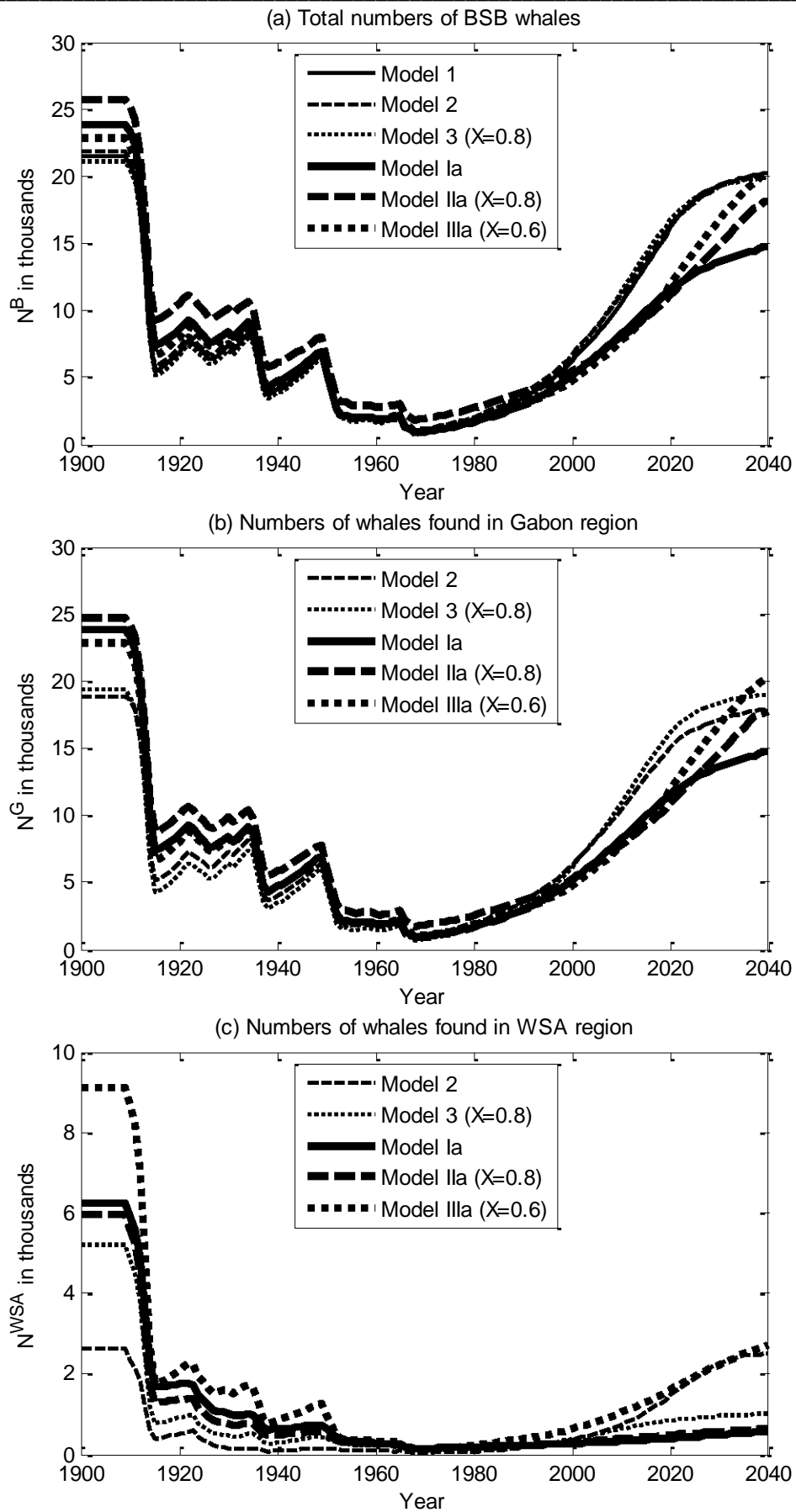


**Figure 5.14 (a)-(c):** Comparison between all the models of the total number of Breeding Stock B whales, as well as number of whales estimated to be in Gabon and WSA. Note that Model 1 is missing from (b) and (c) since for this model the breeding stock is not split into sub-stocks, i.e. the regional split does not feature.

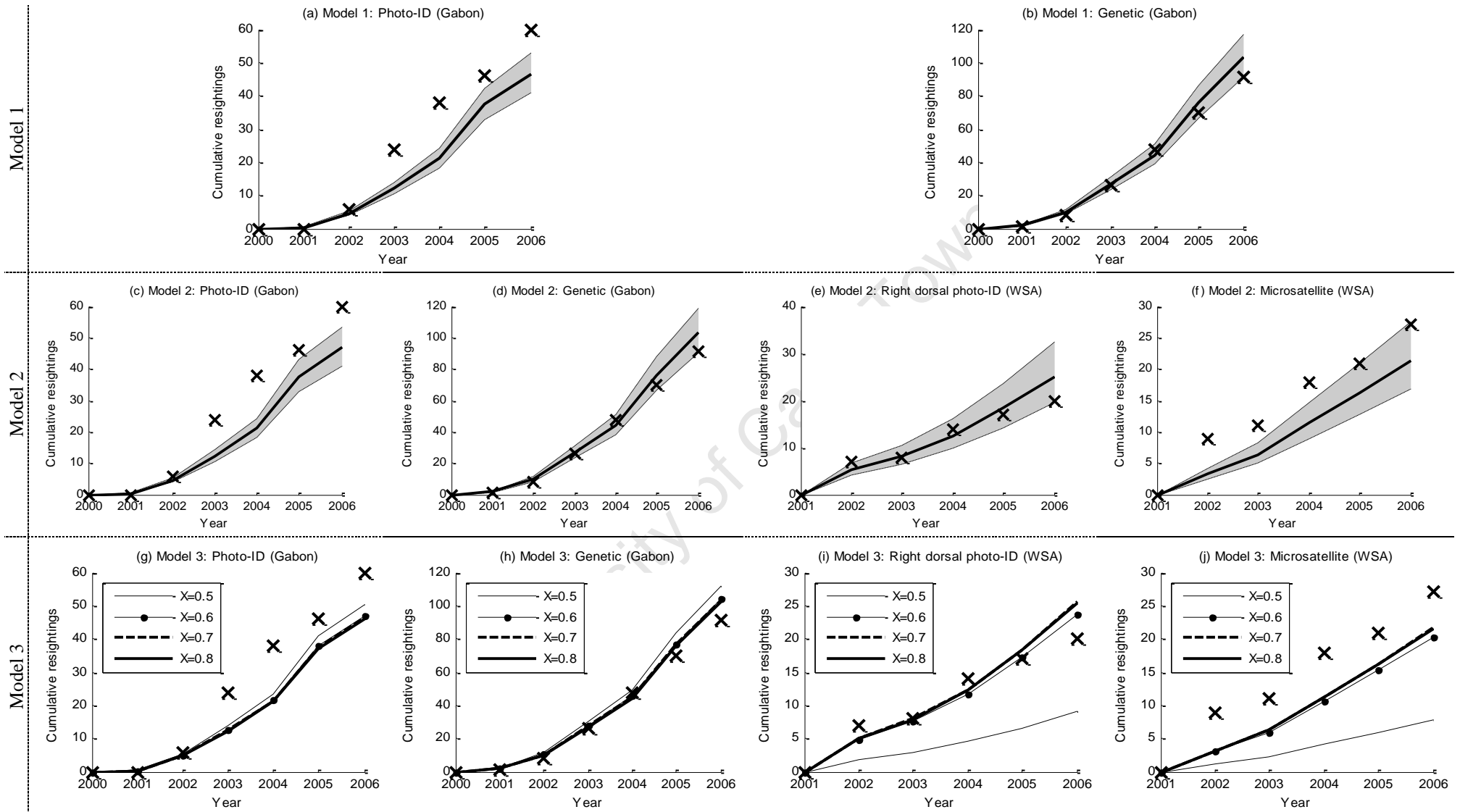


**Figure 5.15 (a)-(j):** The observed cumulative resightings (marked by X's) compared to the numbers predicted by **Models 1-3**. In (a)-(f) the thick solid line is the median estimate and the 90% probability envelope is indicated by the shaded region. In (g)-(j) the lines show the median estimates for each value of  $X$  (in some cases these lines are very close and so not distinguishable on the plots). The probability envelopes are not shown for these medians.

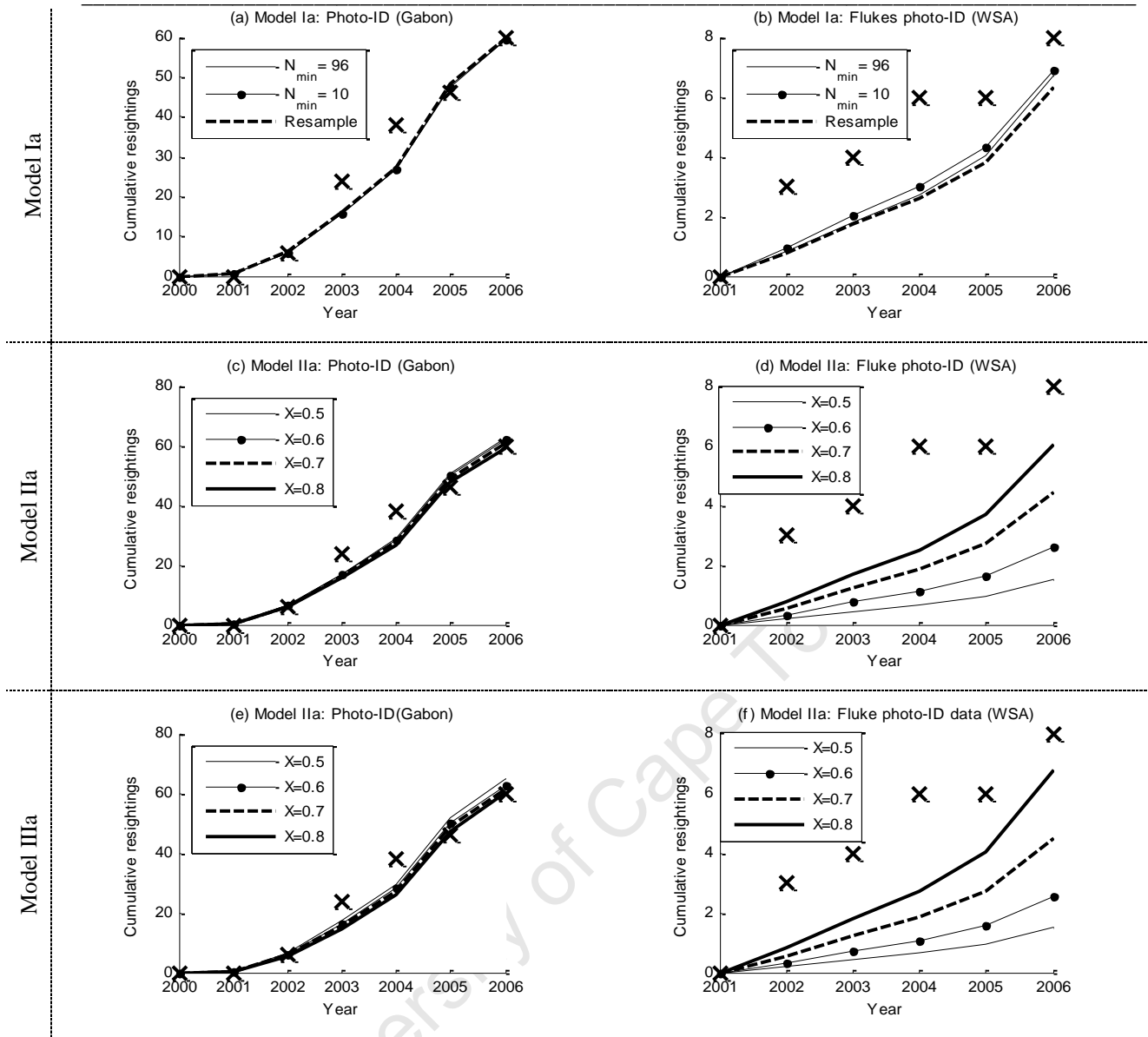


**Figure 5.16 (a)-(f):** The observed cumulative resightings (marked by X's) compared to those predicted by **Models Ia-IIIa**. In (a)-(b) the fits for Model Ia are shown for three different variants. Plots (c)-(f) show the fits for Models Ia and IIa for a range of  $X$  values.

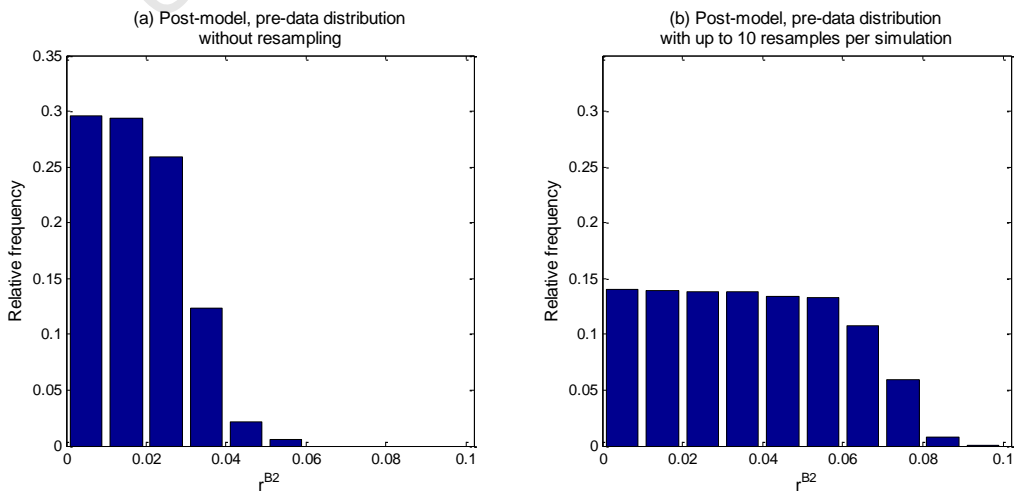


**Figure 5.17 (a)-(b):** The post-model, pre-data distribution of  $r^{B2}$  for **Model Ia** without and with re-sampling (Approach 1 of Appendix 5.2).

## Appendix 5.1

**Input data and lower priority stock structure models for Southern Hemisphere humpback whale assessments as recommended by IWC SC 62**

This Appendix tables the input data selected at IWC SC 62 (Morocco 2010) for assessment modelling of Breeding Stock B and gives the model diagrams and descriptions of the six lower priority models (not presented in this thesis) put forward by the IWC SC. West South Africa is denoted as WSA.

**Table A5.1.1:** Input data selected for use in assessment modelling, specified by reference case and variants (IWC, 2011).

Data category	Population	Reference case	Variants
Capture-recapture	Gabon	Microsatellites* (males only)	Flukes Microsatellites (both sexes)
	WSA	Microsatellites*	Right dorsal fin Flukes
$N_{min}$	Gabon	68 haplotypes	None
	WSA	24 haplotypes	None
Catch allocation (north of 40°S)	Gabon	Congo and 50% Angola	Congo and Angola Congo only
	WSA	50% Angola, Namibia and WSA	Namibia and WSA Angola, Namibia and WSA
Catch allocation (south of 40°S)	Gabon	Hypothesis 1	None
	WSA	Hypothesis 1	None
Migration to unknown breeding ground	WSA	25% (for Model Ie)	None
Migration to Antarctic	WSA	50% (for Model Id)	100% 0%
Struck and loss rate	Both	0.15	0
*In the case of capture-recapture data, microsatellites will only be used as a reference case if genotyping errors can be incorporated into assessment models. Otherwise flukes will be used.			

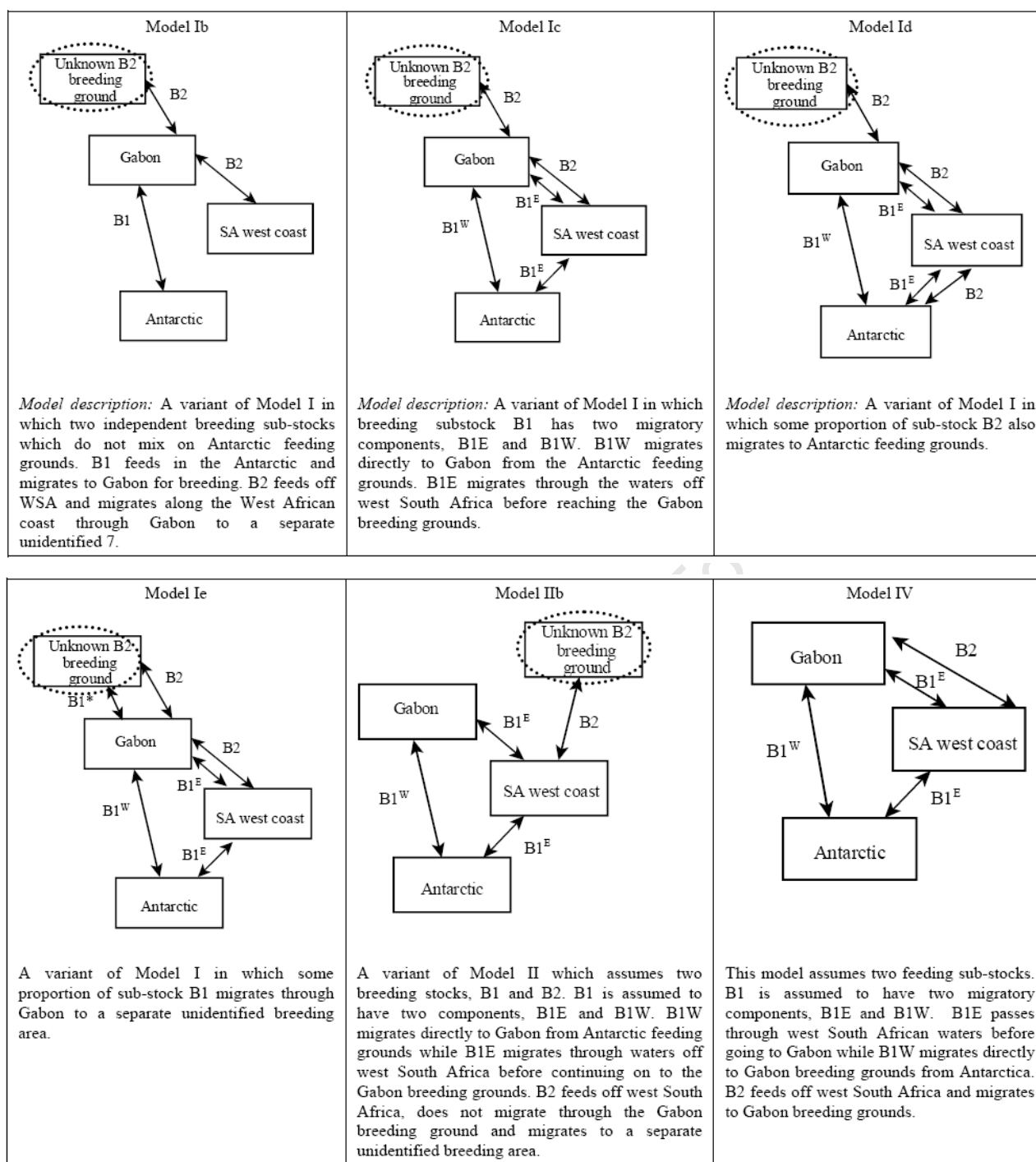


Figure A5.1.1: Lower priority stock structure models identified for Breeding Stock B assessment modelling.

## Appendix 5.2

### Prior incoherence within a Bayesian assessment of the Southern Hemisphere humpback whale Breeding Stock B population

This problem is explained in the context of the simpler<sup>52</sup> Model Ia.

In the assessment procedure, any parameter combination ( $r$  and  $\ln(\tilde{N}_{\text{tar}})$ ) that lead to population estimates going below  $N_{\text{min}}$  are penalised by adding 1000 to the negative log likelihood for each year the population is below  $N_{\text{min}}$  (i.e. the longer the population remains below  $N_{\text{min}}$ , the greater the penalty will be; effectively this penalty is sufficiently large as to prevent trajectories dropping below  $N_{\text{min}}$ ). For the B2 population, the introduction of these new  $N_{\text{min}}$  values results in some parameter values being rejected that might otherwise provide good fits to the trend and abundance data (in particular certain combinations of low  $\ln(\tilde{N}_{\text{tar}}^{B2})$  and high  $r^{B2}$  are rejected). As such, the final assessment results yield a lower  $r^{B2}$  and, as a direct consequence of the favoured high  $\ln(\tilde{N}_{\text{tar}}^{B2})$  and this lower  $r^{B2}$ , a higher  $K^{B2}$  than would otherwise have resulted.

Essentially, there are now two independent pieces of information informing the realised prior distributions (or the post-model pre-data distributions) of the  $r^{B2}$  and  $\ln(\tilde{N}_{\text{tar}}^{B2})$  parameters (namely the  $N_{\text{min}}$  constraints in addition to the standard explicit prior distribution). This results in incoherent joint prior distributions and can turn an uninformative prior distribution into one that is in fact informative (Brandon *et al.*, 2007). A coherent joint prior thus needs to be constructed.

The essence of the problem is that by introducing an (in this case informative)  $N_{\text{min}}$  constraint, the parameter space that is sampled is effectively no longer uniform as certain combinations of  $r^{B2}$  and  $\ln(\tilde{N}_{\text{tar}}^{B2})$  values are excluded. This is illustrated in Figure A5.2.1. The problem was discussed at the December 2010 MARAM<sup>53</sup>/DAFF<sup>54</sup> International Stock Assessment Workshop at the University of Cape Town, and several approaches were proposed.

#### Approach 1: Re-sampling

An approach for dealing with an ( $r^{B2}, \ln(\tilde{N}_{\text{tar}}^{B2})$ ) parameter combination that does not adhere to the  $N_{\text{min}}$  constraint is to re-sample the parameter values until a biologically feasible combination has been found. Various re-sampling schemes are given in Brandon *et al.* (2007). The paper emphasises that no one method has been conclusively deemed better than the others and all schemes produce slightly different results. In the case of a data-poor assessment, these differences can be quite substantial. Thus sensitivity to re-sampling scheme needs to be investigated. The following re-sampling strategy was proposed:

If a biologically unfeasible solution is obtained for a particular parameter combination ( $r^{B1}, r^{B2}, \ln(\tilde{N}_{\text{tar}}^{B1}), \ln(\tilde{N}_{\text{tar}}^{B2})$ ), then  $r^{B1}$  and  $\ln(\tilde{N}_{\text{tar}}^{B1})$ , as well as  $r^{B2}$ , are kept and  $\ln(\tilde{N}_{\text{tar}}^{B2})$  is re-sampled until an acceptable solution is found.

<sup>52</sup> Simpler in relation to Models IIa and IIa, as there is no sub-structuring of B1 in Model Ia.

<sup>53</sup> Marine Resource Assessment and Management Group, University of Cape Town

<sup>54</sup> Department of Agriculture, Forestry and Fisheries, South Africa

For the sake of efficiency, the number of times  $\ln(\tilde{N}_{targ}^{B2})$  is re-sampled has to be limited. In the results of this assessment,  $\ln(\tilde{N}_{targ}^{B2})$  is re-sampled up to 10 times. If after 10 attempts no suitable value has been found,  $r^{B2}$  is also re-sampled. This approach was implemented and the results are presented in the thesis.

Approach 2: Re-parameterise in terms of  $N_{min}$

This approach uses  $r^{Bi}$  and  $\tilde{N}_{min}^{Bi}$  as estimable parameters, instead of the standard  $r^{Bi}$  and  $\ln(\tilde{N}_{targ}^{Bi})$ .  $\tilde{N}_{min}^{Bi}$  is drawn from a uniform prior distribution with the corresponding  $N_{min}$  constraint as a lower bound, and some arbitrary, sufficiently high number as an upper bound. Exploration of this method has commenced, and the results will be presented at a later date.

Approach 3: Use of copulas<sup>55</sup>

Owing to time constraints, this method has not been explored at this point, but will hopefully be investigated and incorporated into future assessments.

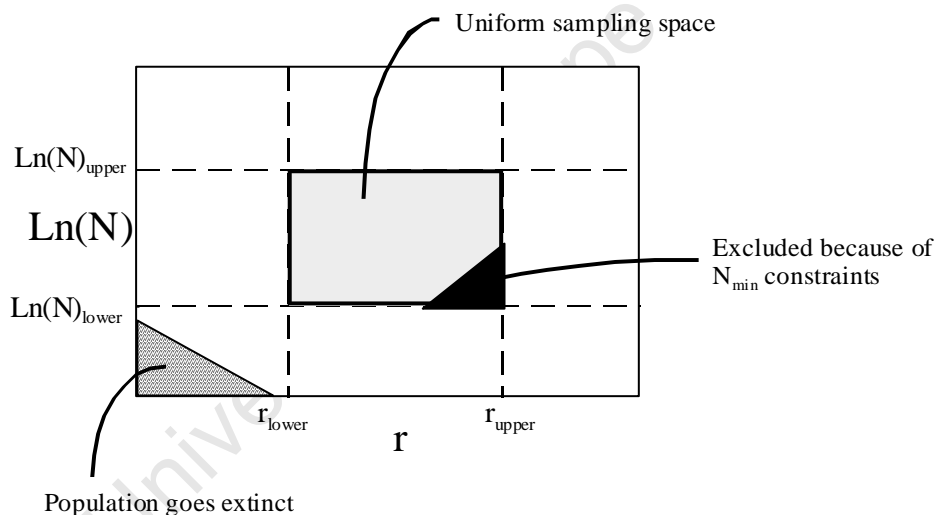


**Figure A5.2.1:** Schematic illustration of the parameter space available for sampling. The outside box contains a large range of possible  $(r, \ln(N))$  combinations, while the inner box encloses a reduced range that represents what are considered realistic parameter values, from which the  $(r, \ln(N))$  values for the Bayesian assessment are drawn.

<sup>55</sup> ‘Copulas are functions that join multivariate distribution functions to their univariate marginal distributions’ (Jaworski, 2009).

## 6 Initial results for a combined assessment of all seven Southern Hemisphere humpback whales breeding stocks

### 6.1 INTRODUCTION

Over the last 10 years or so, various assessments have been carried out for each of the seven Southern Hemisphere humpback whale breeding stocks. One recurring problem encountered in these assessments has been the question of catch allocation. Catch records give historic catches by position (Allison, 2006). In the low latitude wintering and breeding areas, it is fairly straightforward to allocate the catches to the various breeding stocks as these stocks tend to move in shallow waters along the coast (Johnson and Wolman, 1984) and as such have well-defined breeding regions. However in the high latitude Antarctic feeding areas, where mixing between various breeding populations occurs, catch allocation becomes more difficult.

Since several breeding stocks compete for food in the feeding grounds, density dependence becomes an important issue. Carrying capacities (quantities that assessments aim to estimate) would be strongly influenced by feeding ground dynamics (IWC, 2009b), so that care needs to be taken in allocating the feeding ground catches to various breeding stocks. Over the years, various hypotheses have been proposed to deal with these catch allocations (these are summarised in Findlay *et al.*, 2009). The latest of these, referred to as Hypothesis 1 (IWC, 2010), divides the high-latitude waters into nucleus and margin regions, the former being associated with single breeding stocks while the latter is shared between two neighbouring stocks (see Figure A3.1.1 of Appendix 3.1). Hypothesis 1 was recommended as a reference case by the IWC SC sub-committee on Southern Hemisphere humpback whales (IWC, 2010) and is currently in use for the Southern Hemisphere humpback whale assessments. In this hypothesis, catches taken in a nucleus region are allocated to the associated breeding stock, and catches in the margin areas are split equally between neighbouring stocks.

The intersessional IWC meeting in Seattle, February 2009, recommended the development of a model combining multiple breeding stocks, as this would allow flexibility in the placement of the boundaries between the nucleus and margin regions. Such an assessment would provide a platform to explore a widening range from which the high latitude catches from a particular breeding stock might have been taken and immediately compensate any adjustment with the neighbouring stocks. As such possible “double-counting<sup>56</sup>” of catches would be avoided in regions where two or more breeding stocks overlap. This assessment could further be extended to place Bayesian priors on the nucleus and margin boundaries, so that they might be estimated by the model rather than fixed to some pre-determined values.

The assessment reported here is the first step within the larger assessment exercise outlined above. It aims to combine all breeding stocks into one assessment, splitting catches in margin regions in proportion to the

---

<sup>56</sup> If a model’s sensitivity to catch-allocation is to be explored, different boundaries to those given in Hypothesis 1 (see Appendix 3.1) may be set. For conservative assessments (that take a pessimistic view of the stock’s status), it may be required to allocate catches from a far larger area than that given by the nucleus region to the stock in question – catches, which under the reference Hypothesis 1, would be allocated to a neighbouring stock. As stocks are generally assessed independently, such catches would be “double-counted”.

abundances of the respective neighbouring populations, rather than by a fixed (and potentially questionable) ratio. The results reported here were presented at the 62<sup>nd</sup> meeting of the IWC SC, Morocco, 2010 for initial discussion.

## 6.2 DATA

### 6.2.1 Historic Catch data

There are two sources of historic catch data.

- i) Catches north of 40°S, given by region and easily allocated to the respective breeding stocks (see Table A3.1.1 of Appendix 3.1). Records of a series of Russian catches are also available by 10 degree longitude and latitude bands and these catches have been incorporated into Table A3.1.1.
- ii) Catches south of 40°S, which are given according to assumed nucleus and margin regions (see Figure A3.1.1 of Appendix 3.1) and are shown in Table A3.1.2.

### 6.2.2 Abundance and trend data

These data include absolute abundance estimates, relative abundance estimates and capture-recapture information, and are given in Appendix 3.2. Table 6.1 (a) and (b) of the Results section (6.4) summarize the data associated with each breeding stock. Note that the Chittleborough (1965) and JARPA series have at this stage not been incorporated, as the other information is sufficient for the purposes of this initial assessment.

## 6.3 METHODS

### 6.3.1 Breeding stock population dynamics

Each population's dynamics is modelled by the Pella-Tomlinson equation:

$$N_{y+1}^i = N_y^i + r^i N_y^i \left( 1 - \left( \frac{N_y^i}{K^i} \right)^\mu \right) - C_y^i \quad i \in \{A, B, C1, C3, D, E, F, G\} \quad (6.1)$$

where

- $N_y^i$  is the number of whales in the breeding population  $i$  at the start of year  $y$ ,
- $r^i$  is the intrinsic growth rate for breeding population  $i$  (the maximum per capita the population can achieve when its size is very low),
- $K^i$  is the carrying capacity for population  $i$ ,
- $\mu$  is the “degree of compensation” parameter, which is set at 2.39, and hence fixes the level at which MSY is achieved at  $MSYL = 0.6K$ , as conventionally assumed by the IWC SC, and
- $C_y^i$  is the total catch (in terms of animals) for breeding population  $i$  in year  $y$ .

#### *Breeding Stock C sub-structure*

C1 and C3 are sub-stocks of Breeding Stock C, which is assumed to follow the Sabbatical model (Johnston and Butterworth, in prep., see also Chapter 4). Every year there is a probability  $\alpha^{C1}$  that an animal from sub-stock C1

travels to the C3 region instead of C1 and similarly a probability  $\alpha^{C3}$  that an animal from sub-stock C3 travels to the C1 region instead of C3. The observed numbers in regions C1 and C3 each year are then given by  $\eta^{C1}$  and  $\eta^{C3}$  respectively, and these are the variables to which observations apply (both capture-recapture and survey data). The observed populations are given by:

$$\eta_y^i = (1 - \alpha^i)N_y^i + \alpha^j N_y^j \quad \left\{ \begin{matrix} i \\ j \end{matrix} \right\} = \left\{ \begin{matrix} C1 \\ C3 \end{matrix} \right\} \text{ or } \left\{ \begin{matrix} C3 \\ C1 \end{matrix} \right\} \quad (6.2)$$

Note that for simplicity, this assessment uses  $\alpha^{C1} = 0.01$  and  $\alpha^{C3} = 0.05$ . Future assessments will allow these values to be estimated.

#### Breeding Stock B sub-structure

In view of the current debate within the IWC SC humpback working group on the sub-structuring of Breeding Stock B, this assessment assumes a single homogeneous Breeding Stock B (i.e. no B1 and B2 sub-stocks). Once a reference case model has been agreed upon, the assessment will be updated to incorporate it.

*Note that other than for Breeding Stock B and Breeding Stock C, no sub-structure has been assumed for the other stocks.*

#### 6.3.2 Catch Allocation

For catch allocation purposes for regions where more than one stock/sub-stock of whales are present, complete mixing is assumed and catches each year are allocated amongst the stocks in proportion to their relative abundances.

Catches north of 40°S are available by area and thus easily allocated to the respective breeding stocks (see Table A3.1.1 of Appendix 3.1). The feeding ground regions south of 40°S are split into Nucleus and Margin regions (see Figure A3.1.1 of Appendix 3.1). Catches taken in any of the nucleus regions are allocated to the corresponding breeding stock. Catches taken in a marginal region are allocated to the neighbouring stocks in proportion to the population abundances. For example, if  $N^1$ ,  $N^2$  and  $N^3$  are three neighbouring populations, the feeding ground catch allocated to population 2 is given by:

$$C_y^{feed,2} = C_y^{nucleus2} + C_y^{margin,12} \frac{N_y^2}{N_y^1 + N_y^2} + C_y^{margin,23} \frac{N_y^2}{N_y^2 + N_y^3} \quad (6.3)$$

where

- $C_y^{feed,2}$  is the total feeding ground catch in year  $y$  from breeding population 2,
- $C_y^{nucleus2}$  is the catch in year  $y$  taken from the nucleus feeding grounds associated with breeding stock 2,
- $C_y^{margin,12}$  is the catch year  $y$  taken from the marginal feeding grounds shared between stocks 1 and 2, and
- $C_y^{margin,23}$  is the catch year  $y$  taken from the marginal feeding grounds shared between stocks 2 and 3.

The total catch for breeding stock  $i$  is given by:

$$C_y^i = C_y^{breed,i} + C_y^{feed,i} \quad i \in \{A, B, C, D, E, F, G\} \quad (6.4)$$

#### Breeding Stock C catches

Note that Equation (6.4) applies for the combined Breeding Stock C. The feeding ground catches for stock C are further split in proportion to the respective C1 and C3 population sizes. The breeding ground catches, which are given for regions C1 and C3, need to be adjusted to take into account the movement within the stocks. The C1 and C3 catches are thus given by:

$$C_y^{Ci} = C_y^{breed,Ci} + C_y^{feed,C} \frac{N_y^{Ci}}{(N_y^{C1} + N_y^{C3})} \quad \begin{matrix} \{i\} \\ \{j\} \end{matrix} = \begin{matrix} \{C1\} \\ \{C3\} \end{matrix} \text{ or } \begin{matrix} \{C3\} \\ \{C1\} \end{matrix} \quad (6.5)$$

where

$$C_y^{breed,Ci} = C_y^{Ci,reported} \frac{(1 - \alpha^{Ci}) N_y^{Ci}}{((1 - \alpha^{Ci}) N_y^{Ci} + \alpha^{Ci} N_y^{Cj})} + C_y^{Cj,reported} \frac{\alpha^{Ci} N_y^{Ci}}{(\alpha^{Ci} N_y^{Ci} + (1 - \alpha^{Cj}) N_y^{Cj})} \quad \text{and}$$

$C_y^{Ci,reported}$  is breeding ground catch allocated to sub-stock  $Ci$ .

#### 6.3.3 Estimation procedure

Initially, the standard Bayesian SIR approach adopted in the past for assessments of individual breeding stocks was attempted, where for each breeding population  $i$  ( $i \in \{A, B, C1, C3, D, E, F, G\}$ ), values of  $r^i$  and  $\ln \tilde{N}_{target}^{i,obs}$  are randomly drawn from prior distributions and a downhill simplex method of minimisation is used to calculate  $K^i$  such that the model estimate of  $N_{target}^i$  is identical to  $\tilde{N}_{target}^{i,obs}$ .

The approach outlined above whereby  $K$  values are found by working back from a prior distribution on an abundance estimate is known as the ‘backwards’ method (Butterworth and Punt, 1997, see Appendix 3.3). This approach, however, led to time-intensive processes and poor performance in finding solutions necessary to be able to implement the conventional SIR approach. This poor performance was because of the complexity of the problem due to the interaction amongst the populations<sup>57</sup>.

An alternative approach is the ‘forwards’ method (see Appendix 3.3). Here, uniform priors are assumed on  $r^i$  and  $K^i$ , and a maximum (penalised) likelihood estimate (the penalty corresponding to the log of the joint priors) is found (here using AD Model Builder). In other words, a combination of  $r^i$  and  $K^i$  values is found that is the most likely given the abundance and trend data (equations for the likelihood function are given in Chapter 3). Once this maximum likelihood solution has been obtained a Markov Chain Monte Carlo (MCMC) approach is used to obtain a set of equally likely values of  $r^i$  and  $K^i$ , allowing posterior distributions to be computed (see Section 2.5).

<sup>57</sup> Catches are split in proportion to the population abundances. Thus a change in any one of the seven populations effects a change in all of the other six.

The exercise reported here intends only to produce some initial results and these results should be considered as preliminary only. There are problems associated with the ‘forwards method’ – the model dynamics are such that a uniform prior on  $K$  is in fact informative regarding the intrinsic growth rate parameter  $r$ . This is illustrated in more detail in Appendix 3.3. Future adjustments will aim to address this issue by varying the priors for  $K$  in a way that sees them correspond more closely to post-model pre-data distributions for intrinsic growth rate parameters that are near uniform.

The prior distributions used in this initial illustrative assessment are given below.

$$\begin{aligned}
 r^j &\sim \text{U}[0, 0.106] \text{ (i.e. the same uniform prior for all populations)} \\
 K^A &\sim \text{U}[0, 35000] \\
 K^B &\sim \text{U}[0, 40000] \\
 K^{C1} &\sim \text{U}[0, 25000] \\
 K^{C3} &\sim \text{U}[0, 25000] \\
 K^D &\sim \text{U}[0, 50000] \\
 K^E &\sim \text{U}[0, 45000] \\
 K^F &\sim \text{U}[0, 25000] \\
 K^G &\sim \text{U}[0, 25000]
 \end{aligned}$$

A large interval was placed around feasible<sup>58</sup>  $K$  values to obtain the distribution bounds. The uninformative  $r$  prior is bounded by zero (negative rates of growth are biologically implausible) and 0.106 (this upper limit corresponds to the maximum growth rate for the species as agreed by the IWC SC (IWC, 2008)).

#### 6.3.4 Contributions to the likelihood function and priors

The data given in Appendix 3 include absolute abundance estimates, relative abundance estimates and capture-recapture information. The incorporation of these data into the likelihood function is described in Appendix 5, and is given by the following equations:

Absolute abundance data	-	Equation (3.1)	(Chapter 3)
Relative abundance data	-	Equation (3.5)	(Chapter 3)
Capture-recapture data	-	Equation (3.12)	(Chapter 3)

The intrinsic growth rates  $r$  for each of the breeding stocks, while not being identical, are nevertheless likely to be somewhat similar to each other. To incorporate this into the model, it is assumed that the  $r$  values are realisations of an underlying normal distribution,  $N(\bar{r}, \sigma^2)$ , where  $\bar{r}$  is the mean of the eight  $r^j$  values, and  $\sigma$  is an estimate of the spread about the mean, set here to be 0.02. As such, a term has been added to the log priors in the log posterior computation to ensure that solutions for which the variability amongst the eight  $r$  values is not extreme are favoured:

<sup>58</sup> These ‘feasible’  $K$  values are based on estimations for the respective breeding stocks from previous assessments (see Table 6.2).

$$-\ln p_{prior} = \sum_{i=A}^G \frac{(r^i - \bar{r})^2}{2\sigma^2} \quad (6.6)$$

### 6.3.5 $N_{min}$ constraints

Normal procedure in humpback whale assessments is to enforce an  $N_{min}$  constraint based on the observed minimum number of haplotypes a population could have had (see Section 3.2.3). These values are available from Rosenbaum *et al.* (2006b). However considering the complexity of this assessment, these minima have not been included in this exploratory phase, but will rather be incorporated in future work.

## 6.4 RESULTS

### *Convergence*

Figure 6.1 (a)-(h) show the MCMC output chains for Breeding Stocks A to G. The plots show every 1000<sup>th</sup> value from a ten million long chain, for which the first one million steps have been discarded for “burn-in”. Note that the magnitudes of the variations in the chains may be slightly misleading as the vertical axes have different scales to better reflect the variations. Figure 6.2 shows the same chains on a single plot. Figure 6.3 shows a similar plot to Figure 6.2, except for an initial chain with length of 20 million.

### *General assessment results*

Table 6.1 (a) and (b) give the MCMC results for each of the eight breeding populations (including the C1 and C3 sub-stocks of Breeding Stock C). These results are from a chain of 10 million in length, with the first 1 million discarded for burn-in and every 1000<sup>th</sup> value sampled. In each case the median values for the estimated growth rate  $r$  and the pristine population levels  $K$  are shown. The values of  $N_{min}$  and  $N_{min}$  as a fraction of pristine population size are also given. Estimates of current (2010) abundance are given, as well as an estimate of current extent of recovery to the pristine level,  $N_{2010}/K$ . Lastly the estimated extent of recovery for 2040 ( $N_{2040}/K$ ) is given, where  $N_{2040}$  is the projected population size in 2040 under the assumption of zero future catch. The tables give the median values for the above-mentioned quantities, as well as the 90% probability intervals. The recent abundance and trend information used in the assessment are also shown in Table 6.1 (a) and (b).

Figure 6.4 (a)-(d) and Figure 6.5 (a)-(d) show the median population trajectories for each of the eight populations, along with the 90% probability envelopes. Note that in some cases, these probability envelopes are exceptionally narrow (see for example Breeding Stock A, B and E in Figure 6.4 (a) and (b), and Figure 6.5 (b) respectively).

### *Fit to abundance and trend data*

On all plots in Figure 6.4 and Figure 6.5, recent abundance estimates are indicated with a solid circle. Fits to other trend data used for the respective populations are also shown. In some cases (e.g. Breeding Stocks E and F, Figure 6.5 (b) and (c) respectively), the qualitative fits to both the abundance and trend data are good. Figure 6.5 (a) and (d) on the other hand (Breeding Stock D and G) show a relatively poor fit to the recent abundance index.

## 6.5 DISCUSSION

### *Convergence*

In the MCMC process, once thinning has taken place, the resulting plot of the parameter values against iteration number should display a collection of seemingly random points. The plots shown in Figure 6.1 however show clear trends, indicating that the samples are dependent.

An approach to address the issue of dependence in the samples is to extend the length of the chain and increase the thinning interval, in the hope of attaining reasonably independent samples. The MCMC chains were accordingly extended to 20 million in length. After discarding the first million for burn-in and sampling every 1000<sup>th</sup> value, the chains illustrated in Figure 6.3 were obtained. These still show a lack of stability, suggesting that even an increased thinning interval is unlikely to improve the results substantially.

This lack of stability in the chains suggests that the interdependence of the populations does indeed complicate convergence considerably (as the results do not seem to converge even if the chains are simply lengthened). A possible solution is to reduce the ranges of the prior distributions on  $K$ . These were initially made large to ensure that the global minima were included, but reducing the ranges will increase the efficiency of the estimation processes. The observation was indeed made at the SC meeting that the ranges used were unnecessarily large (J. Jackson, *pers. comm.*). Some manual exploration of the likelihood profile<sup>59</sup> might be required for this, and this approach will be developed and investigated in preparation for an updated presentation of the work at future IWC conferences.

### *General assessment results*

The results seem to favour fairly high  $r$  values, with the estimated values for Breeding Stocks A, B and C falling outside the range of previous assessment results (see Table 6.2). A feature that merits further investigation is that the posterior for Breeding Stock E is concentrated entirely at 0.106, the upper bound of the prior distribution. The results of an assessment of this stock presented to the IWC SC in 2005 (Johnston and Butterworth, 2005) showed an even higher estimated  $r$  value of 0.122 (Table 6.2). It should be noted that that assessment used an upper limit of 0.126 for the uniform prior distribution on  $r$ . Since the lower limit of 0.106 implemented in this assessment results in a concentration of the estimated  $r$  values at this limit, this suggests that the data currently available for the Breeding Stock E supports a higher growth rate than that considered biologically plausible. This may reflect some immigration to the stock (Brandão and Butterworth, 2006).

The estimated  $K$  values coincide reasonably well with the results of previous assessments presented in Table 6.2. A point to note is that earlier assessments of Breeding Stock B (prior to the work presented in Chapter 5 of this thesis) were exclusively for the breeding sub-stock B1, and the  $K$  estimate for sub-stock B1 given in Table 6.2 is accordingly much lower than that for the entire breeding stock given in Table 6.1a.

The narrow probability envelopes indicated for some of the populations may in part be explained by the fact these envelopes were derived from MCMC output chains shown in Figure 6.2. The more stable a chain is around its median value, the smaller the probability interval will be. Breeding Stock E and sub-stock C3 serve as an

---

<sup>59</sup>Since there are 16 parameter values to be estimated (eight  $r$  and eight  $K$  values), a manual exploration of the likelihood is not straightforward and will have to be conducted on a grid-search basis in order to refine the ranges on the  $K$  priors.

illustration of this: the chain illustrated in Figure 6.2 for Breeding Stock E has very little variation, and Figure 6.5 (b) shows a narrow probability interval. The chain in Figure 6.2 for sub-stock C3, on the other hand, is much less stable, and Figure 6.4 (d) shows a much wider probability envelope. The other breeding stocks show similar patterns. Another point to note regarding the size of the probability envelopes is that, in general, the more trend data that are available, the narrower the probability envelope becomes. Breeding Stock E, for example, has a long relative abundance series consisting of 17 estimates over 23 years (Table A3.2.23 of Appendix 3.2). Figure 6.5 (b) shows a correspondingly narrow probability envelope. Breeding sub-stock C3 on the other hand has no trend information available, and Figure 6.4 (d) accordingly shows a much wider probability envelope. Other factors may have an influence as well, but it seems as though the width of the 90% probability interval of any particular breeding stock is primarily influenced by the trend data available.

#### *Fit to abundance and trend data*

Overall, this assessment has provided relatively good fits to the trend and abundance data. It is difficult to infer exactly what the driving forces behind the fits observed are, as there is substantial interdependence amongst the breeding stocks within the model (as catches in the margin regions are allocated to breeding stocks in proportion to the sizes of the stocks estimated to be present in the region). As such, a good fit to trend data for one population, may result in a poorer fit for either of its neighbouring populations.

#### *Conclusion*

Given the lack of convergence mentioned above, and the fact that the prior distributions on  $K$  are not entirely uninformative, the results here need to be considered preliminary. The purpose of this exercise has been primarily to illustrate an approach which will be developed further for presentation and discussion at future IWC SC meetings. It should also be noted that as data are updated and models for the individual populations are developed and changed (as for Breeding Stock B at the last IWC SC 62 (2010) meeting), these updates will need to be incorporated into the combined assessment. As such this assessment exercise is likely to remain a continuous work in progress.

In closing, one added advantage in attempting a combined assessment is that populations, for which less data are available, can be informed in an internally consistent way by data relating the other populations. Since it is assumed that the  $r$  values are normally distributed about some mean value, populations for which more data are available can be a driving component behind the  $r$  estimation, something not possible when the populations are individually assessed (unless a posterior for one is taken as a prior for another). Estimation in this manner provides a valuable advantage, as it is difficult to estimate parameters such as the growth rate for breeding stocks with little data (e.g. stocks C3, E and F).

## **6.6 FUTURE WORK**

Future work will entail investigation into the lack of convergence, which will involve:

- Manual exploration of the likelihood profile to refine the prior distributions on  $K$ .
- Adjustment of the  $K$  priors to obtain uninformative distributions.

Further, the model will be extended to allow for uncertainty in the placement of the Antarctic boundaries governing the allocation of high latitude catches amongst breeding stocks. This extension will be attempted

through the placement of priors on the current boundaries and computing posterior distributions in similar fashion to the  $r$  and  $K$  parameters.

Ideally, the more conventional Bayesian approach used in the assessments of the individual stocks should also be implemented here. A major limitation, however, is computing power, given the complicated nature of this problem. The use of importance functions for the estimable parameters may greatly increase the efficiency, but the estimation process is likely to remain time-intensive, thus hindering the ease of exploration of the model.

#### *Input data*

The input data for this assessment will need to be updated, including the incorporation of  $N_{min}$  constraints and the inclusion of any data currently omitted, such as the Breeding Stock B capture-recapture data arising from the IWC SC 62 (2010) meeting.

#### *Stock-structure*

As analyses of the individual stocks progress and views on stock-structure are developed, these findings will need to be incorporated into future work of this assessment. One such example is the sub-stock structure of Breeding Stock B, currently under assessment. On completion of this assessment, provisionally at IWC SC 63 (2011), the final stock-structure will need to replace the current structure used for Breeding Stock B in the combined assessment.

There are other benefits to the development of a combined assessment. Currently, stocks are assessed on an individual basis and as such no movement between stocks can be accommodated. IWC (2006) reports on the genetic identification of a Gabon (Breeding Stock B) juvenile male that was sighted two years before in Madagascar (Breeding Stock C). This sighting suggests movement between stocks may be possible (especially considering that Breeding Stocks B and C share feeding grounds). While there has been only one such observation, and the extent of such movement may be small, an assessment that allows for possible mixing between the stocks could be useful (IWC, 2009a). Similar allowances could be made for other neighbouring breeding stocks.

**Table 6.1 (a):** MCMC results for breeding population A to C3 for a chain of 10 million, with the initial 1 million discarded for burn in and every 1000<sup>th</sup> value sampled, to give the median values as well as the 5<sup>th</sup> and 95<sup>th</sup> percentiles (the latter are given in parenthesis).

	Breeding Stock A	Breeding Stock B	Breeding sub-stock C1	Breeding sub-stock C3
<b>Recent abundance</b>	6251 (2005)	7196 (2003)	5965 (2003)	None
<b>Trend information</b>	Breeding ground index of abundance IDCR/SOWER feeding ground index of abundance	IDCR/SOWER index of abundance Photographic mark-recapture data for all regions combined	Cape Vidal relative abundance estimates Photographic mark-recapture data	Photographic mark recapture data
<i>r</i>	0.096 [0.092;0.104]	0.092 [0.089;0.099]	0.097 [0.089;0.104]	0.088 [0.068;0.104]
<i>K</i>	23282 [22920;23509]	18749 [18339;18957]	7515 [7175;7843]	8372 [7600;9448]
<i>N<sub>min</sub></i>	214 [143;306]	285 [217;360]	442 [234;1380]	974 [322;2174]
<i>N<sub>2010</sub></i>	9960 [7579;12846]	10585 [9087;12273]	7307 [6718;7654]	8229 [7366;9377]
<i>N<sub>min</sub>/K</i>	0.009 [0.006;0.013]	0.015 [0.012;0.019]	0.058 [0.032;0.184]	0.116 [0.042;0.237]
<i>N<sub>2010</sub>/K</i>	0.429 [0.325;0.555]	0.566 [0.484;0.659]	0.978 [0.897;1.000]	0.998 [0.912;1.000]
<i>N<sub>2040</sub>/K</i>	0.999 [0.995;1.000]	0.999 [0.998;1.000]	1.000 [1.000;1.000]	1.000 [1.000;1.000]

**Table 6.1 (b):** MCMC results for breeding population D to G for a chain of 10 million, with the initial 1 million discarded for burn in and every 1000<sup>th</sup> value sampled, to give the median values as well as the 5<sup>th</sup> and 95<sup>th</sup> percentiles (the latter are given in parenthesis).

	Breeding Stock D	Breeding Stock E	Breeding Stock F	Breeding Stock G
<b>Recent abundance</b>	21750 (2008)	7090 (2004)	3827 (2002)	6504 (2006)
<b>Trend information</b>	IWC 1996 estimates IDCR/SOWER estimates	Estimates from Noad <i>et al.</i> , 2008 IDCR/SOWER estimates	IDCR/SOWER estimates	IDCR/SOWER estimates
<i>r</i>	0.100 [0.095;0.106]	0.106 [0.106;0.106]	0.064 [0.039;0.095]	0.069 [0.054;0.098]
<i>K</i>	19644 [18984;20227]	27187 [26897;27441]	15362 [14113;17037]	11351 [10501;11948]
<i>N<sub>min</sub></i>	885 [452;1713]	129 [119;139]	498 [198;1087]	627 [369;960]
<i>N<sub>2010</sub></i>	18918 [16813;19927]	8614 [7995;9275]	6167 [4682;7976]	9161 [6355;10970]
<i>N<sub>min</sub>/K</i>	0.045 [0.023;0.087]	0.005 [0.004;0.005]	0.032 [0.014;0.064]	0.055 [0.033;0.081]
<i>N<sub>2010</sub>/K</i>	0.971 [0.863;0.997]	0.317 [0.294;0.341]	0.400 [0.283;0.554]	0.802 [0.547;0.998]
<i>N<sub>2040</sub>/K</i>	1.000 [1.000;1.000]	0.998 [0.998;0.999]	0.972 [0.735;0.999]	0.999 [0.984;1.000]

**Table 6.2:** Estimated *r* and *K* values from previous assessments of the individual stocks.

Breeding stock	Source	<i>r</i> estimate range	<i>K</i> estimate range
Breeding Stock A	Zerbini <i>et al.</i> (in press)	0.062-0.075 (base case 0.069)	20969-24959 (base case 24713)
Breeding Stock B1	Johnston and Butterworth (2008a)	0.042-0.065	8411-10926
Breeding sub-stock C1	Johnston and Butterworth (in prep)	0.049-0.084 (base case 0.075)	8425-8858 (base case 8439)
Breeding sub-stock C3	Johnston and Butterworth (in prep)	0.051-0.060 (base case 0.057)	8786-9369 (base case 8854)
Breeding Stock D	Johnston and Butterworth (2007)	0.056-0.100	12410-22060
Breeding Stock E	Johnston and Butterworth (2005)	0.122	21825
Breeding Stock F	Currently none available	Currently none available	Currently none available
Breeding Stock G	Johnston and Butterworth (2007)	0.062-0.100	10406-11677

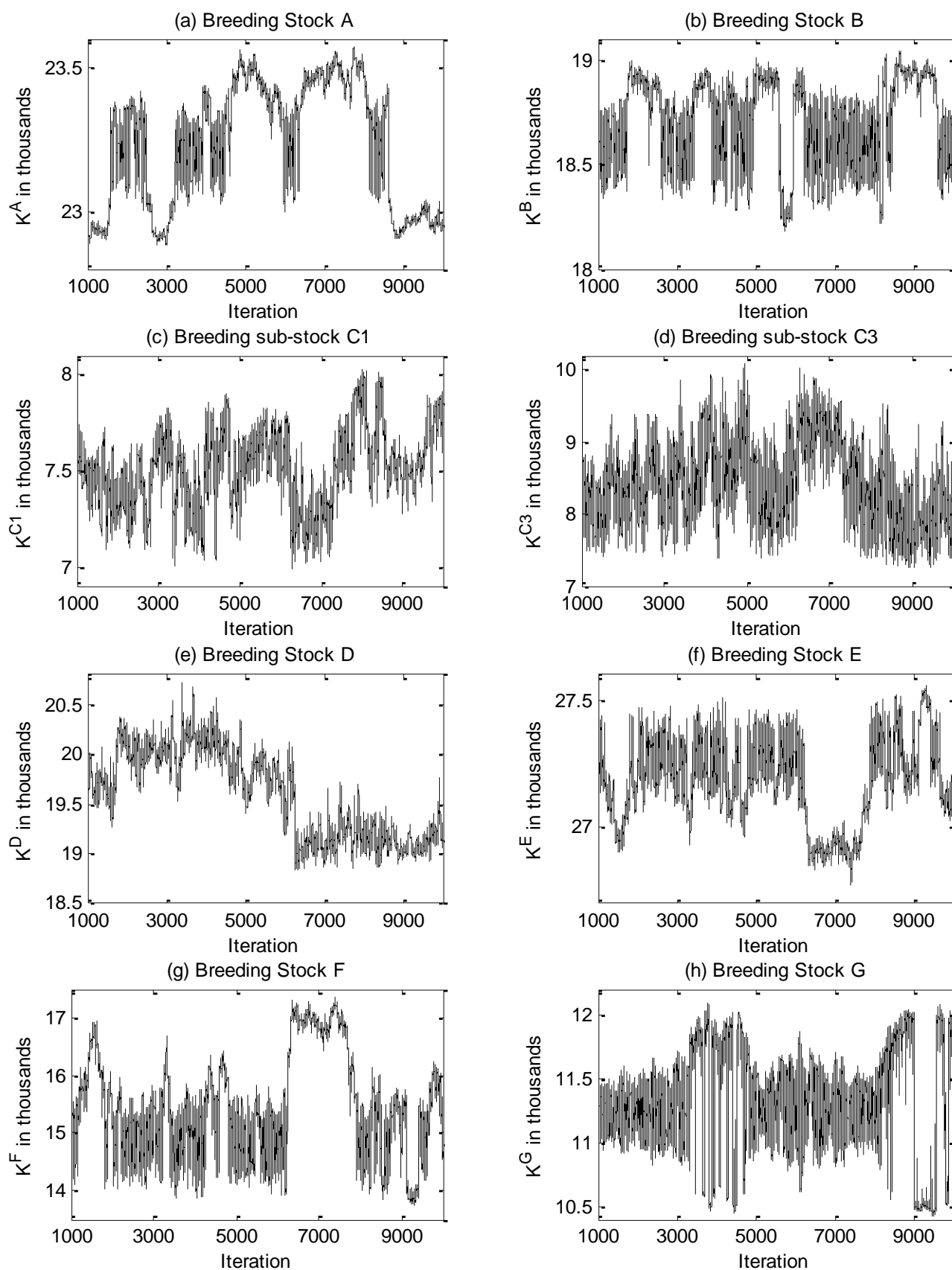


**Figure 6.1 (a)-(h):** MCMC chains for carrying capacity  $K$ : The chains show every 1000<sup>th</sup> value from a 10 million chain (where the first one million were discarded for burn-in).

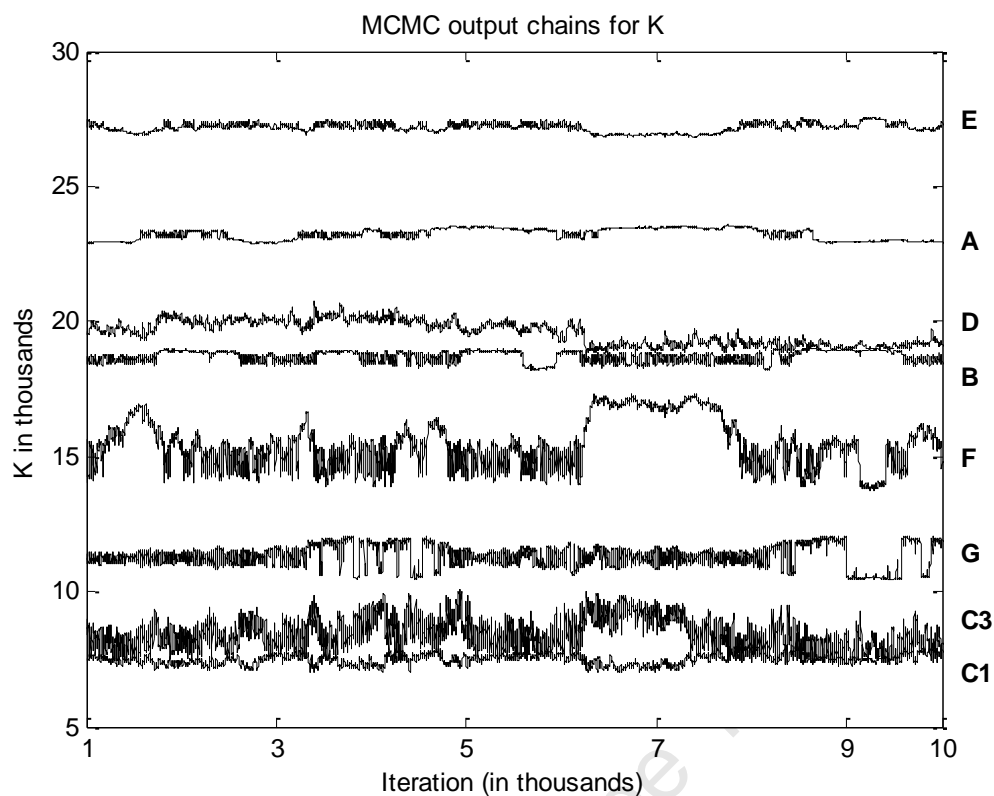


**Figure 6.2:** The MCMC chains for  $K$  from Figure 6.1 plotted on a single graph for all eight populations (every 1000<sup>th</sup> value in a 10 million long chain, with the first one million discarded for burn-in).

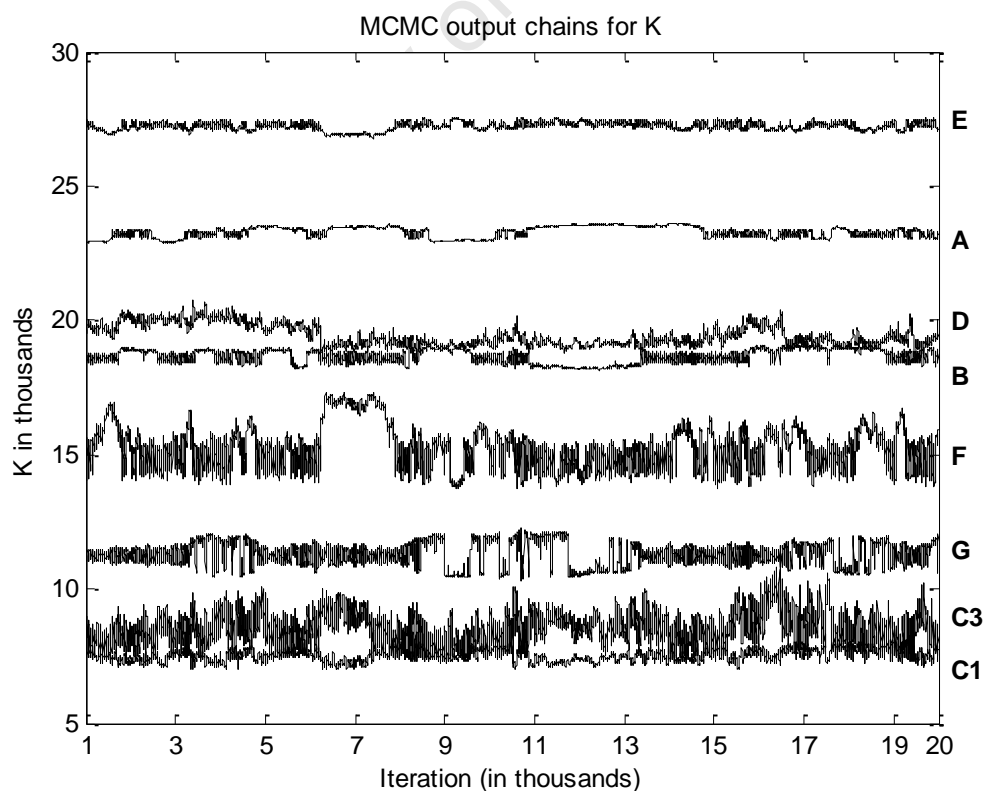


**Figure 6.3:** The MCMC chains generated from taking every 1000<sup>th</sup> value from 20 million long chains, with the first one million discarded for burn-in.

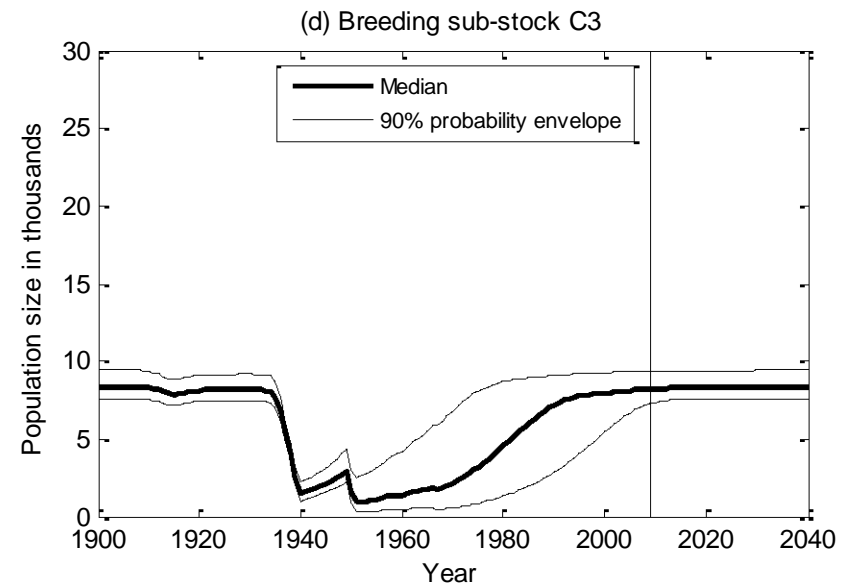
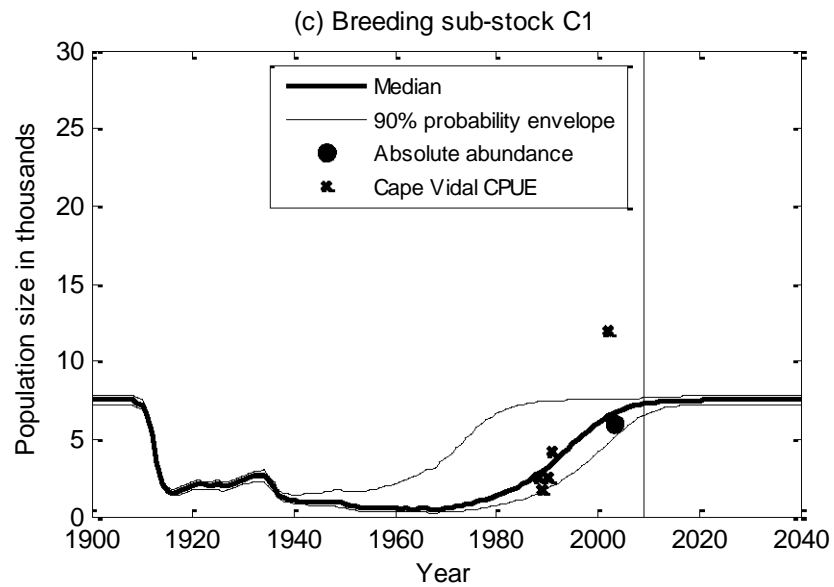
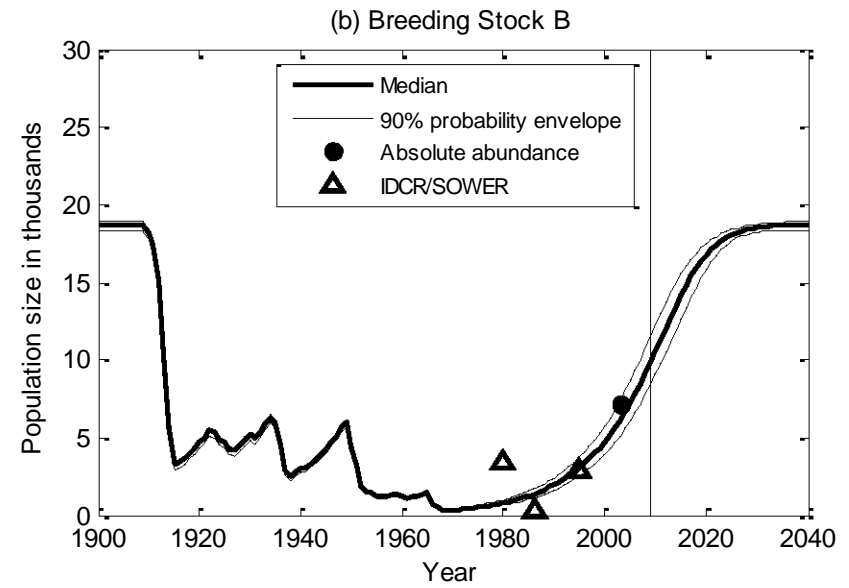
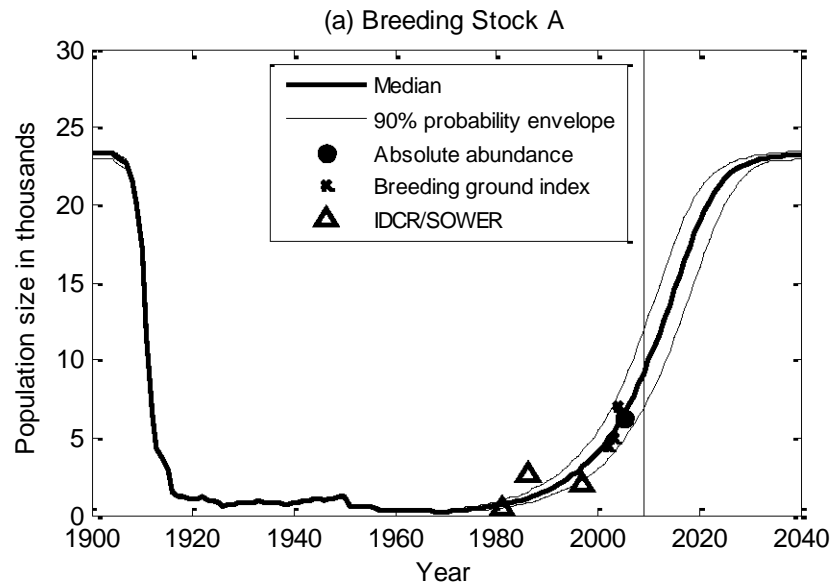


**Figure 6.4 (a)-(d):** Median population trajectories for stocks A-C3. The posterior median trajectories and the 90% probability envelope are shown, as well as the trend data used in the fitting process (see Table 6.1 (a)). Values to the right of the vertical dashed line indicate projections into the future under the assumption of zero catch.

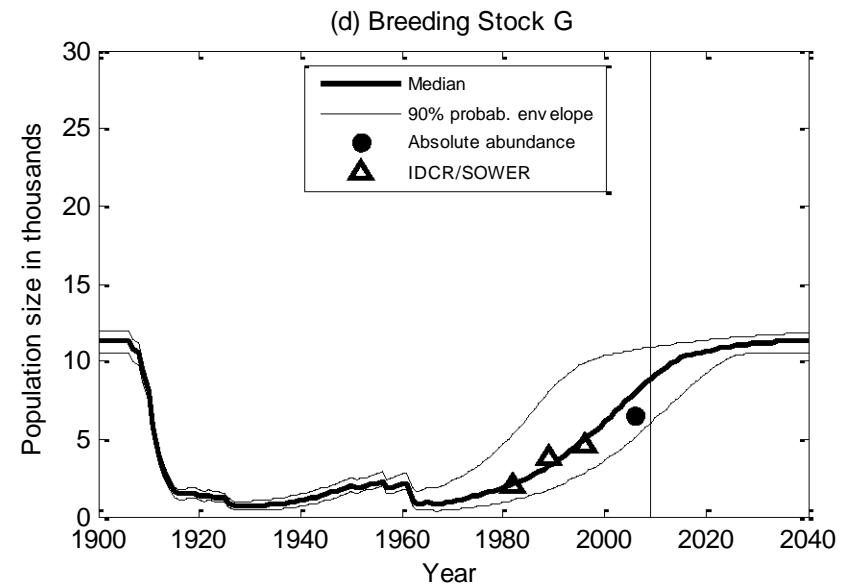
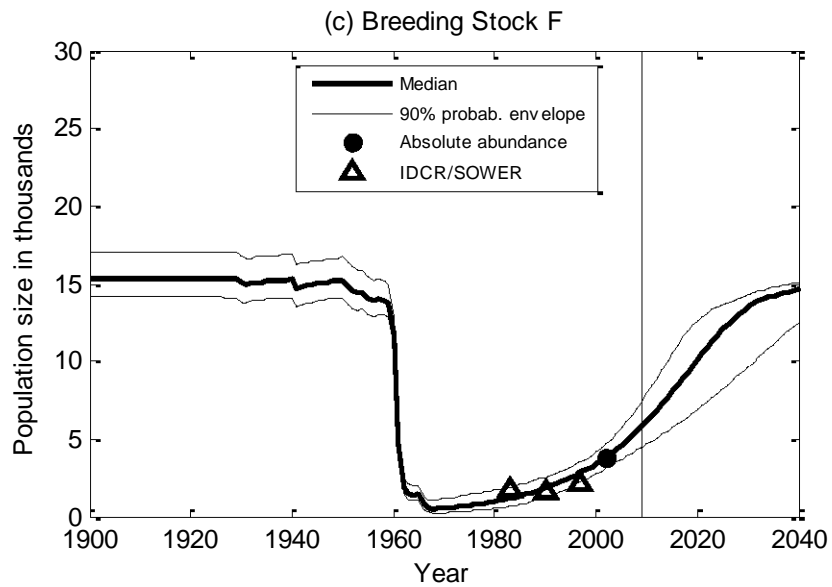
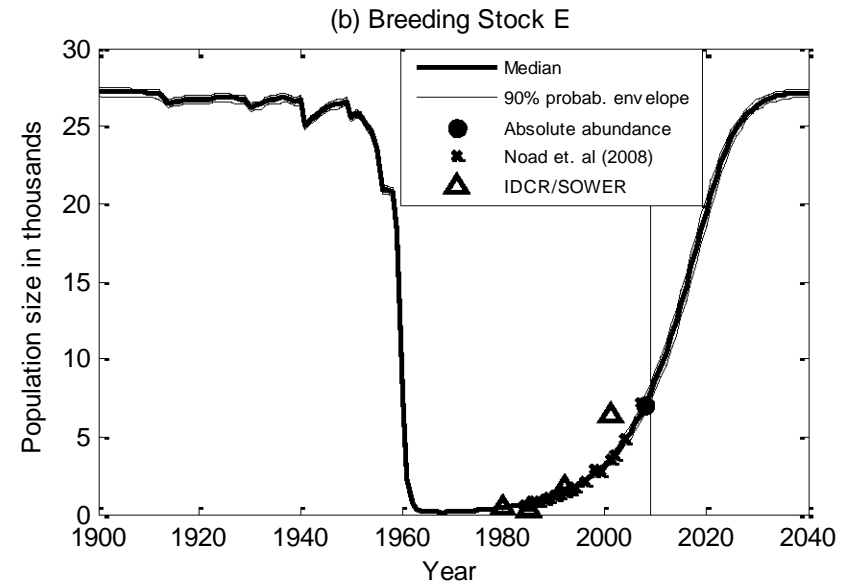
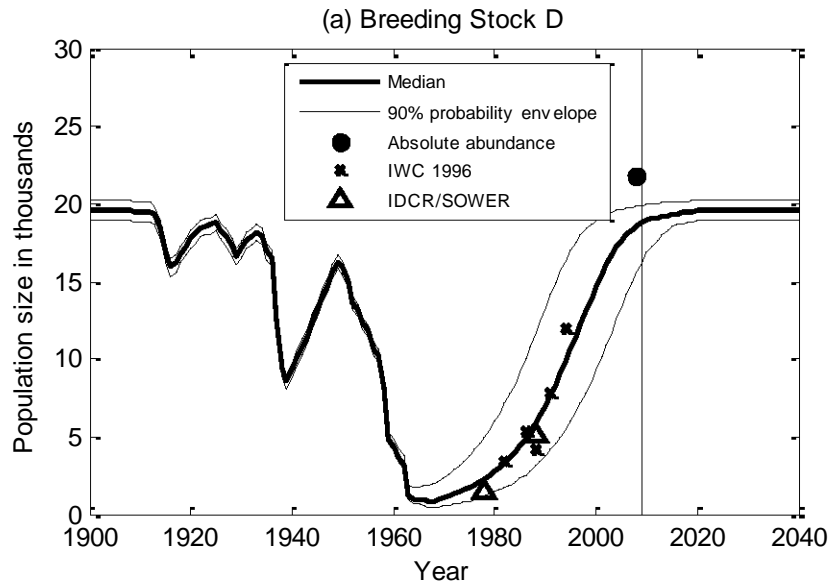


**Figure 6.5 (a)-(d):** Median population trajectories for stocks D-G. The posterior median trajectories and the 90% probability envelope are shown, as well as the trend data used in the fitting process (see Table 6.1 (b)). Values to the right of the vertical dashed line indicate projections into the future under the assumption of zero catch.

**SECTION C:**

**Applications to the South African east coast rock lobster**

**(*Palinurus delagoae*)**

University of Cape Town

## **7 Initial results from an assessment of the South African *Palinurus delagoae* rock lobster resource to investigate the recovery of the resource between two periods of experimental trap-fishing**

### **7.1 INTRODUCTION**

#### **7.1.1 Biological background**

The *P. delagoae* rock lobster is a sociable, migratory species that occurs on rocky as well as trawlable softer substrata of mud or sand off the east coast of South Africa from Durban (30°S) to central Mozambique (17°S) (Berry, 1971). It is a deep-water species (occurring at depths of 100-600m), making biological research difficult, as diving surveys and visual observations cannot be used to obtain information (such as distribution) about the species (Groeneveld, 2000). This information has to instead be obtained from trawl catches and scientific observers on board trawl vessels (Berry, 1971).

#### **7.1.2 Trawl fishery**

Exploratory trawling for *P. delagoae* first commenced in 1920 when the S.S. “Pickle” revealed the existence of large quantities of this species, originally identified as a variant of the related *Palinurus gilchristi*<sup>60</sup> (Berry, 1972). Berry (1972) describes how the species was widely distributed over the estimated 600 sq. miles of trawlable ground north of Durban, and “jackpot<sup>61</sup>” catches were not uncommon, such as a particular catch of over 10 000 lobsters taken in a 1.5 hour drag by a trawler.

These jackpot catches declined with time (the last one recorded was a 5 ton catch in a single drag in 1969 according to Berry, 1972) and after the 1960s the lobster fishery widened its focus to include other species (Groeneveld, 2000). This apparent decline suggests overfishing and is further complicated by the international nature of the fishery – both with respect to foreign vessels fishing in South African waters (Berry, 1972) and the fact the *P. delagoae* is distributed across the international boundary between South Africa and Mozambique.

Trawling still continues, but with a gradually decreasing quantity of *P. delagoae* taken every year (see Table 7.1).

#### **7.1.3 Trap fishery**

Groeneveld (2000) reports on an experimental long-line trap-fishery that was set up off the east coast of South Africa in 1993<sup>62</sup>, to determine the relative abundance trends of the *P. delagoae* population as well as to assess its suitability for trap-fishing. While the initial year’s catch was substantial (89.5t), there was a sharp decline in the years that followed, and the experiment was terminated in 1997 (Groeneveld, 2000). A second experiment was run some years later from 2004-2007 to determine if the stock had recovered and could sustain a trap-fishery

---

<sup>60</sup> *P. gilchristi* is found on the south coast of South Africa. *P. delagoae* was identified as its own species in 1973 (Groeneveld, 2002).

<sup>61</sup> Since the lobsters are sociable animals, they aggregate at times (especially during migrations) to the extent that a particular trawler may fill its nets with a jackpot catch whereas others working alongside catch nothing (Berry, 1971).

<sup>62</sup> A pilot study took place in 1993 to explore the availability and distribution of the lobsters. The structured experiment commenced in 1994.

(Boucher, 2007). The size of the catch taken in 2004 (25.97t) suggests that the stock had recovered somewhat since the first experiment, but again a rapid reduction in the catch in the subsequent year suggested that a long-term trap fishery could not be sustained (Boucher, 2007).

#### **7.1.4 Purpose of the assessment**

The assessment presented here aims to investigate quantitatively the extent, if any, of the recovery of the rock lobster between the two periods of experimental fishing, as well as to assess the current stock levels and potential future sustainable catches. It is of an initial nature and seeks to investigate if the apparent recovery between the experiments suggested by the catch data can be accounted for by the natural growth of the population, or if models with a more complicated spatial structure need to be explored<sup>63</sup>.

## **7.2 DATA**

### **7.2.1 Historic catch data**

#### *Trawl catches*

A trawl catch series for *P. delagaoe* for the years 1985 to 2009 has been provided by the Fisheries Branch of the Department of Agriculture, Forestry and Fisheries (DAFF) and is reproduced in Table 7.1. Berry (1972) provides trawl catches for the years 1961-1971, but it is not known what proportion of these catches were taken off Mozambique, outside South African waters. Catches for the period 1971-1984, and pre-1961 are not on record, as a standardised logbook system for the recording of catch and effort data was not implemented until 1985 (Fennessy and Groeneveld, 1997). These catch series are also shown in Figure 7.1.

#### *Trap catches*

Catch numbers from both experiments have been provided by the Fisheries Branch (DAFF) and are presented in Table 7.1.

#### *Catch-at-length data*

Catch-at-length data for the trap experiments were made available by the Fisheries Branch (DAFF) for 1994-1997 and for the years 2004 and 2007. These data were incorporated in the model to inform selectivity. As no descriptions or explanations accompanied the data, their reliability may be questionable. The data are shown in Figure 7.2 and Figure 7.3. Note that the corresponding data for the years 2005-2006 were not available.

### **7.2.2 Trend information**

The catch per unit effort series used for trend information in the assessment is given in Table 7.3. Its development is described in detail in Appendix 7.1.

---

<sup>63</sup> If the recovery cannot be accounted for by natural population growth, then alternative spatial structures may need to be explored. One such option would be to assume a two-component structure, where the population consists of an exploited and an unexploited subpopulation. Catches taken from the exploited sub-population may thus be augmented over time through migration from the unexploited to the fished sub-population. This will be discussed in more detail later.

### 7.2.3 Tag-recapture data

Tag-recapture data are available from the first experiment and were used to verify the von Bertalanffy growth curve parameters provided in Groeneveld (2000).

## 7.3 METHODS

### 7.3.1 Model Dynamics:

Note that difficulties arising from the use of the simpler Pope equations in an initial assessment attempt led to the use of the Baranov equations given below.

The population dynamics are given by:

$$N_{y+1,0} = R(B_{y+1}^{sp}) \quad (7.1)$$

$$N_{y+1,a+1} = N_{y,a} e^{-(M+S_a F_y)} \quad 0 \leq a \leq m-2 \quad (7.2)$$

$$N_{y+1,m} = N_{y,m} e^{-(M+S_a F_y)} + N_{y,m-1} e^{-(M+S_a F_y)} \quad (7.3)$$

where

$N_{y,a}$  is the number of *P. delagoae* rock lobsters of age  $a$  at the start of year  $y$ ,

$M$  is the natural mortality for *P. delagoae* rock lobster,

$F_y$  is the instantaneous fishing mortality for year  $y$ ,

$R(B_{y+1}^{sp})$  is the recruitment for year  $y+1$  given by the Beverton-Holt stock recruitment relationship (see Equation (7.6)),

$B_y^{sp}$  is the spawning biomass at the start of the year  $y$ ,

$m$  is maximum age considered, and

$S_a$  is the selectivity function, assumed here to be a logistic curve given by:

$$S_a = \frac{1}{1 - e^{-(a-a_s)/\delta}} \quad (7.4)$$

where  $a_s$  and  $\delta$  are estimable parameters.

### Stock-recruitment Relationship

The spawning biomass in year  $y$  is given by:

$$B_y^{sp} = \sum_{a=1}^m w_{a+0.5} f_a N_{y,a} = \sum_{a=a_m}^m w_{a+0.5} N_{y,a} \quad (7.5)$$

where

$f_a$  is the proportion of lobsters of age  $a$  that are mature (assumed knife-edge at age  $a_m$ , taken to be 5 years for this assessment), and

$w_{a+0.5}$  is the mass of an animal at age  $a+0.5$ , as catches are modelled as spread uniformly over the year.

The Beverton-Holt stock recruitment relationship relates the number of recruits at the start of year  $y$  to the mature component of the population, and is given by:

$$R(B_y^{sp}) = \frac{\alpha B_y^{sp}}{\beta + B_y^{sp}} \quad (7.6)$$

with

$$\alpha = \frac{0.8hR_0}{h-0.2} \quad (7.7)$$

$$\beta = \frac{0.2K^{sp}(1-h)}{h-0.2} \quad (7.8)$$

where

$R_0 = K(1 - e^{-M})$  is the recruitment at pristine population level  $K$  (in numbers),

$K^{sp}$  is the pristine spawning biomass at pristine levels, and

$h$  is the steepness of the stock-recruitment curve. It is the ratio of recruitment when the mature population is 20% of its pristine level to recruitment at pristine level, and is taken for this assessment to be 0.75<sup>64</sup>.

### 7.3.2 The likelihood function

#### CPUE contribution

The model treats the CPUE estimates from the GLM output as relative indices of abundance. It is assumed that the observed relative abundance index is log-normally distributed about its expected value:

$$I_y = qN_y^{\text{exp}} e^{\varepsilon_y} \quad (7.9)$$

<sup>64</sup> The value for this parameter was based on assessments for the South Coast rock lobster, *P. gilchristi*, which yielded values ranging between 0.6 and 0.9 for various models (Johnston and Butterworth (2010)).

where

- $I_y$  is the relative abundance (CPUE index) from the GLM assessment for year  $y$ ,
- $q$  is the catchability coefficient,
- $\varepsilon_y$  is an error term assumed to be from  $N(0, \sigma^2)$ , and
- $N_y^{\text{exp}}$  is the model estimate of observed exploitable population size at the start of year  $y$ , given by:

$$N_y^{\text{exp}} = \sum_a S_a N_{y,a} \quad (7.10)$$

The contribution of these data to the negative log likelihood is given by:

$$-\ln L_{\text{CPUE}} = n \ln \sigma + \frac{1}{2\sigma^2} \sum_y (\ln I_y - \ln q - \ln N_y^{\text{exp}})^2 \quad (7.11)$$

The  $\sigma$  parameter is estimated in the fitting procedure by its maximum likelihood value:

$$\hat{\sigma} = \sqrt{1/n \sum_y (\ln I_y - \ln q - \ln N_y^{\text{exp}})^2} \quad (7.12)$$

where

- $n$  is the number of data points in the CPUE series, and
- $q$  is the catchability coefficient, estimated by its maximum likelihood value:

$$\ln \hat{q} = 1/n \sum_y (\ln I_y - \ln N_y^{\text{exp}}) \quad (7.13)$$

#### *Length distribution data contribution*

The model provides estimates of the catch-at-age ( $C_{y,a}$ ) by number, which can be converted into proportions of the catch of age  $a$ :

$$p_{y,a} = C_{y,a} / \sum_a C_{y,a} \quad (7.14)$$

Using the von Bertalanffy growth curve, these proportions at age can be converted to proportions at length, under the assumption that the length-at-age distributions remain constant over time:

$$p_{y,\ell} = \sum_a p_{y,a} A_{a,\ell} \quad (7.15)$$

where  $A_{a,\ell}$  is the proportion of animals of age  $a$  that fall into length group  $\ell$ . The  $A$  matrix has been calculated under the assumption that for each age  $a$ , the length-at-age is normally distributed about the mean length given by the growth curves. The standard deviation used for this normal distribution is taken to be a function of age and proportional to the mean length:

$$\sigma_a = 0.01\bar{\ell}_a \quad (7.16)$$

where  $\bar{\ell}_a$  is the mean length for age  $a$  obtained from the growth curve.

To compute the likelihood contribution, suppose in year  $y$ ,  $r_{y,l}^{obs}$  rock lobsters of length  $l$  are caught. The model gives  $p_{y,l}^{mod}$ , the predicted proportion of the total catch that corresponds to animals of length  $l$ . Under the assumption that these proportions follow a multinomial distribution, the probability that  $r_{y,l_1}^{obs}$  catches are observed for length  $l_1$ ,  $r_{y,l_2}^{obs}$  catches are observed for length  $l_2$ , ... and  $r_{y,l_n}^{obs}$  catches are observed for length  $l_n$ , is given by:

$$P(r_{y,l_1}^{obs} | p_{y,l_1}^{mod}, \dots, r_{y,l_n}^{obs} | p_{y,l_n}^{mod}) = \frac{(\sum_{i=1}^n r_{y,l_i}^{obs})!}{r_{y,l_1}^{obs}! r_{y,l_2}^{obs}! \dots r_{y,l_n}^{obs}!} (p_{y,l_1}^{mod})^{r_{y,l_1}^{obs}} (p_{y,l_2}^{mod})^{r_{y,l_2}^{obs}} \dots (p_{y,l_n}^{mod})^{r_{y,l_n}^{obs}} \quad (7.17)$$

The likelihood contribution then is (after omission of the constant term):

$$-\ln L_{lengthdata} = -\sum_Y \sum_{\ell} r_{y,\ell}^{obs} \ln p_{y,\ell}^{mod} \quad (7.18)$$

### Fishing mortality

The catch of animals of age  $a$  taken in year  $y$  is given by:

$$C_{y,a} = S_a F_y N_{y,a} \frac{1 - e^{-(M+S_a F_y)}}{M + S_a F_y} \quad (7.19)$$

The total catch by weight is then given by

$$C_y^w = \sum_{a=0}^m w_a C_{y,a} \quad (7.20)$$

Thus given  $S_a$ ,  $N_{y,a}$  and  $M$ , an instantaneous fishing mortality has to be found such that the right hand side of Equation (7.15) equals  $C_y^w$  from the catch history. In other words, the roots of the equation

$$g(F_y) = C_y^w - \sum_a w_a S_a F_y N_{y,a} \frac{1 - e^{-(M+S_a F_y)}}{M + S_a F_y} \quad (7.21)$$

have to be found.

The  $F_y$  values have been estimated by adding  $w \sum_y (g(F_y))^2$  to the negative log likelihood<sup>65</sup>, where  $w$  is chosen to be sufficiently large to ensure that Equation (7.21) is always satisfied.

### 7.3.3 Estimation process

A maximum likelihood approach has been implemented, whereby the built-in ADMB minimiser was used to minimise  $-\ln L$  in order to find the maximum likelihood estimates for the estimable parameters. Given the initial nature of this assessment, with its primary purpose being to determine if spatial/stock-structure needs to be considered, the assessment methodology has at this point not been extended to a Bayesian framework.

### 7.3.4 Assumptions made in this assessment

The following assumptions were made on parameter values and relations needed for the assessment:

Growth curve parameters for the von Bertalanffy growth curve:  $\ell_\infty = 130\text{mm}$ ,  $\kappa = 0.13$ ,  $\ell_0 = 1.5\text{mm}$ .<sup>66</sup>

Weight-length relation:  $w(a) = 0.0018\ell^{2.77}$  (Boucher, 2007).

## 7.4 RESULTS

### General assessment results

The key assessment results are given in Table 7.4. The Table gives the maximum likelihood estimates for the pristine population level (in terms of numbers and biomass), as well as 2010 and future abundance estimates (also in terms of numbers and biomass, both in absolute terms and as fractions of the pristine level). The estimated natural mortality is also given. An approximate 95% confidence interval (taken to be  $\pm 1.96$  times the standard error) has been given for each of these quantities. Figure 7.4 illustrates the trajectory of the estimated exploitable population by number and the fit of this trajectory to the CPUE data. The exploitable biomass trajectory in tons is shown in Figure 7.5.

### Estimated catchability coefficients for the trap-fishing experiments

Initially, problems were experienced in obtaining an acceptable fit of the estimated trajectory to the CPUE data. The fit finally obtained (Figure 7.4) was achieved by estimating a separate  $q$  value for the CPUE data from each of the experiments. This  $q$  parameter (described in Equation (7.9)) gives a measure of the catchability of the animals, i.e. given an exploitable population  $N_y^{\text{exp}}$ , how likely it is for any one individual in that population to be caught for a unit level of effort. The value of  $q$  is estimated by its maximum likelihood estimate (see Equation (7.13)) and conventionally a single  $q$  value is estimated for a given CPUE series, as it would usually not be expected for the

<sup>65</sup> A likelihood contribution of this form is required as ADMB requires differentiable calculation processes and as such iterative solutions to equations such as Equation (7.21) (with the number of iterations depending on the convergence criterion) cannot be included.

<sup>66</sup> These parameter values were informed from tag-recapture data provided by DAFF. It was noted (Groeneveld, *pers. comm.*) that an  $L_\infty$  of 130mm is not realistic and that this value should be larger. Future work will accommodate this view and investigate the effect of the value of this parameter on the assessment results.

animals to become more or less ‘catchable’. For this assessment, however, this approach yielded poor fits to the CPUE, with the estimated trajectory seemingly battling to fit both halves of the CPUE series. This outcome may indicate that the CPUE data from the two experiments are in fact not comparable (as they had been hoped to be), but in the absence of the data that would enable the use of an alternative approach to the somewhat unconventional one given in Appendix 7.1, the estimation of separate  $q$  values seemed the most reasonable option. The estimated  $q$  values are given in Table 7.4. Note that a penalty was added to the negative log likelihood when the  $q_2/q_1$  ratio exceeded two, in order to keep the proportional change in catchability between the two experiments to within reason.

#### *Sustainable future catch and maximum sustainable yield (MSY)*

One objective of this assessment was to investigate possible sustainable future catches. Figure 7.6 shows projections into the future under different catch assumptions. Based on this figure, current stock levels (estimated at 4.9% of initial exploitable biomass, see Table 7.4) would be able to sustain an annual catch of at most six tons, for which the stock levels would not show any substantial growth in the future.

The logistic form of the selectivity function prevents an MSY value from being computed explicitly. A crude method to estimate this parameter quickly is to set the catch at a constant value and run the population dynamics for a long period of time. If the catch is at or below MSY, then the population will settle at a non-zero value. As soon as the catch exceeds MSY, the population will die out. This catch value can thus be adjusted until the maximum value is found for which the population does not go into decline. Using this simple method, an MSY of 11 tons was estimated.

#### *Fit to catch-at-length frequency data*

The catch-at-length data were included in the assessment to estimate the selectivity function parameters  $a_s$  and  $\delta$  (Equation (7.4)). Figure 7.7 shows that the selectivity function that best seems to fit the data is an almost knife-edge selectivity at an estimated age of 4.16. Figure 7.8 shows the model predicted catch-at-length frequencies plots against the frequencies observed, for the years where these observations are available. Figure 7.9 plots the residuals (roughly standardised to be homoscedastic by division by the square root of the predicted proportion, as to be expected for a multinomial distribution with small  $p$ ) between the observed and fitted catch-at-length frequencies. It is apparent that the residuals are not randomly distributed – the model systematically overestimates the catch-at-length frequencies for the middle length range, and underestimates them for the lower and higher length ranges.

## **7.5 DISCUSSION**

#### *General assessment results in light of data uncertainty and inconsistencies*

Given the initial nature of this assessment, and the uncertainty about the catch data, care should be taken when interpreting the results presented in Table 7.4, as they are the results of an assessment that requires further development.

A major issue is the uncertainty about the catch data. This assessment does not consider pre-1985 catches (since these are not available<sup>67</sup>) and incorrectly assumes that the population was at its pristine level in 1985. Berry (1972) reports that exploratory trawling started as early as 1920, and while quantities caught are unknown, it is mentioned that catches of over 10 000 lobsters were taken in a 1.5 hour drag, suggesting that these early catches were not insubstantial. The assumption of a 1985 pristine population had to be made in the absence of the early catch data, but is an issue which needs to be addressed in future work, as such an assumption must affect the assessment results quite substantially.

Additionally, some inconsistencies in the catch data provided were evident. Figure 7.1 shows the reported catch series from various sources and highlights a slight discrepancy between the data series provided by the Fisheries Branch of DAFF and that found in Groeneveld (2000) for the overlapping years 1995-1998. While this discrepancy should not have an appreciable impact on this assessment, it should be resolved.

A last concern regarding the treatment of catches in this assessment is that trap and trawl catches have been treated identically. The selectivity-at-age values for animals taken by these two methods are unlikely to be the same<sup>68</sup>, and thus future assessments should try to take this difference into account.

This assessment allowed the natural mortality to be estimated. Exploration of the likelihood profile showed that there was a definite maximum likelihood associated with a particular  $M$  value. Groeneveld (2000) gives 0.09-0.15yr<sup>-1</sup> as a reasonable range, so the  $M$  value supported by the data in this assessment seems rather low (0.067yr<sup>-1</sup>). This last value suggests that the species is longer lived than previously thought. In light of the above discussion regarding catch uncertainty, this result has not been further explored.

#### *Estimated catchability coefficients for the trap-fishing experiments*

These initial results were presented to the DAFF rock lobster scientific working group. This group considered the doubling of the catchability coefficient from the first experiment to the second to be unrealistic, as the same method of trapping was employed for both experiments, so that the two catchability coefficients should be very similar. This critique raises concern about the validity of the model chosen (see section 7.6 on future work). It is interesting to note here that a larger  $M$  value (corresponding to a shorter lived species) would imply more recovery between the two experiments, which would likely result in an even larger ratio between the two catchability coefficients, which seems unreasonable.

#### *Fit to catch-at-length frequency data*

The extension to the model to include length data proved to be challenging. Catch-at-length data for 1994-1997 shows a peak at the 130 + mm length group, whereas the years 2004 and 2007 both show a peak at ~65mm (see Figure 7.8). Closer inspection of the data, as well as the graphic displays given in the experimental reports, revealed that for the second experiment, large numbers of smaller animals were caught in the South region, and that this catch is responsible for the above-mentioned peak at lower lengths. The implication for the assessments is

---

<sup>67</sup> The catches that are available for the years 1961-1970 are considered unreliable as they include an unknown proportion of Mozambique catches (Berry, 1972).

<sup>68</sup> Older more experienced animals, for example, may be able to avoid traps but not trawling.

that the model battles to fit both of these peaks. At this point, it should be noted that the catch-at-length frequency data presented in Figure 7.2 are most likely incomplete. Groeneveld (*pers. comm.*) commented that the peak at length ~65mm that is visible in all the catches taken in the south for the second experiment had also been clearly visible in the catches of the first experiment. This peak is not at all evident in the data plotted in Figure 7.2, strongly suggesting that the data available are in fact incomplete. Thus further comment on the fit to catch-at-length frequencies seems unwarranted.

### *CPUE*

The only abundance trend information available for this assessment is the CPUE series obtained from the GLM described in Appendix 7.1. A concerted effort has been made to obtain a comparable CPUE series for the two trap fishing experiments, but there is still some concern about the validity of the CPUE series chosen. Missing and incomplete data made the work described in Appendix 7.1 difficult, and until the full set of data for the first experiment can be located, a fully comparable CPUE series cannot be obtained. As such the results of the GLM, as well as those of this assessment need to be seen as preliminary. That said, the assessment does suggest that the lobster numbers did not increase substantially in the 10 years between the two experimental trap fisheries, and that the population cannot sustain economic long-term trap fishing, given estimates of current annual sustainable yields in the six ton vicinity.

## **7.6 FUTURE WORK**

### *Catch data*

The main problem remains the uncertainty about the catches. Future work should include continued effort towards locating the missing data for the first trap-fishing experiment, and developing an approach for estimating the missing pre-1985 catch data. If a full set of catch-at-length frequency data is made available, then the selectivity-at-length may be better estimated.

### *Model adjustments*

The concerns raised about the estimated catchability coefficients suggest that the current model may not be appropriate. A second model has been proposed, where the population is assumed to consist of an exploited and an unexploited component:

Fennessy and Groeneveld (1997) explain that the continental shelf off the east coast of South Africa is relatively narrow, and that there are only two primary trawling grounds: one in shallow and one in deep water. The shallow trawling grounds cover an area extending from a few 100 metres to 16km offshore and are closely linked with a region of mud deposition from several rivers in the area, while the deep trawling grounds are situated a little further south at depths of 100-600m (Fennessy and Groeneveld, 1997). These two regions are spatially separated and it is therefore possible that less than the entire rock lobster population is accessible to trawling. Further, the Agulhas Current flows over these trawling grounds at speeds of up to three knots, which is comparable if not greater than the trawl speeds of between two and three knots (Fennessy and Groeneveld, 1997). This current can further limit the areas that can be accessed by the trawlers. The trap-fishing experiment extended to depths of only

425m and is unlikely to have accessed the entire population as juvenile recruitment is thought to take place at depths greater than 400m (Berry, 1973).

The proposed division of the *P. delagoae* population into two will have the one component exploited by the fishery, while the other component will represent the lobsters inaccessible to the trawl and trap fisheries. Net movement occurs from the unexploited to the exploited component, and the apparent recovery between the two trap-fishing experiments may then be accounted for by this movement as well as natural growth.

This model will be implemented to investigate if it can better explain the data available. Further refinements may also be made, such as exploring sex-specific growth curves or developing separate selectivity functions for the trawl and trap catches.

University of Cape Town

**Table 7.1:** Historic catch series for *P. delagoae* rock lobster

Year	Trawl fishery Catch (tons)	Trap fishery		Total Catch (tons)
		Catch (tons)	Catch (numbers)	
1985	27.2 *	0	0	27.2
1986	59.9 *	0	0	59.9
1987	36.8 *	0	0	36.8
1988	30.5 *	0	0	30.5
1989	16.3 *	0	0	16.3
1990	13.7 *	0	0	13.7
1991	22.2 *	0	0	22.2
1992	37.3 *	0	0	37.3
1993	37.8 *	0	0	37.8
1994	24.4 *	89.5 *	24532 °	113.9
1995	10.826 **	50.0 *	21354 °	60.826
1996	10.194 **	39.5 *	23071 °	49.694
1997	10.108 **	7.4 *	6000 °	17.508
1998	5.881 **	0	0	5.881
1999	7.824 **	0	0	7.824
2000	11.113 **	0	0	11.113
2001	8.824 **	0	0	8.824
2002	9.079 **	0	0	9.079
2003	5.372 **	0	0	5.372
2004	4.021 **	25.97 °°	46849 °°	29.991
2005	4.497 **	15.5 °°	29591 °°	19.997
2006	4.604 **	13.62 °°	30567 °°	18.224
2007	5.136 **	11.09 °°	33904 °°	16.226
2008	4.712 **	0	0	4.712
2009	3.912 **	0	0	3.912

\* Groeneveld (2000)

\*\* Fisheries, DAFF data (N. van den Heever, pers. comm.)

° Fisheries, DAFF data (Excel spreadsheet, "Pdsize comp data, 94-97.xls"), possibly incomplete

°° Scientific reports on experiments for 2004-2007

**Table 7.2:** Pre-1985 catches as reported in Berry (1972). Note that an unknown proportion of these catches emanate from Mozambique.

Year	Catch (tons)
1961	300
1962	200
1963	100
1964	200
1965	200
1966	100
1967	*
1968	*
1969	100
1970	100

**Table 7.3:** CPUE series from the GLM assessment, using the results from GLM<sub>3</sub> (see Appendix 7.1).

Year	CPUE
1994	209.26
1995	219.32
1996	83.15
1997	56.00
2004	148.5
2005	177.2
2006	116.24
2007	66.31

**Table 7.4:** Model maximum likelihood parameter estimates. The approximate 95% confidence intervals (taken to be  $\pm 1.96$  times the standard error) are shown in the parenthesis. Table (a) provides the pristine population level in terms of numbers and biomass, and also the estimated natural mortality rate and the two catchability coefficients estimated for the first and the second trap-fishery experiment. Table (b) shows current and future population levels in numbers and biomass, both in absolute terms and in terms of size relative to pristine level.

(a)

Parameter	Estimate	
$N_0^{total}$ (millions)	0.916	[0.644, 1.199]
$B_0^{total}$ (tons)	531	[451, 610]
$M$	0.0724	[0.0246, 0.1201]
$q_1$	0.00059	[0.00051, 0.00067]
$q_2$	0.00118	[0.00100, 0.00136]

(b)

Parameter	Estimate		Estimated fraction of pristine level	
$N_{2010}^{total}$ (millions)	1.915	[1.023, 2.806]	0.209	[0.164, 0.254]
$B_{2010}^{total}$ (tons)	33	[22, 43]	0.061	[0.045, 0.078]
$N_{2025}^{total}$ (millions)	0.516	[0.182, 0.850]	0.563	[0.365, 0.762]
$B_{2025}^{total}$ (tons)	184	[131, 236]	0.346	[0.199, 0.493]
$N_{2010}^{exp}$ (millions)	0.076	[0.059, 0.093]	0.119	[0.093, 0.145]
$B_{2010}^{exp}$ (tons)	25	[12, 38]	0.049	[0.031, 0.067]
$N_{2025}^{exp}$ (millions)	0.285	[0.166, 0.403]	0.446	[0.286, 0.606]
$B_{2025}^{exp}$ (tons)	170	[128, 212]	0.331	[0.196, 0.467]

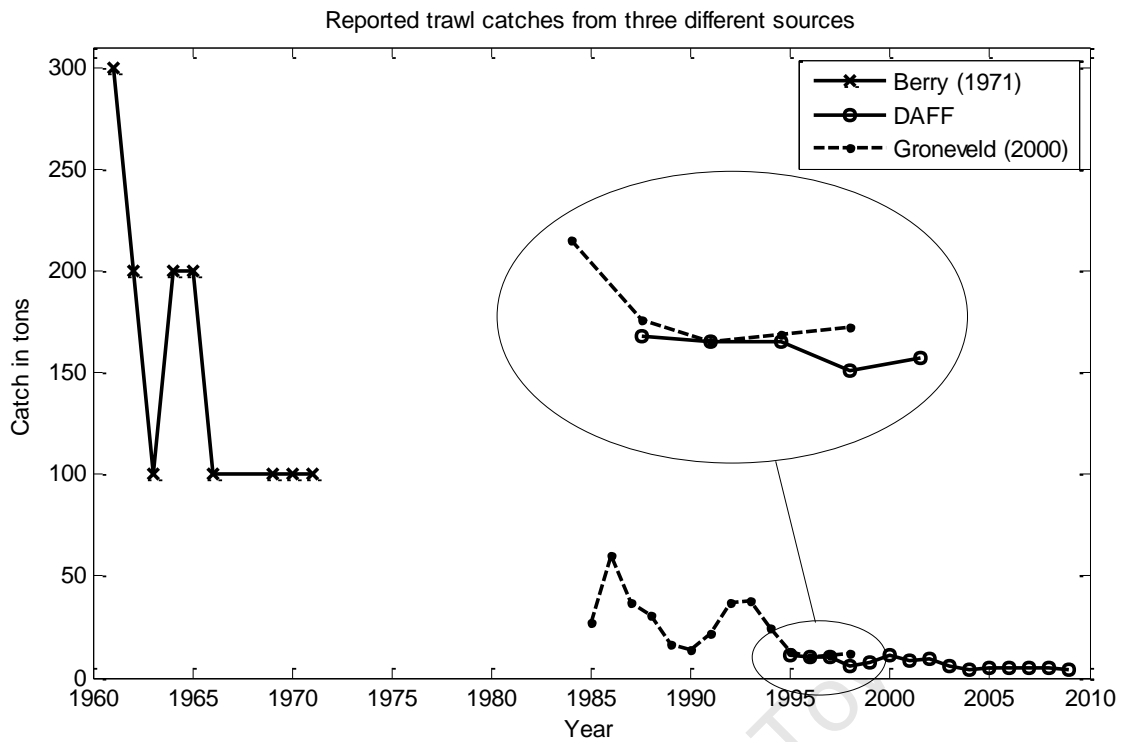


**Figure 7.1:** Reported trawl catches given in Table 7.1. The period where there is an overlap between the data provided by DAFF and those given in Groeneveld (2000) has been enlarged to show the slight discrepancies between the two series.

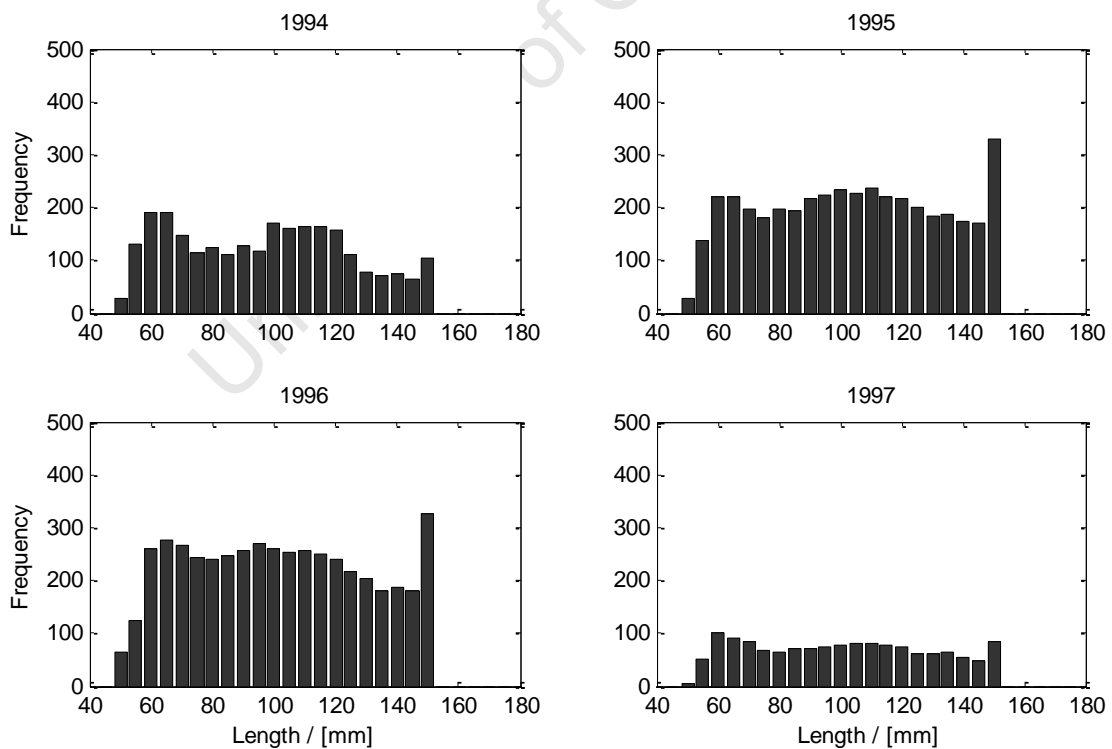


**Figure 7.2:** Catch-at-length frequencies available from the first experiment. Note that these were given without information about region or catch and effort, and are most likely incomplete (see Section 7.5).

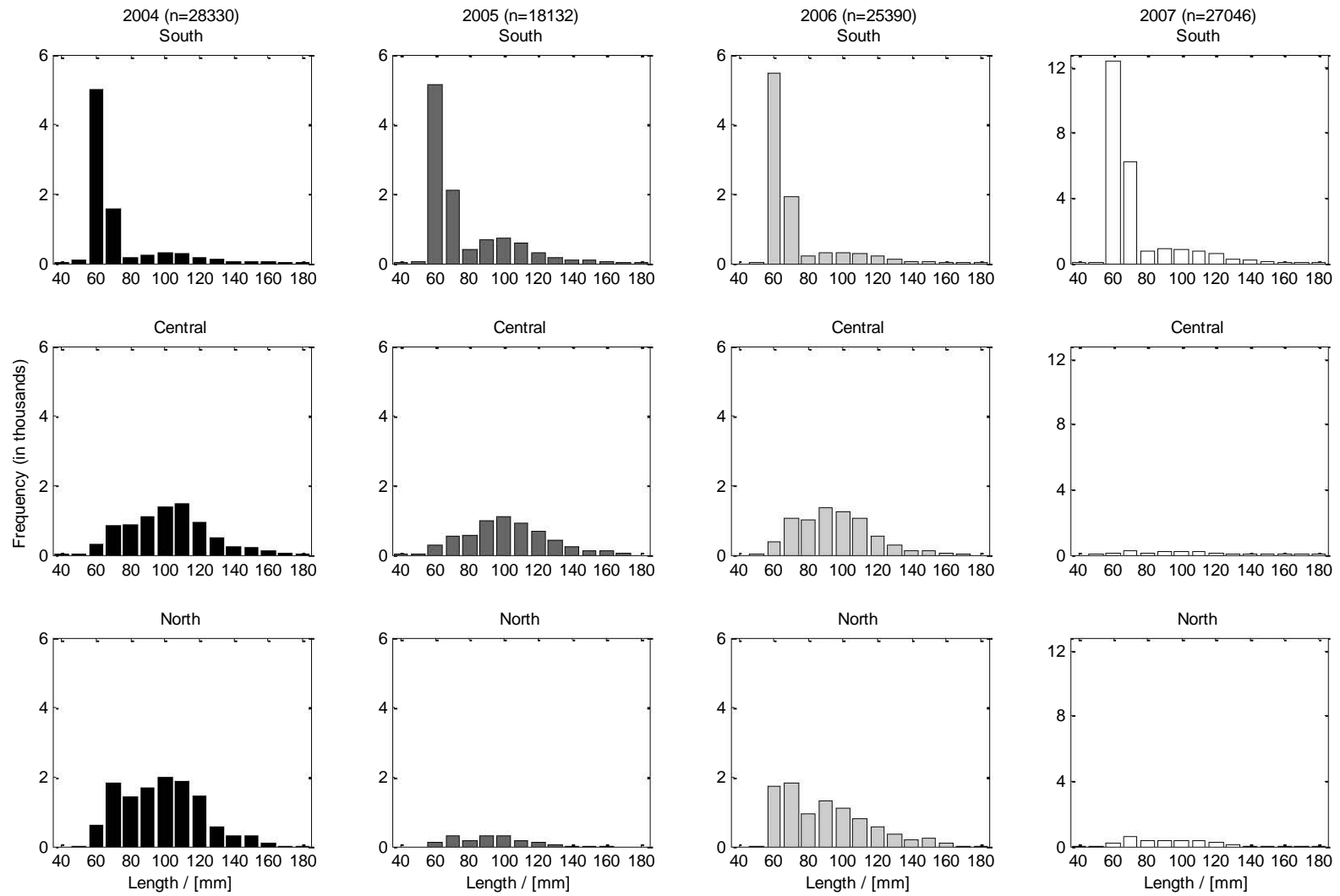


**Figure 7.3:** Reported catch-at-length frequencies from the second experiment, split by region and year. Note the different scale on the vertical axes of the 2007 plots.

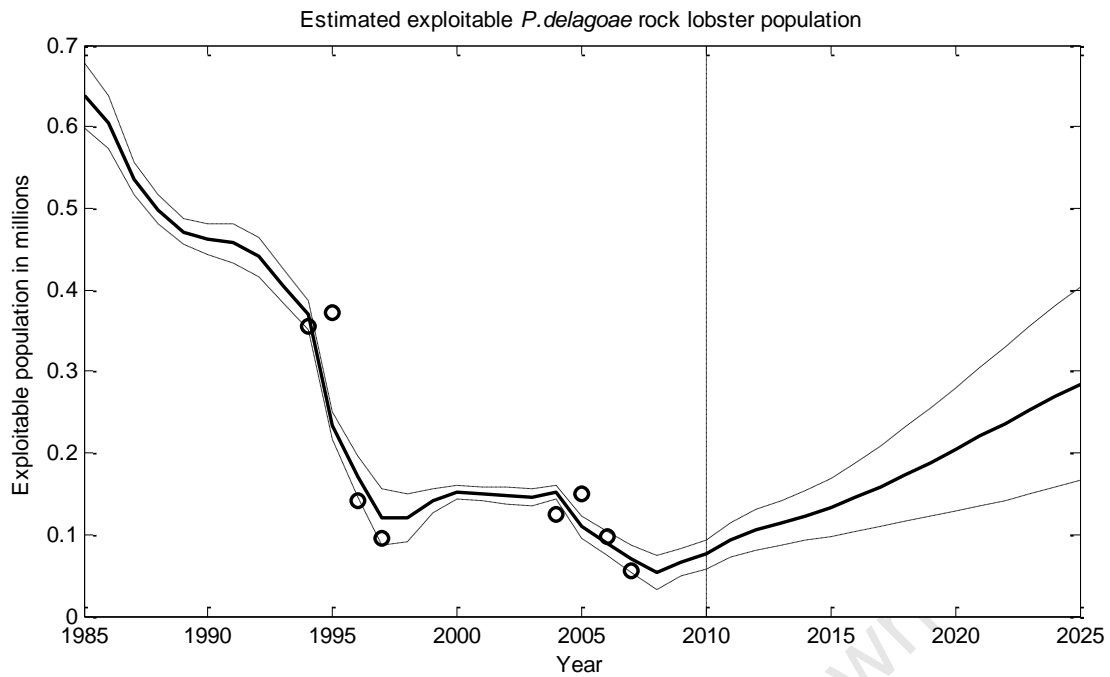


**Figure 7.4:** Estimated trajectory for exploitable population in numbers, showing the fit to the CPUE data (divided by their estimated catchability coefficients). The dashed lines indicate an envelope corresponding to the approximate 95% confidence interval (taken to be  $\pm 1.96$  times the standard error). Values to the right of the vertical dashed line show projections into the future, under the assumption of zero catch.

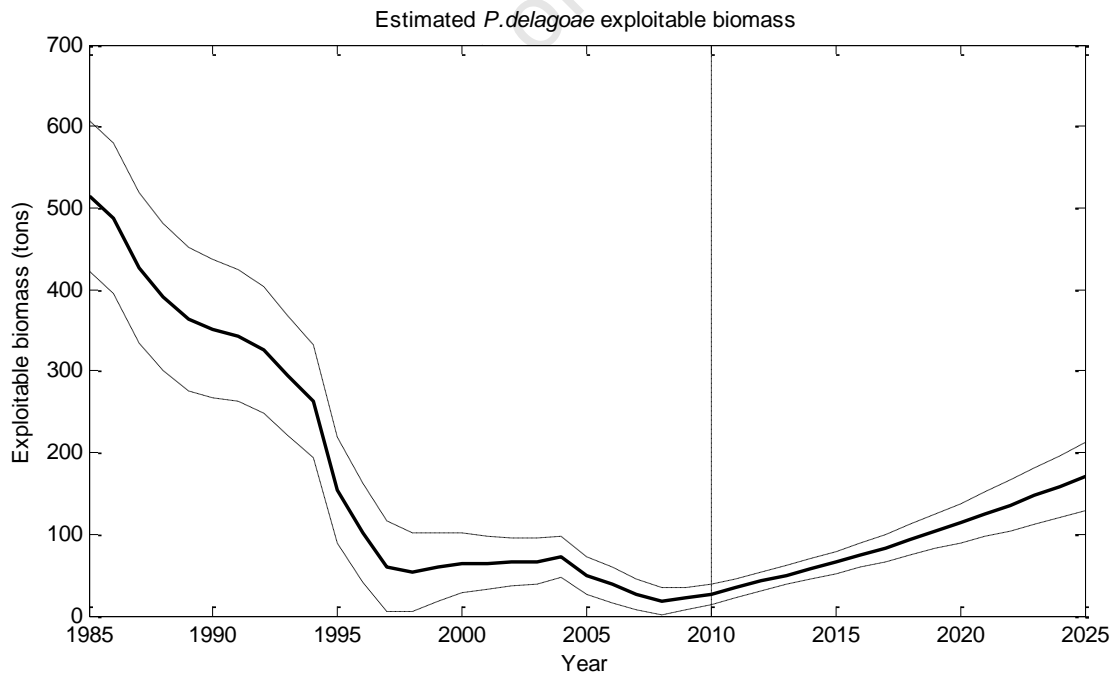


**Figure 7.5:** Estimated trajectory for exploitable biomass (in tons). The dashed lines indicate an envelope corresponding to the approximate 95% confidence interval. Values to the right of the vertical dashed line show projections into the future under the assumption of zero catch.

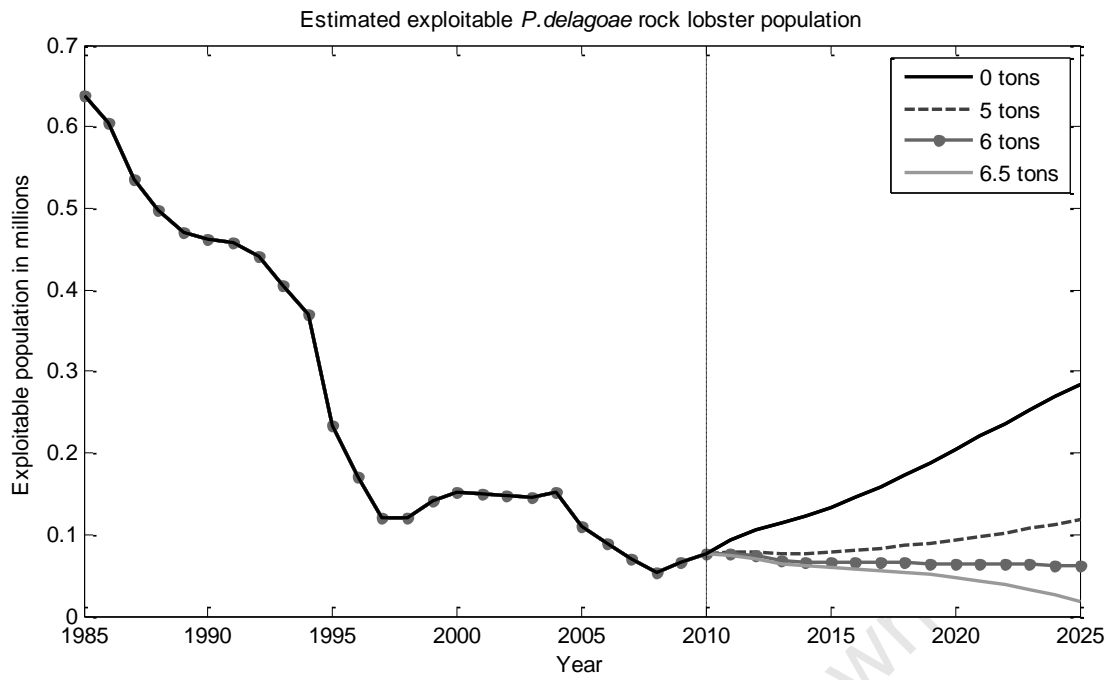


**Figure 7.6:** Estimated population trajectories for four different future catch scenarios. The trajectories to the right of the vertical dashed lines show projections into the future under the assumption of a future annual catch of 0 tons, 5 tons, 6 tons and 6.5 tons.

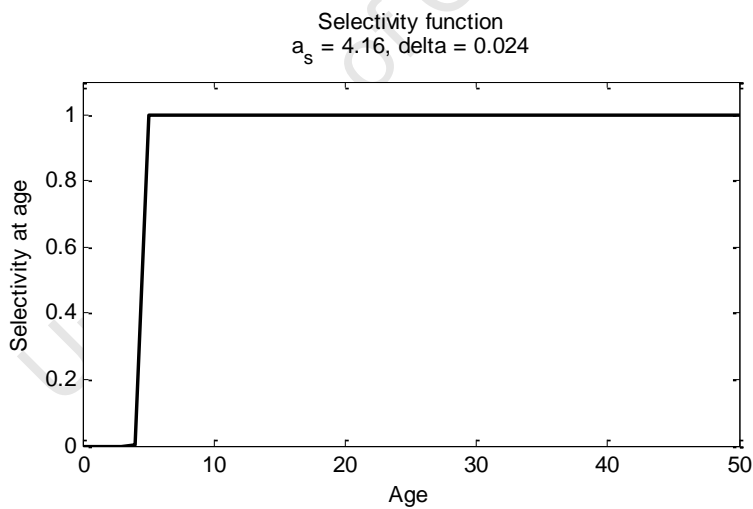


**Figure 7.7:** Logistic selectivity function for estimated values  $a_s=4.16$  yr, and  $\delta=0.024$  yr (see Equation (7.4)).

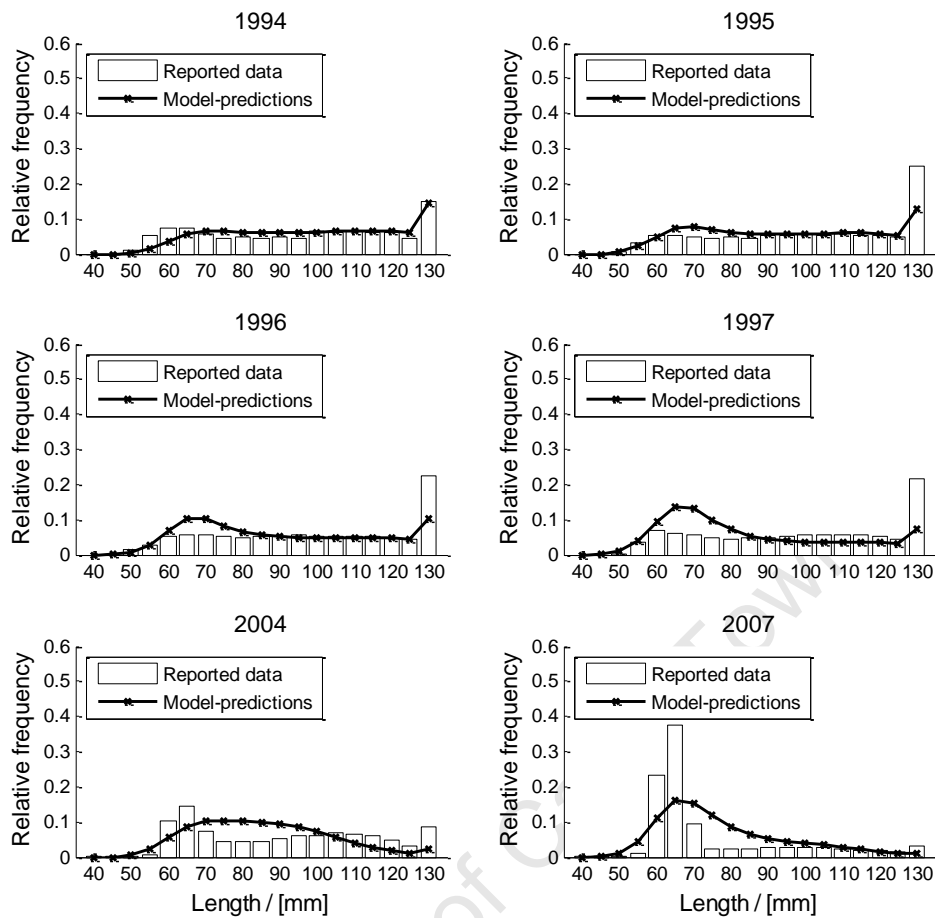


**Figure 7.8:** Fit to length data for 1994-1997, and for the years 2004 and 2007. The white bars show the observed data and the black lines show the model-predicted proportions. The data are not available for 2005 and 2006.

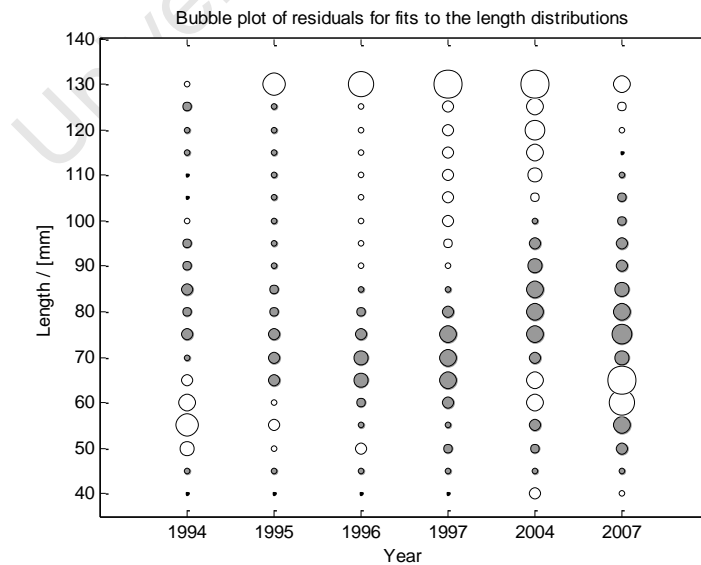


**Figure 7.9:** Bubble plot showing fit to length data. The size (radius) of the bubble is proportional to the corresponding standardised residual ( $\varepsilon_{y,l} = (p_{y,l}^{obs} - p_{y,l}^{mod}) / \sqrt{p_{y,l}^{mod}}$ , where  $p_{y,l}^{obs}$  and  $p_{y,l}^{mod}$  are the observed and model-predicted catch-at-length proportions respectively). The bubbles are white for positive residuals and grey for negative residuals.

## Appendix 7.1

The *P. delagoae* experimental trap-fishery*Trap-fishing experimental setup*

Groeneveld (2000) and Boucher (2007) give the details of the experimental methods employed for the trap-fishery experiments run in 1994-1997 and 2004-2007.

Both experiments consisted of a structured (experimental) and an unstructured (commercial) phase. The structured sampling took place in a grid system, with two long-lines with 50-150 baited traps (each with a soak time of 24-96 hours) set in each grid. These grids spanned the region from 27°S to 31°S from depths of 112.5m to 425m. Based on abundances observed during the one-year pilot study in 1993, the sampling area was reduced to northern, central and southern regions where abundances were thought to be highest (see Figure A7.1.1 below). The majority of the traps were plastic top-entry barrel traps, though some bee-hive traps were also used. The unstructured sampling took place once the structured sampling had been completed. In this phase, there were no restrictions on the placement of the lines or the soaktime, and its primary purpose was to allow for the fishing vessels participating in the experiment to recover costs.

Observers aboard the vessels recorded data for each longline hauled, including numbers and sex of rock lobsters caught, as well as the carapace length (CL) of the first 100 individuals caught with each long-line. The number of traps has been used as the measure of effort.

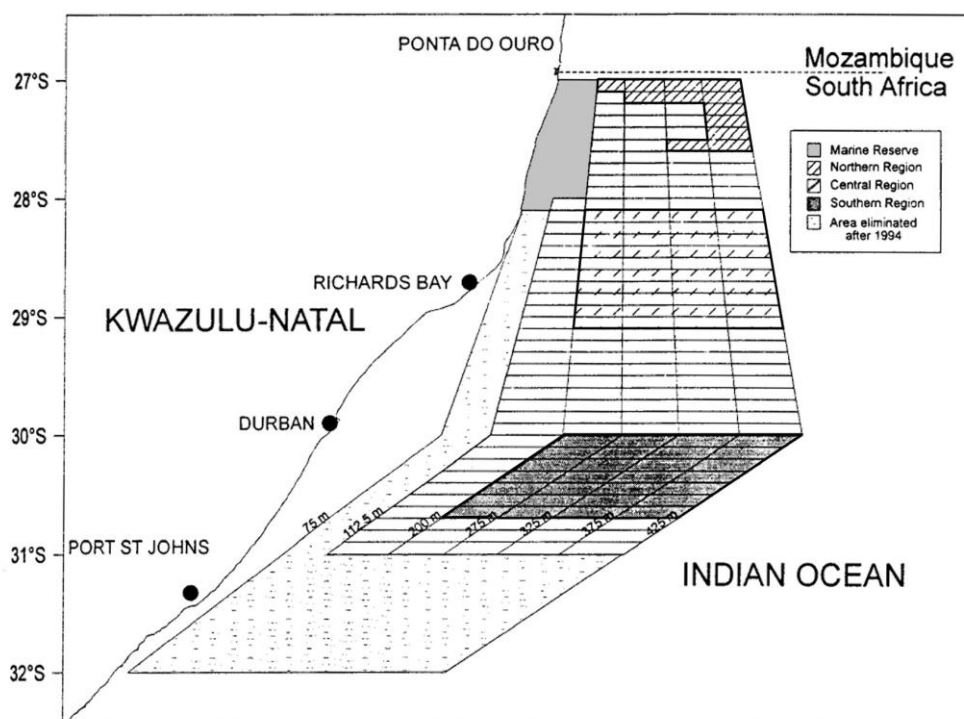


**Figure A7.1.1:** Sampling region for the two trap-fishing experiments (map adapted from Groeneveld, 2000). Indicated are the Northern, Central and Southern regions, as well as a marine protected area and the grid-blocks that were excluded from the survey after the 1993 pilot study.

**GLM**

A generalised linear model (GLM) is a useful tool for standardising CPUE data to obtain a series over several years for which the values are comparable across the years. A GLM takes into account a variety of factors that could influence the CPUE (for example the month or conditions in which the catch was taken) and applies a model to estimate the effect of the factors under consideration. Often these factors are categorical, each with several levels. A GLM allows the data to be standardised across some reference set of levels for each factor.

Unfortunately, the data provided by DAFF for the first experiment (1994-1997) does not contain information about number of traps per line (i.e. there is no measure of effort provided), thus preventing such a GLM from being implemented. A full data set has however been provided for the second experiment (2004-2007). The following approach was devised to produce two individual CPUE series (one for each experiment) that are arguably comparable and can be used jointly in an assessment.

Groeneveld (2000) provides the GLM specifications used to obtain a CPUE series for the first experiment (denoted here as  $CPUE_{Groen}^{94-97}$ ). This GLM was replicated for the 2004-2007 data to obtain a series (denoted as  $CPUE_{Groen}^{04-07}$ ) that is assumed to be comparable to the one given in Groeneveld (2000). A separate “independent” GLM was run on the data from the second experiment, producing  $CPUE_{indep}^{04-07}$ , and a calibration factor was computed between  $CPUE_{Groen}^{04-07}$  and  $CPUE_{indep}^{04-07}$ . This calibration factor was applied to  $CPUE_{Groen}^{94-97}$ , and the resulting series  $CPUE_{indep}^{94-97}$  is assumed to be comparable to  $CPUE_{indep}^{04-07}$ .

**GLM specifications from Groeneveld (2000) for the first experiment ( $CPUE_{Groen}^{94-97}$  and  $CPUE_{Groen}^{04-07}$ )**

A log-normal model was used for these two GLM<sup>69</sup>s, with the following specifications:

*Log-normal model:*

$$\ln(CPUE + \delta) = \mu + \alpha_{year} + \beta_{month} + \gamma_{region} + \lambda_{soaktime} + \varphi_{phase} + \varepsilon \quad (A7.1.1)$$

where:

$\mu$	is the intercept,
$year$	is a factor with 4 levels associated with the years (i.e. the Season-Years: 1994-1997),
$month$	is a factor with 6 levels associated with the fishing month (months May-September),
$region$	is a factor with 3 levels associated with groupings of fishing regions (South, Central and North),
$soak\ time$	is a factor with 3 levels associated with the soak time period (“1” <35 hours, “2”= 36-71 hours and “3” is >72 hours, and
$phase$	is a factor with 2 levels for commercial and experimental phase.

<sup>69</sup> Note that the term “GLM” is conventionally used for generalised linear models. The log-normal model used here is a special case of the generalised linear model and usually referred to as a *general* linear model. For the sake of simplicity, both the generalised linear model and the general linear model will be referred to as GLM hereafter.

The constant  $\delta$  (0.05 of the mean nominal CPUE) was added to allow for the occurrence of zero CPUE values. The error term  $\varepsilon$  is assumed to follow a normal distribution.

The reference levels<sup>70</sup> are the first level for each factor, i.e. year (1994), month (May), area (North), soaktime (0-35 hours), phase (experimental).

The standardised CPUE (weighted according to the open-ocean area of each region) is given by:

$$CPUE_{year} = \sum_{region} [\exp(\mu + \alpha_{year} + \beta_{month} + \gamma_{region} + \lambda_{soaktime} + \varphi_{phase}) - \delta] * A_{region} \quad (A7.1.2)$$

where the area of each region,  $A_{region}$ , given in Table A7.1, and the  $\beta$ ,  $\gamma$ ,  $\lambda$  and  $\varphi$  values were selected to be the GLM parameter outputs for month (July), soaktime (36-72 hours) and phase (commercial) as these are the levels that correspond to the most data points<sup>71</sup>.

#### **Independent GLM assessment on data from second experiment ( $CPUE_{indep}^{04-07}$ ):**

There are three concerns with the above approach:

- (1) The Groeneveld (2000) approach uses two sets of reference/ standard levels: one is the reference level for which the GLM is run (consisting of the first level in each category), and the second is the standard set used in the final CPUE calculation in Equation (A7.1.2) (corresponding to the levels with the most data points). It was considered better to use the standard set (i.e. the levels with the most data points) directly in the GLM, rather than only later in the CPUE calculation.
- (2) The use of  $\delta$  to allow for zero CPUE values can be problematic, as this constant is somewhat arbitrary. It is possible that a Poisson model will be more appropriate, as it can be used for count data (i.e. numbers caught) and can also accommodate zero catch numbers.
- (3) The commercial phase sampling was not systematic and for this reason it would seem better to exclude the commercial catches, as their locations may not be representative of the whole sampling region.

Sensitivity to points (2) and (3) is explored below. Point (1) has however been implemented in all the GLM approaches that follow. As such, the CPUE is standardised to the following levels

Category	Level
Year	2004
Month	September
Region	Central
Trap-type	Plastic top-entry barrel trap
Soak time	35-71 hours
Depth	$\geq 375\text{m}$

as these levels include the most data points in the data set for the second experiment.

<sup>70</sup> A GLM produces an estimate for each level in each category that is a measure of the effect of that level in the model. These estimates are defined relative to a chosen set of reference levels.

<sup>71</sup> This criterion rests on the concept of centering the GLM on the bulk of the data, which hopefully promotes representativity.

The two models explored are the Poisson and the log-normal.

*Poisson model*

The expected number of catches is assumed to follow a Poisson distribution, and is given by:

$$E(C) = Te^L \quad (A7.1.3)$$

where T is an offset corresponding to the number of traps, and L is given by:

$$L = \mu + \alpha_{year} + \beta_{month} + \gamma_{region} + \eta_{trap-type} + \lambda_{soaktime} + \theta_{depth} + \kappa_{line} + \varphi_{phase} \quad (A7.1.4)$$

where:

- $\mu$  is the intercept,
- $year$  is a factor with 4 levels associated with the years (i.e. the Season-Years: 2004-2007),
- $month$  is a factor with 8 levels associated with the fishing month (months May-December),
- $region$  is a factor with 3 levels associated with groupings of fishing regions (South, Central and North),
- $trap\ type$  is a factor with 2 levels associated with the trap type (plastic or bee-hive),
- $soak\ time$  is a factor with 3 levels associated with the soak time period (“1” <35 hours, “2”= 35-71 hours and “3” is >72 hours),
- $depth$  is a factor with 5 levels associated with fishing depth ranges ( “1” for depths < 200m, “2” for 200–274m, “3” for 275-324, “4” for 325-375 and “5” for depths  $\geq$  375m).
- $line$  is a factor with 4 levels associated with line condition (good, tangled, broken and missing, where missing corresponds to a set of data points for which the line condition is missing, all for area South in the year 2007), and
- $phase$  is a factor with 2 levels for the commercial and the experimental phase.

Note that a log link function has been used with the Poisson model.

*Log-normal model*

$$\ln(CPUE + \delta) = \mu + \alpha_{year} + \beta_{month} + \gamma_{region} + \eta_{trap-type} + \lambda_{soaktime} + \theta_{depth} + \kappa_{line} + \varphi_{phase} + \varepsilon \quad (A7.1.5)$$

where the constant  $\delta$  (0.05 of the mean CPUE<sup>72</sup>) was added to allow for the occurrence of zero CPUE values, the error term  $\varepsilon$  is assumed to follow a normal distribution, and the remaining symbols are as explained above.

<sup>72</sup> The effect of  $\delta$  was explored by setting it to a range of values and is discussed further in the results section.

The standardised CPUE series (weighted according to the area of each region) for both models is given by:

$$CPUE_{year} = \sum_{region} ((\exp(\mu + \alpha_{year} + \gamma_{region}) - \delta) * A_{region}) \quad (A7.1.6)$$

where  $A_{region}$  is the ocean surface size of the region concerned, given in Table A7.1. Note that  $\delta$  is zero for the Poisson model.

The two models were run on both the full data set, as well as the data set with the commercial catches excluded, producing four  $CPUE_{indep}^{04-07}$  series that will be discussed in the results section.

**Table A7.1:** Surface areas for the three sampling regions for each of the two experiments. Note that four additional grid blocks were added to the northern sampling region for the second experiment, increasing the sampling area by 60 km<sup>2</sup>, which introduces a small non-comparability factor between the two experiments.

Region	Area (first experiment)	Area (second experiment)
South	414.4 km <sup>2</sup>	414.4 km <sup>2</sup>
Central	340.0 km <sup>2</sup>	340.0 km <sup>2</sup>
North	92.2 km <sup>2</sup>	152.0 km <sup>2</sup>

**Calibration to obtain  $CPUE_{indep}^{94-97}$ :**

The calibration factor is the mean of the  $CPUE_{indep}^{04-07}$  series divided by the mean of the  $CPUE_{Groen}^{04-07}$  series.

$CPUE_{indep}^{94-97}$  is obtained by multiplying  $CPUE_{Groen}^{94-97}$  by the calibration factor, i.e.:

$$CPUE_{indep}^{94-97} = CPUE_{Groen}^{94-97} \frac{\text{mean}(CPUE_{indep}^{04-07})}{\text{mean}(CPUE_{Groen}^{04-07})} \quad (A7.1.7)$$

**Results and discussion**

*CPUE series*

Table A7.2 gives the GLM parameter outputs obtained from the four independent GLMs run on the data from the second experiment, as well as from the GLM run according to the Groeneveld (2000) specifications. The CPUE series obtained from these parameters using Equation (A7.1.6) are given in Table A7.3 in bold text. The scaled CPUE series for the first experiment (obtained using Equation (A7.1.7)) are given in the shaded areas. The corresponding graphical display of these CPUE series is given in Figure A7.1.2. It is interesting to note that the choice of model (log-normal against Poisson) seems to affect the scale of the series but not its trends (see GLM<sub>1</sub> compared to GLM<sub>2</sub>, and GLM<sub>3</sub> compared to GLM<sub>4</sub>, in Figure A7.1.2). The trends of the series on the other hand are primarily affected by the inclusion and exclusion of the commercial catches in the GLM. The differences in trend between the CPUE series from the GLM run according to Groeneveld (2000) specifications and those run according to the alternative specifications may result either from the fact that several factors (trap type, depth and

line condition) were not included in the Groeneveld model, or from the fact that the standard set was used only in the final CPUE calculation and not directly in the running of the GLM.

#### *Model adequacy*

Histograms of the residuals, along with qq-plots to check for normality, are given in Figure A7.1.3. It seems that the residuals for the log-normal model are reasonably normal, or at least more so than the residuals from fitting a Poisson model. For the log-normal model, using the residuals as a check for model adequacy is fairly straightforward, as the residuals should be roughly normally distributed. The Poisson distribution is unfortunately more complicated. While residuals are standardised in an effort to approximate normality, lack of normality in the residuals does not necessarily mean that the model is inappropriate, since a move away from a normal or log-normal model implies that a simple normality check of the residuals may no longer provide sufficient information about model adequacy (the residuals are only expected to be normal in the asymptotic limit).

Probably more important than normality of residuals is the matter of homoscedasticity. If the GLMs are to provide response values (i.e. CPUE values for the log-normal model and numbers caught for the Poisson model) with maximal precision, then variance of observations should be independent of the predicted response value. Thus the standard deviation in the residuals should stay roughly constant across the range of fitted response values. To check for constant variability, the fitted values were ordered and arranged into sets {fitted value<sub>1</sub>-fitted value<sub>24</sub>}, {fitted value<sub>2</sub>-fitted value<sub>25</sub>} and so on. The standard deviations were computed for each group and plotted against the median fitted value of that group. The results are also shown in Figure A7.1.3. The Poisson model (for both GLM<sub>2</sub> and GLM<sub>4</sub>) shows an upward trend, indicating that the model shows more variability in predicting large catches. The log-normal model seems to do reasonably well when the commercial catches are included (GLM<sub>1</sub>), but when they are excluded (GLM<sub>3</sub>), a downward trend becomes apparent, indicating that this model shows more variability in predicting the smaller catches.

#### *Final model choice and possible future improvements*

Given the above considerations, it seems that the log-normal model is preferable, though neither model shows perfect homoscedasticity. An approach to counter-act this effect would be to down-weight the points with high variance in the residuals, and will be explored in future work.

The lack of structure in the commercial sampling phase is still a matter of concern and as such the data excluding the commercial catches are the preferred input for the GLM. The CPUE series resulting from GLM<sub>3</sub> was therefore chosen to provide inputs to the assessment.

The effect of these different CPUE series on the population assessment was investigated by fitting the population model for each of the series. The results are shown in Figure A7.1.4 (a)-(d) and apart from a slight scaling difference in some cases, the differences are minimal. In light of this similarity, it seems acceptable (for the purposes of this initial assessment) to accept GLM<sub>3</sub> as a baseline choice without much further detailed investigation.

*Sensitivity to  $\delta$  in the log-normal model*

With this choice of model made, the selection of the value of  $\delta$  becomes important.  $\delta$  is taken to be proportional to the average of all the CPUE values, i.e.  $\delta = \theta * \text{ave}(\text{CPUE})$ , so to explore the effect of  $\delta$  on the CPUE series and population assessment, the value of  $\theta$  was set to 0.01, 0.05, 0.10 and 0.20. The resulting CPUE series are shown in Figure A7.1.5 (a)-(b). Figure A7.1.5 (a) shows the numerical values of the series, while Figure A7.1.5 (b) shows the proportional changes within each series. These two figures show that changing the value of  $\theta$  affects (a) the magnitudes of the values in the series and (b) the extremity of the 2005 peak. The qq-plots in Figure A7.1.6 seem to suggest that a value  $\theta = 0.05$  results in near normally distributed residuals, and it is interesting to note how these residuals deviate further from normality as  $\theta$  is increased. The results for  $\theta = 0.01$  seem to be the least homoscedastic, but there is not much variation to distinguish the other values of  $\theta$  in terms of homoscedasticity. Thus  $\theta = 0.05$  seems to be the best choice. Figure A7.1.7 shows the estimated trajectory obtained from fitting the population model for each value of  $\theta$ . The value of  $\theta$  seems to have a non-linear effect on the current population level, but the differences are again minimal.

University of Cape Town

**Table A7.2:** GLM results for  $CPUE_{indep}^{04-07}$ . There were no recorded commercial catches for levels marked with a \*. Note that the reference levels (not shown here) have an estimate at zero in the GLM.

Category	Level	GLM1 (Log-normal) (Including commercial catches)				GLM2 (Poisson) (Including commercial catches)				GLM3 (Log-normal) (Excluding commercial catches)				GLM4 (Poisson) (Excluding commercial catches)			
		estimate	s.e.	t(2876)	t pr.	estimate	s.e.	t(2876)	t pr.	estimate	s.e.	t(726)	t pr.	estimate	s.e.	t(726)	t pr.
Constant		-1.520	0.085	-17.97	<.001	-1.183	0.090	-13.12	<.001	-1.764	0.149	-11.87	<.001	-1.410	0.148	-9.54	<.001
Region	North	0.265	0.056	4.71	<.001	0.122	0.062	1.96	0.05	0.640	0.110	5.81	<.001	0.408	0.118	3.46	<.001
	South	0.063	0.082	0.77	0.44	0.082	0.087	0.93	0.35	-0.207	0.171	-1.21	0.23	0.157	0.177	0.89	0.38
Year	2005	-0.261	0.068	-3.81	<.001	-0.101	0.070	-1.45	0.15	0.160	0.142	1.12	0.26	0.198	0.146	1.36	0.17
	2006	-0.429	0.057	-7.59	<.001	-0.340	0.055	-6.17	<.001	-0.217	0.116	-1.87	0.06	-0.110	0.107	-1.04	0.30
	2007	-0.841	0.082	-10.27	<.001	-0.890	0.118	-7.55	<.001	-0.687	0.159	-4.32	<.001	-0.913	0.216	-4.22	<.001
Month	May	-0.086	0.132	-0.65	0.52	0.496	0.134	3.69	<.001	0.661	0.238	2.77	0.01	0.626	0.241	2.60	0.01
	June	0.039	0.109	0.36	0.72	0.386	0.115	3.36	<.001	0.397	0.245	1.62	0.11	0.384	0.244	1.57	0.12
	July	0.360	0.074	4.90	<.001	0.359	0.077	4.70	<.001	0.442	0.130	3.41	<.001	0.297	0.128	2.33	0.02
	August	-0.054	0.079	-0.69	0.50	0.010	0.083	0.12	0.90	0.074	0.175	0.42	0.67	-0.100	0.187	-0.53	0.60
	October	-0.240	0.066	-3.65	<.001	-0.233	0.078	-2.99	0.00	-0.405	0.133	-3.05	0.00	-0.525	0.178	-2.94	0.00
	November	-0.645	0.106	-6.11	<.001	-0.614	0.130	-4.72	<.001	-0.856	0.521	-1.64	0.10	-1.740	2.460	-0.71	0.48
	December	-0.949	0.131	-7.27	<.001	-0.666	0.164	-4.07	<.001	*	*	*	*	*	*	*	*
Trap Type	Bee-hive	0.025	0.291	0.09	0.90	-0.009	0.258	-0.04	0.97	0.482	0.566	0.85	0.40	0.204	0.899	0.23	0.82
	Other	-0.479	0.147	-3.25	0.00	-0.449	0.241	-1.86	0.06	*	*	*	*	*	*	*	*
Soak time	0-34 hours	-0.151	0.066	-2.28	0.00	-0.075	0.064	-1.17	0.24	-0.168	0.114	-1.48	0.14	0.031	0.117	0.27	0.79
	>72 hours	0.277	0.044	6.32	<.001	0.207	0.043	4.83	<.001	0.407	0.100	4.09	<.001	0.497	0.096	5.17	<.001
Depth	< 200m	-0.392	0.332	-1.18	0.20	-0.098	0.296	-0.33	0.74	0.300	1.100	0.27	0.79	-0.440	0.932	-0.47	0.64
	200-274	-0.155	0.064	-2.42	0.00	-0.111	0.069	-1.61	0.11	-0.359	0.121	-2.97	0.00	-0.363	0.131	-2.77	0.01
	275-324	0.051	0.058	0.88	0.40	-0.011	0.062	-0.17	0.86	-0.080	0.113	-0.71	0.48	-0.012	0.113	-0.11	0.92
	325-375	0.343	0.059	5.76	<.001	0.370	0.060	6.22	<.001	0.170	0.109	1.56	0.12	0.265	0.101	2.61	0.01
Line Condition	Broken	-0.466	0.135	-3.46	<.001	-0.651	0.210	-3.10	0.00	-0.504	0.236	-2.13	0.03	-0.727	0.369	-1.97	0.05
	Missing	0.739	0.104	7.10	<.001	1.066	0.129	8.29	<.001	0.552	0.238	2.32	0.02	0.750	0.272	2.76	0.01
	Tangled	-0.709	0.100	-7.09	<.001	-0.571	0.138	-4.14	<.001	-0.669	0.163	-4.10	<.001	-0.527	0.216	-2.44	0.02
Phase	Commercial	0.210	0.048	4.35	<.001	0.146	0.049	3.00	0.00	-	-	-	-	-	-	-	-

**Table A7.3:** Resulting CPUE series from the various GLM runs. GLM<sub>1</sub> uses the log-normal model (with commercial catches included), GLM<sub>2</sub> the Poisson model (with commercial catches included), GLM<sub>3</sub> the log-normal model (without commercial catches) and GLM<sub>4</sub> the Poisson model (without the commercial catches). The second column reports the CPUE series (computed using the GLM parameter output given by Groeneveld, 2000) as well as the CPUE series resulting from this GLM being replicated for the data of the second experiment. In the remaining columns, the bold numbers are the CPUE series resulting from the GLM<sub>1</sub> to GLM<sub>4</sub>. The series in the shaded columns were computed by scaling the Groeneveld (2000) 1994-1997 series by  $\mu_0 / \mu_i$ , where  $i=[1, 2, 3, 4]$ .

Year	Groeneveld (2000) specifications	GLM <sub>1</sub>	GLM <sub>2</sub>	GLM <sub>3</sub>	GLM <sub>4</sub>
1994	522.75	226.10	366.99	209.26	372.34
1995	547.87	236.97	384.63	219.32	390.23
1996	207.72	89.84	145.83	83.15	147.95
1997	139.90	60.51	98.21	56.00	99.65
2004	443.47	<b>198.72</b>	<b>294.54</b>	<b>148.5</b>	<b>257.19</b>
2005	301.08	<b>149.54</b>	<b>266.22</b>	<b>177.2</b>	<b>313.50</b>
2006	282.45	<b>123.98</b>	<b>209.60</b>	<b>116.24</b>	<b>230.40</b>
2007	242.61	<b>76.89</b>	<b>120.95</b>	<b>66.31</b>	<b>103.21</b>
Mean	$\mu_0 = 317.40$	$\mu_1 = 137.28$	$\mu_2 = 222.83$	$\mu_3 = 127.06$	$\mu_4 = 226.08$

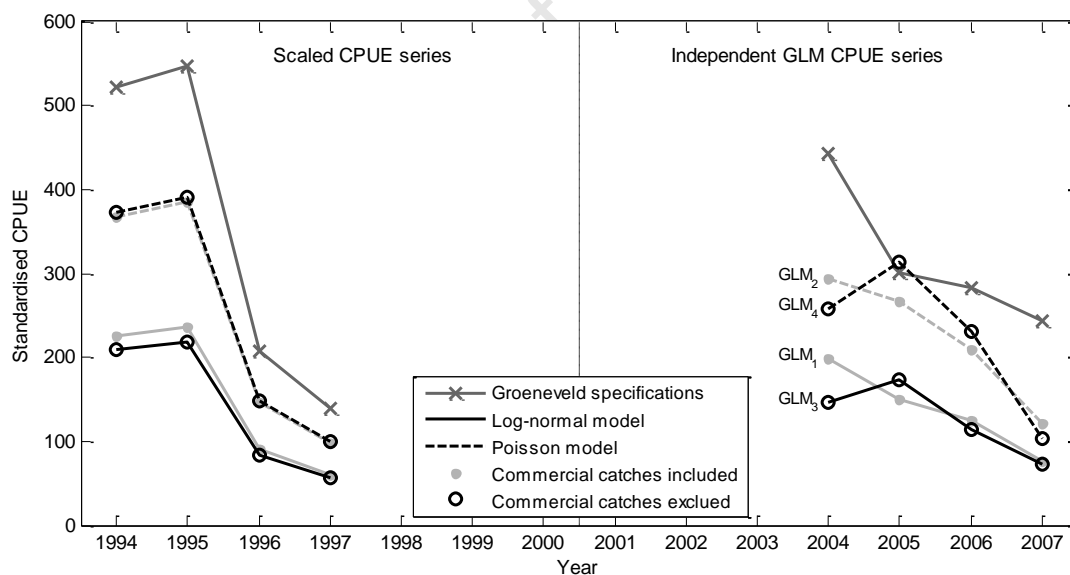


**Figure A7.1.2:** The CPUE series resulting from the various GLM treatments. On the right are the CPUE series calculated directly from the GLM results. The series obtained using the Groeneveld (2000) specification is shown in medium grey; the series obtained when including the commercial catches are shown in light grey; and the series obtained when excluding the commercial catches are shown in black. For the light grey and black series, a solid line indicates that a log-normal model was used, while a dashed line indicates that a Poisson model was used. The series on the left shown in medium grey is the series obtained from the GLM output given by Groeneveld (2000). The remaining series on the left were obtained by scaling the Groeneveld (2000) series, as previously described.

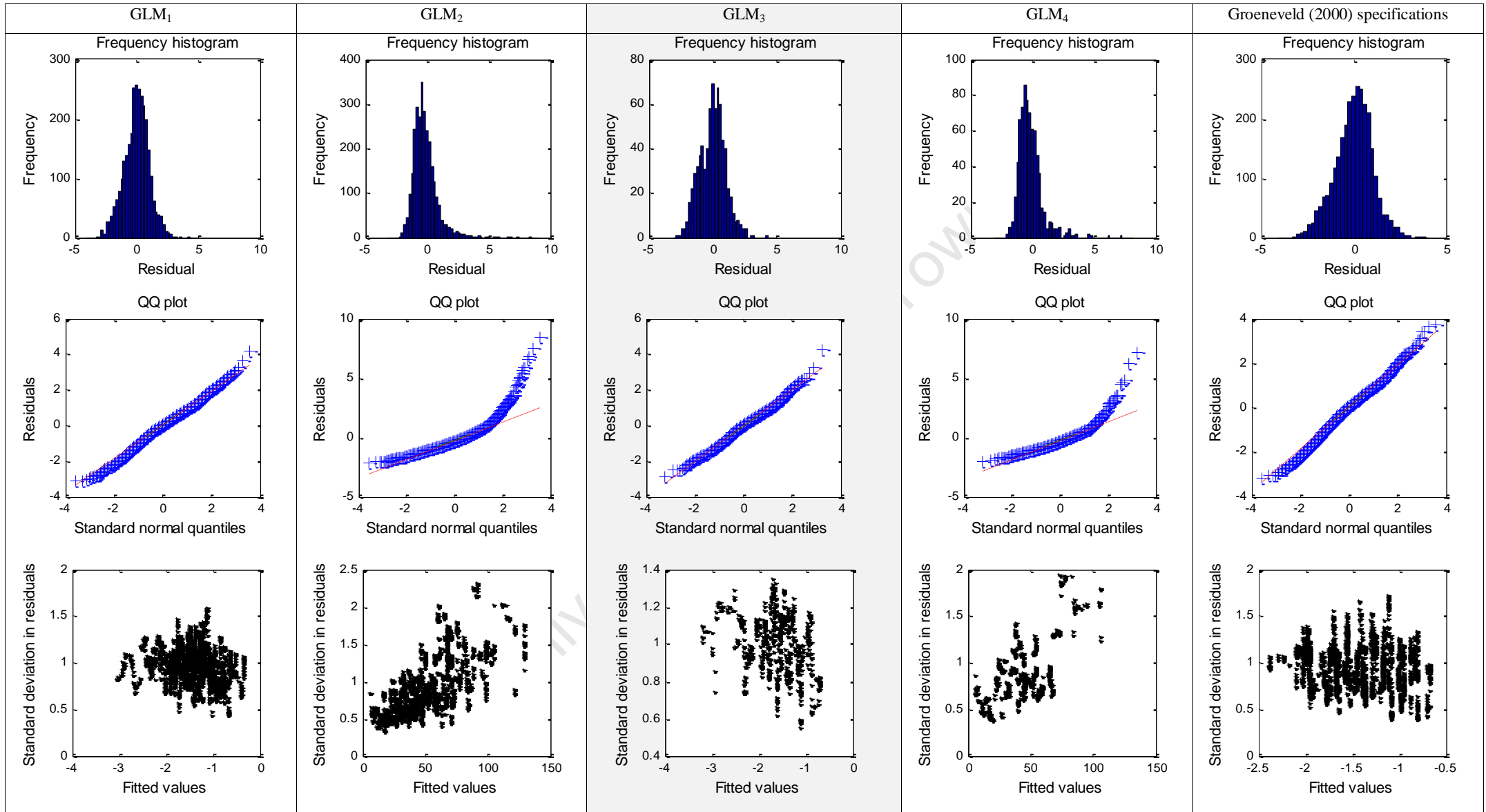


**Figure A7.1.3:** Graphical display of the residuals for the four independent GLMs run on the data from the second experiment, as well as the GLM run according to the Groeneveld (2000) specifications. The rows of plots, working from top to bottom, present histograms, qq-plots and plots of the standard deviation of the residuals against the fitted values. The shaded column highlights GLM<sub>3</sub>, chosen as the reference GLM for the assessment.

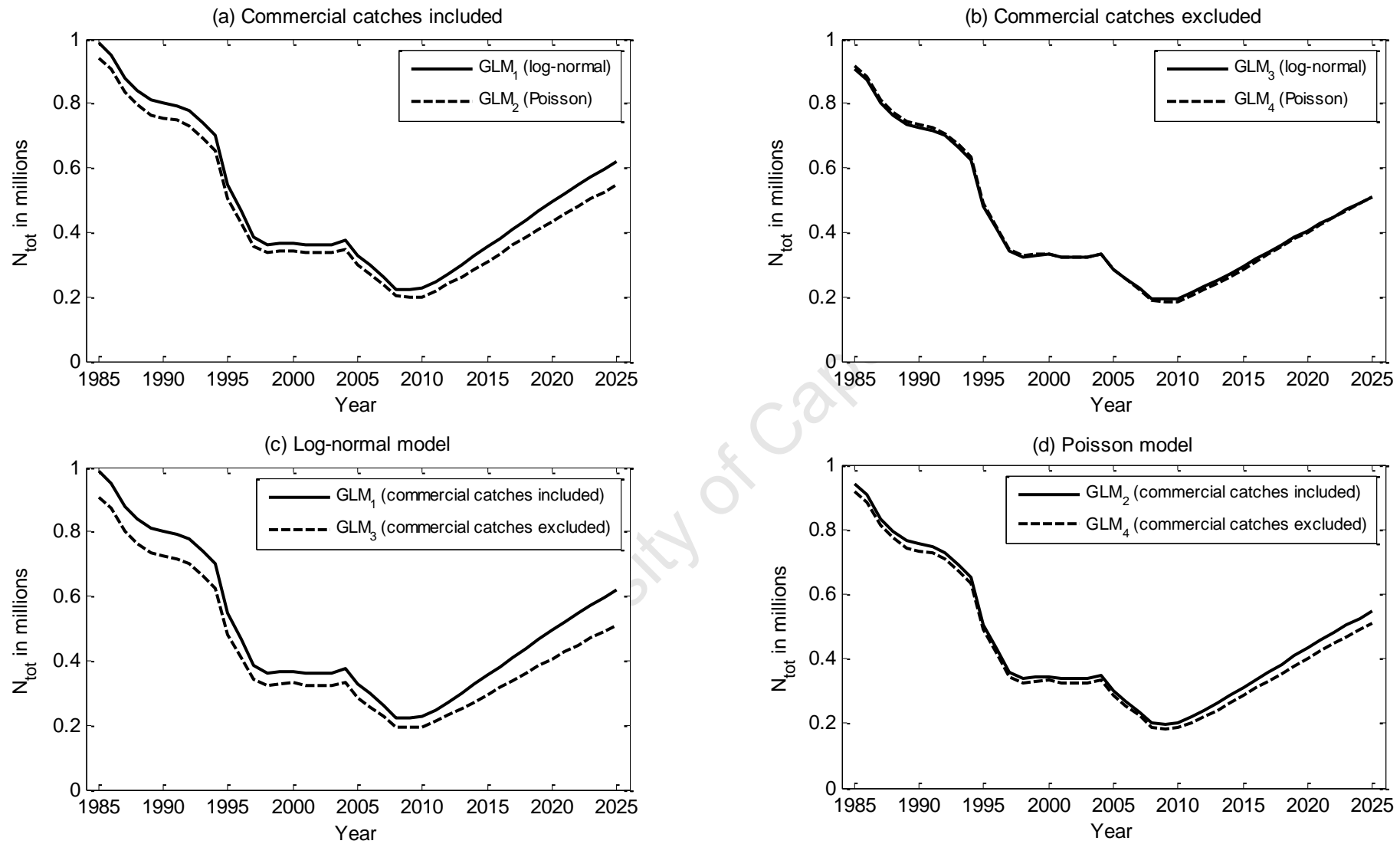


**Figure A7.1.4 (a)-(d):** Estimated population trajectories obtained when the model is run on the CPUE series obtained from each of the four independent GLMs. Figures (a) and (b) compare the log-normal and Poisson model for the case where the commercial catches are included (a) and excluded (b). Figures (c) and (d) compare the inclusion and exclusion for the log-normal model (c) and the Poisson (d).

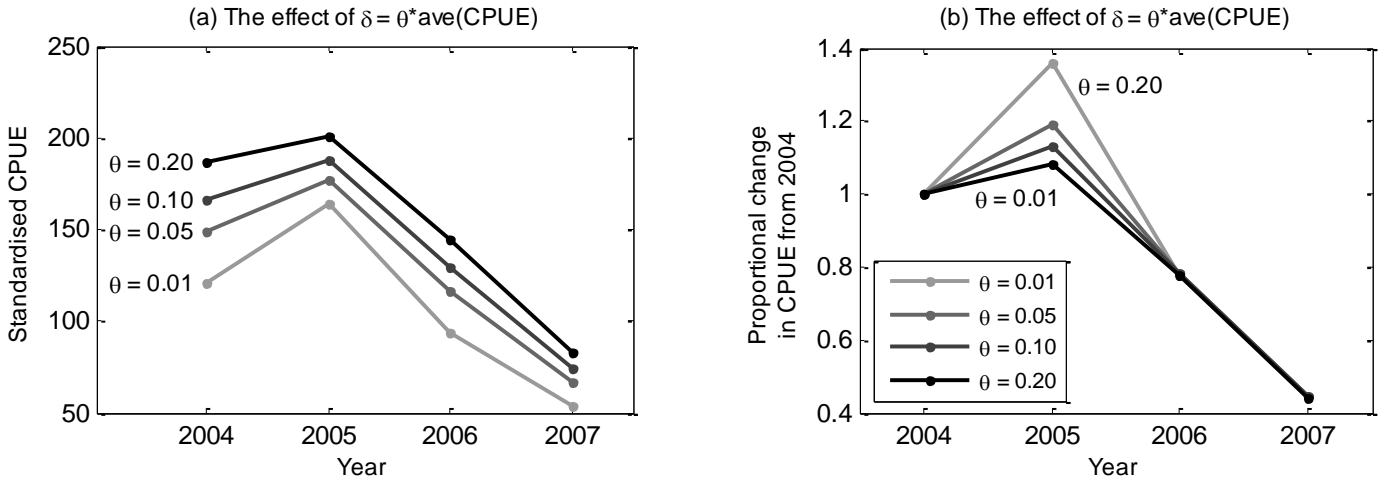


**Figure A7.1.5 (a) and (b):** Comparison of the different CPUE series obtained when varying the value of  $\delta$ . Figure (a) shows the resulting CPUE series, and Figure (b) shows the values of each series in proportion to the first value of that series.

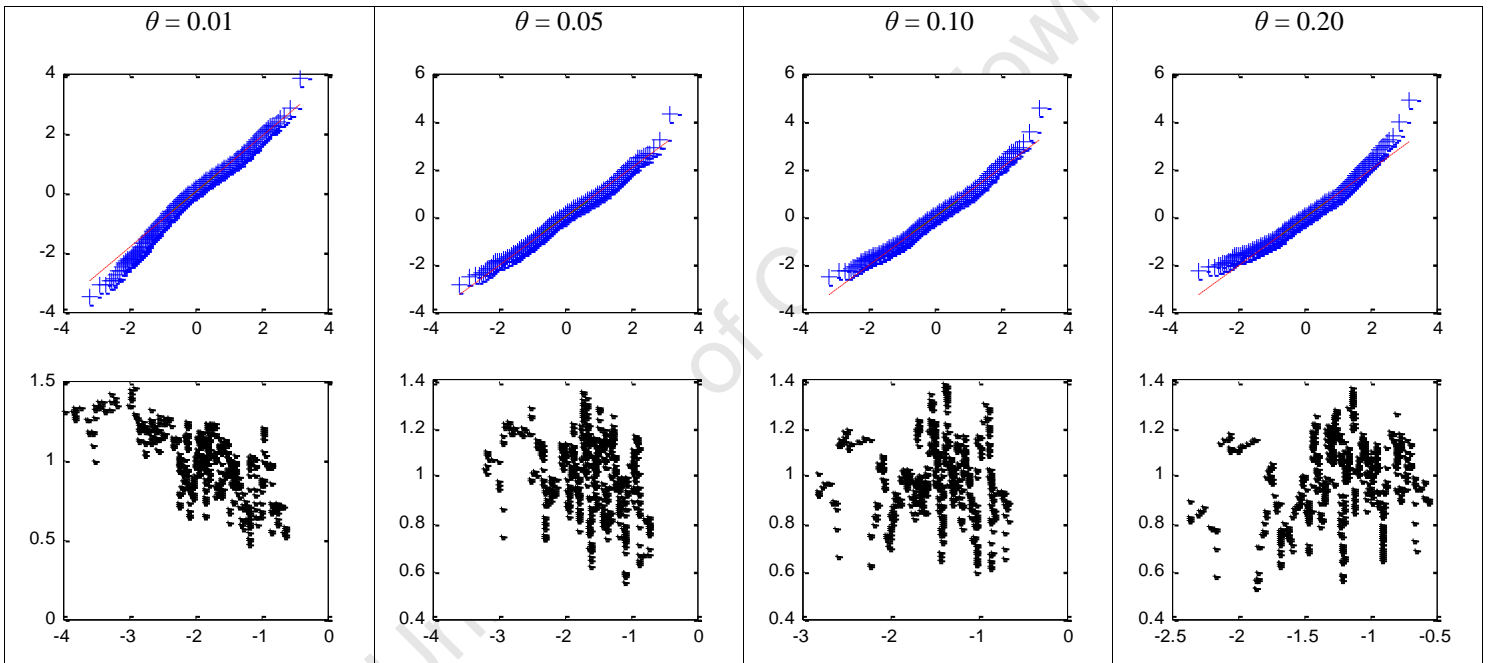


**Figure A7.1.6:** Graphical display of the residuals: qq-plots and the plots of the standard deviation of residuals against fitted values.

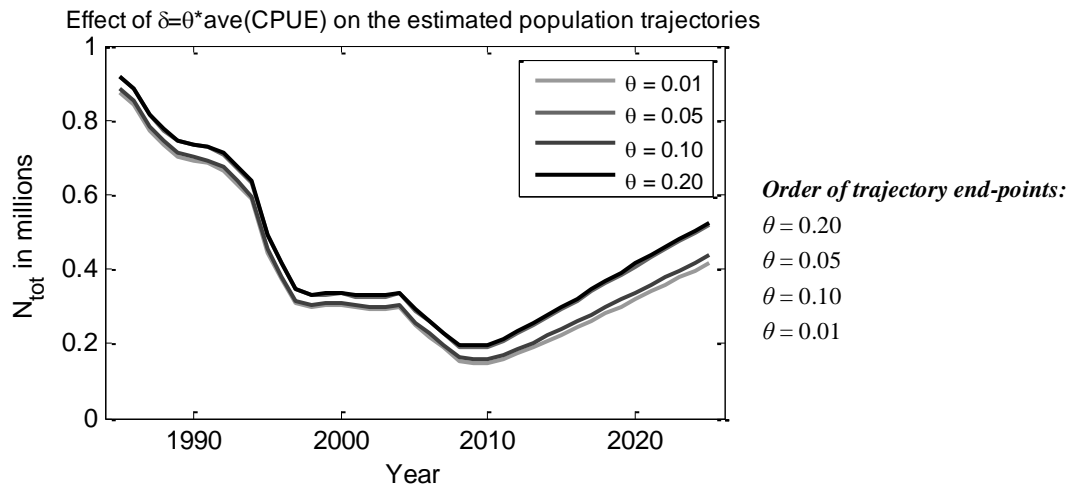


**Figure A7.1.7:** Estimated trajectories for the population (in numbers) for  $\theta$  ranging from 0.01 to 0.20.

University of Cape Town

**SECTION D:**

**Overall discussion and closing remarks**

## 8 Overall discussion and closing remarks

When conducting marine population assessments the standard approach is to start with the simplest possible model to see if this model is compatible with the information available about the population under study. If additional information that suggests some sub-structuring of the population is available, the model needs to be adjusted to incorporate such information. Even if such information is weak, the assessment needs to explore the potential impact on results that might arise if the actual sub-structure is ignored. Should the impact of the population sub-structuring on the assessment results be substantial, more observational data may need to be obtained to strengthen and inform the assessment and any associated scientific advice for management.

Unfortunately, the acquisition of such data is often not a straightforward task. Assessments of an international nature (such as the ones for the humpback whale species presented in this thesis) require collaboration through internet communication, and data sources are often spread across the globe. Thus for any assessment undertaken, sufficient time needs to be factored in for the compilation of available data. Even on a local scale, this compilation is often time-consuming. As the data arise from studies that often span several decades (and thus fall under ever changing scientific management), proper storage of the data becomes vital. Inconsistent attention to archiving can result in the loss or misplacement of data for future studies, as was evidenced in the *P. delagoae* assessment presented in this thesis.

Statistical methods employed in this thesis (such as SIR and MCMC) are powerful methods to combine population dynamics models and real observations to develop a population assessment. Any assessment, however, can only be as good as the data made available to it. Historic data are often incomplete or completely unavailable (such as the early *P. delagoae* catches) and assumptions need to be made to fill the gaps. Further, all data have errors associated with the survey or experimental techniques used to obtain them. As such, inferences drawn from the assessments cannot be taken as absolute truths but should rather be seen as appropriate approximations of reality based on current information. As new information becomes available (from ongoing or new studies and surveys of the population), assessments need to be updated, and alternative models explored if the data provide grounds to do so.

The studies presented in this thesis proved to be both interesting and challenging. Hypotheses and postulates were put forward about the population under study and models were developed to test if they were compatible with the observed data. One of the most challenging aspects of this process was the matter of statistical rigour. The mechanical implementation of a statistically sound process such as SIR or MCMC is on its own not enough, and results cannot be blindly reported without suitable convergence checks. Bayesian methods generally are more difficult to implement successfully than the maximum likelihood approach and so it is often easier to explore a problem first through the maximum likelihood methodology, as was done in Chapters 4 and 7 of this thesis. If the assessments presented there are to carry any weight at a management level, however, they will need to be further developed within a Bayesian framework to better account for the uncertainties in these cases.

Obtaining convergence is by no means the only obstacle in a population assessment. Each assessment brings its own unique set of challenges, such as the issue of prior incoherence explained in Chapter 5, and it soon becomes important to draw on the expertise and experience of others in the field (be it through papers or personal communication). The field of resource assessment accordingly is of an interdisciplinary nature, drawing together

mathematicians, statisticians and life scientists, as well as representatives of the industry and management body concerned with the population under study.

The key contributions made to this field by the work presented in this thesis are conveniently summarised through sequential consideration of the individual assessments.

The assessment of the Southern Hemisphere (SH) humpback whale Breeding Stock C presented in Chapter 4 builds on assessments already completed for this stock and develops an age- and sex-disaggregated model to incorporate catch-at-length frequency data. The study aims to address some more subtle questions that require investigation on a level of detail not available in an age- and sex-aggregated model. Thus, rather than simply update the results of the earlier assessments, this study served to make a contribution through the exploration of data that have up to now not been included in assessments of this stock.

The study presented in Chapter 5 explored a sizeable range of models that capture various stock-structure hypotheses for the SH humpback whale Breeding Stock B that are currently under debate in the Scientific Committee (SC) of the International Whaling Commission (IWC). This stock is at present under assessment, and the study presented in this chapter reflects to a degree the exploratory nature of the debates that take place and postulates that are developed within the SC. The chapter thus presents an interim report on an ongoing study that is to be completed at the SC's next meeting in June 2011.

Although the assessment presented in Chapter 6 is of an initial nature, in particular given the lack of convergence displayed by the results, it is possibly the most distinctive study presented in this thesis because of the unique ideas that it is based upon. It takes the decade-old problem of catch-allocation boundaries for the humpback whale species and proposes a method for allowing uncertainty about these boundaries to be properly addressed within the assessment. The study serves only as a first step towards accomplishing such flexibility, but provides a platform for future work on a complex but highly interesting problem.

Chapter 7 reports on the initial stages of the first comprehensive population assessment of the South African east coast rock lobster (*P. delagoae*). Unlike other rock lobster species in the south, the *P. delagoae* species is currently not under a management scheme. The study aims to investigate if the resource is large enough to support annual fishing on a sustainable basis. Similar to Chapter 6, the work presented in this chapter will be further developed once some of the data issues have been satisfactorily addressed.

Each of the chapters gives a discussion of the future work involved for the respective studies, outlining the issues to be addressed and future model developments that are to take place. This thesis thus serves in part as a progress report on several studies not yet taken to the stage of final results, as well as a presentation of some of the concepts and methodology that the author has learned and further developed over the last two years.

## Acknowledgements

Financial support from the Deutscher Akademischer Austausch Dienst (DAAD), the National Research Foundation (NRF) and the University of Cape Town (UCT) is gratefully acknowledged. I would like to thank my supervisor, Doug Butterworth, for his continued support, patience and guidance over the last two years, as well as the MARAM group at UCT, under whose guidance I have progressively been able to work more independently and gradually become more familiar with the range of approaches used in the field of marine resource assessment.

Numerous people from the IWC SC are to thank for their input into the assessments undertaken in this thesis: for the provision of input data, for advice on biological and ecological issues, for the discussion of the results and for recommendations for future work. In particular, thanks go to Alex Zerbini, Jen Jackson, Cherry Allison, Peter Best, Jaco Barendse, Howard Rosenbaum, Sal Cerchio, Andre Punt and Ken Findlay.

Also, thanks go to the DAFF rock lobster scientific working group for their discussion of and input to the *P. delagoae* assessment presented in this thesis. In particular, my appreciation goes to Andy Cockcroft and Neil van den Heever for their assistance in obtaining the data utilised in the assessment. Thanks also go to Johann Groeneveld and Monique Boucher for provision of background information and their comments on the work.

Lastly, I would like to thank family and friends for their support and encouragement throughout the last two years. Without them, this would not have been rich experience that it proved to be. In particular I'd like to thank Vere Ross-Gillespie for his help with the graphical aspects of this thesis, but more importantly for being my sounding board, proof-reader and general support.

---

**References**

- Allison, C. 2006. Creation of the S.Hemisphere humpback catch series Feb 2006 (Draft). Paper SC/A06/HW47 presented to the Workshop on the Comprehensive Assessment of Southern Hemisphere Whales, Hobart, Australia, April 2006 (unpublished). 9pp
- Andriolo, A., Kinas, P.G., Engel, M.H. and Albuquerque Martins, C.C. 2006. Monitoring humpback whale population in the Brazilian breeding ground, 2002 to 2005. Paper SC/58/SH15 submitted to the IWC Scientific Committee, April 2006 (unpublished). 8pp.
- Baker, C.S., Perry, A., Bannister, J.L., Weinrich, M.T., Abernethy, R.B., Calambokidis, J., Lien, J., Lambertsen, R.H., Urbán Ramírez, J., Vasquez, Q., Clapham, P.J., Alling, A., O'Brien, S.J., and Palumbi, S.R. 1993. Abundant mitochondrial DNA variation and world-wide population structure in humpback whales. *Proceedings of the National Academy of Sciences of the United States of America*, 90: 8239-8243.
- Baker, C. S., Garrigue, C., Rochelle, C., Madon, B., Poole, M., Hauser, N., Clapham, P., Donoghue, M., Russel, K., O'Callahan, T., Paton, D. and Mattila, D. 2006. Abundance of humpbacks in Oceania (South Pacific) 1999 to 2004. Paper SC/A06/HW51 submitted to the IWC Scientific Committee, April 2006 (unpublished). 10pp.
- Bannister, J.L. and Hedley, S.L. 2001. Southern Hemisphere group IV humpback whales: their status from recent aerial survey. *Memoirs of the Queensland Museum*. 47: 587-598. 13pp.
- Barendse, J., Best, P.B., Thornton, M. 2006. Preliminary results of photo-identification of humpback whales on the west coast of South Africa. Paper SC/A06/HW4 submitted to the IWC Scientific Committee, April 2006 (unpublished). 14pp.
- Barendse, J., Best, P.B., Thornton, M., Elwen, S.H., Pomilla, C., Carvalho, I. and Rosenbaum, H.C. 2010. Photo identification of humpback whales *Megaptera novaeangliae* off West South Africa (Breeding Stock B2) and a preliminary (sub-) population estimate. Paper SC/62/SH2 submitted to the IWC Scientific Committee, April 2010 (unpublished), 19pp.
- Berry, P.F. 1971. Spiny lobsters (*Palinuridae*) of the east coast of southern Africa: distribution and ecological notes. *Investigational Report of the Oceanographic Research Institute of South Africa*, 27. 22pp.
- Berry, P.F. 1972. Observations on the fishery for *Palinurus delagoae*. *Oceanographic Research Institute*, Durban, South Africa (unpublished report). 6pp.
- Berry, P.F. 1973. The biology of the spiny lobster *Palinurus delagoae* Barnard, off the coast of Natal, South Africa. *Investigational Report of the Oceanographic Research Institute of South Africa*, 31. 27pp
- Best, P.B. and Brandão, A. 2009. Humpback whaling at Madagascar, 1910-1950. Paper SC/F09/SH2 submitted to the intersessional meeting on Southern Hemisphere humpback whale assessment methodology, Seattle, February 2009 (unpublished). 19pp.
- Best, P.B. 2010. Assessing struck-and-lost rates in early modern whaling: examination of first-hand accounts. Paper SC/62/O2 submitted to the IWC Scientific Committee, April 2010 (unpublished). 6pp.
- Boucher, M. 2007. Recovery of a collapsed spiny lobster *Palinurus delagoae* stock off the eastern South Africa? Insights from an experimental trap-fishery. Thesis submitted in partial fulfilment for the degree M.Sc. (Applied Marine Science) at the University of Cape Town. 40pp.
- Branch, T.A. (in press). Humpback whale abundance south of 60°S from three complete circumpolar sets of surveys. *J. Cetacean Res. Manage.* (Special Issue). 45pp.

- Brandão, A. and Butterworth, D.S. 2006. Concerning demographic limitations on the population growth rate of west Australian (Breeding Stock D) humpback whales. Paper SC/58/SH24 submitted to the IWC Scientific Committee, April 2006 (unpublished). 15pp.
- Brandon, J.R., Breiwick, J.M., Punt, A.E. and Wade, P.R. 2007. Constructing a coherent joint prior while respecting biological realism: application to marine mammal stock assessments. *ICES Journal of Marine Science*, 64(6): 1085-1100.
- Butterworth, D.S. and Punt, A.E. 1997. Some comments on Bayesian synthesis. *Report of the International Whaling Commission*, 47: 158-160.
- Carlin, B.P. and Louis, T.A. 2009. Bayesian methods for data analysis. 3<sup>rd</sup> Ed. Chapman & Hall/CRC Press, Boca Raton. 535pp.
- Carvalho, I., Loo, J., Collins, T., Pomilla, C., Barendse, J., Best, P.B., Hersch, R., Leslie, M.S., Thornton, M., Rosenbaum, H.C. 2010. Temporal patterns of population structure of humpback whales in West coast of Africa (B stock). Paper SC/62/SH8 submitted to the IWC Scientific Committee, April 2010 (unpublished). 13pp.
- Cerchio, S., Ersts, P., Pomilla, C., Loo, J., Razafindrakoto, Y., Leslie, M., Andrianriavelo, N., Minton, G., Dushane, J., Murray, A., Collins, T. and Rosenbaum, H. 2008a. Revised estimation of abundance for breeding stock C3 of humpback whales, assessed through photographic and genotypic mark-recapture data from Antongil Bay, Madagascar, 2000-2006. Paper SC/60/SH32 submitted to the IWC Scientific Committee, April 2008 (unpublished). 20pp.
- Cerchio, S., Findlay, K., Ersts, P., Minton, G., Bennet, D., Meijer, M.A., Razafindrakoto, Y., Kotze, P.G.H., Oosthuizen, H., Leslie, M., Andrianriavelo, N. and Rosenbaum, H. 2008b. Initial assessment of exchange between breeding stocks C1 and C3 of humpback whales in the western Indian Ocean using photographic mark-recapture data, 2000-2006. Paper SC/60/SH33 submitted to the IWC Scientific Committee, April 2008 (unpublished). 15pp.
- Chittleborough, R.G. 1965. Dynamics of two populations of the humpback whale, *Megaptera Novaengliae* (Borowski). *Australian Journal of Marine and Freshwater Research*, 16:33-128.
- Collins, T., Cerchio, S., Pomilla, C., Loo, J., Carvalho, I., Ngousson, S. and Rosenbaum, H.C. 2008. Revised estimates for humpback whale breeding stock B1: Gabon. Paper SC/60/SH28 submitted to the IWC Scientific Committee, April 2008 (unpublished). 17pp.
- Cooch, E and White, G. 2011. Program MARK: "A gentle introduction". 9th Edition. Online book available at <http://www.phidot.org/software/mark/docs/book> (01/04/2011). 850pp.
- Cunningham, C.L. 2002. Improved management of north east Atlantic mackerel, using Bayesian modelling methodologies. Ph.D. thesis. Imperial College of Science, Technology and Medicine, U.K.
- Félix, F., Castro, C., Laake, J.L., Haase, B. and Scheidert, M. (in press). Abundance and survival estimates of the Southeastern Pacific humpback whale stock from 1991-2006 photo-identification surveys in Ecuador. *Journal of Cetacean Research and Management* (Special Issue).
- Fennessy, S.T. and Groeneveld, J.C. 1997. A review of the offshore trawl fishery for crustaceans on the east coast of South Africa. *Fisheries Management and Ecology* 1997, 4:135-147.
- Findlay, K. and Best, P.B. 2006. The migration of humpback whales past Cape Vidal, South Africa, and a preliminary estimate of the population increase rate. Paper SC/A06/HW16 submitted to the IWC Scientific Committee, April 2006 (unpublished). 36pp.

- Findlay, K., Bannister, J.L., Cerchio, S., Jackson, J., Loo, J., Paton, D., Rosenbaum, H., Weinrich, M. and Zerbini, A. 2009. Allocations of catches of humpback whales (1904-1973) for the IWC comprehensive assessment of Southern Hemisphere humpback whales. Paper SC/61/SH31 submitted to the IWC Scientific Committee, April 2009 (unpublished). 33pp.
- Freund, J.E. 2004. Mathematical Statistics with applications. 7th Ed. Pearson Education, Inc., Upper Saddle River. 614pp.
- Gamerman, D. 1997. Markov chain Monte Carlo: Stochastic simulation for Bayesian inference. 1<sup>st</sup> Ed. Chapman & Hall, New York. 245pp.
- Groeneveld, J.C. 2000. Biology and ecology of the deep-water rock lobsters *Palinurus gilchristi* and *Palinurus delagoae* in relation to their fisheries. Ph.D. thesis. University of Cape Town, South Africa.
- Hedley, S.L., Bannister, J.L. and Dunlop, R.A. 2008. Group IV Humpback whales: Abundance estimates from aerial and land-based surveys off Shark Bay, Western Australia, 2008. Paper SC/61/SH23 submitted to the IWC Scientific Committee, April 2008 (unpublished). 17pp.
- International Whaling Commission 1998. Report of the Scientific Committee. *Report of the International Whaling Commission*, 48: 170-182.
- International Whaling Commission 2006a. Report of the Scientific Committee, Annex H: Report of the sub-committee on other Southern Hemisphere whale stocks. *Journal of Cetacean Research and Management*, 8 (Suppl.): 151-170.
- International Whaling Commission 2006b. Report of the workshop on the comprehensive assessment of Southern Hemisphere humpback whales, Hobart, Australia, April 2006. 77pp.
- International Whaling Commission 2007. Report of the Scientific Committee, Annex H: Report of the sub-committee on other Southern Hemisphere whale stocks. *Journal of Cetacean Research and Management*, 9 (Suppl.): 188-209
- International Whaling Commission 2008. Report of the Scientific Committee, Annex H: Report of the sub-committee on other Southern Hemisphere whale stocks. *Journal of Cetacean Research and Management*, 10 (Suppl.): 207-224.
- International Whaling Commission 2009a. Report of the Scientific Committee, Annex H: Report of the sub-committee on other Southern Hemisphere whale stocks. *Journal of Cetacean Research and Management*, 11 (Suppl.): 220-247.
- International Whaling Commission 2009b. Report of the intersessional meeting on Southern Hemisphere humpback whale assessment methodology, Seattle, February 2009. 33pp.
- International Whaling Commission 2010. Report of the Scientific Committee, Annex H: Report of the sub-committee on other Southern Hemisphere whale stocks. *Journal of Cetacean Research and Management*, 11 (Suppl. 2): 218-251.
- International Whaling Commission 2011. Report of the Scientific Committee, Annex H: Report of the sub-committee on other Southern Hemisphere whale stocks. *Journal of Cetacean Research and Management*, 12 (Suppl.): 203-226.
- Jackson, J., Zerbini, A., Clapham, P.J., Garrigue, C., Hauser, N., Poole, M., and Baker, C.S. 2006. A Bayesian assessment of humpback whales on breeding stocks of Eastern Australia and Oceania (IWC Stocks E, E1, E2 and F). Paper SC/A06/HW52 submitted to the IWC Workshop on the Comprehensive Assessment of Southern Hemisphere humpback whales, Hobart, Australia, April 2006 (unpublished). 19pp.
- Jaworski, P. 2009. On copulas and their diagonals. *Information Sciences*, 179: 2863-287.

- Johnson, J.H. and Wolman, A.A. 1984. The humpback whale, *Megaptera novaengliae*. *Marine Fisheries Review* 46(4): 30-37.
- Johnston, S.J. and Butterworth, D.S. 2005. A Bayesian assessment of the west and east Australian breeding populations (stocks D and E of Southern Hemisphere humpback whales. Paper SC/57/SH15 submitted to the IWC Scientific Committee, April, 2005 (unpublished). 25pp.
- Johnston S.J. and Butterworth, D.S. 2007. Corrected assessment results for Southern Hemisphere humpback whales from Breeding Socks D and G. Paper SC/59/SH2 submitted to the IWC Scientific Committee, April, 2007 (unpublished). 5pp.
- Johnston, S.J. and Butterworth, D.S. 2008a. Updated assessments of Southern Hemisphere humpback whale breeding sub-stock B1. Paper SC/60/SH41 submitted to the IWC Scientific Committee, April, 2008 (unpublished). 10pp.
- Johnston, S.J. and Butterworth, D.S. 2008b. Further possible movement hypotheses for C1-C3 humpback whales. Paper MARAM IWS/DEC08/HB/8 submitted to the MARAM International Stock Assessment Workshop, Cape Town, 2008 (unpublished). 5pp.
- Johnston, S.J. and Butterworth, D.S. 2009. Bayesian assessments using models which allow for interchange on the breeding grounds of Southern Hemisphere humpback whale breeding sub stocks C1 and C3. Paper SC/61/SH27 submitted to the IWC Scientific Committee, April 2009 (unpublished). 39pp.
- Johnston, S.J. and Butterworth, D.S. 2010. Updated South Coast rock lobster stock assessments for 2010 and comparisons to the 2008 and 2009 assessments. Paper MCM/2010/APR/SWG-SCRL/04 submitted to the scientific working group of Fisheries Branch, Department of Agriculture, Forestry and Fisheries, South Africa.
- Johnston S.J. and Butterworth, D.S. (in prep.). Bayesian Assessments (and simulation model testing) of Southern Hemisphere humpback whale breeding sub-stocks C1 and C3 using models which allow for interchange on the breeding grounds. 46pp.
- MARAM 2008. MARAM international stock assessment workshop, Cape Town, December 2008: Summary remarks by external panel (unpublished). 3pp.
- Matsuoka, K., Hakamada, T., Kiwada, H., Murase, H. and Nishiwaki, S. (in press). Abundance estimates and trends for humpback whales (*Megaptera novaeangliae*) in Antarctic Areas IV and V based on JARPA sighting data. *Journal of Cetacean Research and Management* (Special Issue).
- McAllister, M.K., Pikitch, E.K., Punt, A.E. and Hilborn, R. 1994. A Bayesian approach to stock assessment and harvest decisions using the Sampling/Importance Resampling algorithm. *Canadian Journal of Fisheries and Aquatic Sciences*, 51:2673-2687.
- McAllister, M.K. and Ianelli, J.N. 1997. Bayesian stock assessment using catch-age data and the sampling-importance resampling algorithm. *Canadian Journal of Fisheries and Aquatic Sciences*, 54:284-300.
- McAllister, M.K. and Kirchner, C. 2002. Accounting for structural uncertainty to facilitate precautionary fishery management: illustration with Namibian orange roughy. *Bulletin of Marine Science*, 70(2):499-540.
- Müller, A., Butterworth, D.S. and Johnston, S.J. 2009. Is the length distribution of C1 and C3 humpback whale catches consistent with an age-structured version of the Resident model? Paper SC/61/SH29 submitted to the IWC Scientific Committee, April 2009 (unpublished). 34pp.
- Müller, A., Butterworth, D.S. and Johnston, S.J. 2010. Bayesian assessments of the Southern Hemisphere humpback whale breeding stock B using three different models for stock-structure. Paper SC/62/SH30 submitted to the IWC Scientific Committee, April 2010 (unpublished). 19pp.

- Noad, M.J., Paton, D.A. and Cato, D.H. 2006. Absolute and relative abundance estimates of Australian east coast humpback whales (*Megaptera novaeangliae*). Paper SC/A06/HW27 submitted to the IWC workshop on the comprehensive assessment of Southern Hemisphere humpback whales, Hobart, April 2006 (unpublished). 15pp.
- Noad, M.J., Dunlop, R.A., Paton, D. and Cato, D.H. 2008. An update of the east Australian humpback whale population (E1) rate of increase. Paper SC/60/SH31 submitted to the IWC Scientific Committee, April 2008 (unpublished). 13pp.
- Olavarria, C., Anderson, M., Paton, D., Burns, D., Brasseur, M., Garrigue, C., Hauser, N., Poole, M., Caballero, S., Flórez-González, L. and Baker, C.S. 2006. Eastern Australia humpback whale genetic diversity and their relationship with Breeding Stocks D, E, F and G. Paper SC/58/SH25 submitted to the IWC Scientific Committee, April 2006 (unpublished). 6pp.
- Pella, J.J. and Tomlinson P.K. 1969. A generalized stock production model. *Bulletin of the Inter-American Tropical Tuna Commission*, 13(3):419-497.
- Press, W.H., Teukolsky, S.A., Vetterling, W.T. Flannery, B.P. 1992. Numerical recipes in FORTRAN: The art of scientific computing. 2<sup>nd</sup> Ed. Cambridge University Press, U.K. 963pp.
- Punt, A.E. 1996. The effects of assuming that density dependence in the HITTER-FITTER model acts on natural mortality rather than fecundity. *Report of the International Whaling Commission* 46: 629-636.
- Robert, C.A. 1994. The Bayesian choice. 1<sup>st</sup> Ed. Springer-Verlag, New York, Inc. 436pp.
- Rosenbaum, H.C., Pomilla, C., Leslie, M. C., Mendez, M. C., Best, P.B., Collins, T., Engel, M.H., Ersts, P.J., Findlay, K.P., Bonatto, S., Kotze, P.G.H., Meyer, M., Minton, G., Barendse, J., Thornton, M. Razafindrakoto, Y. and Ngouesso, S. 2006a. Mitochondrial DNA diversity and population structure of humpback whales from their wintering areas (breeding stocks) in the Indian and South Atlantic Oceans (wintering regions A, B, C, and X). Paper SC/A06/HW41 submitted to the IWC workshop on the comprehensive assessment of Southern Hemisphere humpback whales, Hobart, April 2006 (unpublished). 16pp.
- Rosenbaum, H.C., Pomilla, C., Olavarria, C., Baker, C.S., Leslie, M. C., Mendez, M. C., Caballero, S., Brasseur, M., Bannister, J., Best, P.B., Bonatto, S., Collins, T., Engel, M.H., Ersts, P.J., Findlay, K.P., Florez-Gonzalez, L., Garrigue, C., Hauser, N., Jenner, C., Meyer, M., Minton, G., Poole, M. and Razafindrakoto, Y. 2006b. A first and preliminary analysis of MTDNA sequences from humpback whales for breeding stocks A-G and X. Paper SC/A06/HW59 submitted to the IWC workshop on the comprehensive assessment of Southern Hemisphere humpback whales, Hobart, April 2006 (unpublished). 4pp.
- Rubin, D.B. 1988. Using the SIR algorithm to simulate posterior distributions. P. 395-402 in Bernardo, J.M., DeGroot, M.H., Lindley, D.V. and Smith, A.F.M. (ed.). 1988. Bayesian Statistics 3: Proceedings of the third Valencia International Meeting, June 1-5, 1987. Clarendon Press, Oxford. 805pp.
- Walters. C. and Ludwig, D. 1994. Calculation of Bayes posterior probability distributions for key population parameters. *Canadian Journal of Fisheries and Aquatic Sciences*, 51:713-722.
- Zerbini, A.N., Clapman, P.J. and Wade, P.R. 2008. Plausible maximum rates of population growth in humpback whales. Paper SC/60/SH30 submitted to the IWC Scientific Committee, April 2008 (unpublished). 14pp.
- Zerbini, A. N., Ward, E. J., Kinan, P. G., Engel, M. H. and Andriolo, A. (in press). A Bayesian assessment of the conservation status of humpback whales (*Megaptera novaeangliae*) in the western South Atlantic Ocean. *J. Cetacean Res. Manage.* (Special Issue). 29pp.